The Role of the Autoimmune Regulator Gene (AIRE) in Peripheral T cells

Karen A Adamson

A thesis submitted for the degree of Doctor of Philosophy
University of Edinburgh
2004

To my parents,

for always believing in me.

Declaration

I hereby declare that this thesis has been composed solely by myself and has not been accepted in any previous application for candidature for a higher degree. All the work presented in this thesis, was unless acknowledged, initiated and executed by myself. All sources of information in the text have been acknowledged by reference.

Karen A. Adamson

Contents

Table of Contents

List of Figures

Chapter 4

Chapter 5

List of Tables

Abbreviations

7AAD	7-aminoactinomycin D
A	Adenosine
AIRE	Autoimmune regulator gene
AnnV	Annexin V
AP-1	Activating protein-1
APC	Antigen presenting cell
APECED	Autoimmune polyendocrinopathy candidiasis ectodermal dystrophy
APS1	Autoimmune polyendocrine syndrome type 1
ATF	Activating transcription factor
bHLH	basic helix loop helix
bp	base pairs
BSA	Bovine serum albumin
C	Cytidine
CBF1	C-promoter binding factor 1
CBP	CREB-binding protein
CD	Cluster of Differentiation
cDNA	complementary DNA
CFA	Complete Freund's adjuvant
CFSE	5- and 6- carboxyfluorescein diacetate succinimidyl ester

CM	Complete Media
CMC	Chronic mucocutaneous candidiasis
CRE	cAMP responsive element
CTLA4	Cytotoxic T lymphocyte associated antigen 4
CyChr	Cy Chrome
DC	Dendritic cell
Dl1	Delta-like 1
DNA	Deoxyribonucleic acid
DNase	Deoxyribonuclease
DSL	Delta, Serrate, Lag2
E	Embryonic day
EDTA	Ethylenediaminetetraacetic acid-disodium salt
EGF	Epidermal growth factor
EMSA	Electrophoretic mobility shift assay
FACS	Fluorescence activated cell sorting
FCS	Foetal calf serum
FITC	Fluorescein isothyocyanate
G	Guanosine
GAD	Glutamic acid decarboxylase
GFP	Green fluorescent protein

HDAC	Histone deacetylase
HEL	Hen egg lysozyme
Hes	Hairy enhancer of split
HI	Heat inactivated
HLA	Human leucocyte antigen
HSR	Homogenously staining region
IAA	Insulin autoantibodies
ICC	Immunocytochemistry
IFNγ	Interferon γ
IHC	Immunohistochemistry
IL	Interleukin
ISH	*in-situ* hybridisation
JNK	Jun kinases
kDa	Kilodaltons
LNG	Lin12/Notch/Glp-1
Lta	Lymphotoxin-α
LTβR	Lymphotoxin-β receptor
MACS	Magnetic cell sorting
MAML1	Mastermind-like 1
ME	Mercaptoethanol

MEC	Medullary epithelial cell
MHC	Major histocompatibility complex
MLR	Mixed lymphocyte reaction
mRNA	messenger RNA
NFAT	Nuclear factor of activated cells
NF-κB	Nuclear factor κB
NICD	Notch intra-cellular domain
NK cell	Natural killer cell
NKT	Natural Killer T cell
NLS	Nuclear localisation signal
PBMC	peripheral blood mononuclear cells
PCR	Polymerase chain reaction
PE	Phycoerythin
PEST	Proline-, glutamate-, serine-, threonine-rich sequence
PHD	Plant homeodomain
PML	Promyelotic leukaemia protein
PRR	Proline rich region
PSP	Paraspeckle protein
RAM	RBJκ association molecule
RNA	Ribonucleic acid

RNase	Ribonuclease
RT-PCR	Reverse transcriptase polymerase chain reaction
SAND	Sp100, AIRE-1, NucP41/75, DEAF-1
scc	side-chain cleavage
Sp1	Specificity protein 1
SSCP	Single strand conformational polymorphism
STAT	Signal transducer and activator of transcription
T	Thymidine
T1D	Type 1 diabetes
TACE	TNF-α converting enzyme
TAD	Transcriptional activator domain
TCR	T cell receptor
TEMED	N,N,N`N`-tetramethylethylenediamine
Th	T helper cell
TNFα	Tumour necrosis factor α
TRE	TPA-responsive element
Treg	Regulatory T cell
VNTR	Variable number of tandem repeats

Acknowledgements

Firstly, I would like to thank my supervisors, Dr S Pearce and Prof P Kendal-Taylor in Newcastle upon Tyne, who initiated my interest in Aire. Prof J Seckl for being interested and allowing me to continue investigating this gene upon my move to Edinburgh, and Prof J Lamb and Dr S Howie for their valued supervision when my interest turned to the effects of Aire within the peripheral immune system.

I would like to thank everyone in Molecular Endocrinology for making the move to Edinburgh easy. In particular, thanks to June Noble, Karen French, Karen Chapman and Val Lyons for sharing their experience with me.

A big thank you also to all the members of the Immunobiology group who have been willing to help me out with relearning immunology, especially Sarah Howie for her unending patience. In particular, thanks to Marta Corsin-Jiminez for teaching me how to work with T cells, to Julia Marley for throwing me in at the deep end with 4 colour flow cytometry, to Anne Grant and June Stewart for their help with immunohistochemistry, Lynn Forsyth for introducing me to real time RT-PCR and Linda Wilson for trusting me enough to teach me how to use the confocal microscope. A special thank you to Robert Benson and Mel Leech for their helpful discussion.

And finally, Thomas and Emily, thank you for being so understanding when mummy had to work all weekend.

Abstract

Mutations of the autoimmune regulator gene (AIRE) lead to the development of the multiple organ specific autoimmune disease, autoimmune polyendocrine syndrome type 1 (APS1). Aire is known to have a role in central tolerance through regulating the expression of self-antigens in the thymus. Prevention of autoimmune disease also relies on peripheral control of any autoreactive T cells which do exit the thymus, however, the role of Aire in the maintenance of these mechanisms, if any, is unknown.

Thus, the hypothesis of this thesis was that lack of functional Aire affects peripheral T cell function and that Aire plays a role in peripheral tolerance.

Initially, the disease phenotype and genotype of APS1 patients in the UK was determined. The phenotype of the peripheral lymphocytes of a small number of these patients was determined through assessment of cell surface markers by flow cytometry. The ability of these cells to proliferate when stimulated through the T cell receptor was then assessed, this revealed a trend to a higher maximal proliferative response in patients compared to controls. Cytokine production in response to T cell stimulation showed a trend to a decrease in IFN-γ and TNF-α in patients compared to controls.

The tissue and cellular distribution of Aire in mice was characterised and Aire was found to be expressed in tissues of the immune system along with a number of other tissues, where its expression was predominantly limited to epithelial cells. Given the cellular distribution of Aire, i.e. within speckles in the nucleus, its interaction with nuclear proteins investigated. Aire was found to interact with paraspeckle protein 1.

The role of Aire in CD4+ T cells was then investigated. Aire was found to be up-regulated upon activation through the T cell receptor, at the mRNA and protein level. This up-regulation of Aire could be abrogated by inhibiting signalling through Notch, a developmental gene pathway which may play a role in peripheral tolerance. Thus, it is possible that Aire may be regulated by a component of the Notch signalling pathway, or alternatively by a precursor common to both pathways.

CHAPTER 1

1 Introduction

At the time this thesis was commenced, the autoimmune regulator gene (*AIRE*), had recently been cloned (2,3). *AIRE* was so named, as mutations in this gene cause autoimmune polyendocrine syndrome type 1 (APS1) (OMIM 240300), a rare autosomal recessive disorder characterised by multiple autoimmune diseases (4). These first descriptions of *AIRE* revealed that it is expressed highly within the thymus (2,3). Further descriptions showed that within the thymus, the expression of AIRE is predominantly within the medullary epithelial cells (5,6,7,8). The medullary epithelial cells (MEC) are known to mediate negative selection of T lymphocytes (9), and MEC express tissue specific antigens such that antigens encountered in the periphery are present within the thymus (10,11,12). This promiscuous expression of peripheral antigens and negative selection of T cell clones specific to these antigens is in part under the control of *aire* (13). Therefore, *aire* may play a role in central tolerance through the expression of peripheral antigens and negative selection of thymocytes specific for these antigens. However, it is probable that some autoreactive T cell clones will escape this process of negative selection and will be subjected to mechanisms of peripheral tolerance to prevent the development of autoimmune disease. Whether aire plays a role in peripheral T cells and their responses is the subject of this thesis.

1.1 Autoimmune polyendocrinopathy syndrome type 1 (APS1)

The autoimmune polyendocrinopathy syndrome type 1 (APS1) is characterised by autoimmune hypoparathyroidism, autoimmune adrenal failure and chronic mucocutaneous candidiasis. The *AIRE* gene was originally identified because it is mutations in this gene that cause APS1 (2,14,15,3,1,16,17,18), a rare autosomal recessive form of human endocrine autoimmunity (4). The familial syndrome known as APS1 was first described by Whitaker in 1956 (19), however the first description of hypoparathyroidism associated with candidiasis was in 1929 (20), with the association with hypoadrenalism being reported in 1946 (21). APS1 is also known as Whitaker's syndrome, polyglandular autoimmune disease type 1 or autoimmune polyendocrinopathy, candidiasis and ectodermal dystrophy (APECED).

1.1.1 Prevalence

APS1 is rare with the highest prevalence seen in Finnish and Iranian Jewish populations due to founder effects with a prevalence of approximately 1 in 25000 and 1 in 9000 respectively. In the UK it is estimated to affect approximately 3 per million of the population.

1.1.2 Genetics of APS1

Numerous mutations have been described in the *AIRE* gene (Fig 1.1). In order to make the description of these more meaningful, I shall briefly describe the structure of the *AIRE* gene.

The human autoimmune regulator gene (*AIRE*) is encoded on chromosome 21q22.3 (22), and, as described above, was cloned in 1997 by two independent groups (2,3). It has 14 exons that encode a 2445 base pair transcript. The translated protein has 545 amino acids and a molecular weight of 57.5 kDa (3). The murine *Aire* gene shows a high degree of homology to the human gene (23,5,24).

When cloned, *AIRE* was identified to have many features suggestive of a role as a transcription factor (Fig 1.1). These conserved domains include a nuclear localisation signal, a proline rich region, two plant homeodomain (PHD)-type zinc fingers, four nuclear receptor interaction (L*XX*LL) motifs, an inverted L*XX*LL motif and a variant of this (F*XX*LL) (2,3). Clearly the nuclear localisation signal suggests that this is a nuclear protein, and this in combination with the L*XX*LL motifs and the PHD fingers, which are found in nuclear proteins including transcriptional coactivators, hint at a role in the regulation of gene expression (25). AIRE also contains a SAND domain (**S**p100, **A**IRE-1, **N**ucP41/75, **D**EAF-1); this domain is thought to function as a DNA binding domain and this feature in conjunction with the PHD fingers led Gibson et al to propose that AIRE regulates gene expression by modulating chromatin structure (25). More recently, the DNA binding ability of the SAND domain was confirmed (26). Kumar et al demonstrated that AIRE homodimers and tetramers can bind DNA (27), although this DNA binding may not be mediated by the SAND domain, as the KDWK motif, which mediates DNA

binding via the SAND domain of Sp100 and DEAF-1 is not present in the AIRE protein (28).

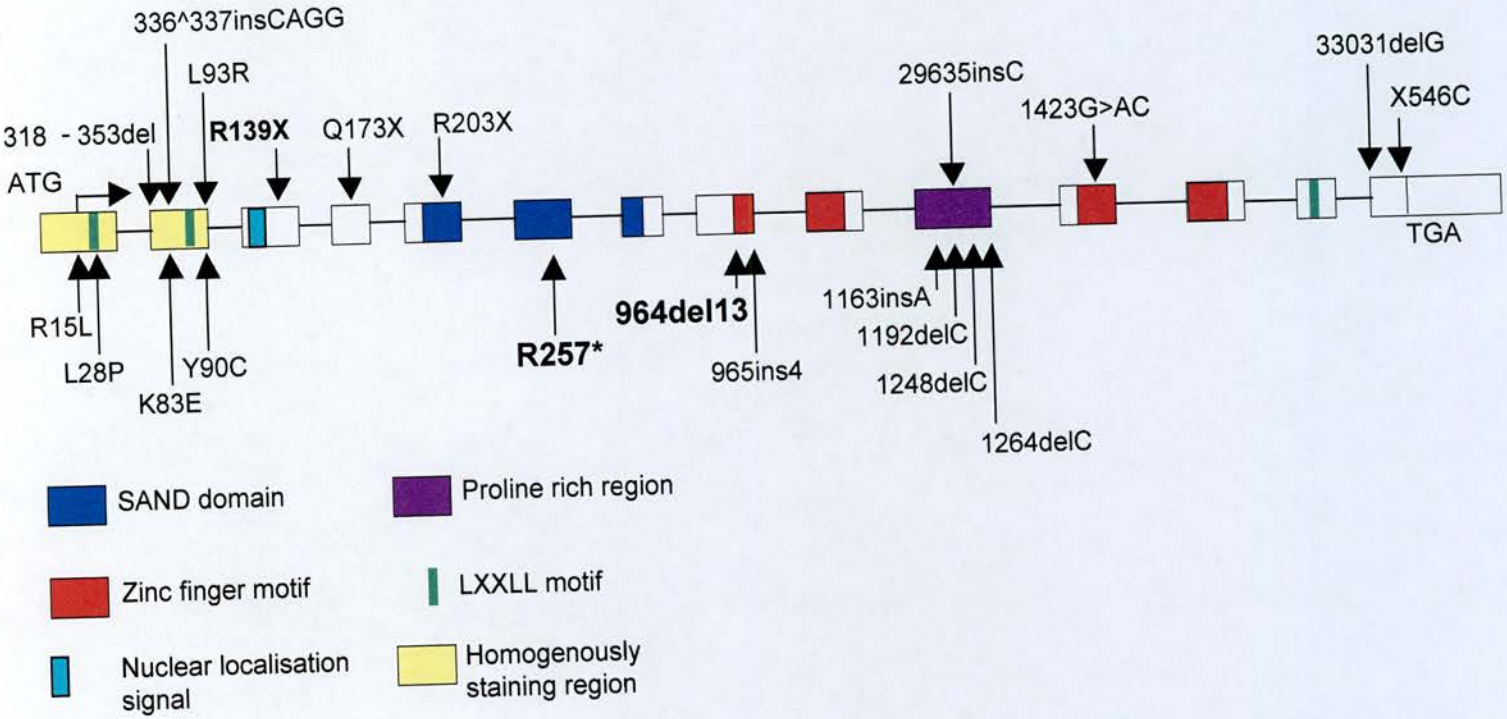

Figure 1.1 The AIRE gene. The 14 exons of AIRE are depicted, with the arrows representing the sites of known mutations. The conserved regions are also shown.

The commonest mutation in the UK APS1 population is a 13 base pair deletion in exon 8 which gives rise to a protein truncated at the start of the first zinc finger motif (1), whilst in the Finnish APS1 population, the major mutation is a nonsense mutation in exon 6 encoding a protein truncated in the SAND domain and containing neither zinc finger (2,3). In addition to these major mutations, there are many other mutations often arising *de novo* in individual families. APS1 is an autosomal recessive disease, thus patients are either homozygotes for the mutation, or more commonly in the case of new mutations, compound heterozygotes. However, despite the wide variety of mutations seen, no genotype-phenotype correlation has been reported, rather it appears that the spectrum of disease present reflects the combination of genetic susceptibility factors and environmental influences acting in individual patients.

As APS1 is characterised by the development of multiple autoimmune diseases, the possibility of an HLA association has been investigated. Unsurprisingly, there is no association between with APS1 and HLA type, as APS1 is caused by mutations in the AIRE gene. However, there may be an association between the development of certain disease manifestations and HLA type. HLA-A3 occurs more frequently in patients with ovarian failure (29), whilst none of 11 APS1 patients with type 1 diabetes, but 15 of 56 APS1 patients without type 1 diabetes had the DQB*0602 allele, which is protective for diabetes (30).

1.1.3 Clinical Features

APS1 usually manifests in early childhood and is characterised by hypoparathyroidism, hypoadrenalism and chronic mucocutaneous candidiasis

(CMC). Clinical diagnosis is based on the presence of two of these three cardinal features (4).

The first manifestation to occur is usually CMC, generally by 5 years of age, although it can occur as early as the first few months after birth (4,31,32). CMC is seen in 73-100% of patients (4,32), although it occurs less frequently in Iranian Jews and when present is less severe (33). CMC affects the oral, vaginal and oesophageal membranes, nails and dermis (4).

Hypoparathyroidism tends to occur next, being present in 76-93% of patients, usually by 10 years of age but can occur as early as 3 months of age and has been reported to occur as late as 44 years of age (4,32,34). Autoantibodies to the extracellular domain of the calcium-sensing receptor have been found in over half of patients with acquired hypoparathyroidism, the majority of whom had APS1 (35).

The third of the cardinal features of APS1, Addison's disease, is usually present by 15 years of age, but has been reported to occur from 36 months to 41 years (4,32). This manifestation occurs in 72-100% of patients with APS1 (4,32,34). Adrenal cortex autoantibodies and steroid-producing cell autoantibodies have been demonstrated in patients with APS1 with Addison' disease (32). The autoantigens recognised by these autoantibodies are P450 17α-hydroxylase (P450 17α-OH), P450 side-chain cleavage (P450scc) and P450 21-hydroxylase (P450 21-OH) (36,37,38,39).

In addition to these manifestations, a variety of other autoimmune diseases occur in APS1. In a major Finnish series of 68 patients, 43% of patients had 4 or more disease manifestations (4). Autoimmune gonadal failure occurs in approximately 17-50% of

patients, these have steroid-producing cell autoantibodies (4,32,34). Malabsorption, occurs in 15-22% of patients (4,32,34), its course often fluctuates, and this has a major impact on all the other manifestations due to effects on the absorption of food and medication. In some patients this is due to coeliac disease (40), however, in many there is no obvious cause. The malabsorption does however appear to be autoimmune in nature, and 48% of APS1 patients were found to have autoantibodies to tryptophan hydroxylase, whilst no patients with other autoimmune diseases or healthy controls were positive for these antibodies (41). In addition, serum from these antibody-positive APS1 patients specifically stained tryptophan-hydroxylase-containing enterochromaffin cells in normal duodenal mucosa and there was an absence of serotonin-containing cells in duodenal biopsy samples from APS1 patients (41). Cholelithiasis occurs in APS1 patients at an earlier age than the general population. This is thought to be secondary to malabsorption, leading to low levels of bile acid in the gallbladder through disruption of the bile acid cycle (42).

Type 1 diabetes (T1D) occurs in 12 to 18% of APS1 patients (4,43). The majority of these patients have islet cell and/or glutamic acid decarboxlyase (GAD) antibodies (43).

Numerous other autoimmune manifestations have been reported. These include thyroid disease, pernicious anaemia, hepatitis, vitiligo and alopecia (4). Autoimmune asplenism may also be present, as a progressive process, leading to characteristic findings on a blood smear, i.e. Howell-Jolly bodies, target cells, burr cells and thrombocytosis (42).

Ectodermal dystrophy also occurs, affecting the nails and teeth, with defective dental enamel formation. At one time this was thought to be a consequence of

hypoparathyroidism, however as it is not seen following surgical hypoparathyroidism and can occur after the correction of the low calcium, this is no longer thought to be the case (32).

1.1.4 Prediction of disease manifestations

A notable feature of the APS1 series reported is the fact that there are unexplained deaths both in patients and their siblings (4,44,45). These are usually attributed to undiagnosed Addison's disease, hypoparathyroidism or fulminant sepsis (possibly secondary to undiagnosed hyposplenism) (45). In view of this, the ability to predict new manifestations to enable targeted screening would be advantageous.

As is the case with most complex autoimmune diseases, in APS1 autoantibodies occur more frequently than the disease for which they are a marker. In APS1 autoantibodies against glutamic acid decarboxylase (GAD) are present more commonly than T1D, being found in 32% of patients (46), making the positive predictive value of GAD65 antibodies for T1D in APS1 approximately 27% (43). Recently it has been suggested that antibodies against the IA-2 tyrosine phosphatase-like protein (IA-2 ab) or insulin (IAA) are better markers of active beta cell loss, with a positive predictive value in APS1 patients of 67% for T1D (30). But it is clear that measurement of autoantibodies alone is not sufficient to predict diabetes development in APS1 patients, therefore at present, the only tool available to the clinician is regular screening (45).

1.1.5 Aire mutations and complex autoimmune diseases

Given the broad spectrum of organ specific autoimmune diseases seen in APS1, it is unsurprising that various researchers have investigated the role of AIRE mutations in complex autoimmune diseases, in particular Addison's disease, autoimmune thyroid disease and diabetes. Three independent groups have found no evidence for heterozygous mutations in AIRE having a role in the development of these autoimmune diseases (47,48,49).

1.2 The autoimmune regulator gene

The structure of AIRE is described in section 1.1.2. Briefly it has features suggestive of a role as a transcription factor including a nuclear localisation signal and several domains capable of mediating protein-protein and protein-DNA interactions.

1.2.1 Subcellular localisation of AIRE

Full length AIRE protein is targeted to the nucleus as predicted by the nuclear localisation signal (50,51,52). Within the nucleus, AIRE is expressed in a characteristic speckled pattern which has been likened to nuclear bodies (50,51,52,8,53). However, AIRE does not colocalise with Sp100 or PML, proteins which are components of nuclear bodies (51,52). In transfected cell lines a fibrillar pattern of cytoplasmic staining is also seen (50,51,52) that is similar in distribution to microtubules and was demonstrated to colocalise with α tubulin and vimentin, which associate with microtubules (52).

The nuclear localisation of AIRE in the presence of a consensus nuclear localisation signal (NLS) is strongly suggestive that this NLS is functional. Proof of this was provided by a construct consisting of the AIRE NLS and green fluorescent protein (GFP). This construct was transiently expressed in COS-1 cells and the GFP was seen to localise to the nucleus (50). In addition to this N terminal NLS, construction of N-terminal deletion AIRE constructs revealed an additional C terminal nuclear transport signal that is functional irrespective of the N terminal NLS (50).

The localisation to microtubular structures is mediated via the N terminal homogenously staining region (HSR), a region which is also required for homodimerisation (50,54).

As might be expected for a protein that is expressed both in the nucleus and cytoplasm, the AIRE protein contains putative nuclear export sequences (28). Although the AIRE nuclear export sequences are not identical to the consensus for the CRM-1-mediated nuclear export system, leptomycin B (LMB), which is a specific inhibitor of the CRM-1-mediated nuclear export pathway, leads to an increase in nuclear localisation of AIRE at the expense of cytoplasmic localisation (50).

1.2.2 Transcriptional activator function of AIRE

The nuclear location and presence of domains associated with other transcription factors such as the proline rich region (PRR) and PHD fingers suggest a role for AIRE in transcriptional regulation. Two independent reports have shown that AIRE can activate transcription in a GAL4-based reporter system (53,54). This transactivation required the presence of more than one activation domain (54).

The possibility that AIRE interacts with the common transcriptional coactivator CREB-binding protein (CBP) has been investigated. CBP is a transcriptional coactivator for many transcription factors (55,56,57,58,59) has histone acetyltransferase activity (60,61) and is localised in PML bodies (62). AIRE was found to interact with CBP through the CH1 and CH3 domains (54), two of CBP's three domains putatively involved in protein-protein interactions.

1.2.3 Regulation of AIRE expression

Until recently, the mechanisms by which AIRE gene expression is regulated were unknown. However, in the last year, data regarding the promoter region of the AIRE gene have been published (63). The AIRE promoter was found to contain a binding site for activating protein-1 (AP-1) at –313 to –291 (63). AP-1 is a family of transcription factors of homodimers and heterodimers of Jun and Fos or activating transcription factor (ATF) proteins. Jun-Jun and Jun-Fos dimers bind to the TPA-responsive element (TRE) and Jun-ATF and ATF homodimers bind the cAMP responsive element (CRE). AP-1 is regulated through transcriptional control, which determines the amount of AP-1 protein present, and by the modulation of its stability through phosphorylation. In addition, the Jun proteins are regulated through interactions with Jun kinases (JNK), as Jun is phosphorylated in response to JNK activation. This phosphorylation enhances the ability of Jun to activate transcription probably through an interaction with CBP (64). The AP-1 band seen in an EMSA, was supershifted only by pan-Jun antibody, not pan-Fos antibody (63).

A CCAAT box was identified in the AIRE promoter, again by EMSA. This binding on EMSA was confirmed to be binding of AIRE promoter to NF-Y protein, a protein known to bind to the CCAAT box, by a supershift assay. The same techniques were used to show that the GC box in the promoter was binding Sp1 (Specificity protein 1). The CCAAT box is present in 30% of eukaryotic promoters and NF-Y (also known as CBF) is its major binding protein. Through binding between the protein and the promoter, NF-Y is able to regulate gene transcription (65). Similarly, it is well recognised that Sp1 binds to the GC box, and through this binding acts as a

transcriptional regulator (66). Thus the promoter region of AIRE contains at least three functional binding sites for common transcription factors.

In addition to binding by these transcription factors, AIRE gene expression is regulated through gene methylation. The AIRE promoter contains a CpG island which is approximately 300bp upstream of the translational start site and includes the first exon, methylation of this region blocks the activity of the AIRE promoter (63). Methylation of CpG islands is known to affect transcription, this is thought to occur through either blocking the binding of transcription factors, or by the binding of other proteins to the methylated residues which then prevent the access of transcription factors to the DNA (67). In two monocytic cell lines (THP-1 and U937) Aire was found to be heavily methylated, whilst a thymic epithelial cell line (TEC1A3) was less heavily methylated (63), in keeping with the hypothesis that gene methylation regulates the level of gene expression (67). Demethylation of these cell lines up-regulated the expression of AIRE, indicating that methylation can silence AIRE expression. Histone deacetylation was also shown to silence AIRE expression (63).

1.2.4 AIRE functions as an E3 ubiquitin ligase

Following the observation that a subset of PHD-containing proteins is able to mediate ubiquitin ligase activity, a Japanese group investigated the possibility that AIRE also has this function. They have demonstrated that the first PHD domain of AIRE does mediate E3 ubiquitin ligase activity, and that disease causing mutations within this domain abolish this activity (68). The ubiquitin pathway participates in

many functions of the cell including signal transduction, cell cycle progression and apoptosis (69,70), all of which play a role in homeostasis of the immune system, thus the elucidation of the target of ubiquitination by AIRE will be an important step towards understanding the role of AIRE within the immune system.

1.2.5 Tissue distribution of AIRE

There are many reports in the literature describing the tissue distribution of Aire using many techniques including RT-PCR, real time RT-PCR, *in-situ* hybridisation, northern blot, western blot and immunohistochemistry in both humans and mouse. There is discrepancy between these reports, thus the following discussion represents a consensus based on the available information, further detail can be found in section 4.1.

Given the importance of Aire in the maintenance of tolerance, its expression within the thymus has been investigated to gain insights into its function. Aire is primarily expressed within the medullary epithelial cells (MEC) in a punctuate pattern, and at the cortico-medullary junction, this expression is seen from E14.5 onwards (71,7,23). In mice in which there is a failure of development of normal thymic architecture, Aire transcripts could not be detected (71). This architectural organisation of the medulla depends on signals from postselection thymocytes, which may be provided by RelB, RelB deficient mice have medullary thymic atrophy, and do not express Aire within the thymus (71,7). As it was postulated that Aire, by virtue of its expression in an area involved in negative selection, is required for this process, the expression of Aire in models of positive and negative selection was investigated. In thymi from mice undergoing negative selection, Aire expression in the medulla and

at the cortico-medullary junction was increased, whilst it was decreased in the positively selecting mice (71).

In addition to expression in MEC, dendritic cells in the thymus and spleen have been documented to express Aire, albeit at lower levels than in MEC (7).

Within the spleen, there is evidence for Aire expression in lymphocytes in the red pulp in both humans and mice (51,6). However, this is disputed by Heino et al, who attribute the mRNA expression detectable in the spleen to expression by splenic dendritic cells (7).

In peripheral blood in humans and in mouse, Aire expression is seen in lymphocytes, neutrophilic granulocytes and monocytes (51,6). Kogawa et al, examined AIRE expression in purified populations of cells from human peripheral blood, and were unable to detect Aire expression in CD4+ lymphocytes, but did see Aire expression in CD14+ cells (72).

There are many differences in the reported tissue distribution of AIRE, but taking all the available data from both humans and mouse, there is some evidence to suggest that AIRE is expressed in many peripheral tissues, including lung, testis, kidney, ovary, adrenal gland, thyroid and gut (2,3,23,5,51,8,6,73,).

1.2.6 Insights into Aire function from knock-out mice

In the last year, two groups have published data on two different Aire deficient mouse strains (13,74).

The first, published by Ramsey et al, has a targeted disruption of the Aire gene in exon 6, and as such closely mimics the major Finnish mutation (74). These mice

develop multiple organ specific autoimmune diseases and have circulating autoantibodies. The major organs affected are the liver, which had periportal accumulation of lymphocytes, the adrenal glands, which were atrophied, and the ovaries, which were also atrophied. The thyroid and pancreas appeared normal (74). No differences in T and B cell ratio or distribution were observed in the thymus, lymph node or spleen, and no defect in T cell maturation within the thymus was seen. The number of apoptotic thymocytes was unchanged, suggesting no difference in the number of thymocytes undergoing negative selection. There was no evidence for an increase in the number of activated lymphocytes, based on flow staining for CD62L and CD44. Activation of cells from the lymph node via the T cell receptor (TCR) using anti-CD3 antibodies revealed no difference in the up-regulation of the activation markers, CD25 and CD69. The naïve phenotype of the T cells in the Aire deficient mouse led to the suggestion that the mice had not been challenged as they were housed in a sterile facility. Therefore, the response to immunisation was assessed. The mice were immunised with hen egg lysozyme (HEL) in complete Freund's adjuvant (CFA), followed by *in vitro* restimulation of draining lymph node cells. The cells from the Aire deficient mice exhibited a 3-5 fold increase in proliferation compared to wild type mice (74).

A mixed lymphocyte reaction using cells from Aire knockout and wild type mice was used to determine whether normal tolerance to self was present. No proliferation was detected in any of the combinations of cells used leading the authors to conclude that tolerance to self and antigen processing by MHCII is normal and that this experiment shows that "no major disturbances were evident to cause a difference in thymic negative selection" (74). However, if autoreactive T cell clones were not

deleted in the thymus, and are therefore present in the population of CD4 T cells used in this MLR, it is probable that the clone would either be present at too low a level allow a response to be seen, or that the APC used (CD4 depleted splenocytes) would not stimulate the T cell clone present. Thus, although the statement quoted above is true, I am not convinced that this experiment could be expected to demonstrate the kind of difference they were looking for. To further determine whether these mice have any alterations in lymphocytes, TCR Vβ chain usage was assessed. No differences were observed in the thymus, but three out of 24 Vβ families were different in the spleen in Aire deficient mice compared to controls (74). Based on these data the authors hypothesise that lack of Aire leads to a defect in peripheral tolerance.

In contrast, Anderson et al, generated an Aire deficient mouse, in which the Aire protein was truncated after exon 1 (13). Autoimmune disease was documented in the salivary gland, ovaries or testis, thyroid, liver, stomach and retina in these mice; circulating autoantibodies specific for these organs were also present. As with the Aire deficient mouse generated by Ramsey et al, no differences in immune cell numbers or distribution was seen. There were also no differences in lymph node cell production of IL2, IL4 or IFNγ, after stimulation with anti-CD3/28 antibodies. However, an increase in the number of thymic MEC, and an increase in activated/memory ($CD44^{hi}CD62L^{lo}$) peripheral CD4+ and CD8+ cells was observed. Further experiments in irradiated mice and in which Aire deficient thymi were transplanted into athymic mice, lead to the conclusion that the presence of Aire in the stromal cells of the thymus is necessary to prevent autoimmune disease in the periphery (13). The issue of whether Aire expression in the target organs is required

to prevent autoimmune disease was addressed. Transfer of Aire deficient lymphocytes into wildtype mice lead to the development of autoimmune disease. Thus the presence of Aire in these organs is not sufficient to prevent autoimmune disease (13).

The role of Aire in the MEC of the thymus was then investigated, in particular, whether Aire plays a role in the ectopic expression of peripheral antigens by these cells. A substantial decrease in the number of genes expressed was observed in the Aire deficient mice, with a bias towards ectopically expressed tissue specific peripheral antigens. Therefore, Aire appears to play a role in central tolerance through regulating the expression of peripheral antigens within the thymus (13).

The biological significance of this finding was confirmed in work by Liston et al. They utilised the Aire knock-out mouse generated by Ramsey et al and crossed this with a TCR transgenic mouse which expresses the TCR for a dominant peptide of HEL which also expresses HEL under control of the rat insulin promoter (75). This leads to expression of HEL in the pancreas and in small amounts circulating in the periphery. This promoter has previously been shown to drive the ectopic expression of peripheral gene in the thymus (76) and insulin is one of the genes whose thymic expression is regulated by Aire (13). The authors were unable to demonstrate expression of HEL protein in the thymus of Aire wild-type mice, however, a defect in negative selection of HEL specific T cells was observed (75). Taking this data in conjunction with that of Anderson et al, there is a strong argument for Aire playing a role in central tolerance through driving the ectopic expression of peripherally restricted antigens, and thus allowing negative selection of autoreactive T cells to take place.

Following the description of these two Aire knock-out mice, it was observed that the phenotype was remarkably similar to that seen in the lymphotoxin-α (Lta) and the lymphotoxin-β receptor (LTβR) deficient mice (77). In the Lta and LTβR deficient mice, a 75-80% decrease in Aire expression was seen in thymus. This reduction in Aire was enough to cause a decrease in the thymic expression of insulin, one of the peripheral antigens under the control of Aire in the thymus. These mice had normal thymic medullary epithelial cell development, but these cells expressed less Aire than the wild types. In addition, thymic Aire expression is up-regulated by *in vivo* treatment of both wild-type and Lta knock-out mice with an agonist LTβR antibody. The down-regulation in Aire observed in the absence of the lymphotoxin pathway, which leads to a decrease in the ectopic expression of peripheral antigens in the thymus, was sufficient to cause a breakdown in tolerance, as evidenced by autoantibody production (77).

1.2.7 Summary

Aire is required to prevent the development of autoimmune disease, but its presence does not appear to be required in the target organs of autoimmunity to prevent disease. Within the immune system, Aire is primarily expressed in the thymic MEC, where it plays a role in directing the ectopic expression of tissue specific antigens, thus allowing negative selection of autoreactive T cell clones. Further evidence for a role for Aire in central tolerance, is provided by Park et al. In an *in-vitro* negative selection system, inhibition of Aire using a dominant-negative construct increased recovery rates of thymocytes, showing that Aire expression on the APC may play a role in inducing thymocyte apoptosis (78).

Aire is also expressed in peripheral lymphoid tissues. However, whether it has a role in the peripheral immune system, is currently unclear.

1.3 T cell activation and effector function

It is clear that Aire has a role in central tolerance, but the presence of Aire in the peripheral immune system raises the question, what is its role here? The work in this thesis was limited to examining the role of Aire in CD4+ T cells as it is these cells that induce the broad range of effector functions that comprise peripheral immunity. Thus the following discussion is primarily limited to CD4+ T cells.

1.3.1 T cell development

Immature double negative T cell precursors migrate from the bone marrow to the thymus, where they enter into the cortex. Following TCR gene rearrangement, those double positive thymocytes able to recognise self-MHC are positively selected. During this process the double positive thymocyte becomes a single positive thymocyte, with the co-receptor (i.e. CD4 or CD8) appropriate for the MHC type against which the cell is selected being retained, and the other being lost. Those that are not positively selected will die by neglect.

In addition to positive selection, developing T cells are negatively selected to select out clones reactive against self-antigen. This process mainly occurs at the cortico-medullary junction and within the medulla, although it could occur anywhere within the thymus, if a self-peptide/MHC complex is recognised by the thymocyte. The self-antigen/MHC complexes that mediate this process can be presented by DCs, macrophages or medullary epithelial cells. The self-antigen is either internalised by the DC/macrophage as it migrates to the thymus or is generated from apoptotic thymocytes. The self-antigen present on thymic epithelial cells represents the ectopic

expression of tissue specific genes, thus explaining the paradox of how T cells can be negatively selected against tissue restricted antigens, these include insulin, glucagon, glutamine acid decarboxylase (GAD) 65 and 67, thyroglobulin, thyroid peroxidase and myelin basic protein (79,80,81). The expression of some of these antigens has recently been shown to be under the control of Aire as described in section 1.2.6 (13).

1.3.2 T cell activation and development of effector phenotype

The mature, naïve CD4+ T cell then leaves the thymus and circulates in the peripheral blood passing through lymphoid tissue. Activation of naïve CD4+ T cells takes place in the lymphoid tissue upon encounter of the appropriate specific antigen for that T cell on an APC expressing co-stimulatory molecules. Activation of a naïve T cell through the TCR alone, in the absence of co-stimulation will lead to anergy, a state of inactivation that renders the cell unable to proliferate and differentiate into an effector cell. In contrast, ligation of the TCR in the presence of co-stimulation, usually provided by CD80 or CD86 on the APC signalling through CD28 on the T cell, leads to activation and clonal expansion of the T cell. This requirement for co-stimulation is important in tolerance to self antigens, as self antigens will generally not be presented by an activated APC, therefore, this process ensures tolerance to tissue specific antigens that are not expressed within the thymus.

Following TCR engagement in the presence of a co-stimulatory signal, the naïve T cell re-enters cell cycle and divides rapidly. The co-stimulatory signal, delivered via CD28, promotes the synthesis of IL2, which drives these processes. Signalling through the TCR leads to the generation of the transcription factor NFAT (nuclear

factor of activated T cells) that binds to the IL2 promoter to activated transcription. As cytokine mRNAs are inherently unstable, the stabilisation provided by the co-stimulatory signal is important in increasing the synthesis of IL2. Co-stimulation through CD28 ligation also induces NF-κB and AP-1, transcription factors that increase IL2 transcription. In addition to an increase in IL2 production, synthesis of the α chain of the IL2 receptor (CD25) is up-regulated, the association of the α chain with the β and γ chains increases the affinity of the receptor for IL2 and drives the cell through the rest of the cell cycle. As well as up-regulation of CD25, the early activation marker, CD69, is up-regulated in the activated T cell.

These proliferating T cells are then able to differentiate and adopt a specific effector phenotype of T helper (Th) 1, Th2 or T regulatory (Treg) cell. This differentiation is dependent on the cytokine milieu and co-stimulation by other molecules e.g. ICAM-1/LFA-1, ICOS/B7, which is itself determined by the APC in response to the conditions in which it first encounters the antigen it is expressing.

The effector phenotype of the T cell was first characterised by the cytokines produced (82). Th1 cells primarily secrete IL2, IFNγ and TNFα and their major role is to activate macrophages to allow killing of intracellular pathogens. The differentiation into a Th1 cell is directed by the presence of IFNγ, which induces expression of the transcription factor, T-bet (83) mediated by STAT1 (84).

The major role of Th2 cells is activation of B cells, leading to antibody production to facilitate the clearance of extra-cellular pathogens. Their differentiation is induced by the presence of IL4 (85) acting through STAT6 (86), leading to the up-regulation of

the transcription factor GATA3 which regulates expression of many of the Th2 cytokines (87) including IL4 and IL5.

Differentiation of effector function occurring in the presence of IL10 and/or TGFβ leads to the development of T regs. A subset of Tregs can be characterised by their surface expression of CD25 and in murine systems the transcription factor, Foxp3, is required for the differentiation and function of Tregs.

1.3.3 The role of developmental gene pathways in mature T cells

As described above the presence of specific cytokines and transcription factors can drive the differentiation of CD4+ T cells into different effector functions. However there is increasing evidence that signalling through developmental pathways may also contribute to this process. One of these pathways, the Notch signalling pathway (described in detail in section 6.1.1), is recognised to have a role in the lineage decisions of developing T cells, and more recently interest has turned to the role of this pathway in mature T cells.

In 2000, Hoyne et al demonstrated that presentation of antigen by DCs in the presence of the Notch ligand, Serrate, induces the development of a regulatory population of T cells, which are able to transfer tolerance (88). More recently, it has been shown that up-regulation of the Notch pathway, by overexpression of one of the ligands (Jagged), induces the development of functional antigen specific regulatory T cells (89). The same is true of overexpression of one of the Notch receptors (Notch3), when regulatory T cells are generated which are able to protect against the development of experimental autoimmune diabetes (90). Signalling mediated by a

specific ligand-receptor combination (Delta-like1 and Notch3) has been shown to generate a Th1 phenotype (91). Thus, there is evidence to suggest that Notch signalling may play a role in determining the effector phenotype of T cells.

1.4 Summary

Aire plays a role in central tolerance to self antigens, but the role of Aire in the peripheral immune system remains to be elucidated. However, following recent evidence regarding the importance of transcription factors in the development of T cell effector function, it is tempting to speculate that Aire, which is also a transcription factor, may have a role in T cell effector function.

Thus, the hypothesis of this work was that lack of functional Aire affects peripheral T cell function. In order to test this the following aims were addressed.

1. Characterisation of the phenotype and genotype of patients with APS1 in the UK
2. Investigation of whether there are differences in peripheral lymphocyte subsets and in the T cell proliferative response in APS1 patients compared to controls.
3. Characterisation of the tissue and cellular distribution of Aire mRNA and protein in the adult and embryo.
4. Characterisation of the expression of Aire in immune cell subsets and the effect of activating these cells on Aire expression.
5. Investigation of an interaction between Aire and the Notch signalling pathway, as this pathway is involved in the development of effector function.

CHAPTER 2

2 Methods

All reagents were obtained from Sigma (Poole, Dorset, England) unless otherwise stated.

2.1 Patient Recruitment

The initial cohort of patients was recruited by Dr S Pearce, by writing to all endocrinologists in the UK to ask if they were aware of any patients with APS1. Following this patients were referred to Dr Pearce and myself for mutational analysis to enable a diagnosis of APS1 to be made.

2.2 DNA extraction

DNA was extracted from 10mls of whole blood collected into an EDTA tube. The DNA was extracted using the Nucleon BACC2 kit (Amersham Biosciences, UK). Briefly, cells were lysed as per the manufacturers instructions and deproteinised with sodium perchlorate. Chloroform and Nucleon resin was used to extract the DNA, which was precipitated from the aqueous layer with absolute ethanol. The resulting DNA was resuspended in TE buffer and the DNA concentration quantified using a photospectometer.

2.3 *AIRE* mutational analysis

All patients were screened for the common UK mutation, 964del13, and the major Finnish mutation, R257*, by PCR and restriction digest. Novel mutations were

sought by single strand conformational polymorphism (SSCP) analysis of all 14 exons.

2.3.1 PCR of *AIRE*

Genomic DNA was used as a template for PCR utilising primers (Table 2.1) that encompassed each of the 14 exons of *AIRE*. PCR was performed with 200ng DNA, 50 pmol of each primer, 200μM dNTP's, 1mM $MgCl_2$, 50mM KCl, 10mM Tris-HCl (pH 8.3) and 1 U *Taq* DNA polymerase (Gibco BRL) in a final volume of 50μl. An initial denaturation step at 94°C for 5 minutes was followed by 35 cycles of amplification, each cycle consisted of 30 s at 93°C, 30 s at a primer pair dependent annealing temperature (see Table 2.1) and 30 s at 72°C. After these 35 cycles, a final extension step of 72°C for 5 min was performed. PCR products were run out on a 1.5% agarose gel, and visualised with ethidium bromide.

2.3.2 Screening for the common UK mutation 964del13

PCR of exon 8 was performed as described above yielding a product of 229bp (Figure 2.1). The resulting PCR product was digested with the restriction enzyme, *Bsr*BI, the restriction site for which is abolished in the presence of the 964del13 mutation (Figure 2.2). Thus, digest of the wild type sequence gives 2 products, 140 and 89 bp, whilst if the mutant sequence is present 1 product of 216 bp is seen (Figure 2.2).

Exon	Primer sequences	Size of product (bp)	Annealing Temperature (°C)
1	F: AAGCGAGGGGCTGCCAGTTC R: GGGACTATCCCTGGCTCACAG	258	65
2	F: TCCACCACAAGCCGAGGAGAT R: AGCTGGGCTGAGCAGGTGACA	389	62
3	F: CTGAGGTTGGGACCCTGCTCC R: CTGGAGACCCTGGCTGGCTTC	231	63
4	F: GGCACTCACCCCCACTGAGAG R: GCCCTGCTCTGACCCCTGAC	202	63
5	F: GCCCAGTGCTGCCTGCTTCTG R: CCATCTTGGAGCCTGGGTCTC	256	63
6	F: TGCAGGCTGTGGGAACTCCAC R: GGGGCATCAAGAGCCAGGCTC	303	59
7	F: CATGTCCACCCTCGCTGCTGA R: AGAAAAAGAGCTGTACCCTGTGG	278	63
8	F: CACCCCAGCCCAGTCTGCATG R: CTTCAGGGTCAGTGGGTGGAG	229	63
9	F: CTGTCACCCGCTCTGTTGTTC R: GTGGCCATGTGGACAGGAGG	205	63
10	F: CCCAGCAGTCACTGACTCCTG R: CGTAGGTCCTGGGCTCCTTGA	311	62
11	F: CTCGGGTTCGGGTTCAGCTAC R: TGTGGGTGTGGGTTCAGGCCT	233	63
12	F: CATACCCCGGAGGTGGCACTC R: CAGCACCGGCATGCATGGAGG	205	64
13	F: CTGTGGGAGTTGGGCTGACCT R: AGTGGAGGAGCACCAGGAGG	141	60
14	F: ATGGCCATGATTGTGTGGCTG R: CTCAGCACTCTCTCATCAGAG	188	59

Table 2.1 Primer sequences and annealing temperatures for amplification of AIRE.

F = forward
R = reverse

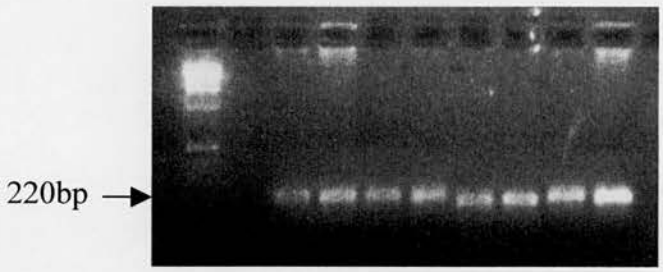

Figure 2.1 PCR of genomic DNA for exon 8 of AIRE yields a product of 229bp

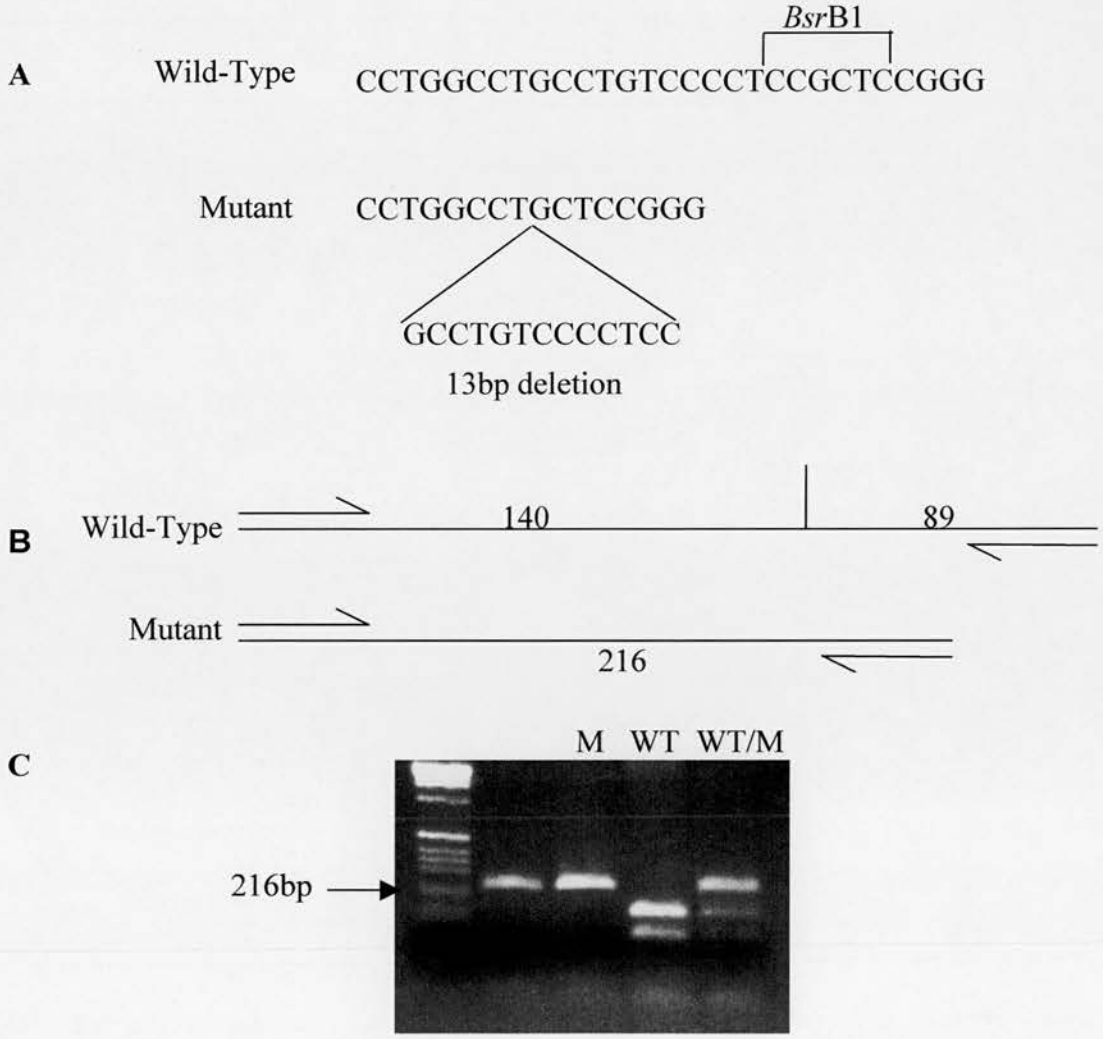

Figure 2.2 **A** The 13bp deletion in exon 8 abolishes the BsrB1 restriction site. **B** Map of restriction products from digest of wild-type and mutant products. **C** Results of restriction digest of PCR product from wild-type, mutant and a compound heteroygote.

2.3.3 Screening for the common Finnish mutation R257*

PCR of exon 6 was performed as described to give a product of 303bp (Figure 2.3). The resulting PCR product was digested with the restriction enzyme, *Taq1*, one of the restriction sites for which is abolished in the presence of the R257* mutation (Figure 2.4). Thus, digest of the wild type sequence gives 3 products, 171, 62 and 72 bp, whilst if the mutant sequence is present 2 products of 171 and 134 bp are seen (Figure 2.4).

2.3.4 SSCP to identify novel mutations in AIRE

Following analysis for the two common mutations as described above, there remained unidentified alleles. DNA from these patients was subject to PCR for exons 1,2,3,6,7,8,9,10,11 and 14, as described in section 2.3.1. The PCR products were analysed for SSCPs using precast 12.5% polyacrylamide gels that were run on the Phast minigel electrophoresis system (Pharmacia LKB), for 150-185 V-h at 10°C. The gels were then fixed in an aqueous solution of 10% ethanol and 0.5% acetic acid and stained with a 0.1% aqueous silver nitrate solution for 30 minutes. After two washes in dH_2O, the colour was set using an aqueous solution of 1.5% sodium hydroxide and 0.15% formaldehyde for 20 minutes and fixed in 1mM EDTA. Samples from patients known not to have mutations in the exon concerned were included on all gels as a control.

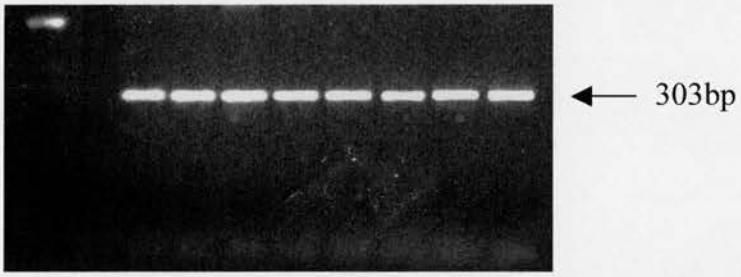

Figure 2.3 PCR of genomic DNA for exon 6 of AIRE yields a product of 303bp

A

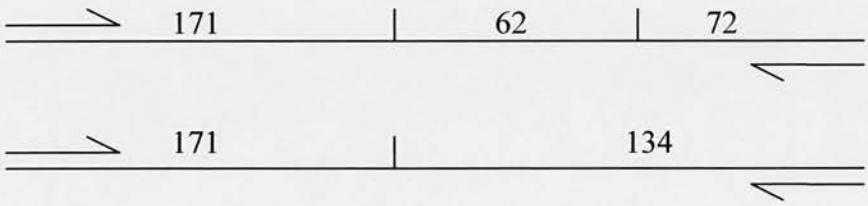

B

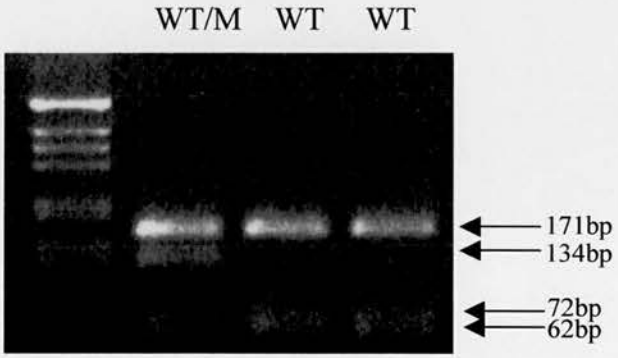

Figure 2.4 Genotyping for the common Finnish mutation R257* A Map of restriction products from digest of wild-type and mutant products. **B** Results of restriction digest of PCR product from a wild-type and a compound heteroygote.

2.4 Determination of MHC haplotype

The presence/absence of a non-Aspartate 57 allele (HLA DQB*0201,0302,0501 and 0604) or the "protective" HLA DQB*0602 was determined by low resolution HLA typing using primers supplied by the Blood Transfusion Service (Newcastle upon Tyne). Further high resolution typing was carried out by the Blood Transfusion Service (Newcastle upon Tyne). HLA typing on an additional 7 patients was performed using an HLA-DQB high resolution kit from Protrans (Quest Biomedical, Solihull, UK) as per the manufacturers instructions.

2.5 Determination of *IDDM2* alleles

The *IDDM2* locus is the variable number of tandem repeats in the 5' polymorphic region of the insulin gene. This was examined utilising the *Hph*I polymorphism, which is effectively in complete linkage disequilibrium (0.002 recombination rate) with the INS VNTR alleles (92,93). Genomic DNA was amplified by PCR using oligonucleotide primers to produce a 440bp fragment (Fig 2.5). The primer sequences were 5' - TCC AGG ACA GGC TGC ATC AG - 3' and 5' - AGC AAT GGG CGG TTG GCT CA - 3'. PCR was performed with 250 ng of DNA, 200µM of dNTP's, 0.75 mM of $MgCl_2$, 1x PCR buffer and 1U of *Taq* DNA polymerase (Life Technologies Inc., Paisley, UK) in a final volume of 50µl. After an initial denaturation at 94°C for 5 minutes, 28 cycles of PCR amplification were performed, with each cycle consisting of 1 minute at 94°C, 1 minute at 58°C and 1 minute at 72°C. The PCR product was digested overnight at 37°C with the restriction enzyme *Hph*I. This yields fragments of 240bp and 160 bp in patients homozygous for the A

allele; 280bp and 160bp in patients homozygous for the B allele and 160bp, 240bp and 280bp in heterozygotes. These fragments were resolved by electrophoresis on a 2% agarose gel (Fig 2.5). The A allele at the *Hph1* polymorphism is carried on the same haplotype as the Class I VNTR alleles, and the B allele is on the class III VNTR haplotype. Because of the near complete disequilibrium between alleles of the *Hph1* SNP and the VNTR genotypes, the A and B alleles have been considered as containing the same information as *INS* VNTR genotypes for the purposes of this study.

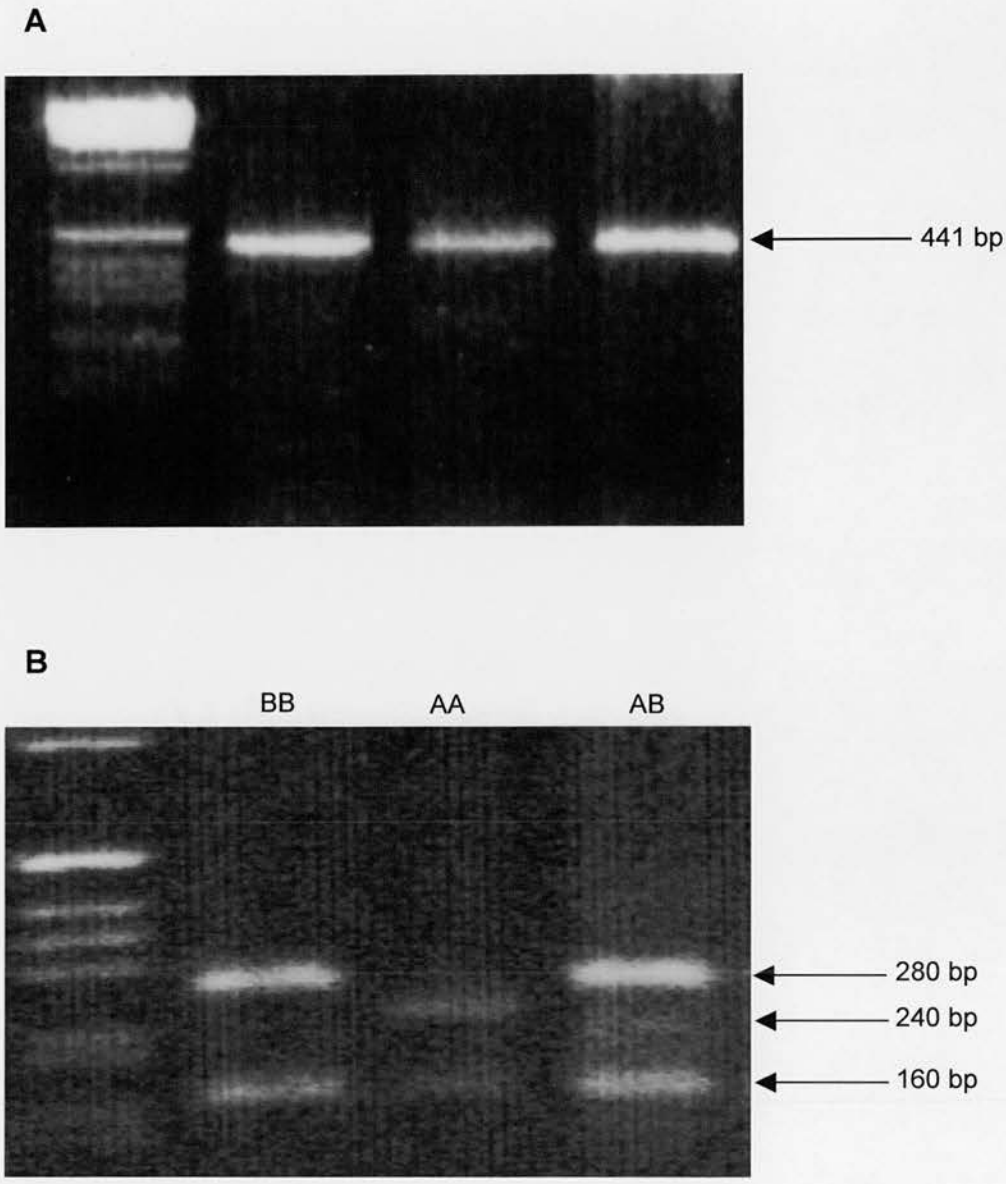

Figure 2.5 Determination of INS VNTR allele A PCR of exon 6 **B** Restriction digest with *Hph1* gives products of 160, 240 and/or 280bp

2.6 Isolation of human peripheral blood cells

Blood was collected for isolation of peripheral cells into a heparinised tube from APS1 patients, controls and normal volunteers.

2.6.1 PBMCs

Blood was collected from APS1 patients and controls. After dilution in an equal volume of PBS, the blood was layered onto Histopaque, and centrifuged at 1000g for 20 minutes. The cloudy interface containing the PBMCs was removed and the cells washed in PBS prior to counting on a haemocytometer.

2.6.2 Adherent cells

Blood was collected from healthy volunteers, diluted in an equal volume of PBS and layered onto Histopaque and centrifuged as described above. Following removal of the PBMCs these were resuspended in serum-free media (Complete RPMI minus serum) at 10^7cells/ml and incubated in a 75cm^2 flask for 60 minutes in a humidified incubator, 37°C 5% CO_2. After this culture period, the cells were washed with PBS to remove any non-adherent cells, and the adherent cells were removed using a cell scraper.

2.7 Staining of human cells for flow cytometry

Human PBMCs were isolated as in section 2.6.1, all staining was performed in a 96 well round bottom plate. $5x10^5$ cells were added to each well in a final volume of 200µl of FACS buffer, the antibodies and isotype controls used can be found in table 2.2. The combination of antibodies used together is shown in table 2.3. After staining

for 30 minutes, the cells were washed twice using FACS buffer and resuspended in 100µl of FACS buffer and 100µl of FACS fix prior to analysis on a FACSCalibur flow cytometer (Becton Dickinson) using CellQuest Software (Becton Dickinson). The appropriate isotype controls and single stains were used to optimise the settings prior to each run.

Antibody to	Fluorochrome	Manufacturer
CD3/4/8	PECy5/PE/FITC	Dako
TCR-αβ	FITC	BD Pharmingen
TCR-γδ	FITC	BD Pharmingen
CD19	FITC	Dako
CD8	FITC	BD Pharmingen
CD45RO	FITC	Dako
Vα24	FITC	Dako
CD94	PE	BD Pharmingen
CD45RA	PE	Dako
CTLA-4	PE	BD Pharmingen
CD69	PE	Dako
CD8	PECy5	Dako
HLA-DR	CyChr	BD Pharmingen
CD25	PE-Cy5	Dako
CD4	APC	BD Pharmingen
IgM	FITC	BD Pharmingen
IgG2a	FITC	BD Pharmingen
IgGa	PE	Dako
IgG2a	PE	Dako
IgG1κ	CyChr	BD Pharmingen
IgG1κ	APC	BD Pharmingen

Table 2.2 Anti-human antibodies and isotype control antibodies used for flow cytometry

FITC	PE	CyChr/PE-Cy5	APC
Isotype control	Isotype control	Isotype control	Isotype control
CD8	CD4	CD3	
TCR-αβ	CD94	CD8	CD4
TCR-γδ	CD94	CD8	CD4
CD19	CD45RA	HLA-DR	
CD8	CD69	CD25	CD4
CD45RO	CD45RA	CD25	CD4
CD8	CTLA4	CD25	CD4
Vα24	CD94	CD8	CD4

Table 2.3 Antibodies used for phenotyping peripheral cell subsets in APS1 patients. The table shows the combinations of fluorochrome antibodies used, details of the method used are in section 2.7

2.8 Human PBMC proliferation assay

Human PBMCs were isolated as in section 2.6.1 and added to 96 round bottom well plates, previously coated with anti CD3ε antibody (0.1μg/ml or 1μg/ml) alone or with plated bound anti-CD3ε plus anti-CD28 antibody (1μg/ml), at $2.5x10^5$ cells/well. Cells were cultured in CM. Cells were incubated in a humidified incubator, 37°C 5% CO_2. At 48 hours the plates were pulsed with 0.5μCi of tritiated thymidine and harvested 16 hours later. Plates were read using a liquid scintillation counter Betaplate 1205 (Wallac, Milton Keynes, UK).

2.9 Cytokine analysis of supernatants from stimulated human PBMCs

The concentrations of IL2, IL4, IL5, IL10, IFN-γ and TNF-α were determined using a Human Th1/Th2 CBA (cytokine bead array) kit as per the manufacturers instructions. Briefly, samples and standards were incubated with detection beads for 3 hours then washed in wash buffer followed by centrifugation at 300g for 5 minutes. The beads were then resuspended in wash buffer prior to analysis on a FACSCalibur (Becton Dickinson) with CellQuest software.

2.10 Animals used

CD1, BALB/c and C57BL/6J mice (B&K, Hull, England) were housed in the University of Edinburgh Animal Facilities in accordance with local guidelines. Embryonic tissue was taken at embryonic (E) days 14.5, 16.5 and 18.5 from time-mated pregnancies, where embryonic day 0 (E0) was determined by detection of the vaginal plug.

2.11 Tissue collection

Mice were sacrificed in accordance with Home Office guidelines. Tissue for in-situ hybridisation was collected into an RNase free tube on dry ice and stored at -70^{0}C until required. Tissue for RNA extraction was collected into Trizol in an RNase free tube on ice and stored at -70^{o}C until required. Tissue for immunohistochemistry was fixed in 4% buffered formalin and processed into paraffin blocks. Tissue for protein extraction was stored at -20^{o}C until required.

2.12 Determination of RNA expression

2.12.1 RNA extraction

RNA was obtained from whole tissues and cells by extraction using Trizol (Life Sciences, Paisley, UK), as per the manufacturers instructions. Tissue samples were homogenised first using an electric homogeniser. Briefly, chloroform was added and the samples centrifuged at 13000g for 15 minutes. The aqueous RNA containing layer was removed and the RNA precipitated using isopropyl alcohol. The pellet was

obtained by centrifugation at 13000g for 10 minutes, and then washed in 70% ethanol. After drying the pellet was resuspended in nuclease free water and quantified using a spectrophotometer. All samples were DNase treated using RQ1 RNase free DNase (Promega, Southampton, UK) in accordance with the manufacturers instructions. To ensure that there was no residual DNA contamination, the RNA was used in a PCR with primers for the housekeeping gene, β-actin. The lack of a PCR product was consistent with no DNA contamination. In one reaction, DNA was used rather than RNA to check the PCR reaction had worked. The reaction mix used was 1x buffer, 100μM dNTPs, 20pmol primers, 2.5mM $MgCl_2$, 0.5U Taq and 50ng RNA. The reaction conditions were 94°C for 2 minutes followed by 30 cycles of 94°C for 30 seconds, 58°C for 1 minute, 72°C for 2 minutes with a final denaturation step of 94°C for 2 minutes. Primer sequences are F 5`-CCA CCA ACT GGG ACG ACA TG, R 5`-GTC TCA AAC ATG ATC TGG GTC ATC which yield a 153bp product.

2.12.2 RT-PCR

RNA (2μg) was reverse transcribed in a reaction containing 1x buffer, 5mM $MgCl_2$, 1mM dNTPs, Oligo dT primers (1:20), RNase inhibitor (1:40) and RT (1:20). Reaction conditions were 42°C for 30 minutes then 99°C for 5 minutes, the resulting cDNA was stored at –20°C prior to use in the PCR reaction.

5μl of cDNA was used as the template for PCR with primers to amplify a 418bp fragment of murine Aire. The reaction contained 1x buffer, 1mM MgCl2, 1mM dNTP's, 5pmol/μl primers, 0.05%W-1 and 1U Taq (Gibco), reaction conditions were 96°C for 3 minutes followed by 30 cycles of 96°C for 45 seconds, 56°C for 30

seconds and 70°C for 90 seconds. (Primers; F –AAG AAG CCA GAT GGC AAC TT; R –CGA GGA TGA GTG TGC CGT GT) (nucleotide numbers 550-569 and 948-967; accession number NM_009646.1)

2.12.3 *in-situ* hybridisation

Generation of cRNA probe

Aire was amplified from mouse thymus by RT-PCR as described above and 3µl of this PCR product was cloned into PGEMTeasy vector (Promega) by an overnight incubation at 4°C with T4 DNA ligase (Promega). 2µl of this ligation reaction was used to transform competent cells (JM109) by heat shock at 42°C for 45 seconds. These cells were plated out overnight on ampicillin containing LB plates and colonies were picked the following day. An individual colony was used in a 5 ml starter culture of LB that was incubated overnight at 37°C. The plasmid was obtained from 1.5ml of this starter culture using Promega Wizard SV miniprep kit as per the manufacturers instructions. The presence of the insert was confirmed by restriction digest with *EcoR1* (Promega). Following this 2ml of the starter culture was used in a 100ml culture from which the plasmid was obtained by midiprep using the Promega Wizard Plus Midiprep DNA purification system as per the manufacturers instructions. The insert was confirmed by sequencing and the orientation by restriction digest with *Nco1* (Promega). The plasmid was cut with *SalI* to generate the template for the anti-sense probe and with *AatII* to generate the template for the sense probe. After restriction digest the plasmid was extracted with phenol/chloroform. Sense (control) and anti-sense 35S labelled RNA probes were

generated from this plasmid using SP6 and T7 RNA polymerase respectively. Briefly, a reaction containing 1x buffer, 1U of RNA polymerase (SP6 or T7), 10mM DTT, RNase inhibitor, 1.5mM ATP, 1.5mM CTP, 1.5mM GTP, 20μM UTP, 5μM 35S UTP and 1μg of template. This reaction was incubated for 90 minutes at 37°C (T7) or 40°C (SP6) followed by DNase treatment with *DnaseI* (Promega). The probe was purified by passing through a Nick column (Amersham), counted in a β counter and stored at –70°C until required.

in-situ hybridisation (ISH)

Tissue was obtained from 6-8 week old CD1 mice, and C57BL/6J embryos. Frozen sections (10 microns) were cut and mounted onto poly-l-lysine coated slides. Sections were fixed in 4% paraformaldehyde, washed in PBS and acetylated (0.25% acetic anhydride in 0.1M triethanolamine, pH8.0). After prehybridisation in a SSC humidified chamber, the sections were hybridised at 50°C overnight with 35S labelled probe (1x 10^7 cps/slide) in a SSC humidified chamber. Slides were washed then RNase treated for 1 hr at 37°C, followed by further washes and dehydration in alcohol. Slides were dipped in Kodak NTB2 emulsion (Kodak, Hemel Hempstead, UK) and developed 2 weeks later. Tissue was counterstained with haematoxylin and eosin, then coverslipped.

2.12.4 Real Time RT-PCR

A Taqman based system and ABI Prism 7700 sequence detector was used for real time RT-PCR. This system utilises the 5`exonuclease activity of Taq polymerase and

FRET (Fluorescent Resonance Energy Transfer). A fluorescently labelled probe which has a high energy reporter and a low energy quencher is used in addition to primers. When the probe is intact, energy transfer ensures that the probe does not fluoresce (FRET). The probe used anneals to the cDNA between the two primers, and as the primer is extended by the Taq polymerase its exonuclease activity cleaves the probe. As the quencher and the reporter are no longer in close proximity, the amount of fluorescence increases.

All reagents were obtained from Applied Biosystems (Warrington, UK). Reverse transcription was performed using the Multiscribe RT™ kit and random hexamer primers, as per the manufacturers instructions. Briefly 400ng of RNA was reverse transcribed in a reaction containing 1x TaqManRT buffer, 5.5 mM $MgCl_2$, 500μM dNTP's, 2.5μM Random Hexamers, 0.4U/μl RNase inhibitor, 1.25U/μl MultiScribe RT, at 25°C for 10 minutes, 48°C for 45 minutes and 95°C for 5 minutes.

Primers were designed using Primer Express for murine Aire (F – 5`CCT GGA TTT CTG GAG GAT TCT CT3`(nucleotides 282-304); R - 5`CCG TCC AGG ATG CTA TGC A3`(nucleotides 339-356); Probe – 5`6FamCGG CTG TAC CGC TCC AGA TTG TAG TCC T Tamra3`(nucleotides 308-335)) (Sequence accession number NM_009646.1), and murine Hes1 (F – 5`GGC TTT TCG GTG ACC CAT CT3`; R – 5`CGC GGT ATT TCC CCA ACA3`; Probe – 5`6FamTTC TCC TTC TGG CCT GCA GCC G Tamra3`) and PCR was performed using Taqman Universal PCR Master Mix™ with 300nM primers and 200nM probe plus 1x 18S primer/probe as an internal calibrator for each sample. All samples were run in triplicate. Data were

analysed using the comparative C^T method (Applied Biosystems). cDNA from whole thymus from an adult CD1 mouse was used as a positive control for all runs involving expression within tissue; in experiments involving the in-vitro culture of T cells, the media control sample was used as the calibrator; all mRNA levels were determined in relation to the calibrator sample.

The comparative C^T method uses the cycle number at which the fluorescence increases above baseline, the cycle threshold (C^T). This value is obtained for both the gene of interest and the internal control (18S) and one is subtracted from the other to give the change in cycle threshold (ΔC^T) to compensate for small differences in loading. This value is then normalised against the designated calibrator in the experiment ($\Delta\Delta C^T$). The following calculation is then carried out $2^{-\Delta\Delta CT}$, this gives a value of 1 to the calibrator sample and all other samples as a fold change in gene expression compared to this.

2.13 Determination of Protein Expression

2.13.1 Antibodies used

A rabbit polyclonal anti-human AIRE antibody (designated 2328.1) was raised by Dr S Pearce (University of Newcastle upon Tyne), by giving 6 injections of a peptide consisting of AIRE amino acids 147-165 conjugated to BSA. The immunoglobulin (Ig) was then Protein A purified from serum as per the manufacturers instructions (HiTrap Protein A affinity column, Amersham Pharmacia Biotech, Bucks, England). For some experiments, the Aire antibody was FITC conjugated using a FluoroTag kit (Sigma); the molar fluorescence/protein ratio of the conjugated antibody was 3.2.

The anti-PSP1 antibody was a kind gift from Prof A Lamond, University of Dundee.

2.13.2 Characterisation of anti-AIRE antibody

Western blotting of murine thymic protein with the rabbit polyclonal anti-human AIRE antiserum (Section 2.13.5) revealed a band of the expected molecular weight of Aire (58kDa) (Fig 4.6). The amino acid sequence of the peptide used for immunisation is homologous between mouse and human at 11 out of 19 amino acids. Specificity in mouse was further confirmed by immunohistochemistry (Section 2.13.7), in control sections by preabsorption with peptide in excess, and incubation of additional control sections with Protein A purified Ig from preimmune serum (Fig 2.6). Staining was within the nucleus in a punctate pattern, consistent with the subcellular expression previously reported (51).

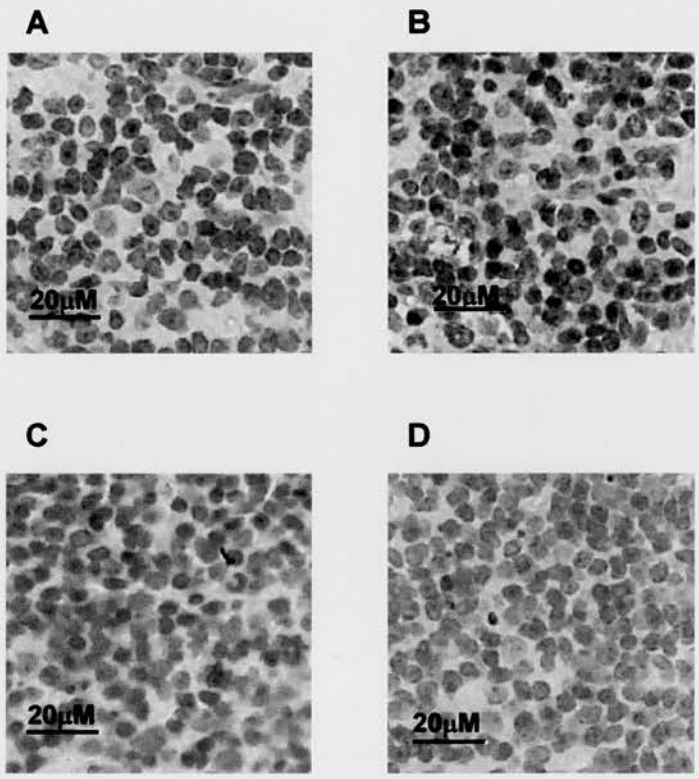

Fig 2.6 Immunohistochemistry of murine thymus.
A Negative control; **B** Incubated with Aire antiserum; **C** Incubated with preimmune serum; **D** Incubated with Aire antiserum preabsorbed with peptide.

2.13.3 Protein extraction

Cells were resuspended in protein lysis buffer (approx 10^6 cells in 200µl), followed by sonication on ice for 30 seconds in 5 second bursts, followed by protein quantification. For extraction of protein from tissue, a small amount of tissue was homogenised in protein lysis buffer. Following centrifugation at 13000g for 5 minutes the supernatant was removed and the amount of protein contained quantified as described below.

As Aire is a nuclear protein expressed at low levels, to increase the yield of Aire protein, protein was extracted from nuclei only. Cells were resuspended in nuclear lysis buffer at 1-2x10^8/ml, passed through a 25G needle and centrifuged at 1800g for 15 minutes at 4^0C. The resulting pellet was resuspended in the same amount of nuclear lysis buffer and sonicated for 30 seconds on ice in 5 second bursts, quantified then stored at -20^0C until required.

2.13.4 Protein Quantification

Protein content was estimated using a BCA kit (Biorad) as per the manufacturers instructions. Briefly, 50µl of sample or standard was added to 2 ml of Biorad protein assay reagent inverted to mix and incubated at room temperature for 15 minutes. The absorbance at 595nm was read in a spectrophotometer. The absorbance was plotted against the concentration of the BSA standards using Excel to generate a standard curve from which the values for the samples were derived.

2.13.5 Western blotting

Proteins were resolved on a 10% SDS/acrylamide separating gel, overlaid with a 4% stacking gel. For blots with protein extracted from tissue, 30μg of protein was loaded per well, for blots with immunoprecipitated proteins 5μl of the immunoprecipitated protein was loaded per well. Gels were run at 100 volts for 2 hours and then transferred onto a nitrocellulose membrane at 150 volts for 30 minutes. After blocking with 5% SMA for hungry babies in TBST for 2 hours the membrane was incubated with primary antibody overnight at room temperature (anti-Aire antiserum 1:50 for tissue, 1:150 for immunoprecipitated protein; anti-PSP1 antibody 1:2000; both in 5% SMA for hungry babies in TBST). The membrane was then washed 3x15 minutes in TBST followed by incubation with goat anti-rabbit HRP antibody (Dako) at 1:2000 in TBST for 2 hours at room temperature. An ECL plus kit (Amersham Biosciences) was used as the chemiluminescent substrate, this was detected using ECLplus radiographic film (Amersham) and developed using an Xograph Compact X4.

2.13.6 Immunoprecipitation

1μg of protein was precipitated using 2 μg of antibody in a final volume of 1ml with PBS plus protease inhibitor cocktail and 1mM sodium orthovanadate (lysis buffer). This was incubated at 4°C for 1 hour, following which 30μl of Protein A-sepharose was added for a further 1 hour at 4°C. This was washed with 1 ml of ice cold lysis buffer 3 times; each wash was followed by centrifugation at 13000g for 5 minutes at 4°C. After a final centrifugation the beads were resuspended in 25μl of 2x sample buffer and 25 μl of 10% SDS, and stored at –70°C until required. Prior to use

samples were boiled for 5 minutes to dissociate the protein from the antibody, this was followed by centrifugation at 13000g for 5 minutes to spin down the beads, the supernatant was then loaded onto an SDS/polyacrylamide gel as described in section 2.13.5.

2.13.7 Immunohistochemistry (IHC)

All IHC was performed on a Biogenex Optimax plus automated staining system (Biogenex, Berkshire, UK). Tissue was taken from C57/BL6J and CD1 mice into 4% buffered formalin then processed into paraffin blocks. Three μm sections were cut and mounted on Vectabond treated slides (Vector Laboratories, Peterborough, England). Slides were dewaxed in xylene, and rehydrated. Antigen retrieval consisted of microwaving the sections at 1000W for 3x5 minutes in Vector antigen retrieval solution (Vector Laboratories) that was diluted 1:100 in deionised water. Slides were blocked with 2% hydrogen peroxide for 15 minutes, washed then blocked with 20% goat serum. The AIRE antibody was preabsorbed with 20% mouse serum and 20% goat serum overnight at 4°C. Slides were incubated with primary antibody or preimmune serum (0.675ng Ig/slide) or primary antibody that had been pre-incubated with the peptide used to raise the antibody (peptide was used at 10x excess), for 2 hours at room temperature, washed, incubated with a goat biotinylated anti-rabbit secondary antibody (1:400) (DAKO, Ely, Cambridgeshire, UK), washed then Vector RTU ABC (Vector Laboratories) was applied and positive signal was detected by the addition of diaminobenzidine (DAB) (DAKO). The slides were counterstained with haematoxylin and coverslipped. Avidin/biotin blocking (Avidin/Biotin blocking kit, Vector Laboratories) was used on all tissues.

2.13.8 Immunofluorescence

For all immunofluorescence, cells were resuspended at 10^8 cells/ml in PBS, 5µl was added to each slide (Superfrost plus, BDH, Poole Dorset UK) and smeared into a thin film, air dried, fixed in 90% dry acetone/ 10% methanol for 10 minutes, washed in PBS then blocked with Dako diluent (Dako) for 10 minutes.

For single stains, the slides were incubated with primary antibody, washed and incubated with secondary antibodies (See table 2.4 for antibodies used). All incubations were at room temperature for 30 minutes. Slides were then incubated with ToPro3 (Molecular Probes) diluted 1:200 in PBS for 10 minutes to allow visualisation of the nucleus. Slides were coverslipped using Mowiol mounting medium. Images were captured using a Leica TCS NT confocal system (Leica Microsystems, GmBH Mannheim, Germany). Control slides which had no primary antibody added to them were included in each experiment.

Primary antibody	Secondary antibody	Tertiary antibody
Anti-Aire (1:50)	Goat anti-Rabbit ~ (1:100)	Donkey anti-Goat 568* (1:200)
Anti-Hes1 (1:30) #	Donkey anti-Goat 568* (1:200)	

Table 2.4 Antibodies used for single stains
~ Dako
*Molecular Probes, Leiden, The Netherlands
Santa Cruz Biotechnology, Santa Cruz, California

For double staining for Aire and PSP1, slides were stained with the antibodies shown in table 2.5. All incubations were for 30 minutes at room temperature except for that

with Aire-FITC that was at 4°C overnight. Slides were washed with PBS between each incubation. The nucleus was counterstained with ToPro3 prior to coverslipping as described above.

Order antibodies applied in	Antibody	Concentration	Manufacturer
1	Anti-PSP1	1:50	N/A
2	Goat anti-rabbit Alexa 568	1:200	Molecular Probes
3	Aire-FITC	1:5	N/A
4	Mouse anti-FITC	1:10	Dako
5	Goat anti-mouse Alexa 488	1:200	Molecular Probes

Table 2.5 Double staining of cells for Aire and PSP1

For double staining with Aire and other nuclear proteins, slides were first stained for Aire as described above for a single stain, this was followed by incubation with either anti-PML antibody (1:10), anti-sc35 antibody (1:1000) or anti-coilin antibody (1:100), all antibodies were a kind gift of Prof A Lamond, Dundee. After washing with PBS, the slides were incubated with goat anti-mouse Alexa 488 (Molecular Probes). For double staining with Aire and cell surface markers, slides were first stained for Aire as described above for a single stain, this was followed by incubation with FITC conjugated cell surface marker (anti-CD4, 8 or IgD^b, Pharmingen) (1:10), washed, incubated with mouse anti-FITC antibody (1:10), washed then incubated with goat anti-mouse Alexa 488 (Molecular Probes) (1:200). All incubations were

for 30 minutes at room temperature, after the final wash cells were counterstained with ToPro3 and coverslipped as described above.

2.14 Cellular isolation from murine spleen

Spleens from C57BL/6J or BALB/c mice were mechanically disrupted by being ground through a 40μM cell strainer in PBS to give a single cell suspension. The cell suspension was centrifuged at 300g for 7 minutes and the resulting pellet was resuspended in 4mls of red cell lysis buffer plus 1ml of cold PBS, incubated on ice for 3 minutes after which 10mls of cold PBS was added followed by centrifugation at 300g for 7 minutes. The cells were counted using a haemocytometer with trypan blue exclusion.

The cell type required e.g. CD4+, CD19+, was then isolated using MACS beads (Miltenyi Biotech, Germany) as per the manufacturers instructions. For positive selection kits (CD19), the splenocytes were resuspended in 90μl of MACS buffer plus 10μl of antibody micro-beads per 10^7 cells and incubated at 4^0C for 15 minutes. The cells were washed by adding an excess of MACS buffer and pelleted by centrifugation at 300g for 7 minutes. The cell pellet was resuspended in 500μl of MACS buffer per 10^8 cells and cell separation was performed on an AutoMACS machine (Miltenyi Biotech, Germany) using a Possell program. For negative selection kits, e.g. CD4+ and Pan T cell, the splenocytes were resuspended in 40μl of MACS buffer plus 10μl of Biotin-Ab cocktail and incubated at 4^0C for 10 minutes. A further 30μl of MACS buffer was added plus 20μl anti-biotin beads per 10^7 cells followed by incubation at 4^0C for 15 minutes. The cells were washed by adding an

excess of MACS buffer and pelleted by centrifugation at 300g for 7 minutes. The cell pellet was resuspended in 500µl of MACS buffer per 10^8 cells and cell separation was performed on an AutoMACS machine (Miltenyi Biotech, Germany) using a Deplete program.

Cells were then counted using a haemocytometer with trypan blue exclusion. $6x10^5$ cells were kept for FACS analysis to check the cell purity (Section 2.18), the remainder were used for culture.

2.15 Culture of CD4+ T cells

2.15.1 Activation with anti-CD3 and anti-CD28 antibodies

Murine CD4+ T cells were cultured in complete media at $2x10^6$/ml in 24 well plates (96 well plates for proliferation assays). The plates were first coated with anti-CD3ε antibody, 1ml (100µl for 96 well plates) of anti-CD3ε antibody at 0.1µg/ml was added to each well and incubated for 2 hours at 37^0C. The plates were then washed with PBS to remove any unbound antibody. Cells were plated out at the density described above plus soluble anti-CD28 antibody (1 or 5µg/ml). The cells were incubated in a humidified incubator, 37^oC 5%CO_2, for 24, 48 or 72 hours and then harvested.

2.15.2 Co-culture with Delta-like1 expressing L cells

Delta-like 1 (Dl1) expressing L cells (A kind gift from Prof M Dallman, Imperial College, London) were used in co-culture experiment with murine CD4+ T cells. The Dl1 L cells and the parental L cells were cultured in HAT media, with geneticin

selection for the Dl1 L cells. Once the cells were sub-confluent, trypsin and EDTA was used to remove them from the flask, once the cells were lifted from the flask the trypsin/EDTA was inactivated by the addition of CM, the cells were then washed in CM and counted using a haemocytometer.

Prior to co-culture the cells were mitomycin C treated, 0.5mg of mitomycin C in 10mls CM was added to the L cells, and cells were incubated at 37°C for 1 hour. Following this the cells were washed 3 times in CM prior to counting. The cells were then plated out in complete media at $2x10^5$/ml and C57BL/6J CD4+ T cells were added at $2x10^6$/ml in a final volume of 2mls in 24 well plates and 200µl in 96 well plates and incubated for 24 hours in a humidified incubator, 37°C 5%CO_2.

2.16 Proliferation assay – murine CD4+ T cells

Murine CD4+ T cells were cultured in 96 round bottom well plates as described in Section 2.15. Cells were incubated in a humidified incubator, 37°C 5%CO_2, for 24, 48 or 72 hours. Sixteen hours prior to the end of the culture period, the plates were pulsed with 0.5µCi of tritiated thymidine. At the end of the culture period the plates were harvested, then read using a liquid scintillation counter Betaplate 1205 (Wallac, Milton Keynes, UK).

2.17 CFSE staining of CD4+ T cells

All tubes were wrapped in foil to prevent fading of the CFSE. A stock solution of 1mM CFSE was made up in DMSO. CD4+ T cells were resuspended at 10^7/ml in PBS and incubated at 37°C for 10 minutes, followed by the addition of 1uM CFSE.

Cells were stained for 15 mins at 37°C, then 100ul of HI FCS was added per ml of cells to inactivate the CFSE. Cells were washed twice in complete media at 300g for 7 minutes.

Following the culture period, cells were stained with anti-CD4-PE antibody, as described in Section 2.18, and analysed the same day.

As CFSE staining was used to confirm the absence of cell division, a positive control of CD4+ T cells activated with anti-CD3ε and anti-CD28 antibodies was performed (Fig 2.7).

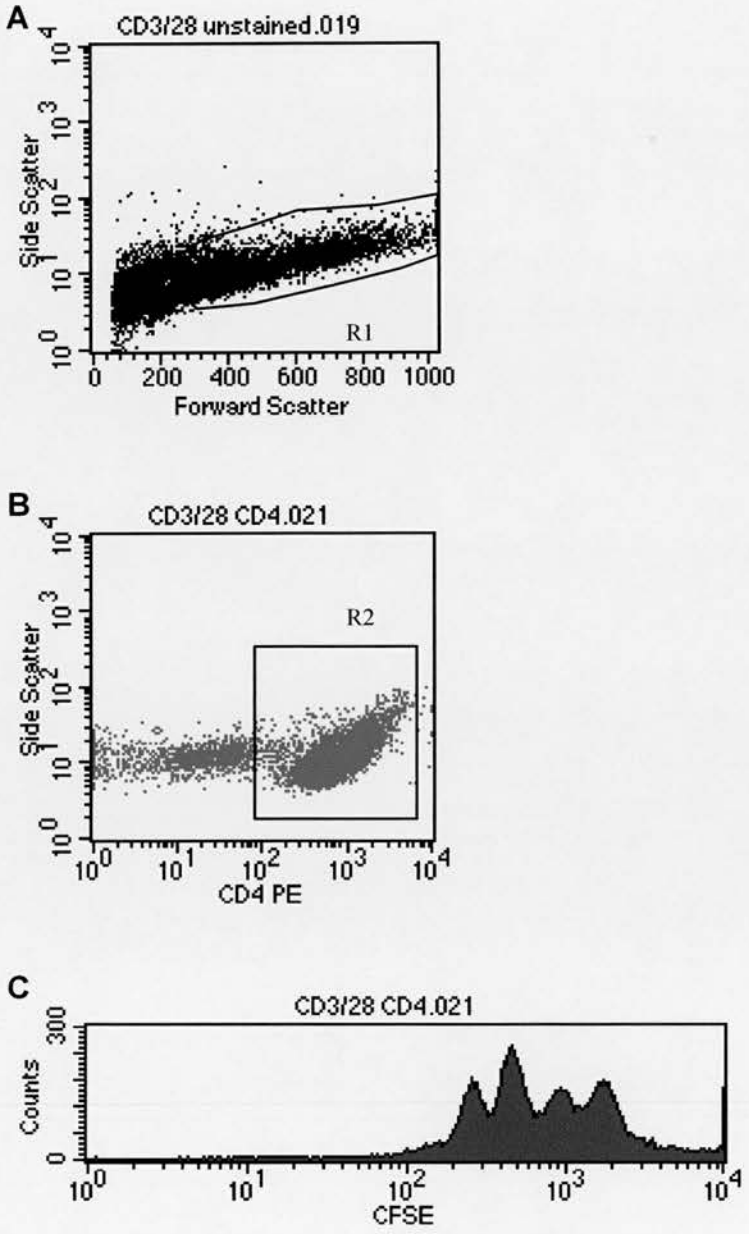

Fig 2.7 CFSE staining of antiCD3/CD28 activated T cells. A Dot plot showing the lymphocyte gate; **B** Dot plot gated on the lymphocyte gate showing the CD4+ cell gate; **C** Histogram gated on CD4+ cells demonstrating division of the proliferating cells by CFSE staining.

2.18 Analysis of murine cell surface molecule expression by flow cytometry

Flow cytometric analysis was carried out on a FACSCalibur (BD Pharmingen). $2x10^5$ cells were added to each well of a 96 well plate in a final volume of 200µl of FACS buffer plus 10% mouse serum (Scottish Antibody Production Unit) and either 0.5µg of FITC labelled or 0.2µg of PE labelled antibody (see table 2.6 for details of antibodies used). The cells were incubated in the dark at 4^0C for 30 minutes. Cells were washed twice in FACS buffer and resuspended in 100µl of FACS buffer and 100µl of FACS fix and stored at 4^0C for a maximum of 3 days.

Antibody	Fluorochrome	Isotype	Manufacturer
Anti-CD4	PE	RIgG2bκ	BD Pharmingen
Anti-CD25	FITC	rIgMκ	BD Pharmingen
Anti-CD69	PE	HsIgG	BD Pharmingen
Anti-CD3	PE	HsIgG1	eBioscience
Anti-CD19	PE		BD Pharmingen

Table 2.6 Antibodies used for cell surface marker identification in mouse

The amount of apoptosis was assessed by flow cytometry using an AnnexinV/7AAD kit (BD Pharmingen) as per the manufacturers instructions.

2.19 Materials

Complete HAT Culture Media ± Geneticin: RPMI 1640 with 10% HI FCS, 100U/ml penicillin/streptomycin (Gibco), 2mM L-glutamine (Gibco), 15μg/ml hypoxanthine (Gibco), 0.2μg/ml aminopterin (Gibco), 5μg/ml thymidine (Gibco), 6μg/ml mycophenolic acid and 250μg/ml xanthine ± 500μg/ml geneticin (Gibco). Kept at 4^0C.

Complete RPMI culture media (Human): RPMI 1640 with 10% heat inactivated (HI) foetal calf serum (FCS), 50μM β-mercaptoethanol (ME), 100U/ml penicillin/streptomycin (Gibco), 2mM L-glutamine (Gibco). Stored at 4^0C.

Complete RPMI Culture Media (Mouse): RPMI 1640 with 10% HI FCS, 100U/ml penicillin/streptomycin (Gibco), 2mM L-glutamine (Gibco). Stored at 4^0C.

DEPC H_2O: Add 5 drops of diethyl pyrocarbonate to 500mls dH_2O.

FACS buffer: 0.5% BSA, 0.1% NaN_3 in PBS.

FACS fix: 4% paraformaldehyde in PBS

γ-secretase inhibitor: The g-secretase inhibitor II (MW167) (Merck Biosciences, Darmstadt, Germany) was dissolved in 10mM DMSO to give a final concentration of 1 mM.

2x hybridisation buffer (for *in-situ* hybridisation): 1.2M NaCl, 20mM Tris (pH7.5), 2x Denhardts solution, 2mM EDTA, 2mg salmon sperm DNA, 2g dextran sulphate, 2mg yeast tRNA in DEPC H_2O. Aliquot and store at –20°C.

LB: 2.5g Yeast, 5g Tryptane, 5g NaCl make up to 500ml with dH_2O and pH with NaOH to pH7.5. Autoclave the same day.

LB agar: As for LB above plus 7.5g Agar. To pour plates melt LB agar by heating, allow to cool to hand hot and add ampicillin (50μg/ml). Pour plates and allow to set.

MACS buffer: 0.5% BSA in PBS

Mowiol mounting medium: 2.4g of Mowiol is added to 6g glycerol and stirred briefly with a pipette, then 12ml of dH_2O is added followed by stirring at room temperature overnight. The following day, 12ml of 0.2M Tris (pH 8.5) is added then heated to 50^0C for 1-2hours whilst stirring. Once the Mowiol has dissolved, clarify by centrifugation at 5000x g for 15 mins. DABCO was added to 2.5% and aliquots were stored at -20^0C.

Nuclear protein lysis buffer: 0.01M Hepes, 0.1mM EGTA, 0.5mM PMSF, 10mM KCl, 0.04mM DTT, 1mM $MgCl_2$, 1x Protease inhibitor in dH_20.

4 x pH 8.8 buffer: 1.5M Tris, 0.4% SDS in dH_2O, autoclave and store at room temperature.

4 x pH 6.8 buffer: 0.5M Tris, 0.4% SDS in dH_2O, autoclave and store at room temperature.

2x prehybridisation buffer (for *in-situ* hybridisation): 1.2M NaCl, 20mM Tris (pH7.5), 2x Denhardts solution, 160µM EDTA, 10mg salmon sperm DNA, 2mg yeast tRNA in DEPC H_2O. Aliquot and store at $-20^{o}C$.

Protein lysis buffer: 50mM Tris pH7.5, 0.32M Sucrose, 1mM EDTA pH8, 1x Protease inhibitor cocktail, 1mM PMSF in dH_20.

Red cell lysis buffer: 1mM NH_4HCO_3, 114 mM NH_4Cl in dH_2O

5 x Running buffer: 0.12M Tris, 1M Glycine, 0.5% SDS in dH_2O

2x sample buffer: 50mM Tris pH6.8, 100mM DTT, 2% SDS, 0.1% bromophenol blue, 10% glycerol in dH_20. Store at $-20^{0}C$.

20xSSC: 3M NaCl, 0.3M Trisodium citrate in dH_2O, pH to 7.

10% separating gel: 10% polyacrylamide, pH 8.8 buffer plus 0.05% APS and 0.05% TEMED.

4% stacking gel: 4% polyacrylamide, pH 6.8 buffer plus 0.05% APS and 0.1% TEMED

TBST: 0.9% NaCl, 100mM Tris pH7.5 in dH_20 plus 0.01% Tween 20.

Transfer buffer: 0.19M Glycine, 0.02M Tris, 20% Methanol in dH_2O

CHAPTER 3

3 Characterisation of APS1 patients in the UK

3.1 Introduction

The absence of functional AIRE, as seen in patients with APS1, causes a wide spread defect in self-tolerance, as evidenced by the development of multiple autoimmune diseases (4). APS1 most frequently manifests in early childhood. The first endocrine component occurred as early as 19 months of age in a large Finnish series, with additional disease manifestations developing throughout life (4). Forty three percent of these Finnish patients had 4 or more disease manifestations (4). A variety of different mutations in AIRE are present in patients with APS1 (2,3,1,15,17) either homozygously or in combination with another mutation in AIRE i.e. compound heterozygote. There is no genotype-phenotype correlation, and at the present time, prediction of the development of new manifestations or complications of APS1 is not possible (1).

Type 1 diabetes and APS1

Type 1 diabetes (T1D) occurs in 12-18% of Finnish APS1 patients (4,43). T1D as a disease has a significant impact on an individual's health, thus the ability to predict its development would be advantageous. In 1999, Ward et al described 2 siblings with APS1 who were discordant for T1D, and suggested that the IDDM2 locus may have role in the development of the T1D associated with APS1 (94). This led to work considering the role of this locus in APS1 patients in the UK.

The effect of non-functional AIRE on T cell function

Aire is known to be important in central tolerance as demonstrated in murine experimental models (13,75), where it is required to delete organ specific T cells within the thymus (75). However, the role of Aire in peripheral T cell function is less well understood. Given that diabetes, in common with the other autoimmune diseases seen in APS1, is T cell mediated, it seems logical to consider the effect non-functional AIRE has on T cell function. Ramsey *et al* noted that the lymphocytes of an Aire knockout mouse have an uncontrolled proliferative response when re-challenged in vitro with HEL compared to wild type littermates (74), suggesting that Aire may have a role in regulating the immune response in the periphery, but at present there are no data in the literature on how lack of Aire affects the function of peripheral lymphocytes from APS1 patients.

The aims of this chapter were

1. to characterise the phenotype and genotype of patients with APS1 in the UK
2. to determine whether diabetes susceptibility can be predicted in UK APS1 patients
3. to investigate whether there are differences in peripheral lymphocyte subsets and in the T cell proliferative response in APS1 patients compared to controls.

3.2 Patient characteristics

Patients with APS1 in the UK were sought as described in 2.1. 13 patients formed the original cohort. These patients were genotyped by Dr S Pearce in Newcastle prior to the start of this thesis (1). The remaining patients were genotyped in Newcastle where this thesis was commenced. 33 British APS1 patients were studied; the mean age was 24.2 years, range 9-56, with 24 males and 9 females. These patients were members of 28 unrelated kindreds with subjects 5 and 27, 9 and 13, 10 and 12, 11 and 15 and 19 and 21, being full siblings (Table 3.1). Diagnosis in the proband of a family was based on the presence of at least two out of three cardinal features, chronic mucocutaneous candidiasis (CMC), primary hypoparathyroidism and primary adrenal failure. In a sibling of an index case, one of the cardinal features was sufficient for the diagnosis of APS1 (4).

29 of the 33 patients (80.56%) had primary hypoparathyroidism, 28 (77.78%) had chronic mucocutaneous candidiasis, 23 (63.89%) Addison's disease, 9 (25%) gonadal failure, 8 (22.22%) type 1 diabetes, 8 (22.22%) malabsorption, 6 (16.67%) hepatitis, 4 (11.11%) alopecia, 3 (8.33%) keratopathy and 3 (8.33%) ectodermal dystrophy. In addition, the following manifestations were present in individual patients, ankylosing spondylitis, hypothyroidism, red cell aplasia, diabetes insipidus, pernicious anaemia, hypertension, epilepsy, cataracts, gallstones and pulmonary fibrosis.

The majority of patients with APS1 have multiple manifestations of the syndrome, representing a significant disease burden for the individual patient.

23 of the 33.patients (70%) studied here have 4 or more manifestations of APS1 (Fig 3.1), compared to 43% of Finnish APS1 patients (4).

This difference is most likely because APS1 is more readily recognised in the genetically isolated population of Finland where it is much commoner. Thus, due to this greater awareness patients may be diagnosed with less manifestations of the disease than here in the UK where a patient with CMC and Addison's may not immediately be recognised as having APS1.

	Sex/Age at assessment	HP*	AD*	CMC*	T1D*	Other
1	M 10	Y			Y	M,H
2	M 15	Y	Y	Y	Y	
3	M 20	Y	Y	Y	Y	A,T
4	M 24	Y	Y	Y	Y	GF
5	M 33 (sib of 27) #	Y	Y	Y	Y	A
6	M 37		Y	Y	Y	M, RCA, OC
7	M 41	Y	Y	Y	Y	M,GF, K, PA
8	F 52 #	Y	Y	Y	Y	GF
9	M 9 (sib of 13)	Y	Y	Y	N	
10	F 10 (sib of 12)	Y		Y	N	
11	M 10 (sib of 15)	Y			N	
12	M 13 (sib of 10)			Y	N	H
13	M 12 (sib of 9)	Y	Y	Y	N	M
14	F 13	Y		Y	N	
15	F 13 (sib of 11)	Y		Y	N	M,H,P, K
16	M 14	Y	Y		N	
17	F 15	Y	Y	Y	N	H
18	M 15	Y			N	H,Ch
19	F 16 (sib of 21)	Y			N	
20	M 17	Y	Y	Y	N	M,GF
21	M 19 (sib of 19)	Y	Y	Y	N	H,GF
22	M 20	Y	Y	Y	N	M,GF
23	M 23	Y	Y		N	
24	F 26	Y	Y	Y	N	M,T
25	F 26	Y	Y	Y	N	GF
26	M 26	Y	Y	Y	N	T
27	M 26 (sib of 5) #		Y	Y	N	
28	M 27	Y	Y	Y	N	
29	M 36	Y		Y	N	
30	F 37	Y	Y	Y	N	GF,AS
31	M 37	Y	Y	Y	N	A,GF
32	M 51	Y	Y	Y	N	A,K
33	M 56	Y	Y	Y	N	A

Table 3.1 Clinical Characteristics of UK APS1 patients

*Y= present, N= absent.
HP – Hypoparathyroidism; AD – Addisons disease; CMC – Chronic mucocutaneous candidiasis; T1D – Type 1 diabetes; M – Malabsorption; K- Keratopathy; A – Alopecia; GF – Gonadal Failure; H – Hepatitis; AS- Ankylosing Spondylitis;
T – Hypothyroidism; RCA – red cell aplasia; PA – Pernicious anaemia;
Ch – Cholelithiasis; P – Pulmonary fibrosis, OC - Oral Carcinoma; C - Cataracts.
These patients are deceased

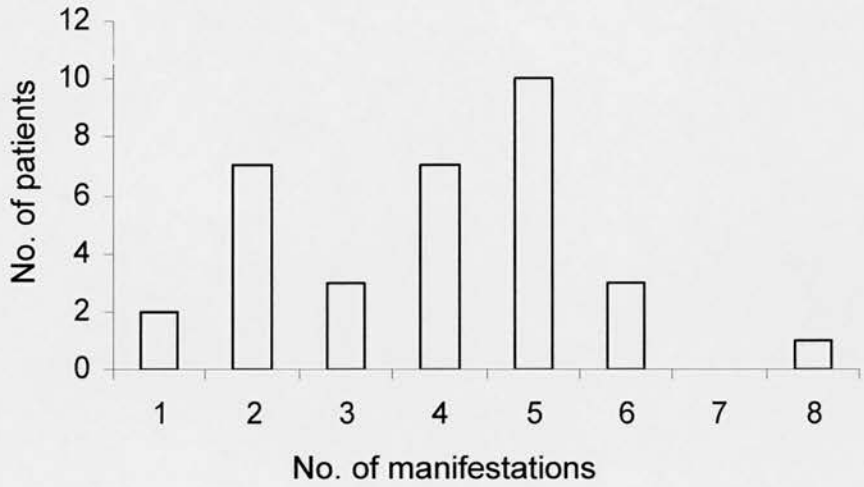

Figure 3.1 Number of manifestations of APS1 per patient

3.3 AIRE mutations present in APS1 patients

Mutational analysis of the original cohort of patients by Dr Pearce showed that the commonest mutation in the UK is 964del13 (71% of mutant alleles) (1), whereas in the Finnish population the mutation R257* predominates (85% of mutant alleles) (2,3).

The common UK mutation, designated 964del13, is a 13bp deletion in exon 8 which gives rise to a non-functional AIRE-1 protein of 372 amino acids, truncated at the start of the first zinc finger motif. The major Finnish mutation is a nonsense mutation in exon 6, R257*. This encodes a non-functional 256 amino acid protein, truncated in the SAND domain and containing neither zinc finger.

All patients were screened by PCR and restriction digest for 964del13 and R257* as described in section 2.3 (Table 3.2). The common UK mutation 964del13 was present in 31 of the 33 patients (94%), accounting for 46 of the 66 alleles (70%) as 15 of these patients are homozygotes for this mutation, the remainder being compound heterozygotes. This is in accordance with previously reported findings (1). In addition, 3 of 33 patients were heterozygous for the Finnish major mutation R257*, accounting for 3 out of 66 alleles (4.5%).

There remain 11 unidentified alleles in 11 patients. One of these patients was from the original cohort and therefore had already been screened for a second mutation by SSCP. The DNA from the remaining 10 patients was subject to PCR and SSCP (Section 2.3.4) targeted at the exons where mutations in AIRE cluster. The exons

screened were exons 1, 2, 3, 6, 7, 8, 9, 10, 11 and 14. No novel mutations were identified.

	AIRE mutation		AIRE mutation		AIRE mutation
1	964del13 + Un	12	964del13 + Un	23	964del13 + R257*
2	964del13 + Un	13	964del13 + Un	24	964del13x2
3	*964del13x2	14	964del13x2	25	*964del13x2
4	*964del13x2	15	#964del13x2	26	964del13 + Un
5	*964del13x2	16	*964del13x2	27	*964del13x2
6	*x10del + L28P	17	964del13x2	28	964del13x2
7	*964del13x2	18	964del13 + Un	29	*R257* + Y90C
8	*964del13 + Un	19	*964del13 + R15L	30	*964del13 + x10del
9	964del13 + Un	20	964del13 + Un	31	964del13 + Un
10	964del13 + Un	21	*964del13 + R15L	32	964del13x2
11	#964del13x2	22	964del13x2	33	964del13 + R257*

Table 3.2 Aire mutations in UK APS1 patients

The common UK and Finnish mutations, 964del13 and R257* were screened for using PCR and restriction digest, novel mutations were sought using SSCP
*original cohort of patients (1)
#mutational analysis on these patients was carried out by Dr S Pearce

3.4 The prediction of diabetes susceptibility in patients with APS1

Type 1 diabetes (T1D), an autoimmune disease which has multiple susceptibility genes, was reported to occur in 12 to 18% of Finnish APS1 patients (4,43). The pre-clinical phase of T1D is characterised by the presence of autoantibodies, however not all those with autoantibodies will go on to develop T1D. In keeping with this, autoantibodies against glutamic acid decarboxylase (GAD) occur more commonly than T1D, being present in 32% of APS1 patients (46), although the positive predictive value of GAD65 antibodies for T1D in APS1 is only 27% (43). Recently it has been suggested that antibodies against the IA-2 tyrosine phosphatase-like protein (IA-2 ab) or insulin (IAA) are better markers of active beta cell loss with a positive predictive value in APS1 patients of 67% for T1D (30). Therefore, none of these measurements alone are sufficient to predict diabetes development in APS1 patients. The genetic susceptibility loci that contribute the most to diabetes susceptibility are the major histocompatibility complex (MHC) class II genes designated *IDDM1*, and insulin gene polymorphisms (IDDM2) (95). In view of the reported association between *IDDM2* and diabetes susceptibility in a sibpair, this study to define the relationship between *IDDM1* and *IDDM2* and the presence of T1D in a larger group of APS1 patients was undertaken.

3.4.1 Type 1 diabetes and *IDDM1* in UK APS1 patients

In T1D, *IDDM1* contributes 50% of the genetic risk (96). Of the MHC class II genes, HLA DQB and in particular residue 57, determines susceptibility to (or protection

from) type 1 diabetes. Of the MHC class II genes, HLA DQB1*0201 and 0302 alleles are the main predisposing alleles for type 1 diabetes in a non-APS1 population, with compound heterozygosity for these alleles being present in 30% of type 1 diabetes patients (97). In addition a non-Asp residue at position 57 of the DQβ-chain on either DQB allele is present in 98% of type 1 diabetes patients (98). In contrast, HLA DQB1*0602 protects against the development of type 1 diabetes (99). Unlike other autoimmune polyendocrinopathy syndromes, there are no known HLA associations with the cardinal manifestations of APS1. However, Gylling et al. recently suggested that HLA DQβ1*0602 may be associated with protection against the development of T1D in an APS1 population (30).

HLADQB typing (section 2.4) was performed on 25 APS1 patients, 5 of whom have diabetes (Table 3.3). Two of these 5 with type 1 diabetes had a "non-aspartate 57" DQB allele. Of the 20 APS1 patients without type 1 diabetes, 7 had a non-aspartate 57 allele ($p=0.6$, Fisher's exact test). None of the 5 APS1 patients with diabetes carried HLA DQB*0602, however 4 of 20 non-diabetic APS1 patients (20%) did. This difference was not significant ($p=0.38$).

	APS1 with T1D (%)	APS1 without T1D (%)
Non-Asp57 allele present	2 (40)†	7 (35)
Non-Asp57 allele absent	3 (60)	13 (65)
HLA DQB*0602 present	0 (0) ††	4 (20)
HLA DQB*0602 absent	5 (100)	16 (80)

Table 3.3 HLA status of APS1 subjects with and without Type 1 diabetes

HLA DQβ typing was performed utilising PCR to determine the presence or absence of a non-Asp57 allele (as described in section 2.4).
Non-Asp57 alleles are HLA DQB*0201,0302,0501 and 0604, and are present in 98% of non-APS1 type 1 diabetes.
†p=0.6, Fisher's exact test.
††p=0.38, Fisher's exact test.

	APS1 with T1D (%)	APS1 without T1D (%)
HphI AA homozygotes	6 (75)†	8 (32)
HphI AB or BB	2 (25)	17 (68)

Table 3.4 *HphI* genotypes in APS1 subjects with and without Type 1 diabetes

HphI genotype was ascertained by PCR and restriction digest.
AA is equivalent to homozygous class I *INS* VNTR alleles and is a T1D susceptibility genotype in non-APS1 subjects. AB and BB are equivalent to a class I/class III heterozygote and class III homozygote (T1D protective genotypes), respectively.
† p=0.042, Fisher's exact test.

3.4.2 Type 1 diabetes and *IDDM2* in UK APS1 patients

The 5' polymorphic region of the insulin gene (*INS*), located on chromosome 11p15.5, consists of a variable number of tandem repeats (VNTR) and determines susceptibility to T1D (*IDDM2*) (93,92). This *INS* gene polymorphism can be divided into three classes depending upon the number of repeats: the class III allele of the INS gene is dominantly protective for T1D, whereas homozygosity for the class I allele predisposes to T1D (relative risk 1.9-5.0) (92).

Patients were screened by PCR and restriction digest to determine which *IDDM2* allele was present as described in section 2.5. Eight out of the 33 (24%) APS1 subjects had T1D. Of the 8 with T1D, 6 (75%) were homozygous for the *Hph1* A allele, which is in tight linkage disequilibrium with the T1D susceptibility class I VNTR (Table 3.4). In comparison, only 8 out of 25 (32%) APS1 patients without T1D were homozygous for the A allele (OR=6.4, [5-95% CI =1.2-34.7]; p=0.042 Fisher's exact test). The 2 APS1 patients with T1D, who did not carry the homozygous A allele (subjects 4 and 6), were aged 37 and 24 years, respectively. The mean age of the subjects with T1D was 29 (range 10-52) compared to 22.6 (range 9-56) in the APS1 patients without T1D. This older age in the T1D group leaves open the possibility that further cases of T1D may develop in the unaffected APS1 cohort as they age.

3.4.3 Patient genotype-phenotype - Conclusions

The difficulty experienced in predicting new disease manifestations in APS1 combined with the observation that insulin gene polymorphisms segregated with T1D in one sibpair (94) lead to the investigation of this in 33 APS1 subjects from the U.K. In this relatively small cohort, there is an increase in the frequency of *INS* VNTR Class I associated alleles in those subjects with type 1 diabetes compared to those without type 1 diabetes (75% vs. 32%, p=0.042). This suggests an association between the development of type 1 diabetes and homozygosity for Class I *INS* VNTR in patients with APS1, which is similar to that seen in the non-APS1 type 1 diabetes population. Previous studies have shown that 73% of non-APS1 type 1 diabetes patients are homozygous for the class I VNTR, this figure is remarkably similar to the 75% AA genotype in the APS1 type 1 diabetes patients studied here (92). However, this work clearly demonstrates that *INS* gene polymorphisms are not necessary disease alleles for the development of type 1 diabetes in the UK APS1 population.

AIRE is known to be expressed in thymic medullary epithelial cells, its expression is up-regulated in models of negative selection (7,8,71,6) and the ectopic expression of insulin within the thymus is under the control of Aire (13). In addition, there is differential expression of insulin within the thymus of diabetics with the different *INS* VNTR haplotypes. Homozygosity for class I alleles is associated with low levels of insulin, but the protective class III allele is associated with high levels of insulin (80,81). Positive and negative selection of thymocytes can be affected by the

concentration of peptide presented, with higher concentration of peptide leading to negative selection and lower concentrations to positive selection (80). This relationship between *IDDM2* and type 1 diabetes is in keeping with this, however, if thymic expression of insulin is under the control of Aire in humans as seen in the Aire knock-out mouse (13), then insulin would not be expressed in the thymus irrespective of the insulin gene polymorphism present. If this is the case, then it seems unlikely that the positive relationship between lack of diabetes and a protective *IDDM2* allele would exist. Thus it may be that, unlike the Aire knock-out mouse, thymic expression of insulin is not under the control of AIRE in humans. Alternatively, in APS1 insulin may not be the primary autoantigen, but autoantibodies to insulin may appear after tissue damage has occurred mediated through an alternative autoantigen, e.g. GAD.

As in previous studies, no association with a "susceptibility" HLA haplotype was found (100). Gylling *et al* (100) documented an absence of the protective HLA DQB*0602 in APS1 patients with diabetes, whilst non-diabetic APS1 patients showed a significant increase in the prevalence of this haplotype. The results of this work are entirely consistent with this finding.

AIRE plays a role in negative selection within the thymus through the ectopic expression of tissue restricted antigens and the appropriate negative selection of T cells specific for these antigens (13,13,75). In addition, the differential expression of self-peptides in the thymus leads to the regulation of negative selection (80). Thus, the observation of a positive relationship between INS polymorphisms and type 1 diabetes in APS1 is consistent with this mechanism of action of AIRE.

3.5 Characterisation of peripheral lymphocytes in APS1 patients

There are a limited number of reports in the literature of studies on the phenotype or biological function of lymphocytes in patients with APS1 (42,101,102,103,104). To date, there are no data in the literature regarding the proliferative response of T cells from patients with APS1 compared to controls, and limited inconclusive data on alterations in peripheral cell subsets (42,104,103). However, the peripheral control of any autoreactive T cells which exit the thymus is important in preventing autoimmune disease, and the autoimmune diseases that occur in APS1 are T cell mediated. Therefore, the phenotype and biological function of peripheral lymphocytes was investigated in a small number of APS1 patients.

3.5.1 Comparison of peripheral lymphocyte subsets in patients and controls

In 1991, Friedman et al investigated 9 patients with APS1 and found no evidence for a difference in T or B lymphocyte or NK cell populations by flow cytometric staining for CD3, CD4, CD8, CD20, CD5 and CD56 compared to the percentages of these populations in normal children (42). More recently, Sediva et al examined a similar selection of markers in 4 patients with APS1. Two out of 4 patients had elevated numbers of CD4+CD3+ T cells, no other differences were found (103). The lymphocyte subpopulations of 6 patients with CMC, 2 of whom had APS1 were investigated, no difference in CD4+ or CD8+ T cells was observed (104).

This study analysed peripheral blood cell subsets in patients with APS1 in comparison to age and sex matched controls using a wide panel of antibodies. Peripheral blood mononuclear cells (PBMCs) were isolated from whole blood by centrifugation through a Ficoll gradient (Section 2.6). The PBMCs were stained for analysis by flow cytometry with antibodies to cell surface markers (Section 2.7; Table 2.2). Populations of T, B and natural killer T (NKT) cells were delineated using antibodies for CD3, CD19 and CD94 respectively (Figs 3.8, 3.9). CD3+ T cells were then stained for CD4 and CD8 or TCR αβ and γδ (Fig 3.8). CD4+ T cells were further subdivided using antibodies against CD45RA and CD45RO to determine the proportions of naïve and memory cells, and CD25, CD69 and CTLA4 to assess the activation status of the cells. CD8+ T cells were also stained for CD25 and CD69 and CTLA4. CD19+ B cells were stained for CD45RA and HLA-DR. NKT cells were subdivided on CD4 and CD8 and Vα24. Data for cells stained with CTLA4 and Vα24 was not analysed, as this staining was comparable to that obtained with the appropriate isotype control due to the low numbers of resting cells that express these markers. Representative flow cytometry data for one patient (Figs 3.3, 3.5, 3.7) and one control (Fig 3.2, 3.4, 3.6) are shown. No significant differences in cell surface marker expression were seen in patients compared to controls (Figs 3.8-11) in the initial cohort of 2 patients and 3 controls. As this initial data revealed no differences, no further samples were collected.

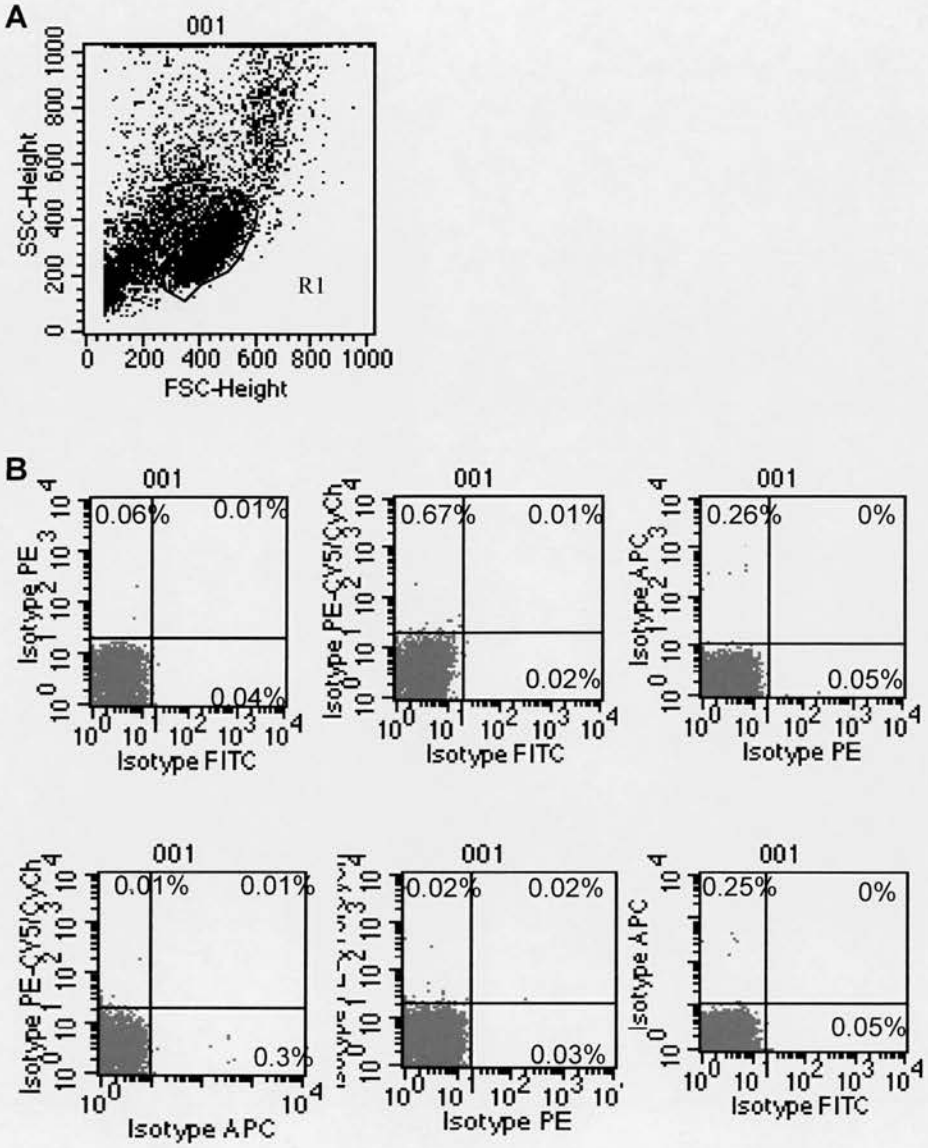

Fig 3.2 Representative FACS plots – Control

A PBMC's from whole blood, with lymphocyte gate (R1)

B Isotype controls gated on R1

The antibodies used are described in section 2.7 and in table 2.3

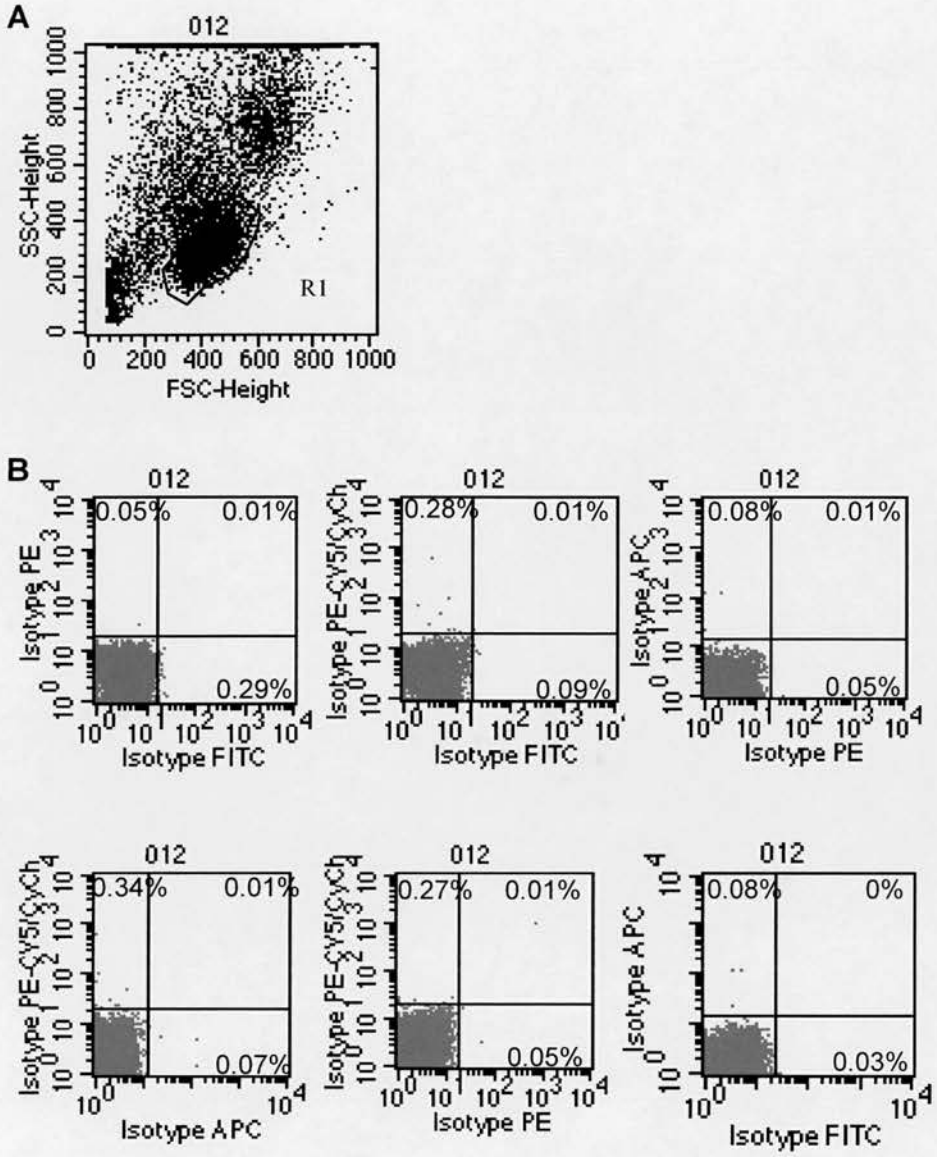

Fig 3.3 Representative FACS plots – Patient

A PBMC's from whole blood, with lymphocyte gate (R1)

B Isotype controls gated on R1

The antibodies used are described in section 2.7 and in table 2.3

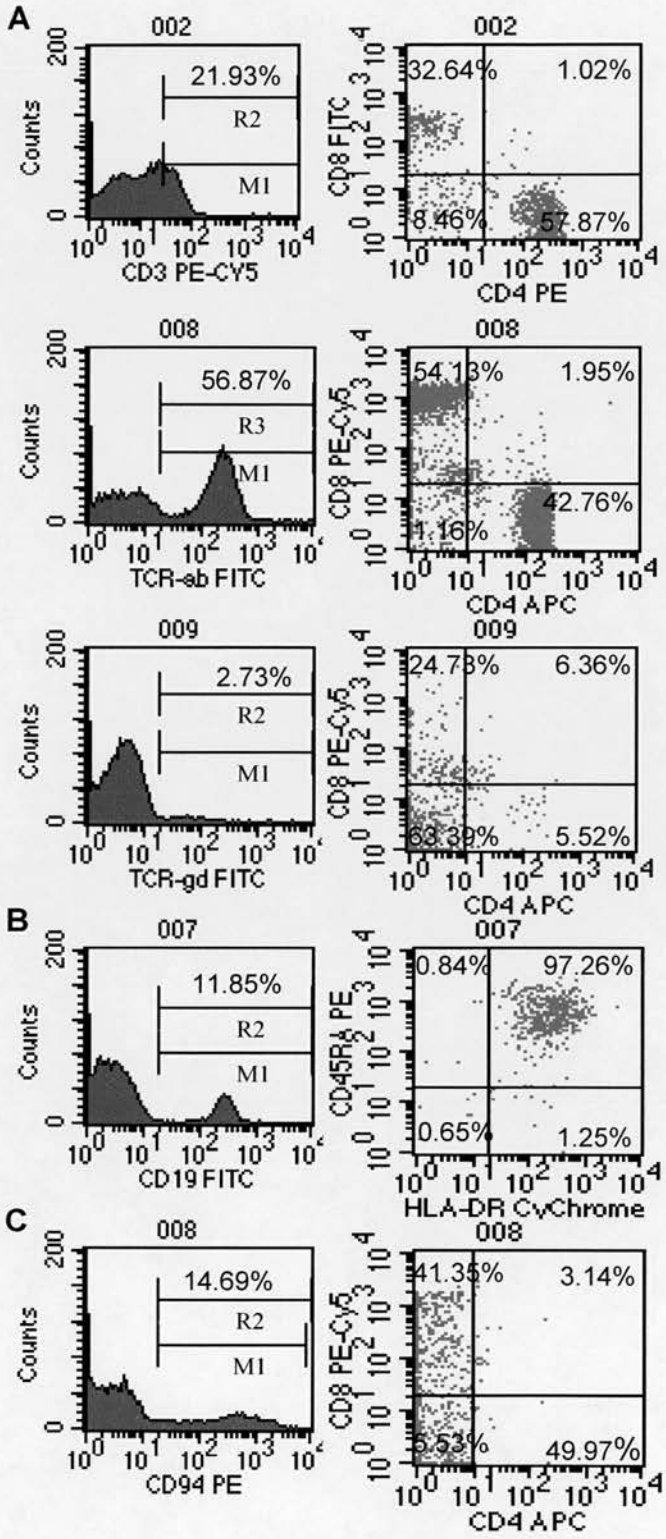

Fig 3.4 Representative FACS data – Control

A Lymphocytes; **B** B cells; **C** NKT cells

All histograms are gated on gate R1 (lymphocytes) and the gate for the corresponding dot plot is shown on the histogram

The antibodies used are described in section 2.7 and in table 2.3

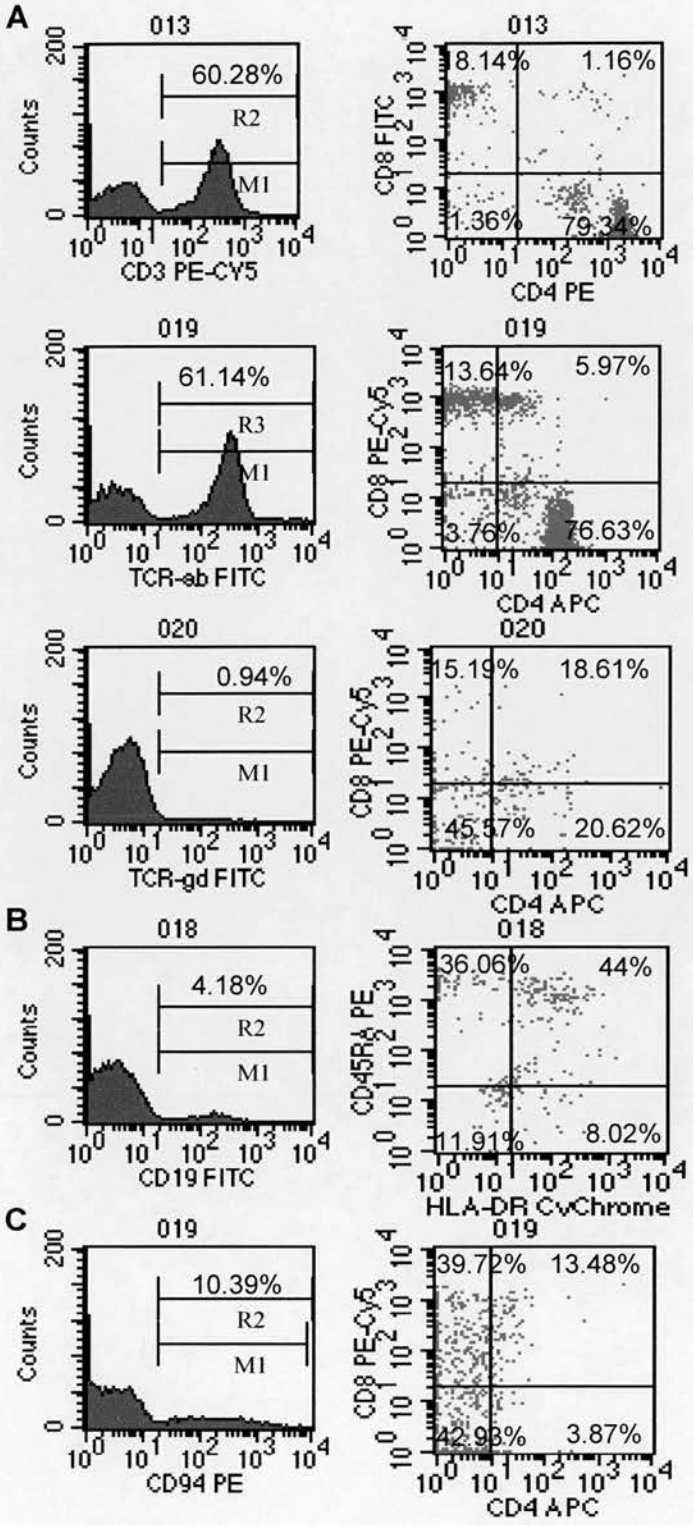

Fig 3.5 Representative FACS data – Patient

A Lymphocytes; **B** B cells; **C** NKT cells

All histograms are gated on gate R1 (lymphocytes) and the gate for the corresponding dot plot is shown on the histogram

The antibodies used are described in section 2.7 and in table 2.3

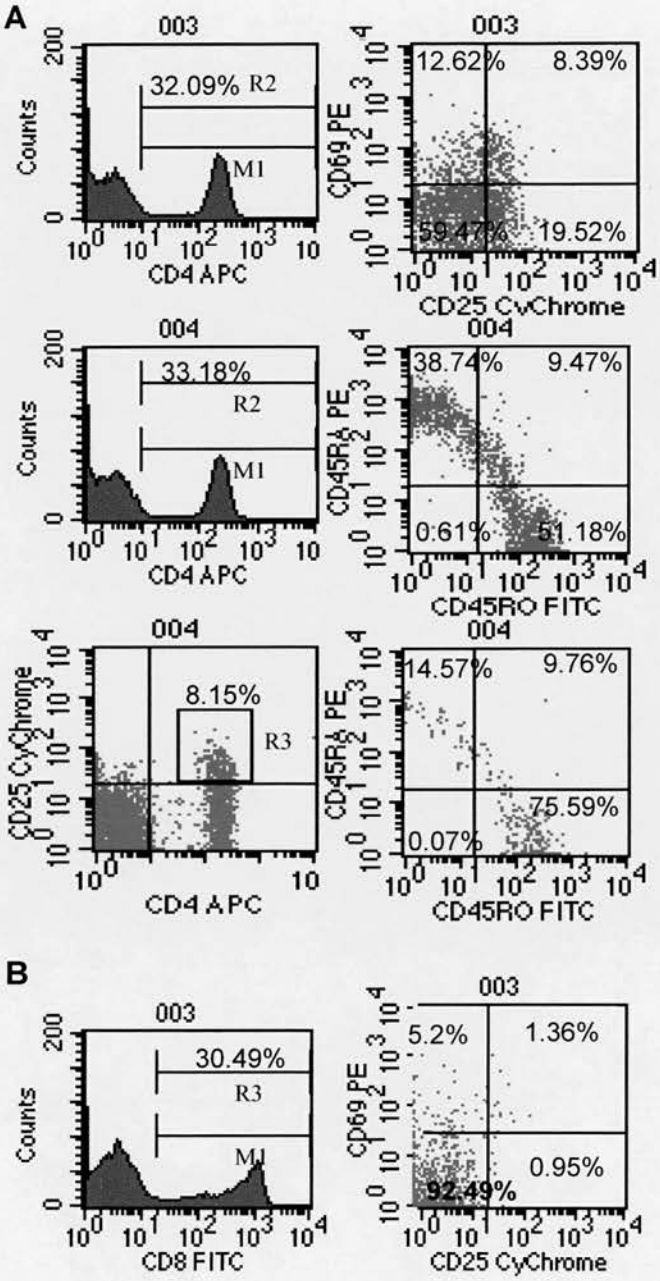

Fig 3.6 Representative FACS data – Control
Characterisation of **A** CD4 and **B** CD8 subsets. All histograms are gated on gate R1 (lymphocytes) and the gate for the corresponding dot plot is shown on the histogram/dot plot
The antibodies used are described in section 2.7 and in table 2.3

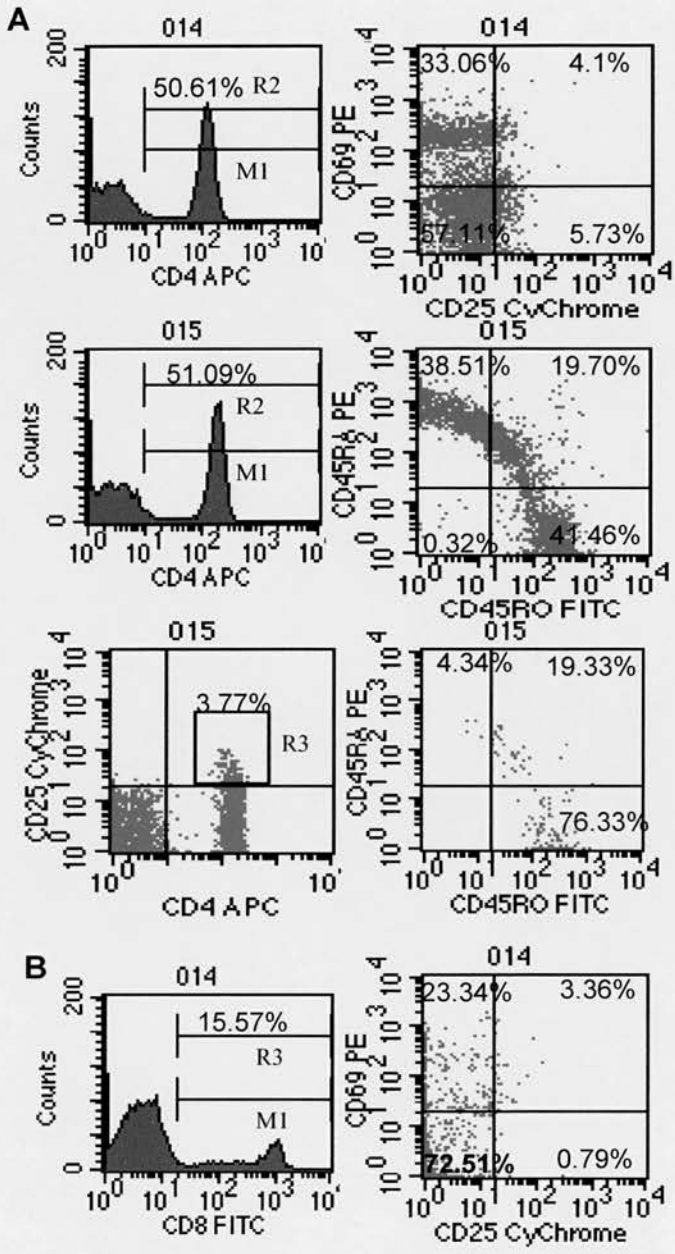

Fig 3.7 Representative FACS data – Patient

Characterisation of **A** CD4 and **B** CD8 subsets. All histograms are gated on gate R1 (lymphocytes) and the gate for the corresponding dot plot is shown on the histogram
The antibodies used are described in section 2.7 and in table 2.3

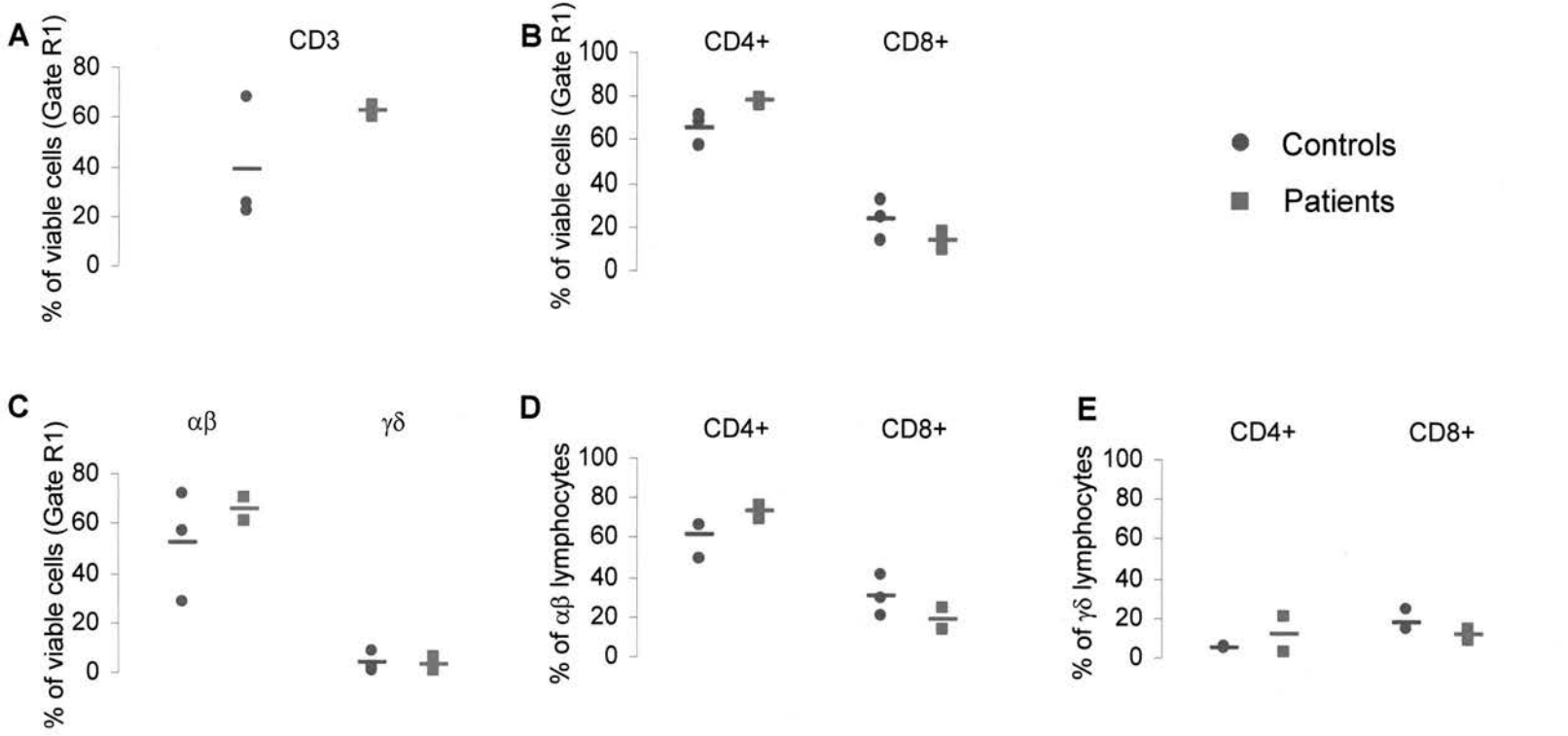

Fig 3.8 Peripheral cell subset analysis in APS1 patients compared with controls. Each data point represents an individual patient or control, the mean is represented by the bar. **A** CD3 positive lymphocytes; **B** CD4+ and CD8+ cells as a percentage of CD3+ cells; **C** αβ, γδ TCR expression on lymphocytes; **D** CD4+ and CD8+ cells as a percentage of αβ TCR lymphocytes; **E** CD4+ and CD8+ cells as a percentage of γδ TCR lymphocytes

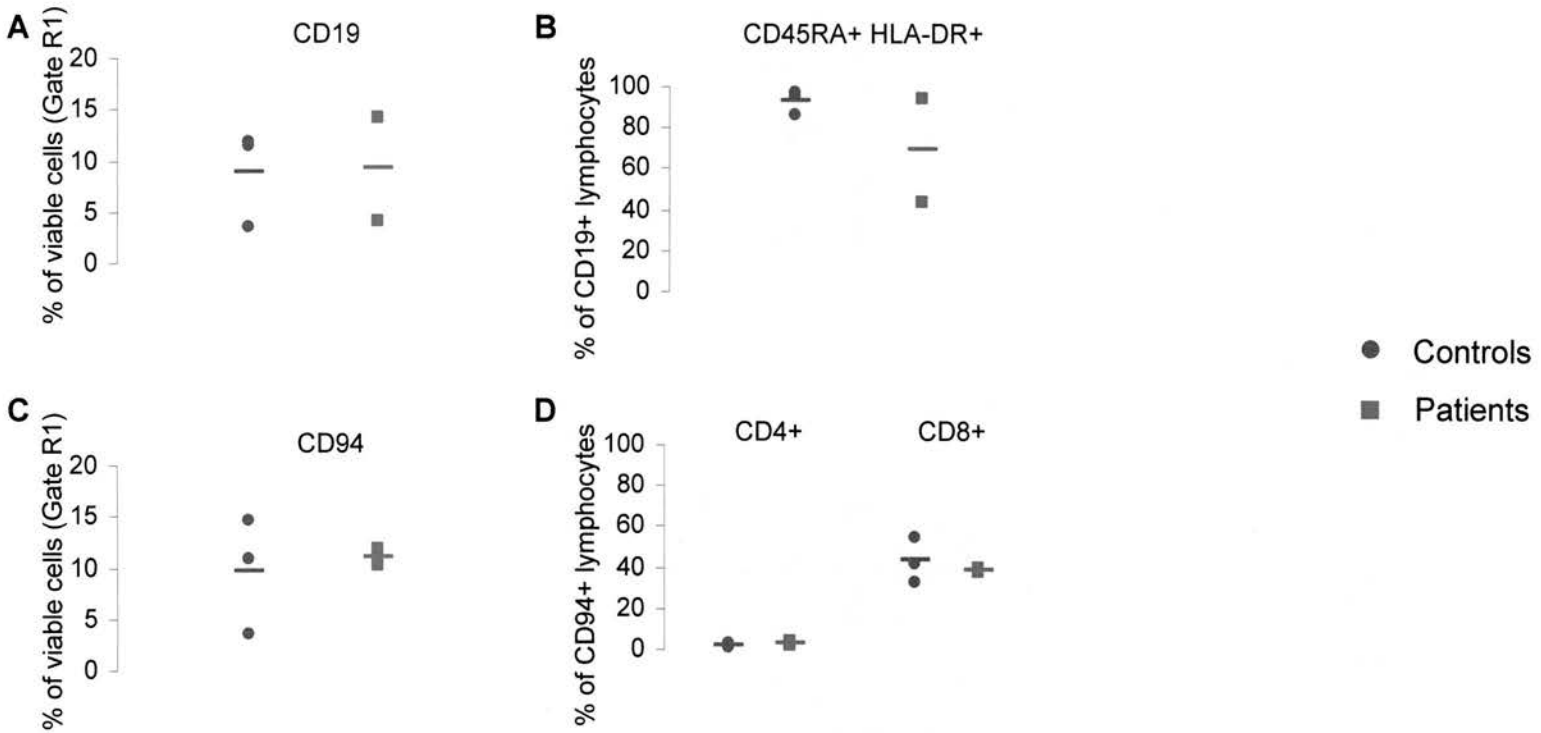

Fig 3.9 Peripheral cell subset analysis in APS1 patients compared with controls. Each data point represents an individual patient or control, the mean is represented by the bar. **A** CD19 positive lymphocytes; **B** CD45RA+ and HLA-DR+ cells as a percentage of CD19+ cells; **C** CD94 positive lymphocytes; **D** CD4+ and CD8+ cells as a percentage of CD94+ lymphocytes

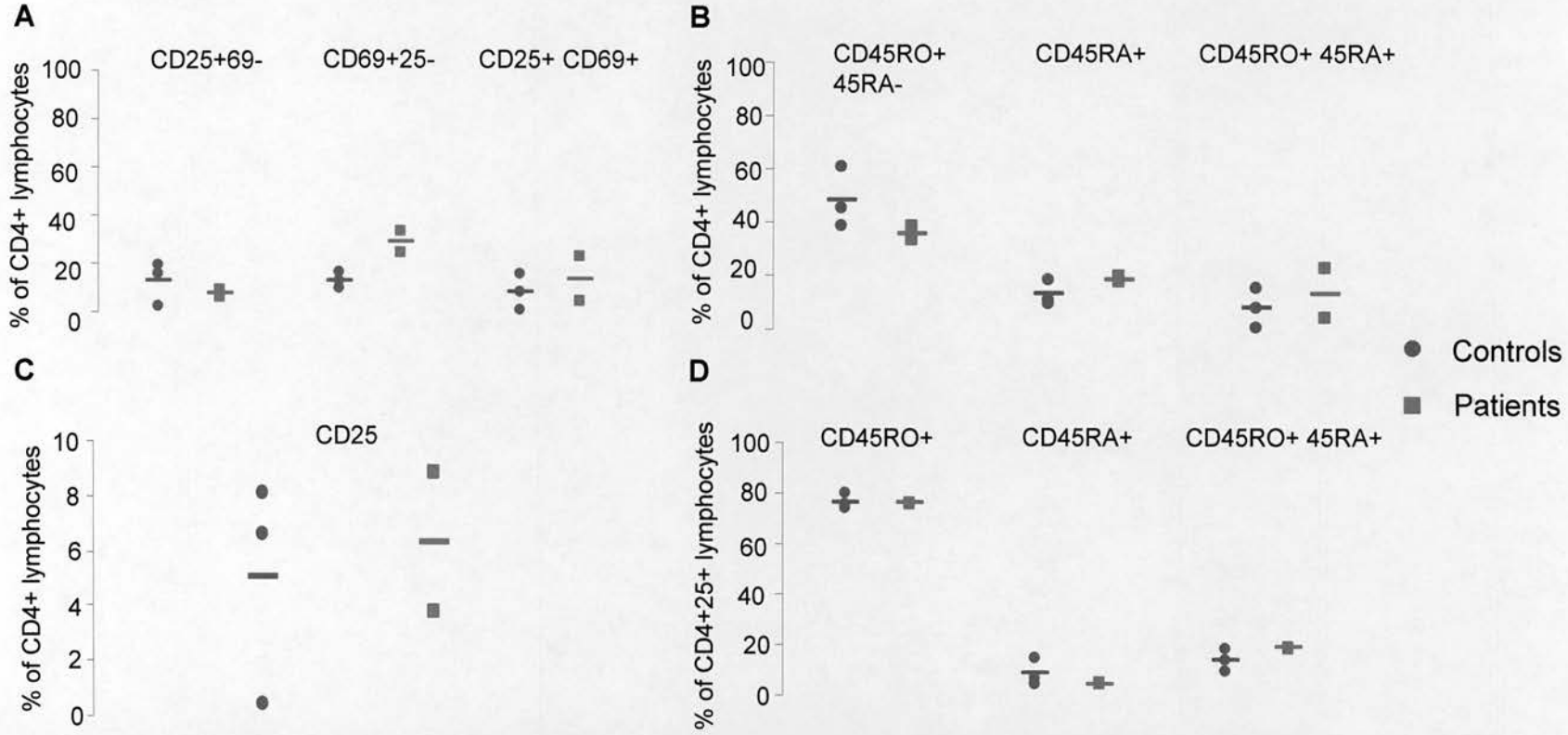

Fig 3.10 Peripheral cell subset analysis in APS1 patients compared with controls. Each data point represents an individual patient or control, the mean is represented by the bar. **A** CD25+ and CD69+ cells as a percentage of CD4+ lymphocytes; **B** CD45RO+ and CD45RA+ cells as a percentage of CD4+ cells; **C** CD25 positive lymphocytes as a percentage of CD4+ cells; **D** CD45RO+ and CD45RA+ cells as a percentage of CD4+25+ lymphocytes

Fig 3.11 Peripheral cell subset analysis in APS1 patients compared with controls. Each data point represents an individual patient or control, the mean is represented by the bar. CD25+ and CD69+ cells as a percentage of CD8+ lymphocytes

3.5.2 Characterisation of the response to T cell receptor stimulation in APS1 patients

Prior to this thesis, there was no information regarding the proliferative response of human T cells lacking AIRE to stimulation through the T cell receptor. Data from the Aire deficient mouse shows an increased proliferative response to an *in-vitro* rechallenge with HEL (74). Kobrynski et al, investigated 6 patients with CMC, 2 of these had APS1. These 2 APS1 patients show a trend to higher proliferation to PHA compared to those with CMC (104).

The response of peripheral blood mononuclear cells to stimulation by anti-CD3 and anti-CD28 antibodies was examined in 3 patients with APS1 and 3 controls. Briefly, PBMCs were isolated as described above and plated into 96 well plates in the presence of varying concentrations of anti CD3 and anti CD28 antibodies for 48 hours. Sixteen hours prior to the end of the culture period the cells were pulsed with tritiated thymidine, the incorporation of which was subsequently assessed (Section 2.8).

The patients with APS1 have a higher background proliferation than controls and a trend to a higher maximal proliferative response (Figure 3.12A). However, there was no difference in the fold change in proliferation over baseline [Stimulation Index, SI] (Figure 3.12B).

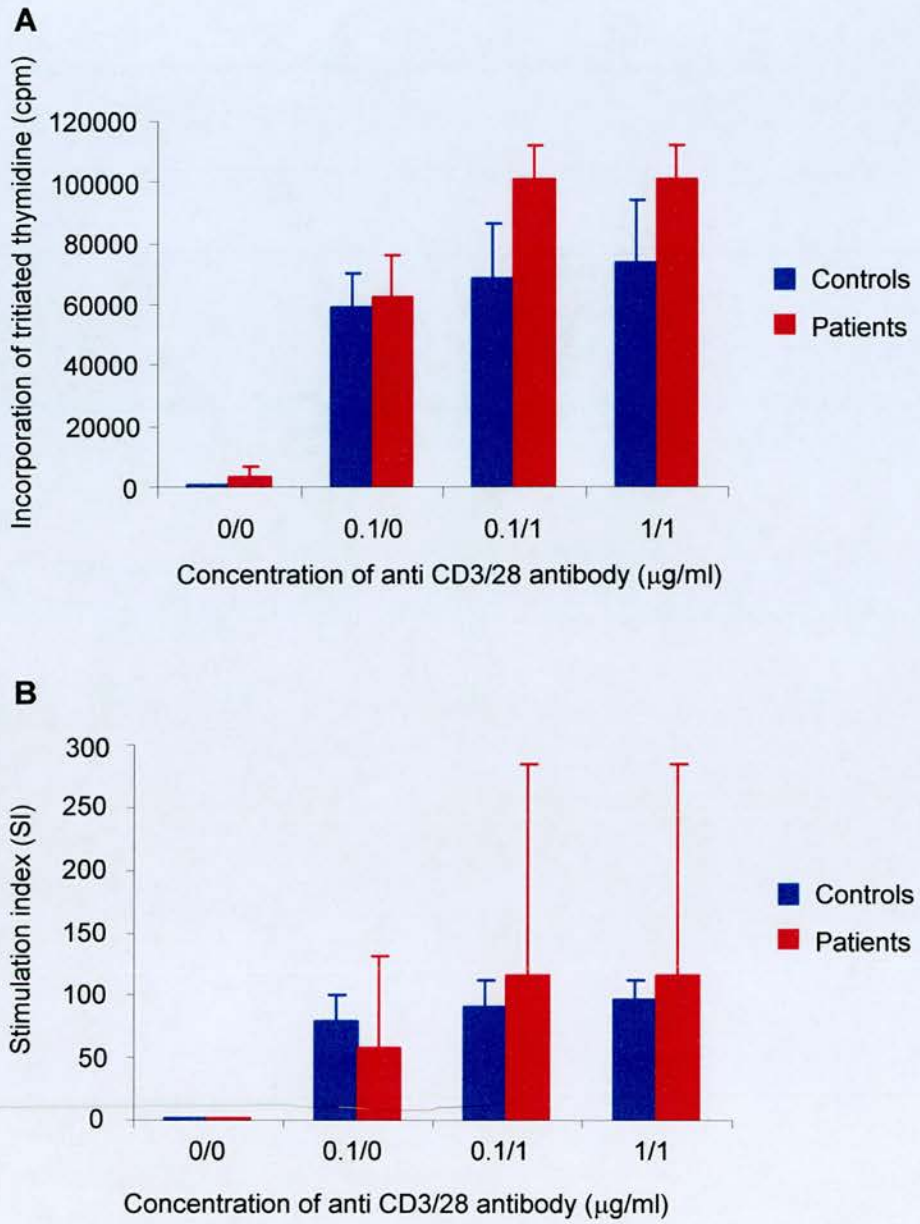

Fig 3.12 Response of PBMCs to stimulation with anti CD3/28 antibodies in APS1 patients and controls.
A Proliferation as assessed by incorporation of tritiated thymidine
B Stimulation index
All data are represented as the mean +/-SD (n=3 per group)

3.5.3 Cytokine secretion by activated human PBMCs

There is limited information on the cytokine profile of peripheral lymphocytes from APS1 patients. Sediva et al, show a trend to decreased IFNγ production by activated PBMCs from APS1 patients compared to controls (103). Additionally, patients with isolated CMC, which is one of the cardinal features of APS1 produce less IFNγ in response to candidal antigens than controls (105,106).

PBMCs were isolated and plated out as described in section 3.5.2, and supernatants were collected at 48 hours for measurement of cytokines. Levels of IFNγ, TNFα, IL-10, IL-5, IL-4 and IL-2 were determined using a human Th1/Th2 cytokine bead array (CBA) kit (BD) (Section 2.9). There was no significant difference in cytokine secretion between the patients and controls (Figs 3.13 and 3.14). In view of this and the difficulty recruiting patients this work was not taken any further.

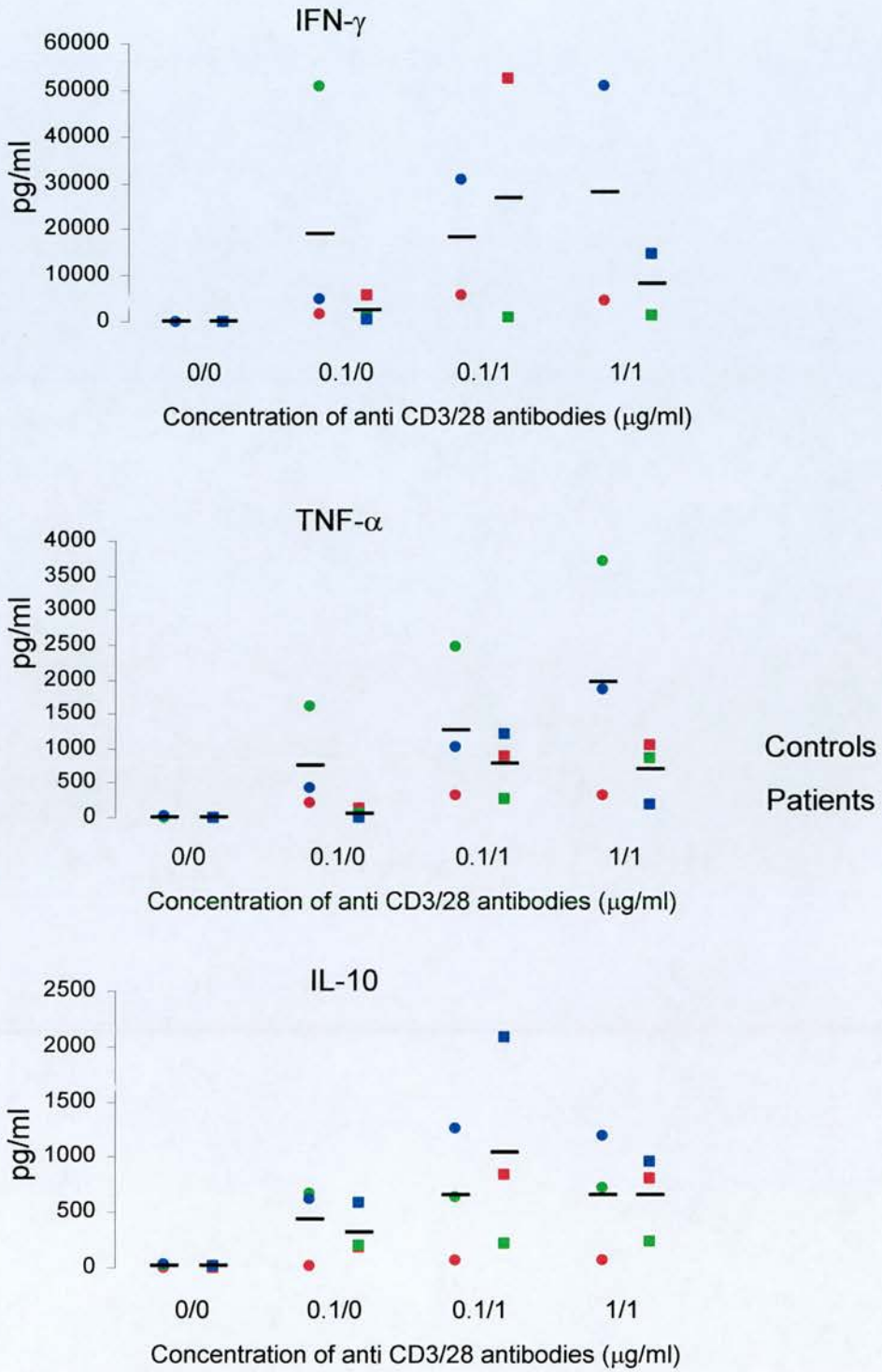

Fig 3.13 Cytokine secretion by patient and control PBMCs in response to anti-CD3 and anti-CD28 antibodies is similar. Individual patients(□)/controls (○) are represented by separate data points, the mean is represented by the bar

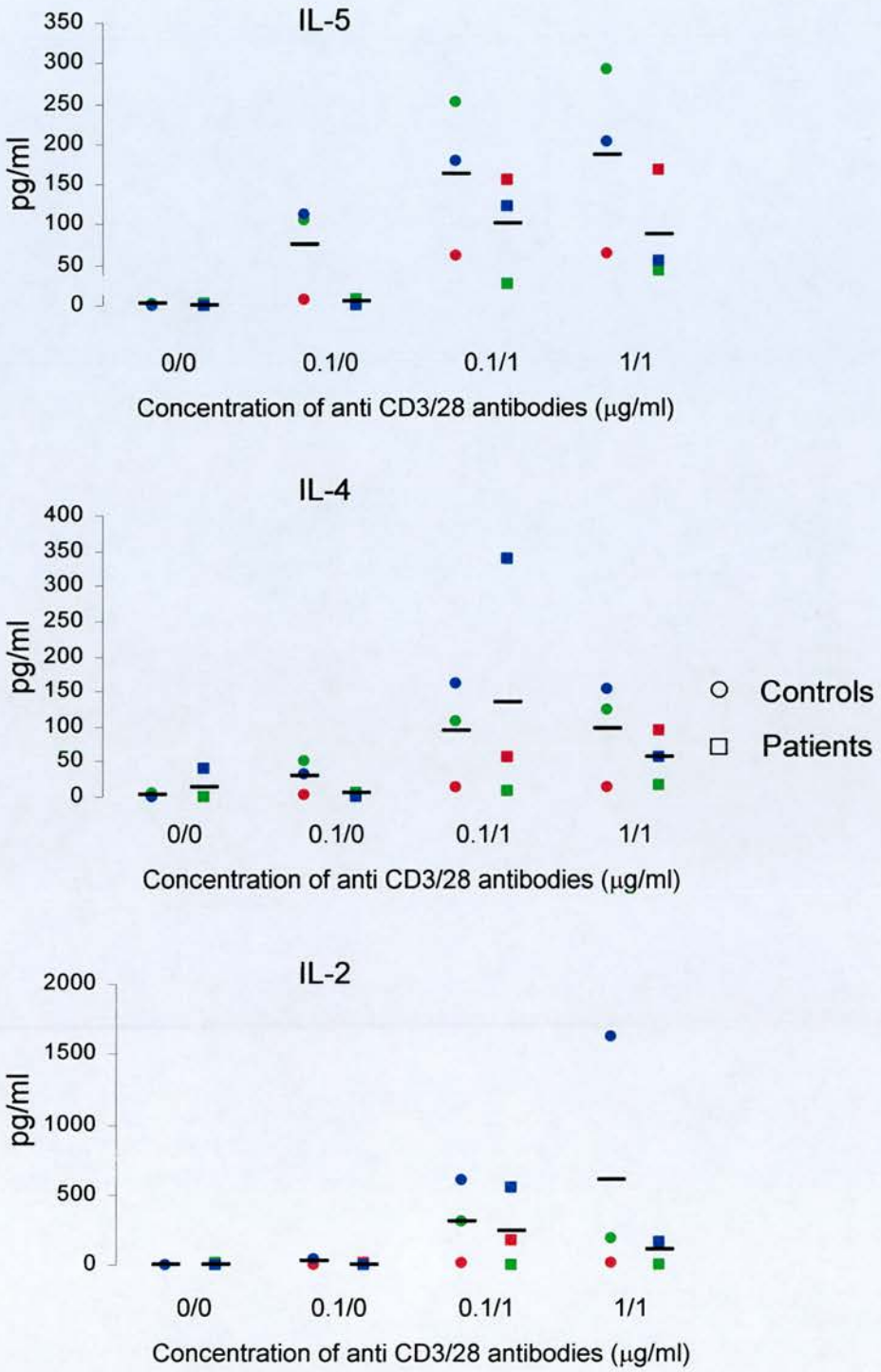

Fig 3.14 Cytokine secretion by patient and control PBMCs in response to anti-CD3 and anti-CD28 antibodies is similar. Individual patients(□)/controls (○) are represented by separate data points, the mean is represented by the bar

3.5.4 Patient T cell function - Conclusions

It is difficult to draw any firm conclusions from this limited data set, even when taken in conjunction with the other data available. However, it seems probable that patients with APS1 have no perturbation in peripheral lymphocyte subsets. There are currently 2 published Aire deficient mice, one of these is designed to mimic the major Finnish mutation by targeted disruption of exon 6, and these mice have no differences in peripheral cell subsets (74). The other Aire deficient mouse has a deletion of exon 2 giving rise to a protein truncated after exon 1. These mice have normal CD4/CD8 subset distributions but an increase in $CD44^{hi}CD62L^{lo}$ CD4+ and CD8+ T cells (13). This difference in the 2 different Aire deficient mice may represent a difference in the generation of the mice. The strain generated by Anderson et al, which has an increase in activated/memory cells, has an Aire protein consisting of just exon 1. This compares to the strain generated by Ramsey et al which has an Aire protein truncated in exon 6, in which no differences are seen in the proportion of activated cells. This is unlikely as there is no phenotype-genotype correlation in APS1, and by extrapolating from data in transactivation studies neither of these proteins would be expected to be functional (54). Alternatively the disparity in activated cells present may be due to, as Ramsey et al state, the fact that their mice have not been challenged as they are housed in a sterile facility. However, as no difference was observed in CD44 and CD62L expression, in Aire deficient mice compared to wild-type mice, after an *in-vitro* re-challenge with HEL, this explanation would also seem unlikely (74).

The situation in patients is further complicated by the fact, that unlike the Aire deficient mice, they are all on varying combinations of treatment for the

manifestations of APS1 that will affect T cell function. In particular, the patients studied here were all on glucocorticoid replacement therapy, oestrogen replacement and Vitamin D_3. Glucocorticoids are immunosuppressive and may therefore affect the proliferative response to anti-CD3 and anti-CD28, they are known to inhibit the production of all the cytokines investigated here and can promote the development of a Th2 phenotype (107). Vitamin D3 may also promote Th2 responses (108), whereas oestrogens can lead to increased antigen specific T cell responses and a skewing to a Th1 phenotype as evidenced by increased interferon γ production (109). Thus, it is not surprising that the data on PBMC proliferation and cytokine production, and resting lymphocyte subsets is equivocal.

3.6 Summary

In keeping with previous studies documenting the phenotype of APS1 patients (4), UK patients have a significant disease burden. Being able to predict new disease manifestations would significantly improve the management of patients with APS1. However, although there is a positive relationship between the *IDDM2* locus and type 1 diabetes in APS1, it does not enable the absolute prediction of diabetes susceptibility.

Patients with APS1 have no differences in cell surface marker expression compared to controls, and although there is a trend to higher background proliferation, the fold change in proliferation and cytokine secretion from stimulated PBMCs is no different. Thus, no firm conclusions could be drawn from these data due to the small number of patients readily available for study, the heterogeneity of the disease and the further confounding factor of the treatment required by the patients.

CHAPTER 4

4 Expression of Aire in adult and embryonic murine tissues

4.1 Introduction

The pattern of human *AIRE* mRNA expression was first described in 1997 by 2 independent groups (2,3). Northern analyses showed mRNA expression in thymus, lymph node and fetal liver. *AIRE* expression was also reported in spleen and tissues affected in APS1, such as adrenal cortex and pancreas by one group (2), but not by another (3). Human AIRE protein expression, as determined by immunohistochemical staining, was seen in thymic medulla, lymph node, spleen and fetal liver (51,8) but expression was not observed in tissues other than these (8).

Reports of the tissue distribution of murine *Aire* mRNA are also discordant. Although *Aire* mRNA could not be detected by northern blot analysis (23,5,73), RT-PCR revealed the presence of *Aire* transcripts in heart, lung, testis (23,8,73), thymus (7,6,73) and lymph node (7,6). There are conflicting reports of *Aire* mRNA expression in spleen (23,7,73), kidney, brain (23,6), and liver (6,73). A single report found *Aire* mRNA in ovary, adrenal gland and thyroid (73).

Aire protein has been found in adult thymic medullary epithelial cells (7,6,74), and in thyroid, gut, pancreas and brain (7,74). Aire protein expression in spleen, lymph node, adrenal gland, lung, ovary, liver, kidney and testis is discordant between studies (7,6,74).

In the murine embryo, Aire expression can be seen using RT-PCR, *in-situ* hybridisation and immunohistochemistry from embryonic day 14.5 in thymic medullary epithelial cells (23,5,7).

Characterising the normal distribution of Aire is crucial to the understanding of its role in maintaining self-tolerance. However, it is clear, there is a lack of consensus regarding the tissue distribution of Aire, and variability in expression as determined by the same technique between studies. Therefore, a comprehensive survey of Aire mRNA expression using RT-PCR, *in-situ* hybridisation and real time RT-PCR, and protein using immunohistochemistry was undertaken in adult murine tissues to clarify this issue. In addition, protein expression in the whole embryo was investigated, as to date Aire expression has only been described in the embryonic thymus.

The aims of this chapter were

1. to characterise the tissue distribution of Aire mRNA and protein in the adult.
2. to characterise the tissue distribution of Aire mRNA and protein in the embryo.
3. to assess differences in level of mRNA expression between the embryo and adult

4.2 Expression of *Aire* mRNA in tissues of adult mice

The tissue distribution and level of mRNA expression in adult mice was investigated using RT-PCR, *in-situ* hybridisation and real time RT-PCR.

4.2.1 RT-PCR

Initial characterisation of mRNA expression was performed on thymus, spleen, liver and 2 of the target organs in APS1 pancreas and adrenal gland, from the out-bred strain CD1, as described in section 2.12.2. Expression was seen in thymus and weak expression was seen in the spleen (Fig 4.1A).

4.2.2 *in-situ* hybridisation

To gain information regarding spatial distribution, *in-situ* hybridisation was undertaken on tissues from CD1 mice. Using this relatively insensitive method, expression could only be determined in the adult thymic medulla (Fig 4.1B).

4.2.3 Real Time RT-PCR

In view of the low level of expression seen using RT-PCR and *in-situ* hybridisation, real time RT-PCR was used to further delineate *Aire* mRNA. For these experiments, adult CD1 thymus was used as a positive control, and was run on all plates as a calibrator. Expression is determined as a fold change compared to this calibrator; n=3 for all tissues examined. The highest expression was seen in C57/BL6J thymus (mean 4.3 fold higher than CD1 thymus; range 0.9-6.5) (Fig 4.2). All other tissues investigated expressed Aire mRNA, at varying levels, that were less than in the

positive control. Low levels of mRNA relative to thymus were seen in spleen, testis, kidney, liver, brain, lung, ovary, heart and gut, with barely detectable expression in adrenal gland.

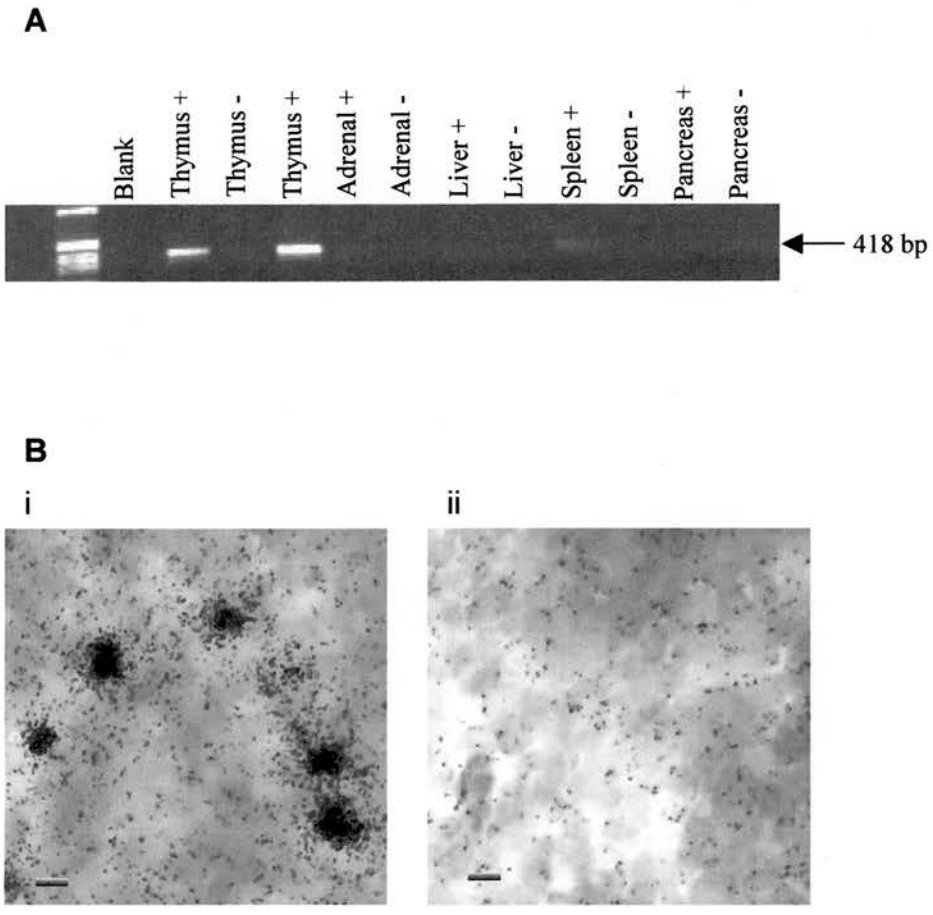

Fig 4.1 RNA expression of Aire in murine tissues. A RT-PCR of whole tissues from CD1 mice using primers specific for *Aire*

B Expression of Aire mRNA is seen in the thymic medulla of CD1 mice by *in-situ* hybridisation; i) antisense probe; ii) sense probe (original magnification x200; scale bar represents 20μm)

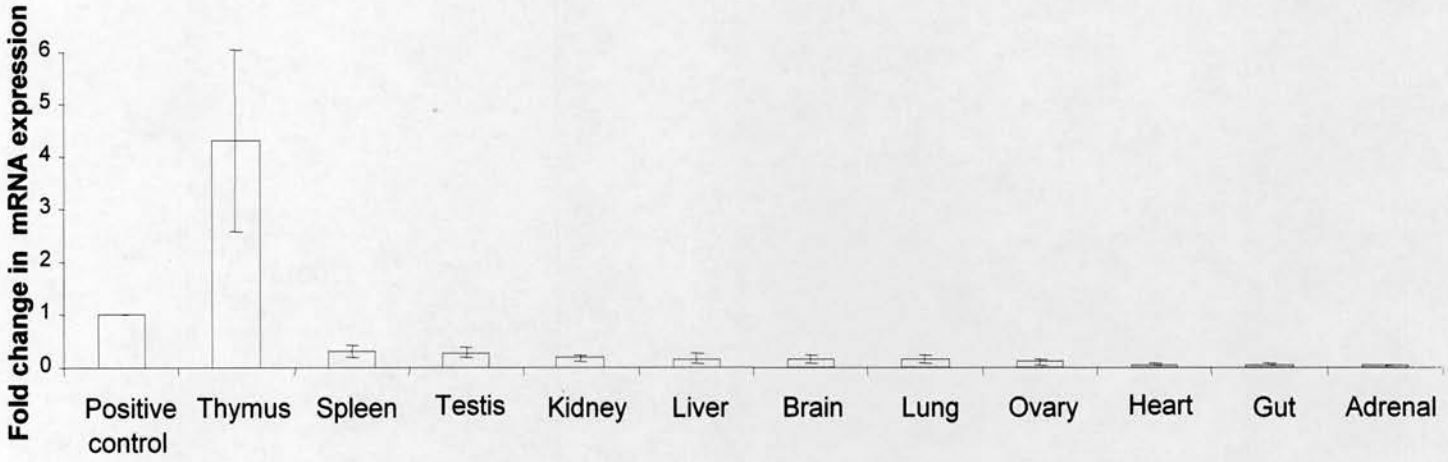

Fig 4.2 *Aire* expression demonstrated by Real Time RT-PCR. mRNA from whole tissues was reverse transcribed nad used as the template for PCR with Aire specific primers and probe. All samples are shown as a fold change in mRNA expression compared to a calibrator which has a value of 1.

4.3 Expression of Aire mRNA in tissues of embryonic mice

Aire mRNA and protein expression have previously been described in the murine thymus from E14.5 (23,5,7). However, there was no data on the distribution of Aire elsewhere in the embryo, in particular in the haematologically/immunologically important organs, liver and spleen. This was investigated at the mRNA and protein level using *in-situ* hybridisation and immunohistochemistry, and the level of mRNA expression was compared to that in the adult using real time RT-PCR

4.3.1 *in-situ* hybridisation

Aire expression was detected by ISH from E14.5 in the thymus of C57/Bl6J embryos (Fig 4.3) this is in keeping with previous reports, Balb/C mice were used in one of these reports (7), the mouse strain used is not specified in the others (23,5,7). No other specific expression was seen by ISH.

4.3.2 Real Time RT-PCR

mRNA from C57/Bl6J spleen, thymus and liver at E16.5 was reverse transcribed to use as the template for real time PCR. No amplification was detected even after 40 cycles from liver. There was however, amplification in both thymus and spleen (Fig 4.4A). In view of the lack of amplification in liver, other tissues, in which *Aire* mRNA expression would be expected to be lower, were not analysed.

4.3.3 mRNA expression in the adult compared to the embryo

In order to determine the relative expression of *Aire* mRNA between the adult and the embryo, real time RT-PCR was performed on spleen and thymus, these tissues were chosen as they express the highest levels of *Aire*.

In the spleen, expression in the embryo at E16.5 was 20 fold less than in the adult (Fig 4.4B). A lower level of expression in the embryo compared to the adult was also seen in the thymus (Fig 4.4C).

A

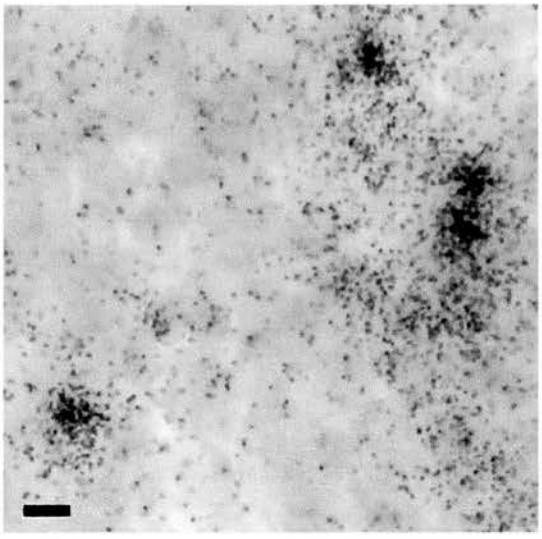

B

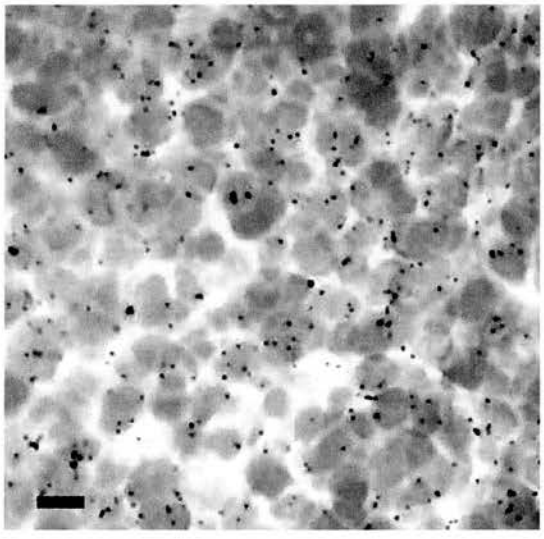

Fig 4.3 *Aire* mRNA expression at E14.5 demonstrated by *in-situ* hybridisation. *Aire* mRNA expression demonstrated by *in-situ* hybridisation in the thymic medulla **A)** antisense probe; **B)** sense probe; scale bar represents 20μM.

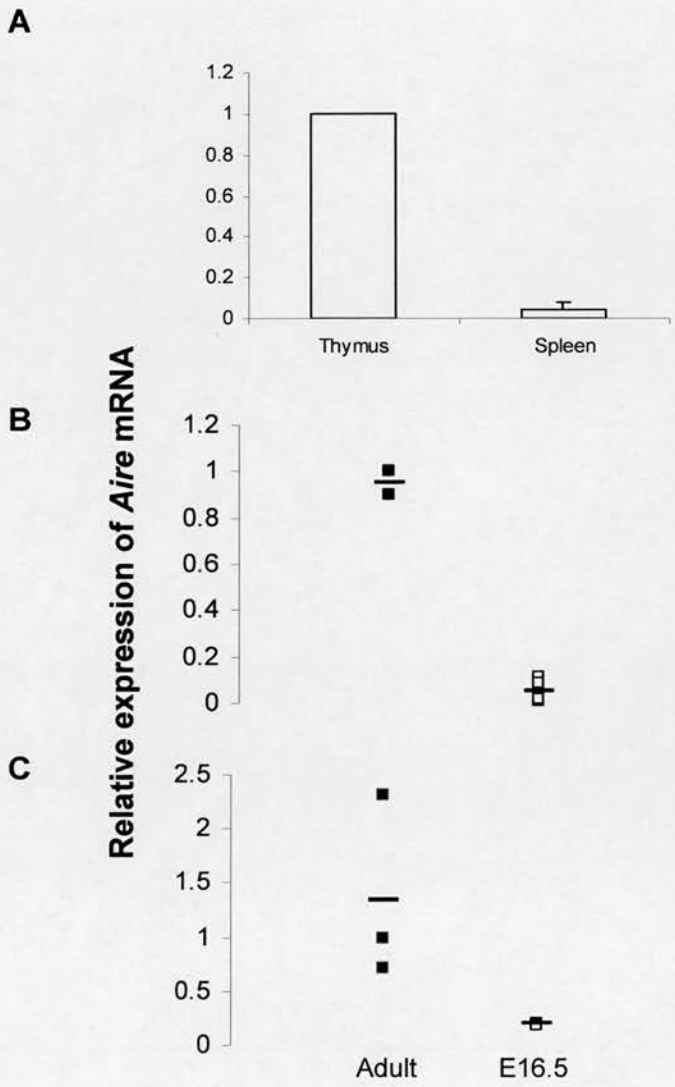

Fig 4.4 *Aire* mRNA expression in embryonic mice demonstrated by real time RT-PCR. A cDNA from whole tissues at E16.5. Data is represented as a fold change in mRNA expression compared to the calibrator sample which has a value of 1; **B+C** Data from individual mice is represented by an individual data point, the mean is shown by the bar. **B** cDNA from whole spleen from adult and E16.5 mice; **C** cDNA from whole thymus from adult and E16.5 mice.

4.4 Expression of Aire protein in tissues of adult mice

Immunohistochemistry was performed on tissues from C57/BL6J mice. Peptide preabsorbed Aire antiserum, preimmune antisera and secondary antibody were used as controls in all tissues examined, and no staining was seen (Fig 2.6).

Aire expression within the thymus (Fig 4.5A) was most marked within the thymic medullary epithelial cells, with occasional medullary and cortical non-epithelial cells also staining. In lymph nodes (Fig 4.5B), the light zone of the germinal centre of the lymphoid follicles showed positive staining, whilst in the dark zone there was some staining but the majority of cells were negative. Positive staining was also seen in the T cell areas of the lymph node. This was also the case in spleen where the positive staining was seen in the nuclei of cells in T cell areas of the white pulp (Fig 4.5C). There was no staining in the red pulp.

In many other tissues including lung, kidney and fallopian tube, there was expression within epithelial cells. This is illustrated in the large airways of the lung (Fig 4.5D) where the only positive staining is in the epithelial cells. No staining was detected within the small airways or alveoli.

Staining was observed in epithelial cells of the kidney (Fig 4.5E), within the tubules and the glomerulus. Similarly, the columnar epithelium of the fallopian tubes also stains positively.

No specific staining was seen in the epithelial cells of the small intestinal villi or in the neuroendocrine cells of the gut, but strong staining was seen in the mucin spaces of the goblet cells (Fig 4.5F). The significance of this is unclear, but loss of goblet cells is a feature of autoimmune disease of the gut (110,111).

Within the testis (Fig 4.5G), Aire staining was seen in the developing spermatocytes, but not in the mature haploid cells, whilst in the ovary, staining was seen in the follicular cells (Fig 4.5H). In the brain, staining was present in the neurones of the hippocampus and cortex. All of this staining was absent in sections incubated with pre-immune serum and was abolished by preabsorption of the Aire anti-serum with a blocking peptide. No staining was seen in the heart (Fig 4.5I), liver (Fig 4.5J) or any zone of the adrenal gland (Fig 4.5K).

This pattern mimics that described above for real time RT-PCR, as tissues where a greater population of cells stain have higher mRNA expression, e.g. thymus, spleen and kidney. The only discrepancies between the real time PCR data and IHC are for liver and heart, as mRNA expression is detectable in these tissues, albeit at low levels, but no staining is seen in these tissues. This may reflect the fact that real time RT-PCR is highly sensitive and is therefore able to detect a very low level of mRNA, whilst protein expression is either absent or not detectable by IHC. Immunohistochemistry was also performed on tissues from the outbred strain CD1, the pattern of staining seen is consistent with that in the inbred strain C57/BL6J (data not shown).

When compared to the study of Halonen et al (6), the obvious discrepancy is that they report staining in the zona glomerulosa of the adrenal gland and in the liver in hepatocytes and Küppfer cells, but as can be seen in figures 4.5J+K, no positive staining was seen here. In view of this, western blotting of liver and adrenal gland was undertaken. This confirms the absence of Aire protein in these tissues in this system (Fig 4.6). Ideally, the antibody used by Halonen et al should be used to investigate the tissues examined here, as this differential staining most likely

represents as difference in the 2 antibodies used. Unfortunately, the antibody used by Halonen et al was not available.

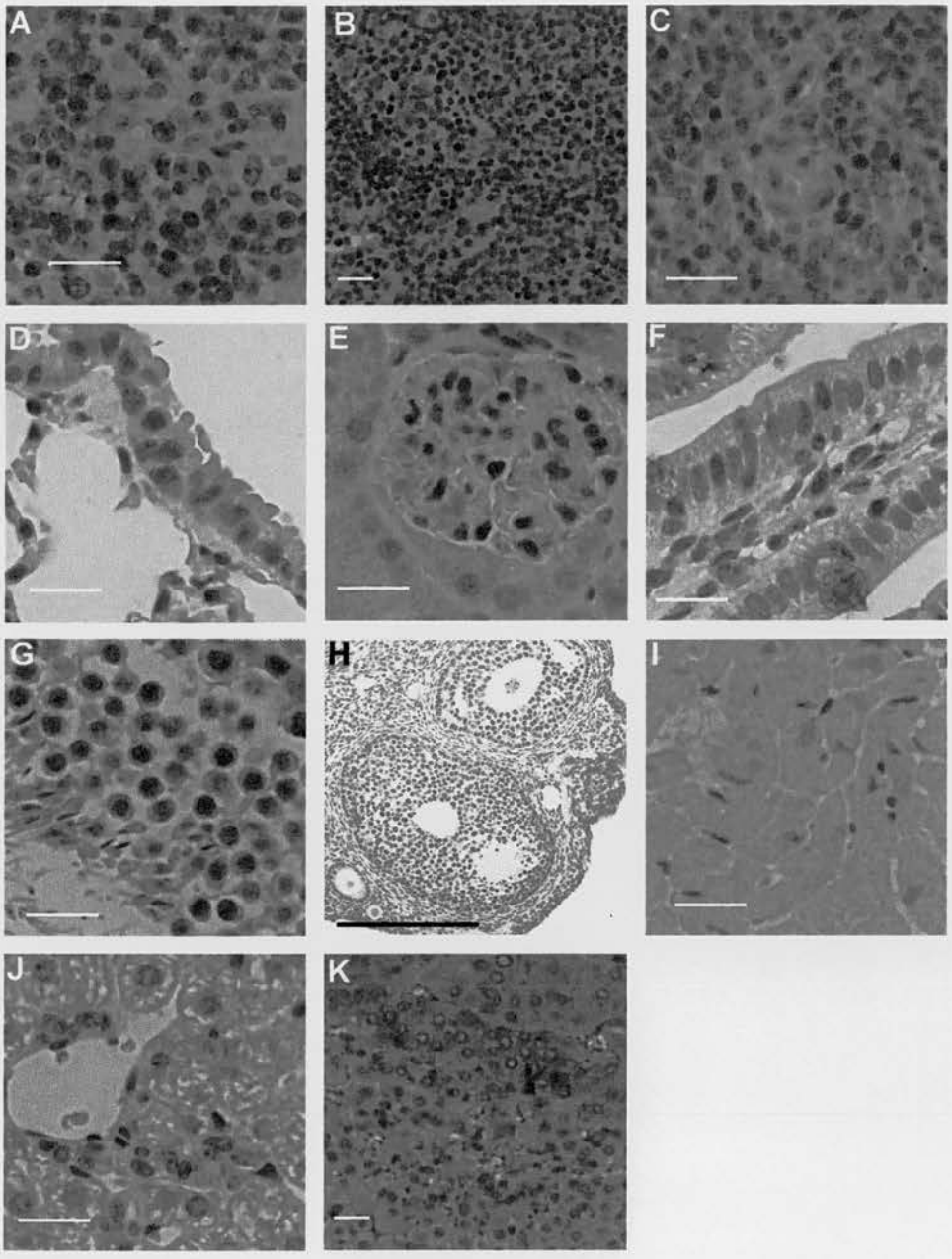

Fig. 4.5 Immunohistochemistry of murine adult tissues demonstrating expression of Aire. A Thymus; **B** Lymph node; **C** Spleen; **D** Lung; **E** Kidney; **F** Gut; **G** Testis; **H** Ovary; **I** Heart; **J** Liver; **K** Adrenal Gland. A,C,D,E,F,G,H,I,J original magnification x200; B,K original magnification x100; scale bar represents 20 μm

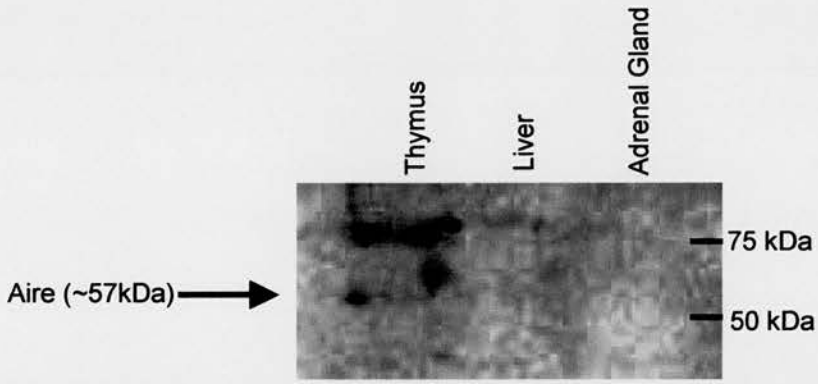

Fig 4.6 Western blot demonstrating lack of Aire expression in liver and adrenal gland. Whole thymus is used as a positive control, and Aire is detected at ~57kDa as expected. No expression is seen in liver or adrenal gland.

4.5 Expression of Aire protein in tissues of embryonic mice

mRNA expression was seen from E14.5, therefore, IHC was undertaken from E14.5. Aire protein expression within the thymus was seen from E14.5 (Fig 4.7A) to term. Unlike the adult, expression was seen at E14.5 in the liver (Fig 4.7C) and remained at E18.5 (Fig 4.7D), presumably reflecting that this is the main site of haematopoiesis in the embryo.

Staining was also observed in the epithelial and interstitial cells of the developing lung (Fig 4.7E+F) in the large airways, as demonstrated in the adult. Unlike the adult, positive staining was detected in the epithelial cells of the gut at E14.5 (Fig 4.7G). This staining decreased but remained present towards term, and was accompanied by the presence of staining in the mucin spaces of goblet cells, in the same pattern as the adult (Fig 4.7H).

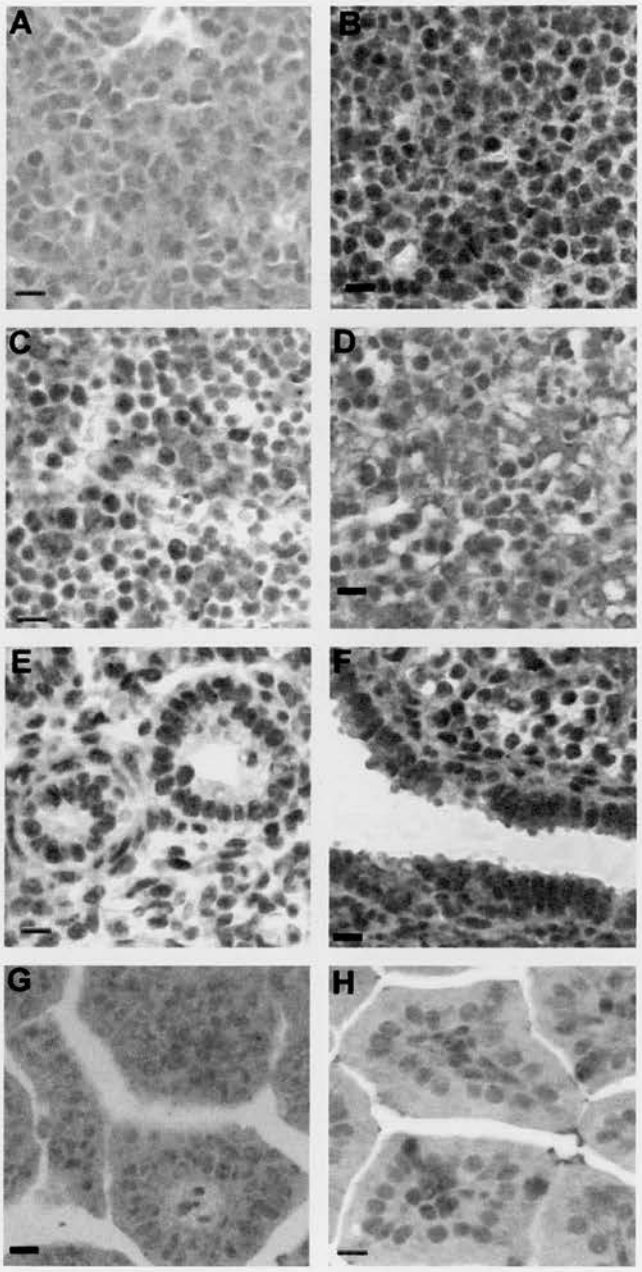

Fig 4.7 Immunohistochemistry of murine embryonic tissues at E14.5 and E18.5. A Thymus E14.5; **B** Thymus E18.5; **C** Liver E14.5; **D** Liver E18.5; **E** Lung E14.5; **F** Lung E18.5; **G** Gut E14.5; **H** Gut E18.5. Original magnification x200; scale bar represents 20μM

4.6 Discussion

These results reveal the presence of Aire protein in immunologically relevant murine tissues and a restricted number of peripheral tissues. In the thymus, mRNA and protein was detected primarily within the medulla as previously published for both human and murine tissue (51,8,7,6). Thymic medullary epithelial cells have a role in tolerance induction through clonal deletion (112), the induction of anergy (113) and by supporting the development of regulatory T cells (114). As patients with APS1 have a breakdown in tolerance leading to autoimmune disease, the expression of Aire in this particular tissue is not surprising. Negative selection of autoreactive T cells within the thymus is an important mechanism in the prevention of autoimmune disease. Therefore, the increased expression of Aire seen in models of negative selection and the absence of Aire in the RelB-deficient mouse, in which there is a defect in negative selection are further important clues to Aire's function, although interpretation of the data in the RelB-deficient mouse is complicated by the fact that it has defective thymic development (71,7). These data, in addition to the recently described Aire knock-out mice, in which there is a defect in ectopic expression of peripheral antigens in the thymus (13) and failure of deletion of organ specific T cells within the thymus (75), show the importance of Aire in the induction of central (thymic) tolerance.

In the lymph node, Aire expression has previously been reported in human and mouse. However, the pattern of expression in lymph node and spleen seen here is different to that reported by Halonen et al (6), who found no staining in B cell areas, compared to the staining in both B and T cell areas demonstrated above. They also

failed to detect Aire in the white pulp of the spleen (6), this is in contrast to the specific staining in the T cell areas of the white pulp shown here (Figure 4.5C).

In addition to the immune system, immunostaining was seen in epithelial cells of the lung, kidney, neurones within the cortex and hippocampus, in the ovary and testis and in the goblet cells of the gut. This goblet cell staining raises concern regarding the specificity of the antibody used here, as this pattern of staining is seen when non-specific staining is present, however, this staining was not seen in the absence of anti-Aire antiserum and in slides stained with pre-immune serum. The expression of the Aire protein in the lung, kidney and brain is more restricted in this study than in the earlier ones (6,115).

These discrepancies may be explained by the use of different antibodies in the two studies. The antibodies may recognise different epitopes, the peptide used by Halonen et al. is slightly different to that used here, as it overlaps the sequence used by 5 amino acids. Strain differences between the inbred C57/BL6J mice used in this study and the outbred NMRI mice used by Halonen et al. (6) may also account for variation in the pattern of staining. However, the pattern of protein expression in the outbred strain CD1 was similar to that in C57/BL6J mice. A study on Balb/C mice (7) revealed protein expression in the thymic medulla as demonstrated here, but not in other tissues examined including testis, adrenal gland, lymph node, spleen and liver.

In the embryo, in common with another report (23), Aire mRNA was detected in the thymus by *in-situ* hybridisation from E14.5. Using the more sensitive technique of

real time RT-PCR Aire mRNA was detected at low level in the spleen. Protein expression was also seen from E14.5 and persisted through to E18.5. Expression was also seen within the embryonic liver from E14.5 and towards term, consistent with the liver's role in haematopoiesis. Expression of protein and mRNA has also been reported in the human fetal liver (8).

In the embryo as in the adult, Aire expression is present in the epithelial cells of the lung and developing renal tubules. Additionally, Aire expression is seen in the epithelial cells of the gut at E14.5, as reported by Halonen et al. (6) in the adult. In the embryo Aire is absent by E18.5, and we observe the same pattern of expression as in the adult, namely expression in the mucin spaces of the goblet cells only.

Positive staining for mRNA by *in situ* hybridisation was only seen in the thymus and not in the other tissues studied. This may reflect either absent or very low levels of expression in these tissues, below the limit of detection of this technique. These findings complement those of others, as this is a common theme in previously published work in mouse and human (23,8,73). In Balb/C mice Aire mRNA could be detected outside the immune system but nested PCR was required due to low levels of signal (7). The presence of low level expression is strongly suggested by real-time PCR. The lack of staining seen in adrenal gland, suggests that the barely detectable signal from real time PCR, may either be from a migrating cell type, as described by Heino et al (7), due to the higher sensitivity of this technique, or Aire mRNA may be shortlived in comparison to protein.

In conclusion, the data described here show that Aire is expressed at the protein and mRNA level in immunologically relevant tissues and in a restricted number of other tissues in the adult. Novel data are presented on the expression of Aire protein in extra-thymic tissues of the embryo. Of particular interest is the expression seen within the immune privileged sites of testis and brain, especially in view of the high proportion of male patients who develop testicular failure (4), and in the goblet cells of the gut, which are lost in autoimmune disease at this site. The role of Aire in these tissues remains to be elucidated, but raises questions regarding the role of Aire in the peripheral immune responses.

CHAPTER 5

5 Cellular localisation and expression of Aire

5.1 Introduction

When transfected into epithelial or monocyte cell lines, human AIRE has been observed to be localised predominantly in the nucleus in a speckled pattern (51,8,52). This speckled pattern is similar to that seen with proteins that form nuclear bodies, but AIRE does not co-localise with promyelotic leukaemia protein (PML) or Sp100 (51,52). It was therefore of interest to determine if AIRE co-localised with any other nuclear proteins.

The previous subcellular localisation of Aire was determined in over-expressing cell lines rather than primary cells, and in common with the tissue distribution of Aire, there is a lack of a consensus about the cellular distribution of Aire. In their work on the distribution of AIRE in human spleen, Heino et al described protein and mRNA expression (8), and Bjorses et al found protein expression in lymphocytes in the red pulp only (51).

In the mouse, Halonen et al found protein expression in the red pulp of the spleen in lymphocytes and neutrophils (6), but in work by Heino et al, no protein expression was detected in the murine spleen, and the mRNA expression seen there was attributed to expression by splenic dendritic cells (7). As shown in the previous chapter, a low level of mRNA expression was detected in the spleen by real time RT-PCR, and protein expression was in the white pulp of the spleen, but not in the red pulp.

It should be emphasised that the staining in all of these previous papers is for Aire alone. No double staining for cell surface markers has been performed, thus any conclusions reached regarding the cell types expression Aire in the spleen are based on morphology and geographical position.

Two groups have investigated AIRE protein expression in peripheral blood in humans, with discordant findings. One group shows that on a smear of peripheral blood leucocytes strong staining was seen in a 'large population' of lymphocytes, neutrophilic granulocytes and monocytes. Paradoxically, in the same paper, once these cells had been prepared as a cytospin, only approximately 5% of the cells expressed AIRE protein (51). Kogawa et al, examined AIRE expression in MACS purified populations of cells from peripheral blood. They found that *AIRE* mRNA was detectable by RT-PCR in CD14 positive cells but not in CD4 positive cells; the same distribution was seen for protein expression, where 93% of CD14+ cells stained for AIRE whilst less than 3% of CD4+ cells were positive (72).

In mouse peripheral blood smears, lymphocytes, polymorphonuclear leucocytes and monocytes stained positively for Aire, but there was no double staining of these cells for cell surface markers (6).

Thus, there was a need to determine Aire expression in immune cell subsets, and to investigate whether this would change on activation of the cells.

The aims of this chapter were

1. to investigate the relationship between Aire and other nuclear proteins
2. to characterise the expression of Aire in immune cell subsets

3. to characterise the effect on Aire expression when these cells are activated

5.2 Interaction with nuclear proteins

It is becoming increasingly evident that the location of a gene within a chromosome territory of the nucleus plays a role in its ability to access the nuclear machinery (116). This nuclear machinery encompasses many functions including transcription, RNA splicing, protein modification and cell cycle control (117). The proteins involved in these activities are contained in subcompartments of the nucleus or nuclear bodies (118). These include PML bodies, coiled bodies, gems, splicing speckles and nucleoli (117).

The pattern of AIRE expression in the nucleus has been noted to be reminiscent of PML bodies, however, AIRE does not co-localise with PML or Sp100, which are components of PML bodies (51,52).

Recently, a novel nuclear domain, termed paraspeckles has been identified (118). Paraspeckles contain paraspeckle protein 1 (PSP1), paraspeckle protein 2 (PSP2) and p54/nrb. p54/nrb has a role in transcriptional control, apoptosis, splicing, dsRNA processing and co-transcriptional control through interacting with steroid hormone nuclear receptors (119,120,121,122,123). PSP2 is a coactivator activator (124). The function of PSP1 is unknown but it may be involved in transcriptional control (118).

The pattern of staining seen with Aire in the nucleus appeared similar to that of PSP1, therefore the possibility that Aire and PSP1 co-localise was investigated.

Human adherent cells were used to investigate the co-localisation of AIRE and PSP1. These cells were chosen as those in peripheral blood, which were likely to express the highest levels of AIRE based on the evidence to date. It was necessary to use

human cells, as the only anti-PSP1 antibody available is an anti-human antibody that does not cross react with mouse.

Both antibodies were raised in rabbit, therefore, the anti-Aire antibody was directly FITC conjugated as described in section 2.13.1. Immunofluorescence was then performed on the adherent PBMCs. The signal from the FITC-conjugated AIRE, although detectable, was weak and was therefore amplified by using an anti-FITC antibody followed by an Alexa Fluor 488 antibody (Molecular Probes). Binding of the anti-PSP1 antibody was detected with an anti-rabbit Alexa Fluor 594 and the images captured using a confocal microscope (Section 2.13.8).

Both proteins were detected within the nucleus in a speckled pattern that co-localised (Fig 5.1). No staining was observed in the absence of the primary antibodies, and staining by the secondary antibodies was specific as demonstrated in figure 5.2. In view of this co-localisation, immunoprecipitation was performed with either anti-PSP1 or anti-AIRE antibodies. The resulting protein was subjected to analysis by western blotting and the membrane was probed with the opposite antibody. This demonstrated an interaction between the two proteins (Fig 5.3).

Immunofluoresence was also performed using anti-AIRE antibody and anti-SC35 antibody, a splicing factor present in the nucleus as speckles. No co-localisation was observed (Fig 5.4).

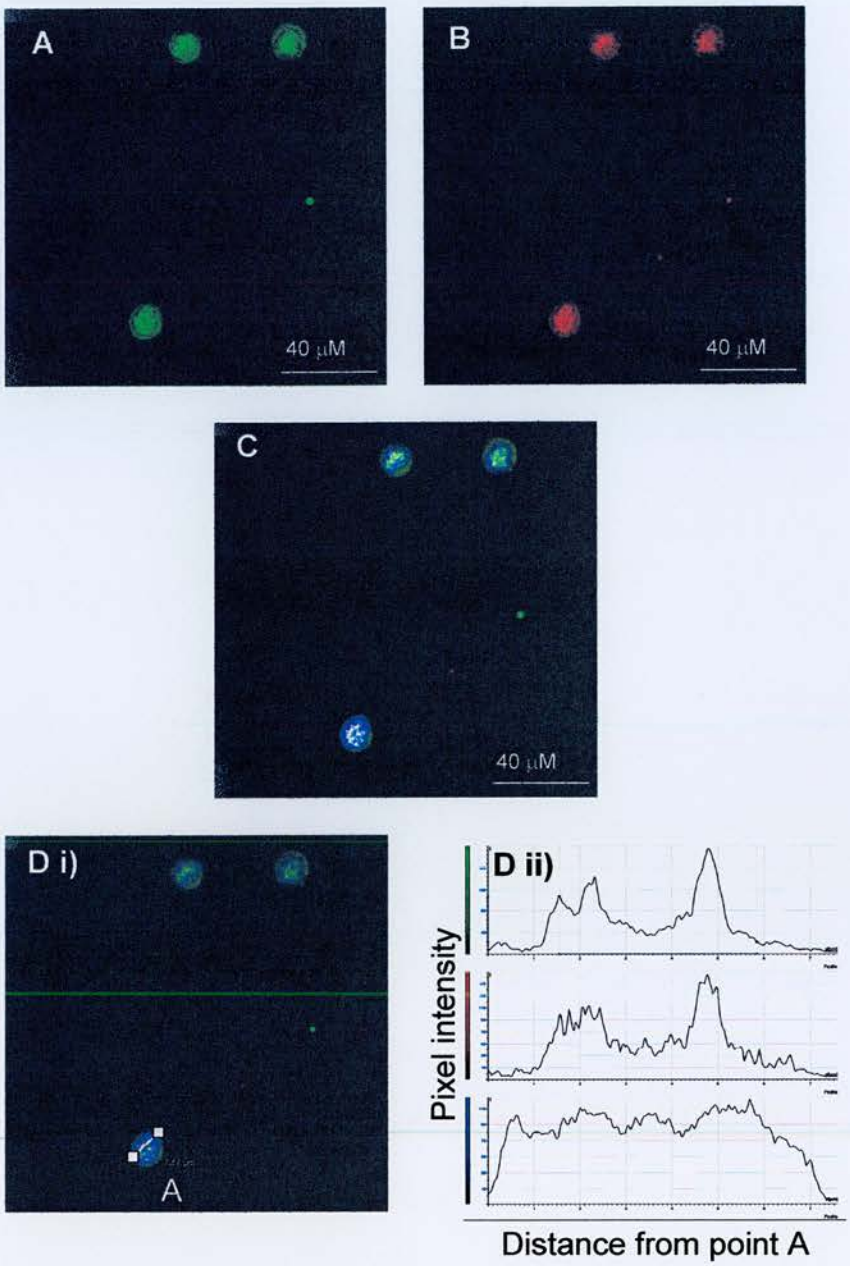

Fig 5.1 Co-localisation of AIRE and PSP1 within the cell. Human PBMCs were adhered for 1 hour in serum free media. The adherent cells were stained for **A** AIRE (green) and **B** PSP1 (red), and co-localisation is seen as yellow (**C**), the nucleus is stained with ToPro3 (blue); images were captured using a confocal microscope. **D i)** Pixel intensity along the line shown is depicted in **ii)** and confirms that there is co-localisation of AIRE and PSP1.

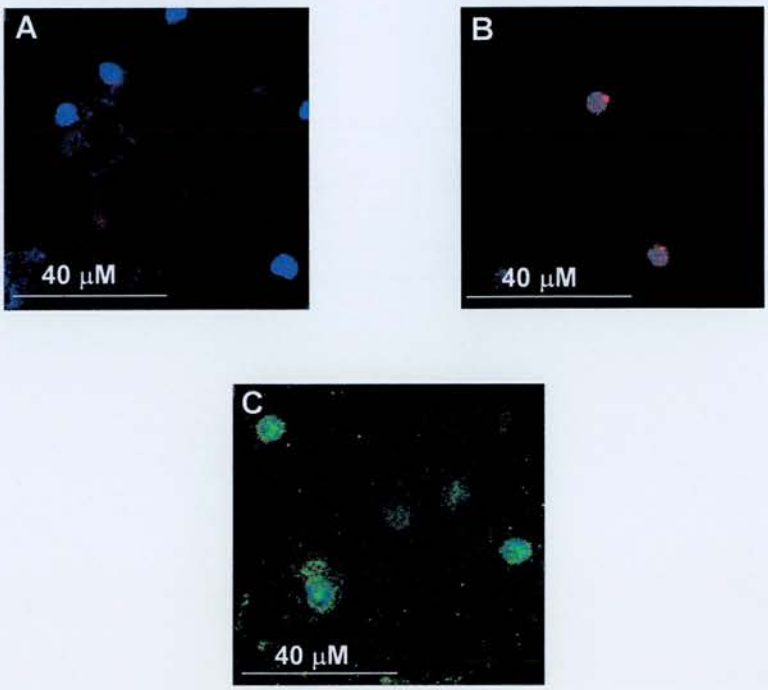

	PSP1 primary	PSP1 secondary	Aire Primary	Aire secondary
A	x	✓	x	✓
B	✓	✓	x	✓
C	x	✓	✓	✓

Fig 5.2 Control slides for double immunofluorescence with anti-AIRE and anti-PSP1 antibodies. The antibodies used are shown in the table. AIRE (green), PSP1 (red) and the nucleus is stained with ToPro3 (blue). No non-specific staining is seen.

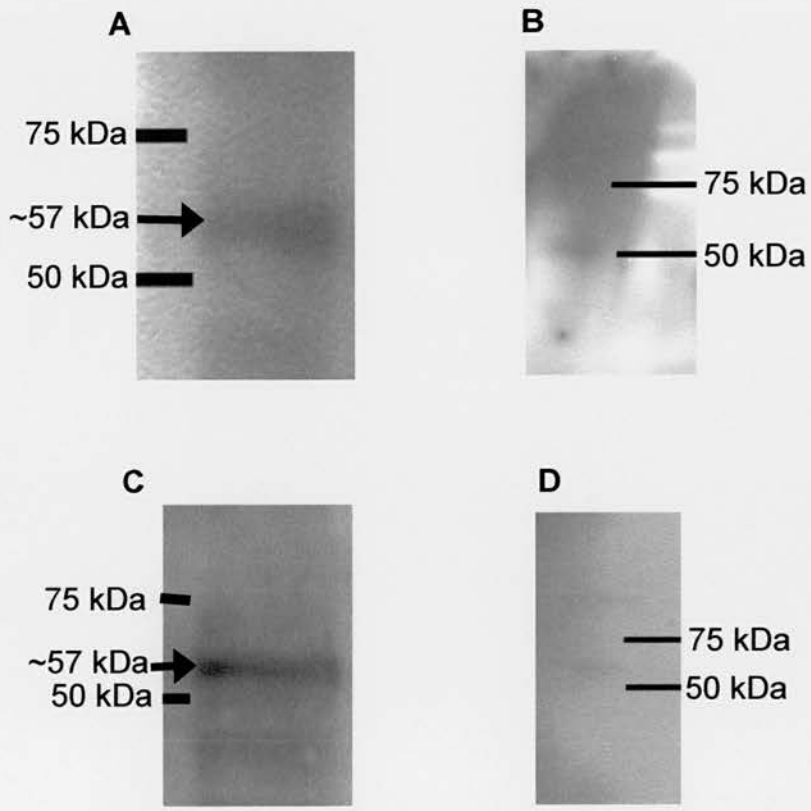

Fig 5.3 Immunoprecipitation of protein from human adherent PBMC's shows an interaction between AIRE and PSP1. A+B Immunoprecipitation with anti-AIRE antibody; **A** Membrane probed using anti-PSP1 antibody; **B** no primary control; **C+D** Immunoprecipitation with anti-PSP1 antibody; **C** Membrane probed using anti-AIRE antibody; **D** no primary control.

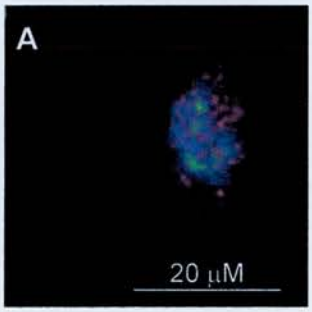

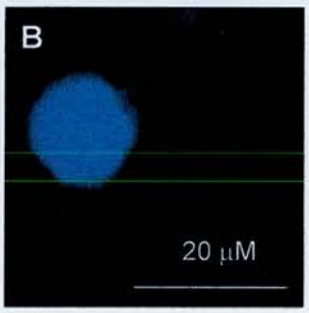

Fig 5.4 AIRE and sc35 do not co-localise. A Human adherent cells were stained with FITC labelled anti-Aire antibody (Green) and anti-sc35 antibody (red). No co-localisation was observed. **B** No primary control.

5.3 Aire expression in lymphocyte subsets

Given the controversy regarding whether Aire is expressed in lymphocytes and which, if any subsets it is seen in, the expression of Aire in immune cell subsets was investigated by immunohistochemistry. Briefly, T and B cells were isolated by mechanical disruption of the spleen, purified by MACS and stained using anti-Aire antibody. FACS analysis to check cell purity was also performed.

5.3.1 Aire expression in splenic B cells

B cells were isolated from the spleens of C57Bl/6J and BALB/c mice by positive selection for CD19 (Miltenyi Biotech). Cell purities as assessed by FACS were 90% and 93% respectively. The majority of these cells (>95%) express Aire protein, but the level of staining seen was not as bright as for NK and T cells (Fig 5.5). To confirm this observation, splenocytes from C57Bl6/J and BALB/c spleens were double stained with the anti-Aire antibody and an anti-IgD^b antibody (Section 2.13.8). Staining for Aire was observed in IgD^b positive cells (Fig 5.8).

5.3.2 Aire expression in splenic T cells

CD3+ T cells were isolated from the spleens of C57Bl/6J and BALB/c mice by negative selection using a T cell isolation kit (Miltenyi Biotech). Cell purities as assessed by FACS were 94% and 95% respectively. The majority of these cells (>95%) express Aire protein (Fig 5.6).

5.3.3 Aire expression in CD4+ and CD8+ T cells

In view of the expression in CD3+ lymphocytes, expression in CD4+ T cells was investigated. CD4+ T cells were isolated from C57/Bl6J and BALB/c spleens by negative selection using a CD4+ T cell isolation kit (Miltenyi Biotech). In 3 separate experiments using pooled C57/Bl6J spleens the cell purity was 85-90%. These cells express Aire protein (Fig 5.7B). CD4+ T cells from BALB/c spleen also express Aire protein (Fig 5.7A). This staining was confirmed to be in CD4+ cells by double staining with anti-Aire antibody and an anti CD4 antibody (Section 2.13.8) (Fig 5.8).

In a preliminary experiment to investigate whether AIRE is expressed in human CD4+ T cells, these cells were purified from a buffy coat by depletion of other cell subsets using a CD4+ T cell isolation kit (Miltenyi Biotech). In contrast to work published by Kogawa et al (72) these cells do express AIRE protein (Fig 5.7C).

Expression of Aire in CD8+ splenocytes was investigated, by double staining with anti-Aire antibody and an anti-CD8 antibody (Section 2.13.8), CD8+ cells also express Aire protein (Fig 5.8).

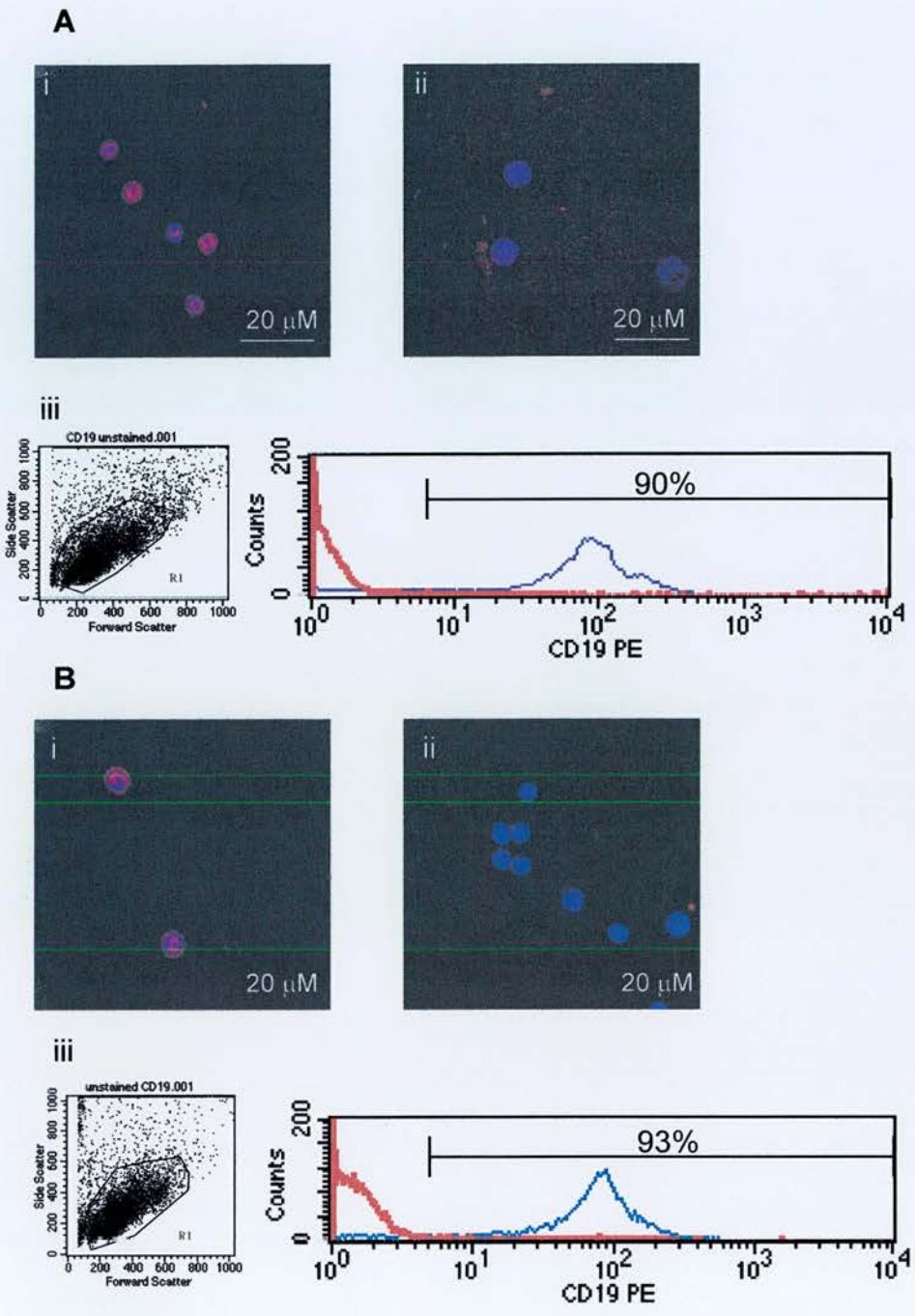

Fig 5.5 Splenic B cells express Aire. Aire expression by IHC in CD19+ splenic cells isolated by MACS. **A** C57/Bl6J **B** BALB/c **i)** Positive staining; **ii)** Negative control; **iii)** FACS analysis to show purity of cells obtained by MACS purification. Isotype control staining is shown by the red line.

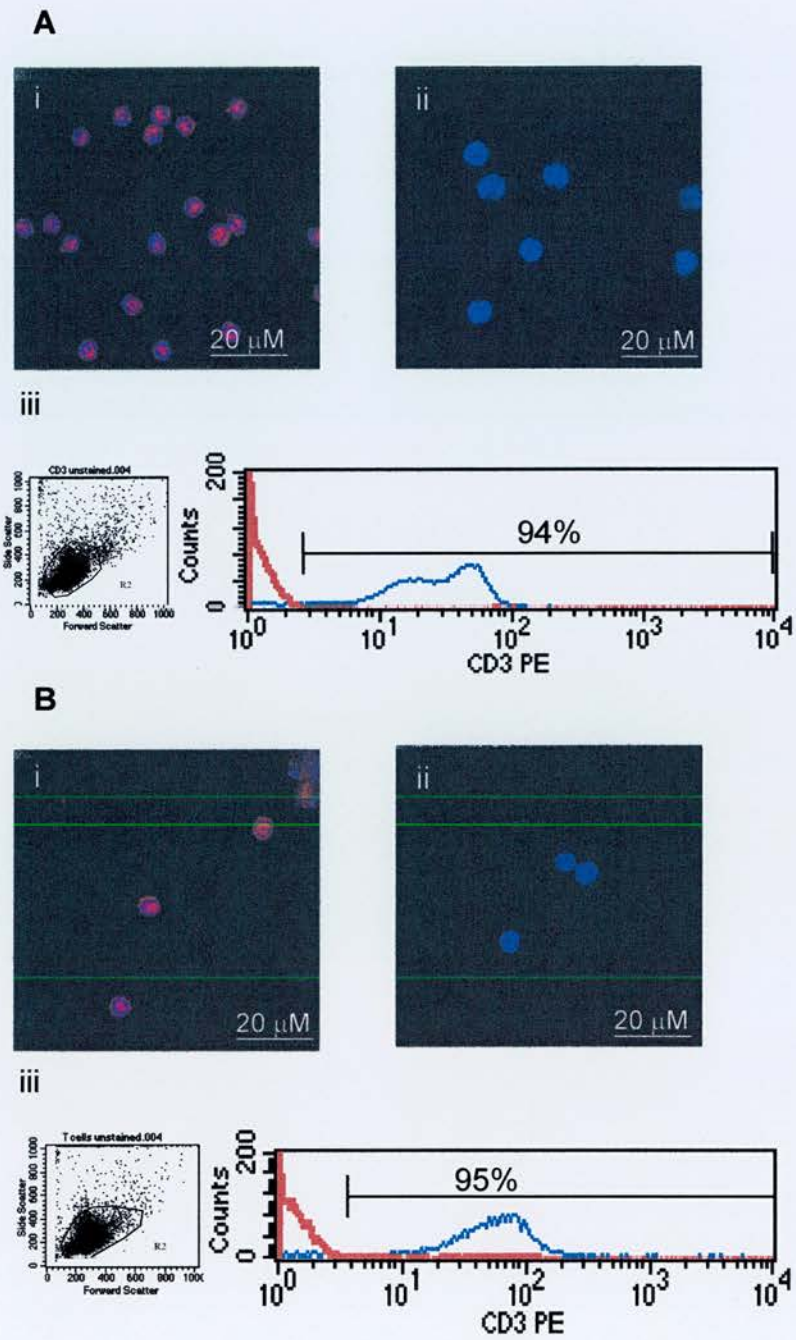

Fig 5.6 Splenic T cells express Aire. Aire expression by IHC in splenic T cells isolated by MACS. **A** C57/Bl6J **B** BALB/c **i)** Positive staining; **ii)** Negative control; **iii)** FACS analysis to show purity of cells obtained by MACS purification. Isotype control staining is shown by the red line.

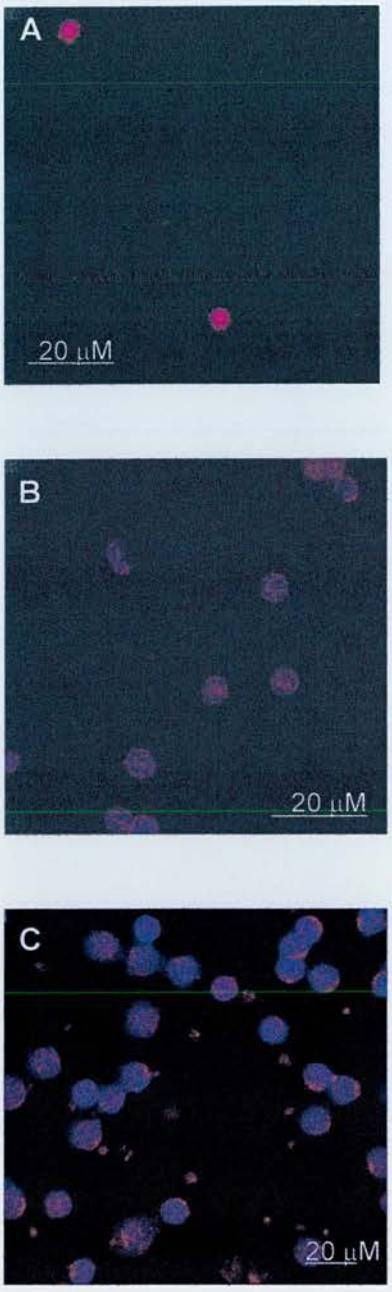

Fig 5.7 Aire is expressed in CD4+ T cells isolated from BALB/c and C57Bl6/J mouse spleen and human peripheral blood. Cells were stained with anti-AIRE antibody (red); the nucleus was stained with ToPro3 (blue). **A** BALB/c CD4+ T cells; **B** C57Bl6/J CD4+ T cells; **C** Human CD4+ T cells.

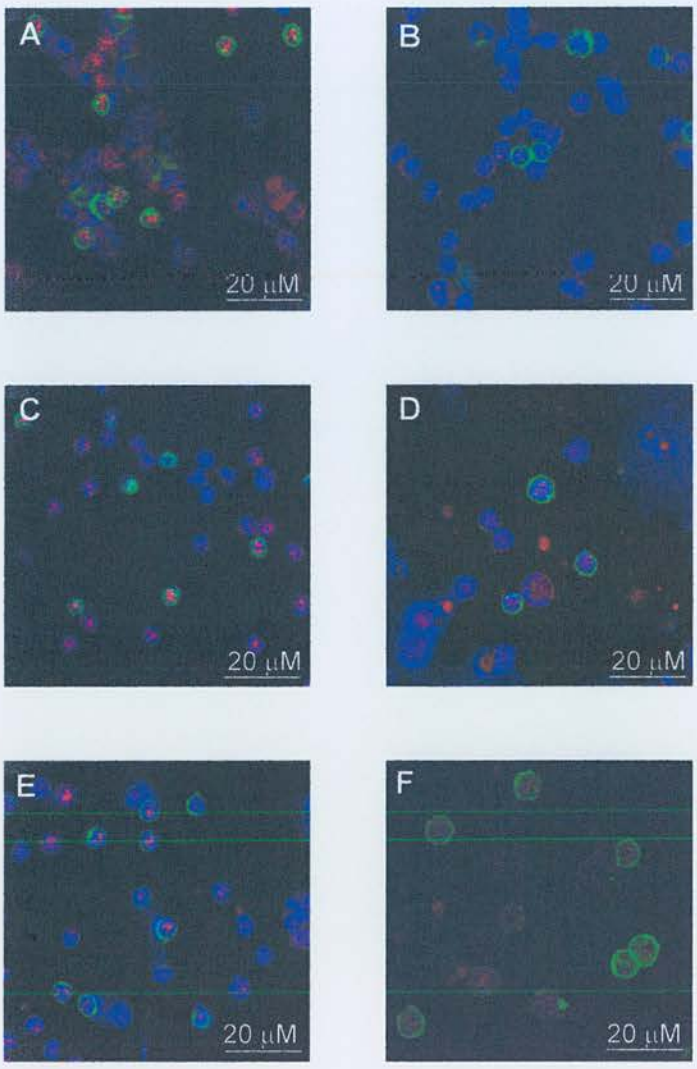

Fig 5.8 Aire protein is expressed in CD4+ and CD8+ T cells and B cells isolated from C57Bl6/J and BALB/c spleen. Splenocytes are stained with anti-Aire antibody (red) and antibodies against either CD4, CD8 or IgD^b (green), the nucleus is stained with ToPro3 (blue). A BALB/c splenocytes stained for Aire and CD4; **B** C57Bl6/J splenocytes stained for Aire and CD4; **C** BALB/c splenocytes stained for Aire and CD8; **D** C57Bl6/J splenocytes stained for Aire and CD8; **E** BALB/c splenocytes stained for Aire and IgD^b; **F** C57Bl6/J splenocytes stained for Aire and IgD^b.

5.4 Aire expression is increased in activated CD4+ T cells

Aire is known to have a role in central tolerance, however, the prevention of autoimmune disease is also dependent on the peripheral control of any autoreactive T cells, which do exit the thymus. The role of Aire in controlling a peripheral T cell response is unknown, but restimulation *in vitro* with HEL, in the Aire deficient mouse leads to increased proliferation compared to wild type (74), and in APS1 patients there was a trend to an increase in maximal proliferation (as described in 3.5.2). Therefore, the role of Aire in peripheral T cells was investigated.

CD4+ T cells were isolated from murine C57/Bl6J spleens, the spleens were mechanically disrupted and the CD4+ cells magnetically isolated by negative selection (section 2.14), cell purity was 85-90%. These cells were then activated using plate bound anti-CD3 antibody at 0.1μg/ml and soluble anti-CD28 antibody at 5 μg/ml for 24 or 48 hours (section 2.15.1), after which cell proliferation, assessed by the incorporation of tritiated thymidine (section 2.16), and up-regulation of activation markers, as demonstrated by FACS analysis, were used to determine activation status. Aire mRNA and protein expression were determined. Each experiment used pooled spleens, typically 4-6, and the data shown is from 7 individual experiments. At both 24 and 48 hours the CD4+ T cells proliferated in the presence of anti-CD3 and anti-CD28 antibodies, indicating that the cells had been activated (Fig 5.9). The activation markers, CD25 and CD69 were also up-regulated as shown by flow cytometry (Fig 5.10 + Fig 5.11).

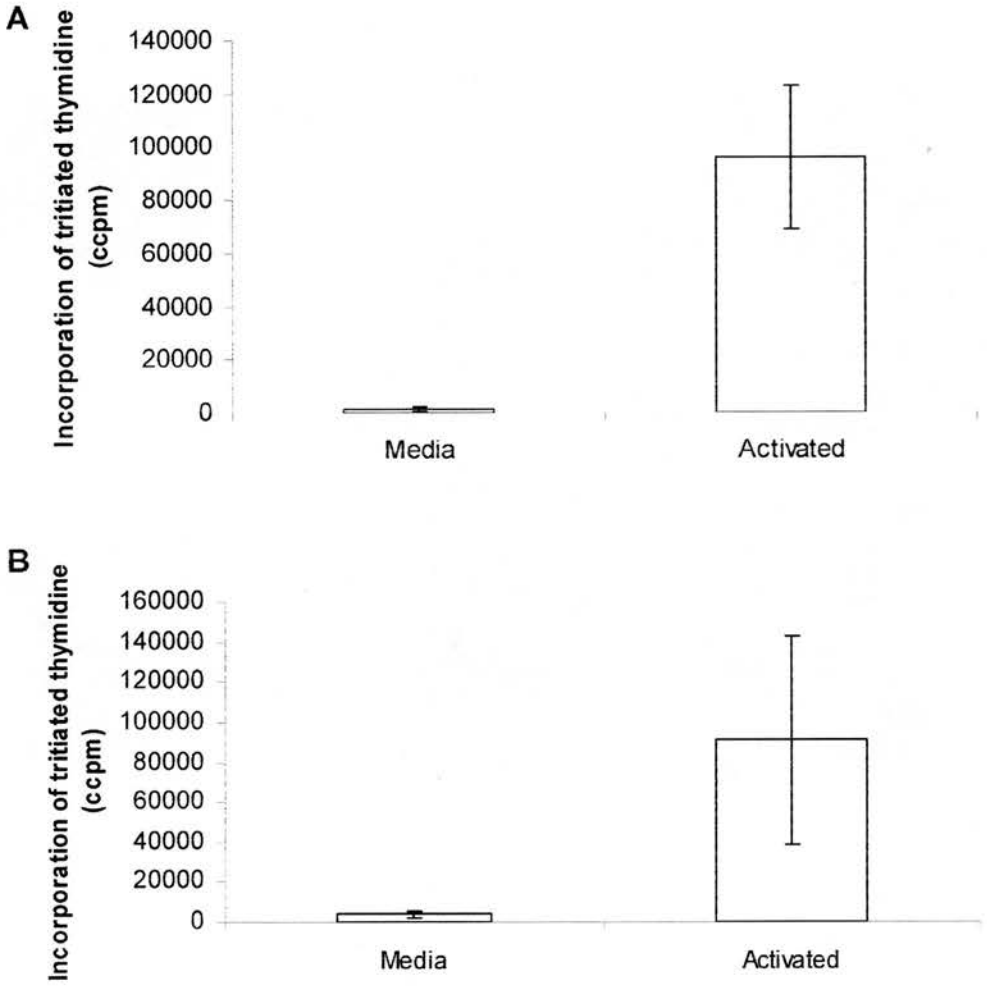

Fig 5.9 Proliferation of C57/Bl6J CD4+ T cells, as measured by the uptake of tritiated thymidine, in response to activation with anti-CD3 and anti-CD28 antibodies. A Proliferation at 24 hours; **B** Proliferation at 48 hours. Data are representative of 3 individual experiments.

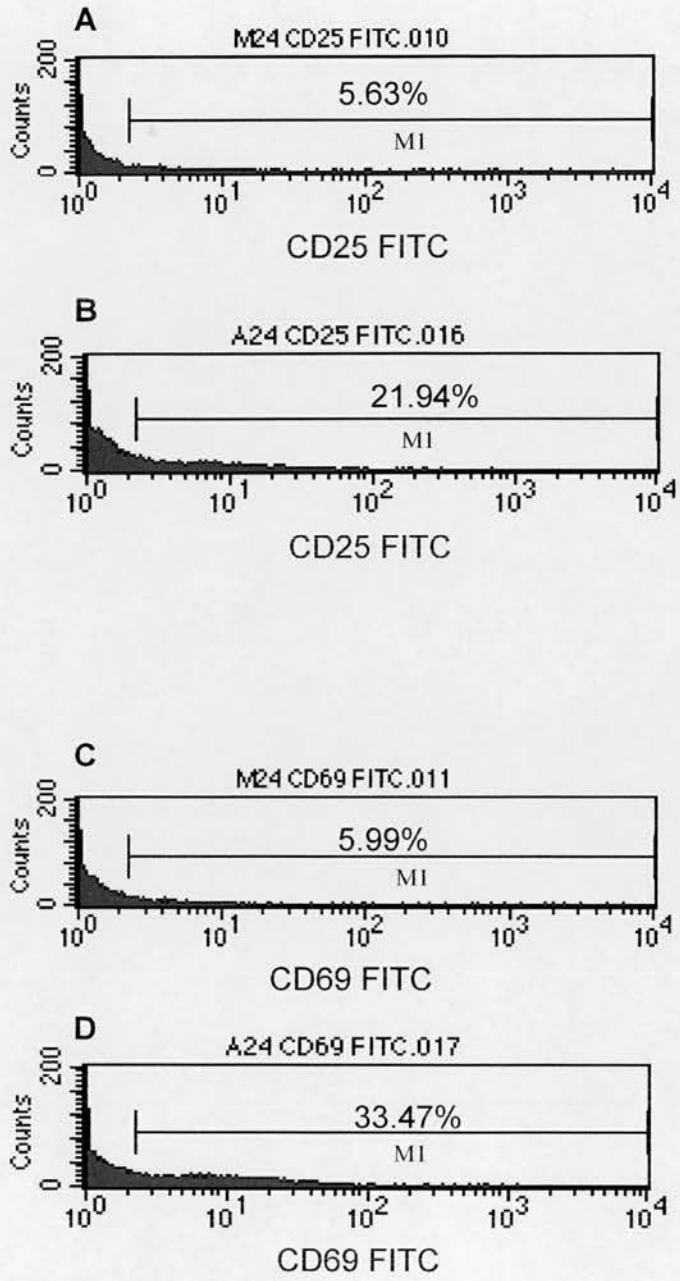

Fig 5.10 CD25 and CD69 are up-regulated upon activation of C57Bl6/J CD4+ T cells at 24 hours. A CD25 expression on resting CD4+ T cells; **B** CD25 expression on activated CD4+ T cells; **C** CD69 expression on resting CD4+ T cells; **D** CD69 expression on activated CD4+ T cells. Data are representative of 4 experiments.

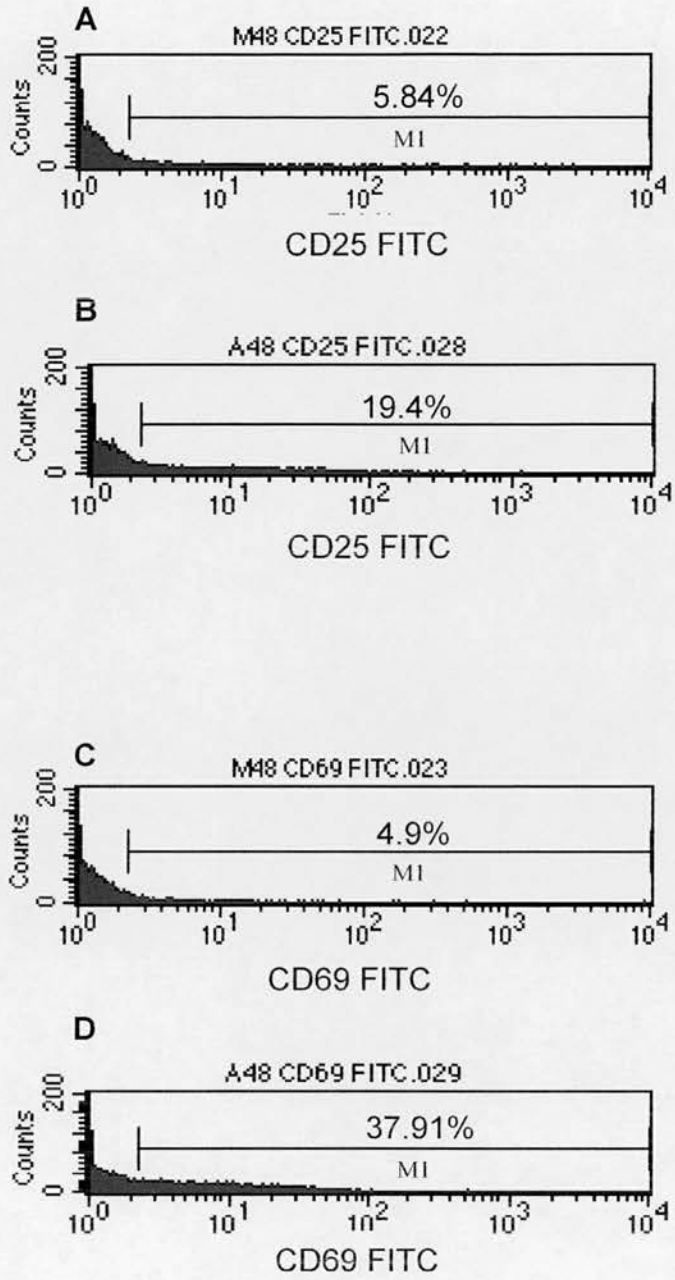

Fig 5.11 CD25 and CD69 are up-regulated upon activation of C57Bl6/J CD4+ T cells at 48 hours. A CD25 expression on resting CD4+ T cells; **B** CD25 expression on activated CD4+ T cells; **C** CD69 expression on resting CD4+ T cells; **D** CD69 expression on activated CD4+ T cells. Data are representative of 4 experiments.

5.4.1 *Aire* mRNA expression in activated CD4+ T cells

RNA was isolated from CD4+ T cells obtained as described above, reverse transcribed and used as the template for real-time RT-PCR using specific primers and probes for Aire (section 2.12.4). Five independent experiments were performed; in experiments 4 and 5 Aire expression was up-regulated at 24 hours. Aire expression remained up-regulated in experiment 4 at 48 hours and was also up-regulated in experiments 2 and 3 (Fig 5.12).

5.4.2 Aire protein expression in activated CD4+ T cells

Immunohistochemistry was performed on CD4+ T cells, using an anti-Aire antibody, the nucleus was delineated by staining with To-Pro3 and images were captured using a confocal microscope (section 2.13.8). Aire protein expression was up-regulated on activation at 24 and 48 hours, the data shown are representative of 3 experiments (Fig 5.13).

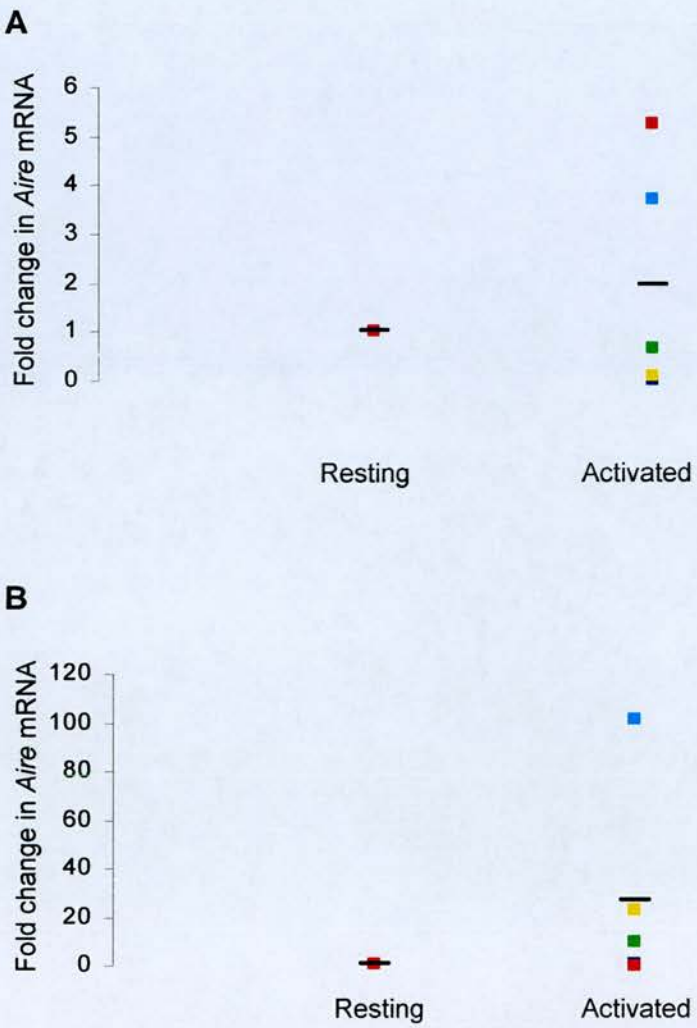

Fig 5.12 Real Time RT-PCR demonstrating *Aire* mRNA expression in activated CD4+ T cells. CD4+ T cells were purified from C57/Bl6J spleens and activated with anti-CD3 and anti-CD28 antibodies for **A** 24 or **B** 48 hours. The resting cells are used as the calibrator for each experiment. Data is plotted as individual data points for each experiment (n=5), the mean is represented by the bar.

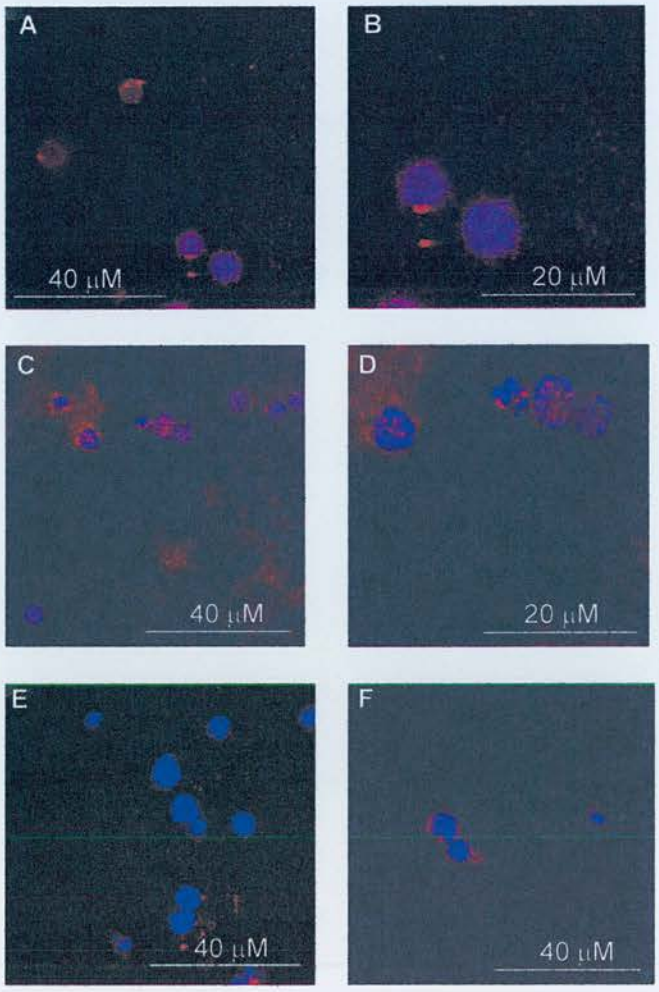

Fig 5.13 Activation of C57/Bl6J CD4+ T cells up-regulates Aire protein expression. Immunofluorescence of resting and anti-CD3/anti-CD28 treated CD4+ cells. Aire (red) Nucleus (blue) **A** Resting cells (original magnification x63); **B** Resting cells (original magnification x126); **C** Activated cells (original magnification x63); **D** Activated cells (original magnification x126); **E** Resting cells – negative control (original magnification x63); **F** Activated cells – negative control (original magnification x63). Data are representative of 3 experiments.

5.5 Aire mRNA and protein expression is also increased in activated BALB/c CD4+ cells

These experiments were also performed using BALB/c mice (as described above and section 2.15.1), however, for these experiments anti-CD28 antibodies were used at 1 μg/ml, as this concentration gave a similar increase in proliferation as 5μg/ml. In addition to investigating protein expression at 24 and 48 hours, a 72 hour time point was included in these experiments and cells were also stimulated with anti-CD3 antibodies alone as well as in combination with anti-CD28 antibodies.

Aire mRNA expression was increased upon activation with anti-CD3 antibody in 3 out of 4 experiments, and in 2 out of 3 experiments with anti-CD3 and anti-CD28 antibodies at 24 hours (Fig 5.14A). At 48 hours *Aire* mRNA expression was increased in 2 out of 4 experiments when CD4+ T cells were activated with both anti-CD3 and anti-CD28 antibodies (Fig 5.14B). No up-regulation in mRNA was seen at 72 hours (Fig 5.14C).

Aire protein expression was up-regulated on activation by 24 hours in these experiments and remained increased at 72 hours, no difference was observed in Aire expression between cells activated with anti-CD3 alone compared to anti-CD3/28 treated cells, this finding was reproduced in 3 separate experiments (Fig 5.15).

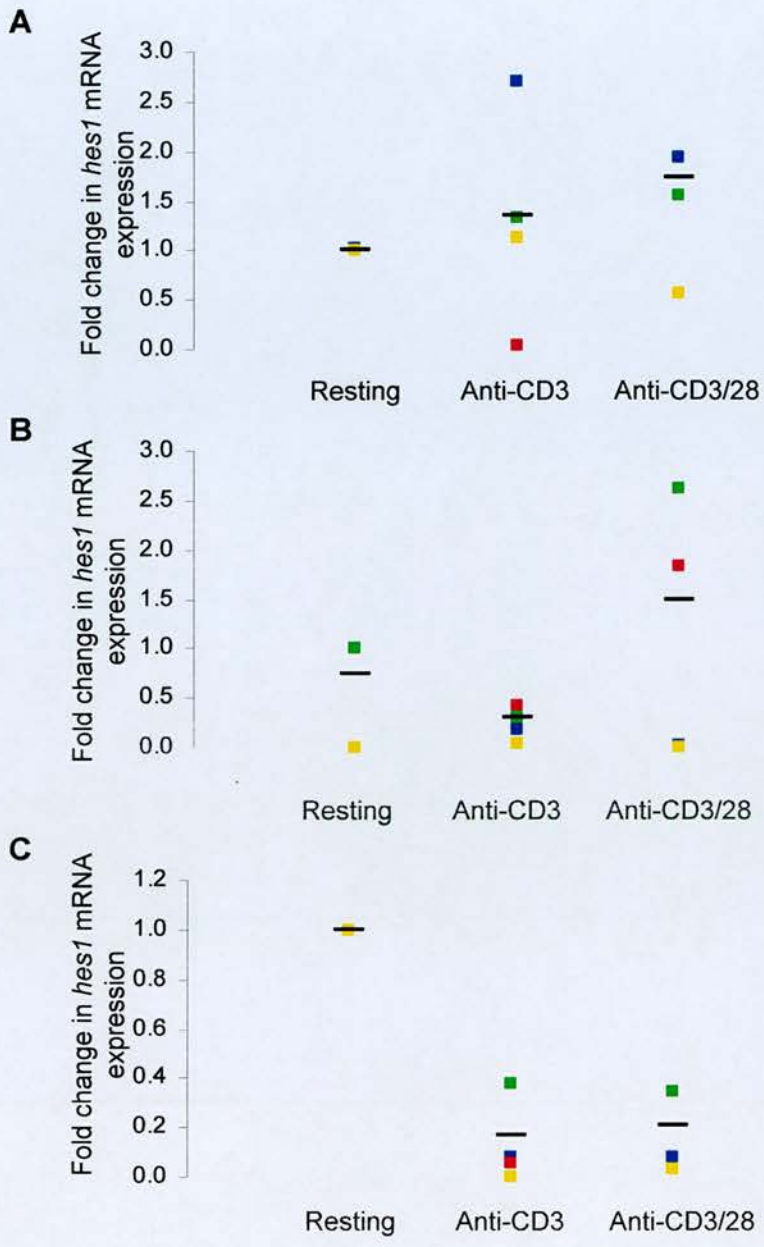

Fig 5.14 *Aire* expression is up-regulated in activated BALB/c CD4+ T cells. *Aire* mRNA expression in resting, antiCD3 activated and anti-CD3/28 activated CD4+ T cells at **A** 24 hours, **B** 48 hours and **C** 72 hours as determined by Real Time RT-PCR. The data points represent individual experiments; data is calibrated to the resting sample in each experiment; the mean is represented by the bar; n=4.

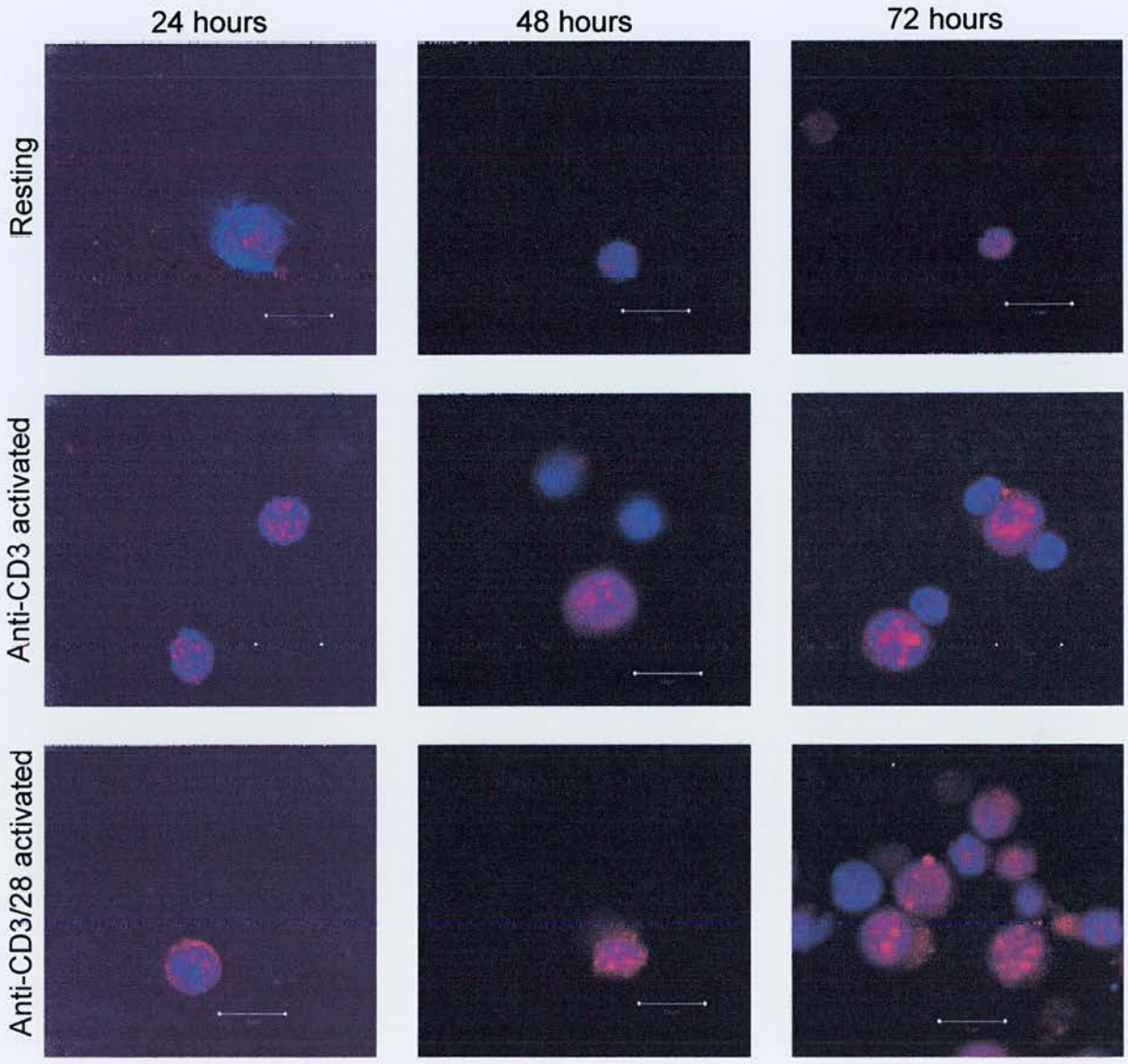

Fig 5.15 Aire protein expression is up-regulated in BALB/c CD4+ T cells activated with anti-CD3 antibody or anti-CD3 and anti-CD28 antibodies.
The scale bar represents 10μM. Data are representative of 3 experiments.

5.6 Discussion

In summary, AIRE is expressed as speckles within the nucleus of human adherent PBMCs where it co-localises with PSP1 but not with sc35. It is important to mention that AIRE and PSP1 are not the same, this was determined by BLAST analysis of protein and mRNA sequences of both Aire and PSP1. PSP1 is thought to be involved in transcriptional regulation, in view of this it would be interesting to investigated whether AIRE and PSP1 co-localise at all points in the cell cycle, as I have observed that the pattern of Aire expression is different in cells which have mitotic spindles present.

In addition to human adherent PBMCs, Aire mRNA and protein is also expressed in murine T and B cells purified from spleen, and preliminary data suggests that in contrast to work described by Kogawa et al (72) Aire protein is expressed in human CD4+ T cells. Upon activation of murine CD4+ T cells, this Aire expression is up-regulated at both the mRNA and protein level. This increase in expression occurs upon activation with anti-CD3 antibody alone and with anti-CD3/28 antibodies, however no obvious difference in protein expression was observed between cells activated through the TCR alone compared to those activated through the TCR with co-stimulation. TCR stimulation in the absence of co-stimulation was included as the human AIRE promoter has been shown to contain a functional AP-1 binding site (63). Analysis of the murine Aire promoter using TESS (http://www.cbil.upenn.edu/tess/), which utilises TRANSFAC v4.0, also revealed an AP-1 binding site. As co-stimulation is required for optimal activation of AP-1

(125), it was possible that Aire may have been up-regulated more in the presence of co-stimulation.

This data, in conjunction with that from the Aire deficient mouse, which has an uncontrolled proliferative response upon rechallenge in-vitro with HEL (74), and the trend to an increase in maximal proliferative response in patients with APS1 (Section 3.5.2 and Fig 3.12A) suggest that Aire may have a role in controlling the proliferative response in the periphery. Thus, functional Aire may be required in lymphocytes to terminate the immune response, and the autoimmune diseases seen in APS1 and the Aire deficient mouse, are a consequence (at least in part) of a failure to terminate/prevent a peripheral immune response. This hypothesis could be investigated by assessing whether Aire protein expression remains up-regulated after proliferation has started to decline. Alternatively, the generation of an Aire conditional knock-out mouse, in which Aire is deficient in T cells only, would help to delineate not only the role of Aire in the proliferative response, but also the role of Aire in peripheral T cells in a broader sense.

The up-regulation in Aire as described above was seen in CD4+ T cells, but Aire is also expressed in CD8+ and B cells. Further investigation of the role of Aire in these cells would be informative, as although CD4+ T cells will play a role in the autoimmune diseases seen in APS1, autoaggressive CD8+ T cells are recognised to play a role in these autoimmune diseases (126) and autoantibody production does occur (127).

CHAPTER 6

6 Interaction of Aire and the Notch signalling pathway

6.1 Introduction

In the previous chapter, it was demonstrated that Aire is present in peripheral CD4+ T cells, and is up-regulated upon TCR mediated activation of these cells. This led to consideration of the possibility that, in addition to Aire's role in the induction of central tolerance, it has a role in T cell effector function. The Notch signalling pathway, a family of highly conserved developmental genes, has a role in determining T cell lineage commitment and has been shown to influence T cell effector function (88,91). Work from the laboratory has shown that this pathway is up-regulated by activation through the T cell receptor (RA Benson PhD Thesis, University of Edinburgh 2004) as described in chapter 5 for Aire. In view of this, the possibility that Aire may interact with the Notch signalling pathway was investigated.

6.1.1 The Notch signalling pathway

The Notch signalling pathway was first identified in Drosophila and plays a role in cell fate in decisions in many organisms (128). There is a wealth of information in the literature, thus in this review, I shall limit myself, where possible, to data from mammals and concentrate on the role of Notch in the immune system.

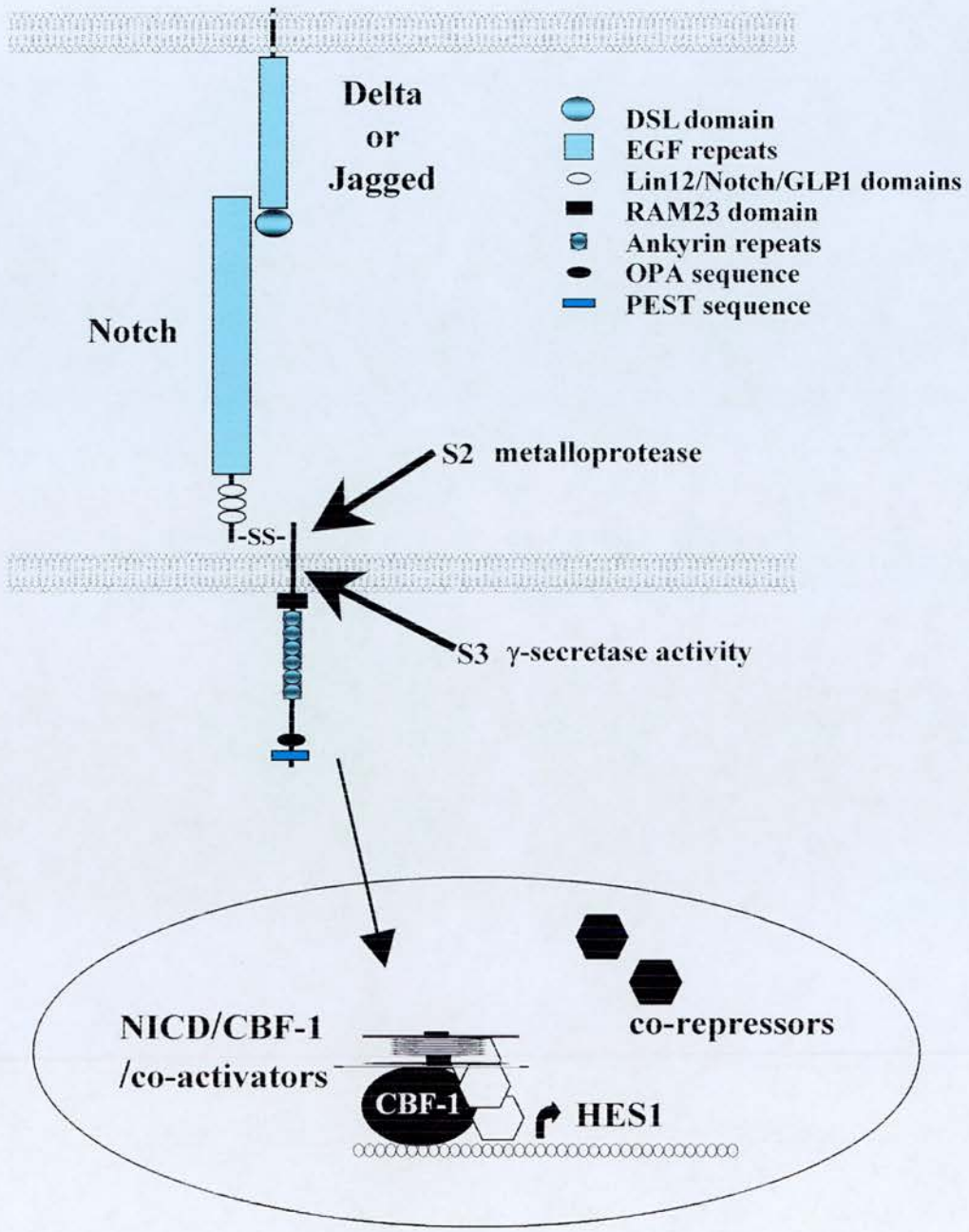

Fig 6.1 Notch signal transduction Binding of Notch by ligand induces an extra-cellular cleavage event, followed by intra-membranous cleavage mediated by γ-secretase. This releases the intra-cellular domain of Notch which translocates to the nucleus, binds to CBF-1 and via recruitment of co-activators activates transcription of *hes1*.See text for detailed description.

Overview of Notch Signalling

There are four single pass transmembrane protein Notch receptors in mammals (Notch 1-4). The extra-cellular portion contains epidermal growth factor (EGF) repeats and three membrane proximal Lin12/Notch/Glp-1 (LNG) repeats; the intra-cellular region contains nuclear localisation sequences, a RAM (RBP-Jκ associated molecule) 23 domain, the ankyrin repeats, a transcriptional activator domain (TAD) and a PEST (proline-, glutamate-, serine-, threonine-rich) sequence (Fig 6.1) (129).

During synthesis, the Notch receptors are cleaved by a furin-like convertase (S1 cleavage), to give a 180kDa fragment consisting of the majority of the extra-cellular domain and a 120kDa fragment which is the rest of the extra-cellular portion and the intra-cellular domain. These are non-covalently associated as a heterodimeric form which is expressed at the cell surface (130).

There are five Notch ligands, Delta-like1, Delta-like3, Delta-like4, Jagged1 and Jagged2. Following binding of the ligand, through its DSL (Delta, Serrate, Lag2) domain, to the extra-cellular domain of the Notch receptor, an extra-cellular cleavage event mediated by TACE (TNF-α converting enzyme), a member of the ADAM metalloprotease family, occurs (S2 cleavage) (131). The membrane tethered intracellular portion that remains after this cleavage event then becomes a substrate for a further cleavage event (S3 cleavage) leading to the release of the intra-cellular domain of Notch (NICD) (132). This proteolytic cleavage event is mediated by the gamma secretase complex. The gamma secretase complex consists of presenilin (133), nicastrin (134), aph-1 and pen-2 (135), and although all components are required for assembly of the gamma-secretase complex, the activity of the complex co-purifies with presenilin (136).

Following this gamma-secretase mediated cleavage event, NICD translocates to the nucleus where it binds to CBF1 (C-promoter binding factor 1) via the RAM 23 domain and ankyrin repeats (129). This binding displaces histone deacetylase (HDAC) and recruits histone acetylases and Mastermind which leads to activation of transcription (137,138).

There are numerous target genes of Notch including a family of basic helix-loop-helix (bHLH) proteins, the HES (Hairy-Enhancer of Split) proteins, that are expressed in the immune system (139) and NF-κB, the expression of which is increased by signalling through Notch (140). Thus up-regulation of the HES genes is commonly used as marker of Notch signalling.

Notch signalling can affect cell fate either through lateral inhibition or inductive signalling. In lateral inhibition, both Notch receptors and ligands are expressed on the same adjacent cell type, and over time through fluctuations in levels of the receptor and ligand, one cell will preferentially express the ligand and the other the receptor. The ligand bearing cell will then adopt the primary cell fate, and the receptor bearing cell, in which active Notch signalling is occurring, will inhibit development of the primary cell fate. In contrast, inductive signalling requires there to be two different cell types, one expressing ligand, and the other expressing receptor. Signalling can then occur in the receptor bearing cell to alter its cell fate.

These cell fate decisions are further influenced by the specific receptor-ligand combination present, as signalling through different combinations can lead to different outcomes.

Notch Signalling in the Immune System

Within the immune system Notch signalling is involved in cell fate decisions involved in lineage commitment such as T/B cell differentiation and αβ/γδ TCR usage. Active Notch signalling is required for T cell commitment, in the absence of Notch there is a block in T cell development and a bias towards B cell development (141), whilst overexpression of Notch leads to an increase in T cell development at the expense of B cells (142). Thymic epithelial cells express Notch ligands of the Delta-like and Jagged families (143), thus it is likely that signalling from these ligands allows the precursor to adopt a T cell fate. The data regarding αβ versus γδ commitment is less clear. However, from the evidence available it seems that Notch signalling favours the development of αβ rather than γδ T cells (143). The final cell fate decision process in which Notch appears to be involved is CD4/CD8 lineage commitment, where Notch signalling promotes the development of CD8+ T cells over CD4+ T cells (144).

Once activated through the recognition of a peptide/MHC complex on a mature DC within the lymph node, the mature peripheral T cell may differentiate into a Th1, Th2 or T regulatory cell, a process that Notch may also be involved in. Signalling mediated by Dl1 and N3 has been shown to generate a Th1 phenotype characterised by an increase in IFNγ production and up-regulation of T-bet expression (91), and signalling through Jagged1 has been shown to generate a regulatory population of T cells which were able to transfer tolerance (88,89).

Two recent studies have shown that Notch receptors are expressed on T cells and their expression is up-regulated following T cell activation (145,146). Through the

use of inhibitors of the gamma-secretase complex, this work also showed that in the presence of decreased Notch signalling, T cell proliferation and secretion of IL2 and IFNγ were reduced (145,146), whilst overexpression of the intra-cellular domain of Notch1 increased proliferation and expression of CD25 (145). Therefore, it is possible that Notch signalling acts in a co-stimulatory manner to enhance T cell function.

The aims of this chapter were

1. to confirm that Notch signalling is up-regulated in activated CD4+ T cells
2. to investigate the effect of inhibiting Notch signalling on Aire expression in activated CD4+ T cells
3. to determine the effect on Aire expression of delivering a direct Notch signal

6.2 Notch signalling is up-regulated in activated CD4+ T cells

The Notch signalling pathway is described in detail above. Briefly, binding of the membrane bound Notch receptor by a ligand (either Delta-like or Jagged) causes cleavage by the γ-secretase complex and release of the intra-cellular portion of Notch which then translocates to the nucleus where it is able to signal. This signalling is then able to increase transcription of Notch target genes, such as Hes1.

To determine whether Notch signalling was occurring upon T cell activation, RNA was used in a Real Time RT-PCR reaction with primers and probe specific for *hes1*. CD4+ T cells were isolated from C57BL/6J spleens by magnetic beads as described in section 2.14, and activated with anti-CD3 antibody (0.1μg/ml) and anti-CD28 antibody (1μg/ml) for 48 hours. *Hes1* mRNA was not detected even after 40 cycles by real-time RT-PCR in resting cells, but was detected in activated cells. In a further 5 experiments, with CD4+ T cells from pooled C57BL/6J spleens activated with anti-CD3 antibody (0.1μg/ml) and anti-CD28 antibody (5μg/ml) for 24 or 48 hours, *hes1* mRNA expression was up-regulated in 2 out of 5 experiments at 24 hours and in the other 3 experiments at 48 hours (Fig 6.2).

To determine that the effect seen was not mouse strain specific, 3 experiments using CD4+ T cells from pooled BALB/c spleens were undertaken. In these experiments, CD4+ T cells were activated with either with anti-CD3 antibody (0.1μg/ml) alone or anti-CD3 (0.1μg/ml) and anti-CD28 (1μg/ml) antibodies for 24, 48 or 72 hours.

In 2 out of 3 experiments, *hes1* mRNA was increased at 24 hours in CD4+ T cells activated with anti-CD3 alone, with a mean fold change in mRNA expression of 2.8±1.9, and increased in CD4+ T cells activated with both anti-CD3 and anti-CD28

antibodies in the 2 experiments for which data are available, mean increase 2.5±0.6. At 48 hours, *hes1* mRNA expression was increased by anti-CD3 alone in 1 out of 3 experiments, increasing from 0.67±0.58 up to 1±0.44, and was increased in all 3 experiments when activated with anti-CD3 and anti-CD28 antibodies, with a mean increase of 2.77±1.7. At 72 hours, a decrease in hes1 mRNA expression was observed in both anti-CD3 and anti-CD3/28 activated cells (Fig 6.3).

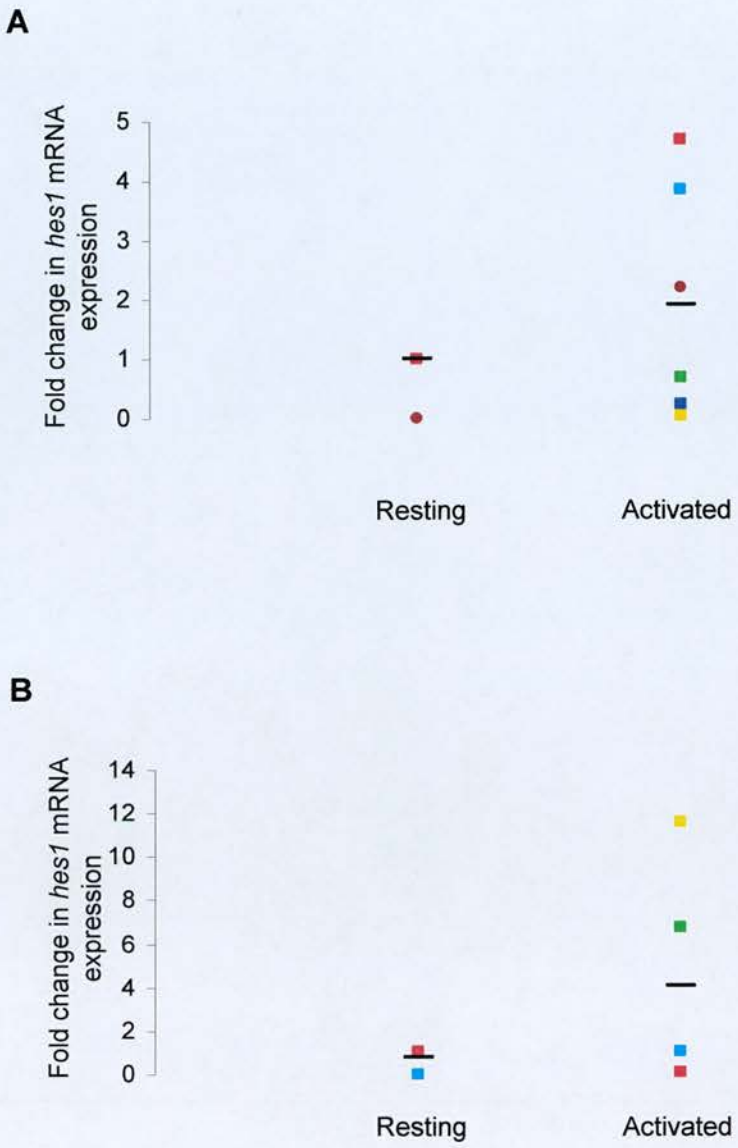

Fig 6.2 *hes1* expression is up-regulated in activated C57BL/6J CD4+ T cells. *hes1* mRNA expression in resting and anti-CD3/28 activated CD4+ T cells at **A** 24 hours and **B** 48 hours, as determined by Real Time RT-PCR. The data points represent individual experiments; the mean is represented by the bar; n=5.

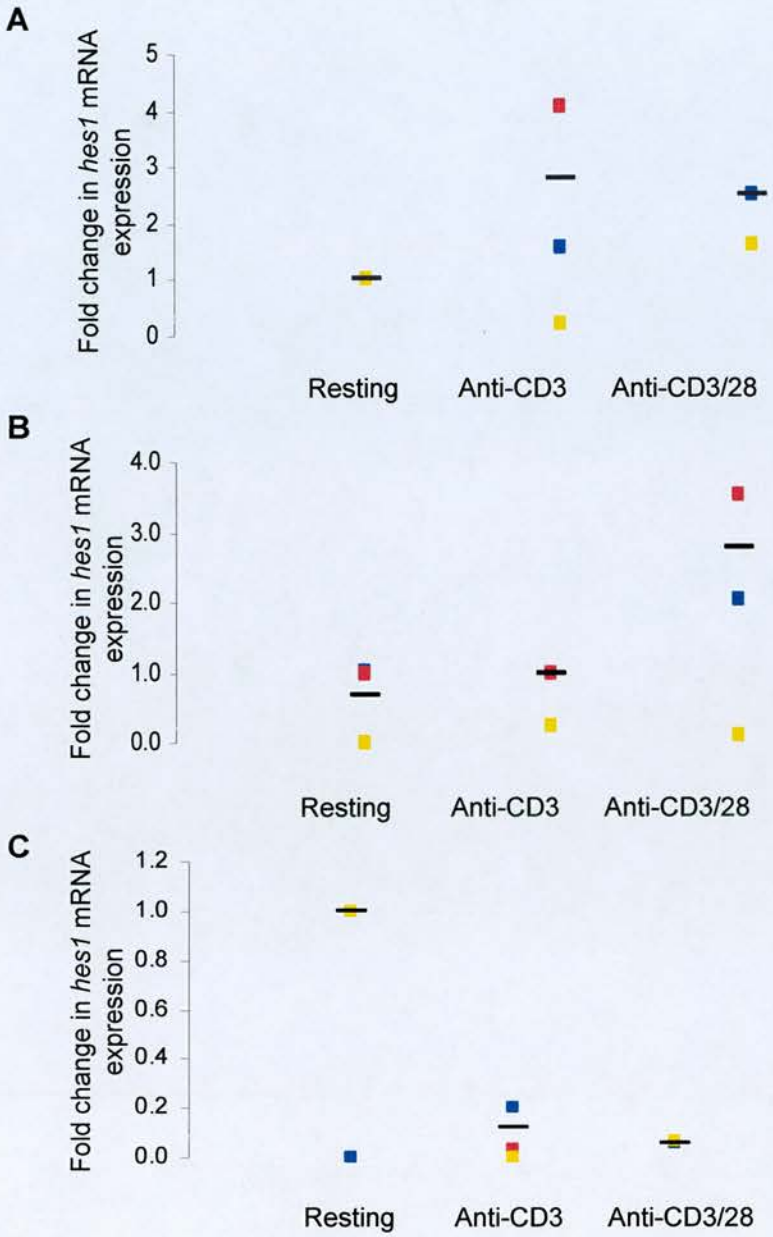

Fig 6.3 *hes1* expression is up-regulated in activated BALB/c CD4+ T cells. *hes1* mRNA expression in resting, antiCD3 activated and anti-CD3/28 activated CD4+ T cells at **A** 24 hours, **B** 48 hours and **C** 72 hours as determined by Real Time RT-PCR. The data points represent individual experiments; data is calibrated to the resting sample in each experiment; the mean is represented by the bar; n=3.

6.3 *Aire* mRNA expression correlates with *hes1* mRNA expression

The data obtained showing up-regulation of *hes1* mRNA expression is very similar to that seen for *Aire* mRNA expression in the same experiments in both C57BL/6J and BALB/c mice (See Fig 5.12 and 5.14 for *Aire* mRNA expression). In view of this the possibility of an interaction between Aire and Notch signalling was investigated further.

6.4 Notch signalling is inhibited by γ-secretase inhibitors

In order to determine whether the up-regulation of Aire seen upon activation is due to the Notch signalling that is occurring in these cells, an inhibitor of Notch signalling was used.

After binding of a ligand to a Notch receptor, an extracellular cleavage event occurs. The remaining membrane tethered intracellular portion of the Notch receptor is then able to be a substrate for the γ-secretase complex. Further cleavage by the γ-secretase complex releases the intra-cellular portion, which translocates to the nucleus where it effects CBF1-dependent signalling. Therefore, by inhibiting γ-secretase activity, Notch signalling can be prevented.

The γ-secretase inhibitor, MW167 has been shown to inhibit the γ-secretase dependent processing of Notch that is required for nuclear translocation of NICD (147,148,149,150), with an IC_{50} of 16μM (151,152). Like the Notch receptors, presenilin, the active component of the gamma-secretase complex, is cleaved during

synthesis, this endoproteolysis is required to generate a functional protein (153). When used at low concentrations MW167 has presenilinase activity (152) i.e. it prevents this endoproteolysis and leads to a decrease in the amount of functional presenilin present.

MW167 or DMSO, as a vehicle control, was added to C57BL/6J CD4+ T cells that were cultured in the presence or absence of anti-CD3 (0.1μg/ml) and anti-CD28 (1μg/ml) antibodies. MW167 was used at 5μM, a dose that will primarily affect presenilinase activity (152) and 20μM at which γ-secretase activity should be affected. Previous work in the laboratory had investigated the effect of MW167 on *hes1* mRNA expression in resting, anti-CD3 antibody stimulated and anti-CD3/28 antibody stimulated BALB/c CD4+ T cells. This work demonstrated a minimal effect on *hes1* in resting cells after 24 hours with 10μM or 20μM of MW167, but a reduction in *hes1* was observed in resting cultures by 48 hours, which neared biological relevance when 10μM was used and was almost undetectable when 20μM of MW167 was used. In anti-CD3 antibody activated cells, 20μM of MW167 was required to reduce *hes1* expression. In anti-CD3/28 antibody activated cells, a decrease in expression was present with 10μM MW167, this decrease reached biological significance when 20μM was used (RA Benson PhD Thesis, University of Edinburgh 2004).

This was confirmed in C57BL/6J mice, in resting CD4+ T cells, *hes1* mRNA expression was detected by real time RT-PCR in the absence of MW167, but was undetectable when 5 or 20 μM of MW167 was added into the culture. In anti-CD3/28 antibody activated CD4+ T cells, *hes1* mRNA expression was reduced by

40% by addition of MW167 at 20 μM (Fig 6.4). It would have been preferable to use a higher concentration of MW167, which would have decreased *hes1* expression further in activated T cells, however this was not possible due to the cost of MW167.

In order to determine that any effects seen by using the γ-secretase inhibitor MW167 were due to inhibiting Notch signalling and not through altering the activation status of the cells, the effect, if any, of this inhibitor on T cell proliferation and up-regulation of activation markers was assessed.

Proliferation of C57BL/6J CD4+ T cells was not affected by MW167 at 5,10 or 20μM at 48 hours (Fig 6.5). In a further 3 experiments using BALB/c CD4+ T cells, proliferation was unaffected by MW167 at 20μM even after 72 hours of culture.

To determine the activation status of the CD4+ T cells, up-regulation of the activation markers, CD25 and CD69 was assessed by FACS staining (Section 2.18). No differences in the up-regulation of either marker was observed by the addition of MW167 at 20μM at 24, 48 or 72 hours in resting, anti-CD3 antibody activated or anti-CD3/28 antibody activated BALB/c CD4+ T cells. Representative data obtained at 48 hours are shown in figures 6.6-6.8 (n=3). In C57BL/6J CD4+ T cells, no difference in up-regulation of CD25 or CD69 was observed in the presence of MW167 at 10μM (n=3).

Notch1 has been documented to have anti-apoptotic effects in T cells (154), and thus it is feasible that by inhibiting Notch with MW167, which will inhibit all Notch signalling, not just that mediated by Notch1, apoptosis may be increased. In view of this, the degree of apoptosis present was assessed by FACS staining for AnnexinV and by staining with 7AAD (Section 2.18). MW167 did not increase apoptosis of

either C57BL/6J (n=4) or BALB/c (n=3) CD4+ T cells at 24, 48 or 72 hours. Representative data for BALB/c CD4+ T cells at 48 hours is shown in figure 6.9.

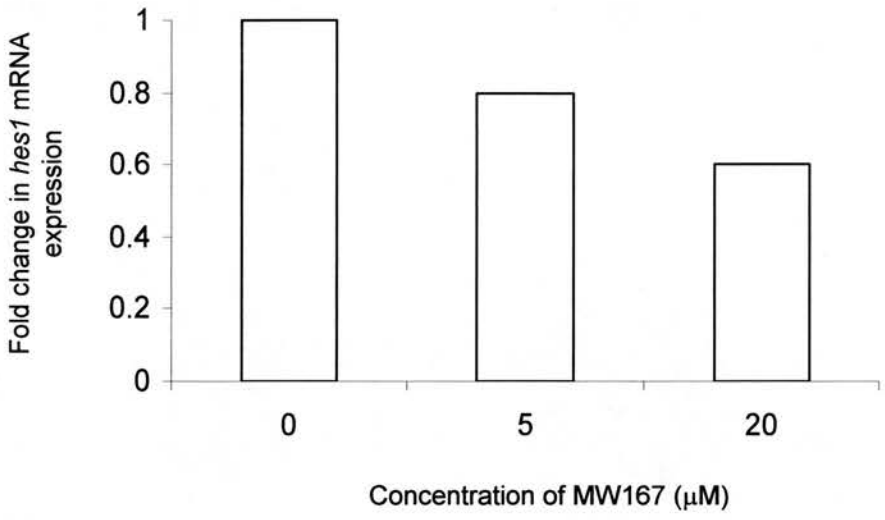

Fig 6.4 Notch signalling is inhibited by the γ-secretase inhibitor MW167. *hes1* mRNA expression in anti-CD3/28 activated C57Bl6/J CD4+ T cells as determined by Real Time RT-PCR. The untreated sample is used as the calibrator.

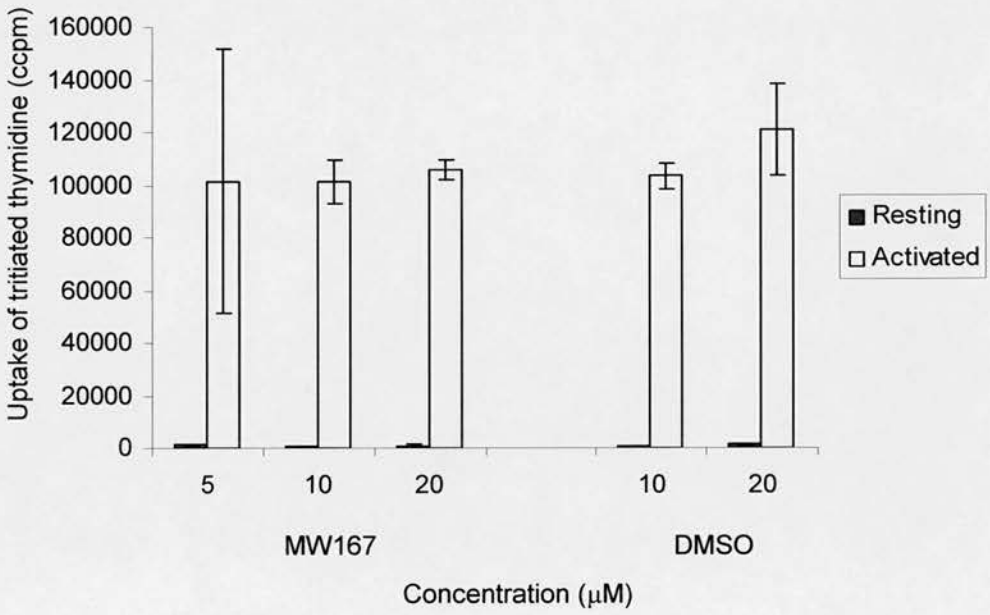

Fig 6.5 Proliferation of C57Bl6/J CD4+ T cells is not affected by the γ-secretase inhibitor MW167. Proliferation of CD4+ T cells as assessed by the uptake of tritiated thymidine 48 hours after activation with 0.1 μg/ml anti-CD3 and 1μg/ml anti-CD28 antibodies in the presence of either MW167 or DMSO as a control.

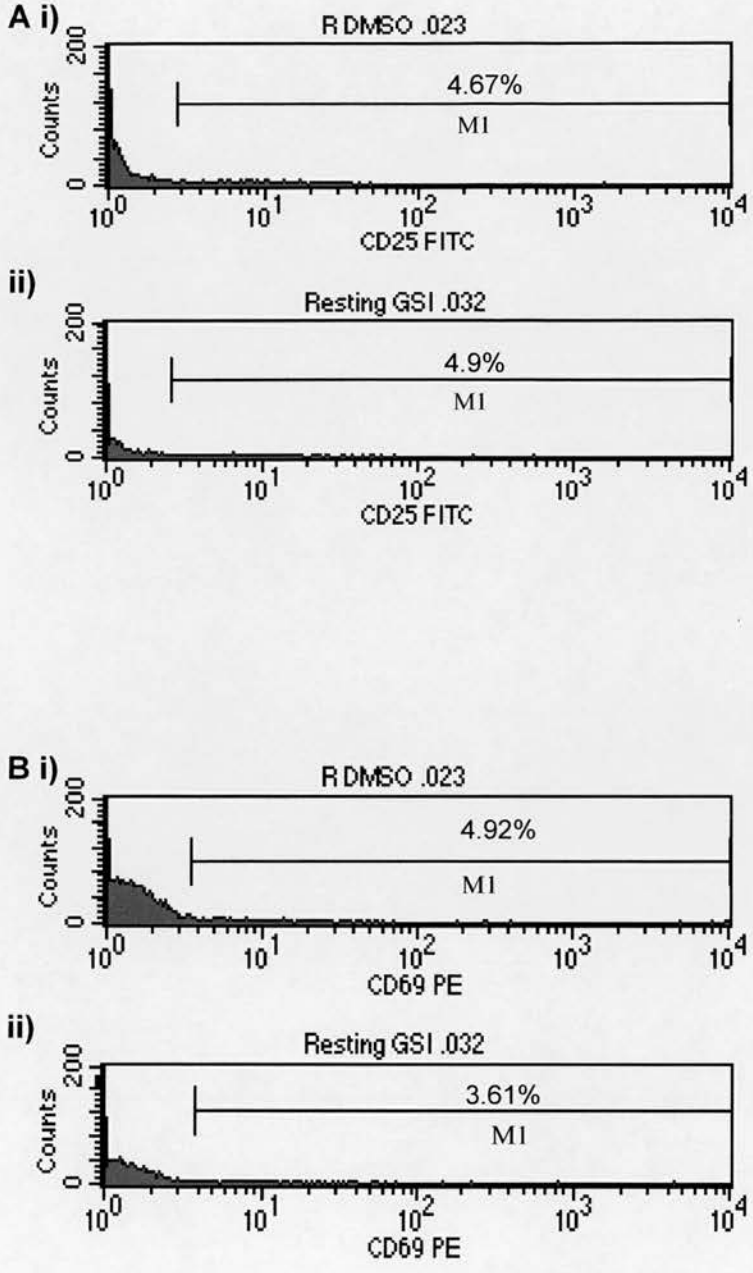

Fig 6.6 MW167 does not affect surface expression of CD25 and CD69 on resting cells. FACS staining of BALB/c resting CD4+ T cells **i)** + DMSO or **ii)** MW167 20mM, with **A** CD25FITC or **B** CD69PE antibodies; n=3.

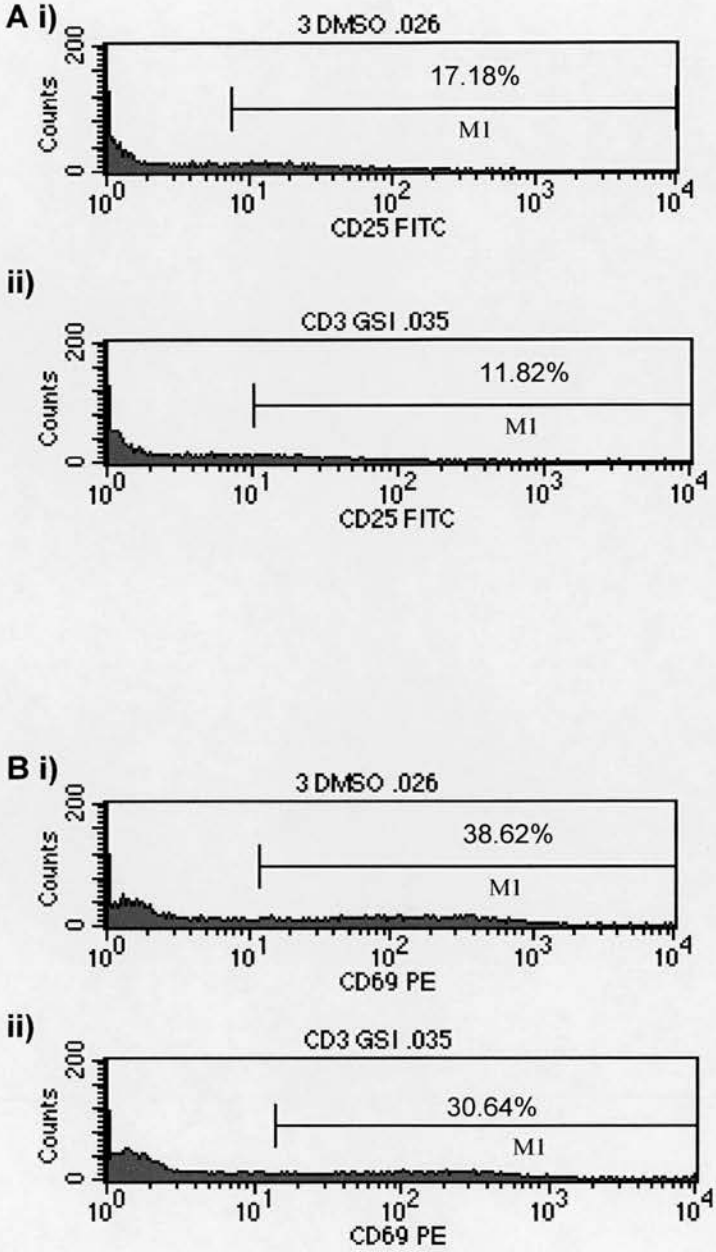

Fig 6.7 MW167 does not affect surface expression of CD25 and CD69 on anti-CD3 antibody activated cells.
FACS staining of BALB/c CD4+ T cells **i)** + DMSO or **ii)** MW167 20mM, with **A** CD25FITC or **B** CD69PE antibodies; n=3.

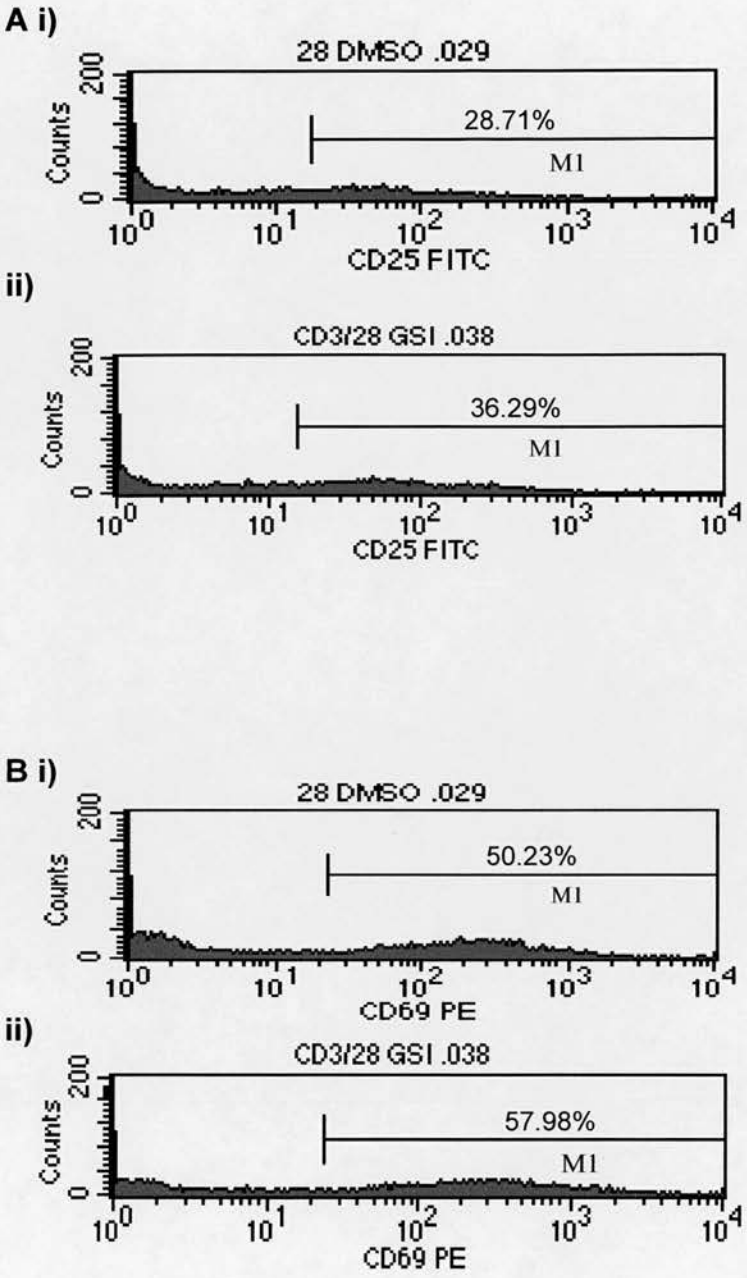

Fig 6.8 MW167 does not affect surface expression of CD25 and CD69 on anti-CD3/28 antibody activated cells. FACS staining of BALB/c CD4+ T cells **i)** + DMSO or **ii)** MW167 20mM, with **A** CD25FITC or **B** CD69PE antibodies; n=3.

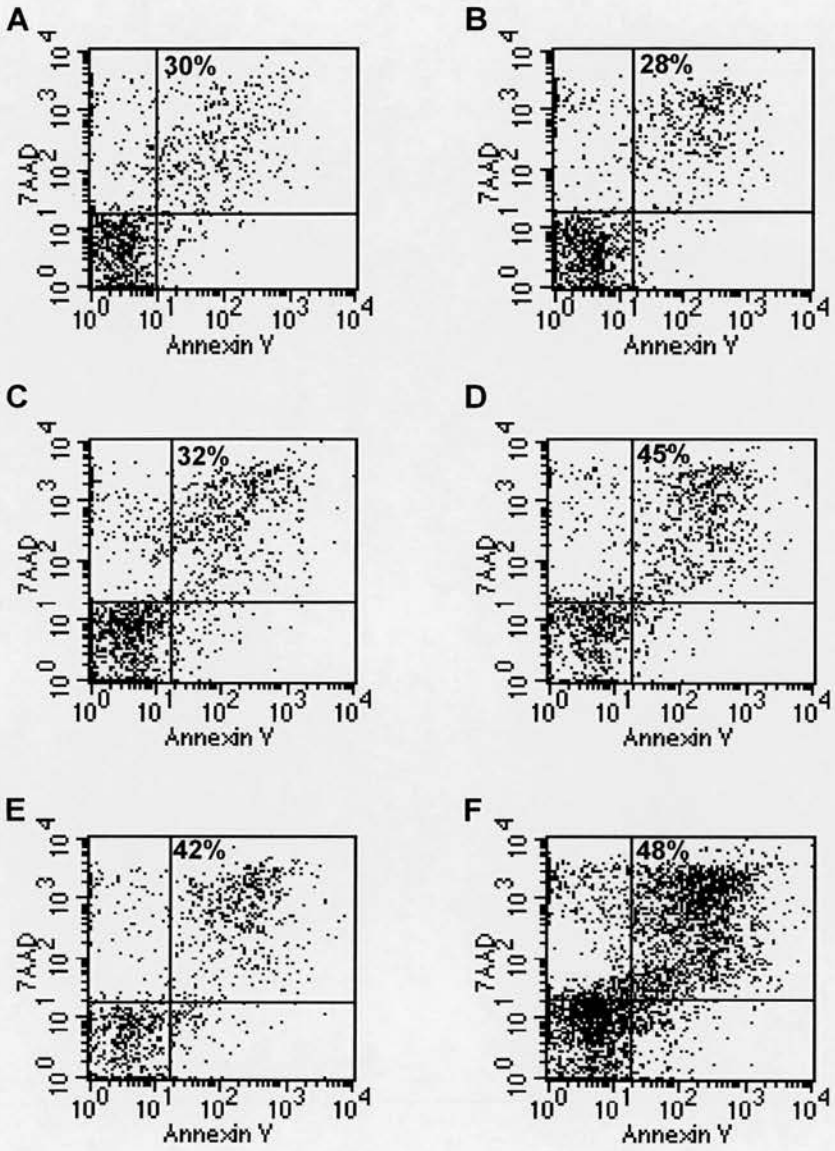

Fig 6.9 Inhibition of Notch signalling does not affect the number of cells undergoing apoptosis. A Resting cells + DMSO; **B** Resting cells + 20μM MW167; **C** Anti-CD3 antibody activated cells + DMSO **D** Anti-CD3 antibody activated cells + 20μM MW167; **E** Anti-CD3/28 antibody activated cells + DMSO **F** Anti-CD3/28 antibody activated cells + 20μM MW167; n=3. Representative data at 48 hours in CD4+ T cells from BALB/c mice is shown.

6.5 Aire up-regulation is decreased by inhibiting Notch signalling

Six experiments were undertaken, using CD4+ T cells magnetically isolated from 4-6 pooled C57BL/6J spleens by negative selection. Cells were activated with anti-CD3 antibody (0.1μg/ml) and anti-CD28 antibody (1μg/ml) and cultured in the presence or absence of 10μM MW167 for 48 hours. As described above, no differences in proliferation, up-regulation of activation markers or apoptosis were observed by addition of MW167. In the 4 experiments in which immunofluorescence was performed, Aire protein was up-regulated upon activation as described in section 5.4.2, and this up-regulation was prevented by addition of MW167 (Fig 6.10).

As the level of Aire protein expression appears to be higher in BALB/c mice than C57BL/6J (fig 5.8), a further 4 experiments using BALB/c mice were performed. CD4+ T cells were magnetically isolated by negative selection, activated with anti-CD3 antibody (0.1μg/ml) alone or anti-CD3 antibody and anti-CD28 antibody (1μg/ml) and cultured in the presence or absence of MW167, at 20μM. In all of these experiments, Aire protein expression was increased at all time points upon activation with either anti-CD3 antibody alone or with both anti-CD3 and anti-CD28 antibodies. Surprisingly however, the up-regulation observed with anti-CD3 antibody alone could not be inhibited by MW167, but that seen with anti-CD3 and anti-CD28 antibodies could (fig 6.11).

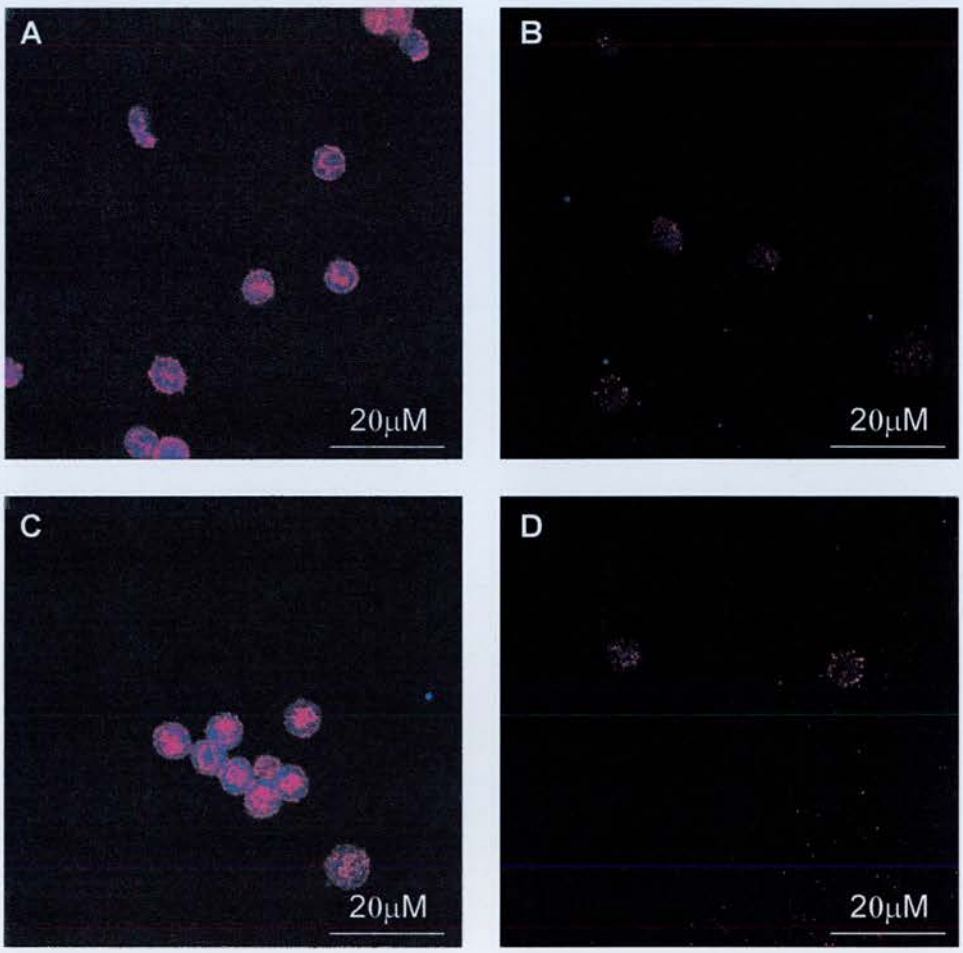

Fig 6.10 Up-regulation of Aire in activated C57BL/6J CD4+ T cells is abrogated by inhibition of Notch signalling. A Resting cells + DMSO; **B** Resting cells + 10μM MW167; **C** Anti-CD3/CD28 Activated cells + DMSO; **D** Anti-CD3/CD28 Activated cells + 10μM MW167. Representative data at 48 hours are shown. n=4.

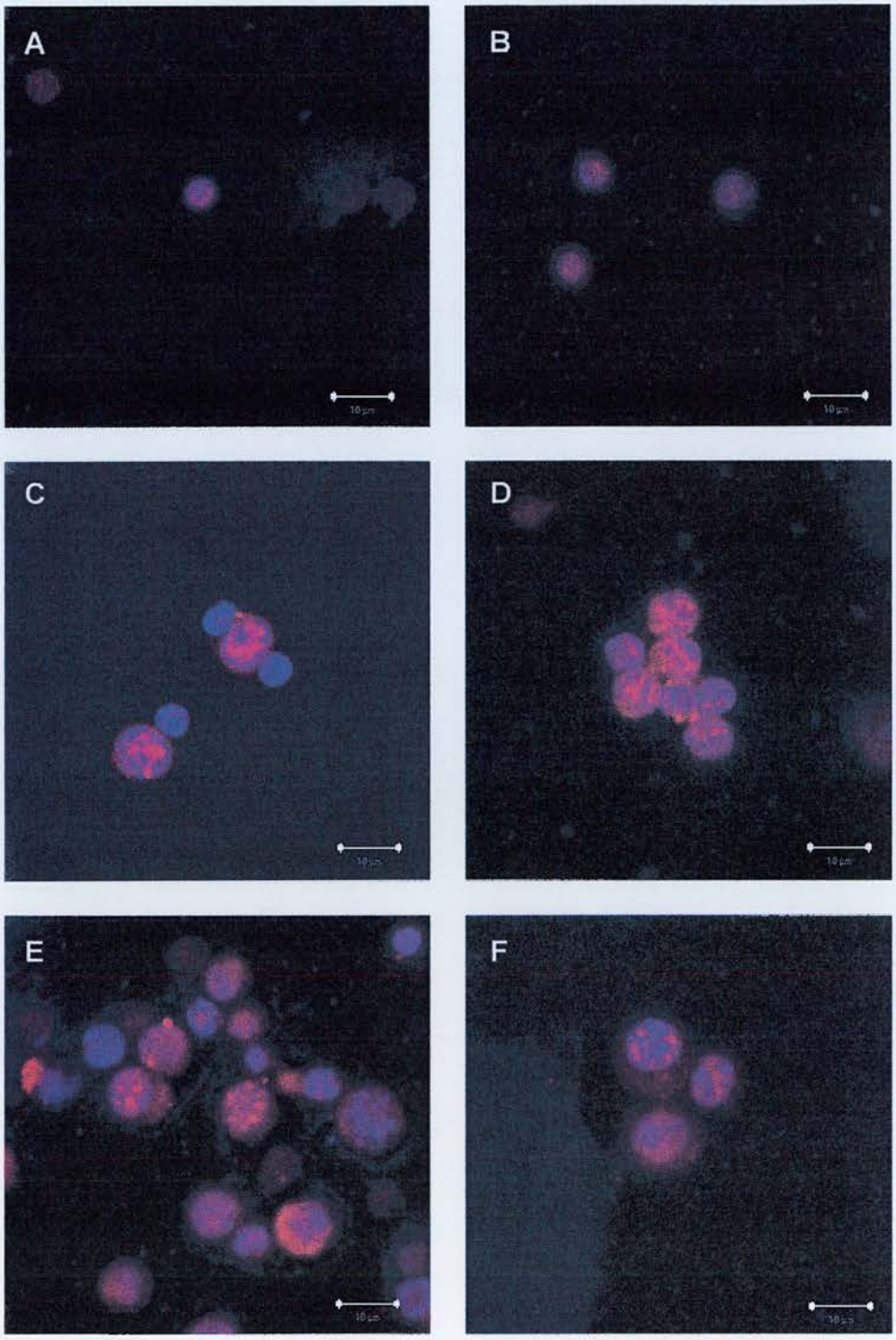

Fig 6.11 Up-regulation of Aire in activated BALB/c CD4+ T cells is abrogated by inhibition of Notch signalling in the presence of co-stimulation. A Resting cells + DMSO; **B** Resting cells + 20μM MW167; **C** Anti-CD3 Activated cells + DMSO; **D** Anti-CD3 Activated cells + 20μM MW167; **E** Anti-CD3/CD28 Activated cells + DMSO.; **F** Anti-CD3/CD28 Activated cells + 20μM MW167. Representative data at 72 hours are shown. n=4.

6.6 Aire expression is up-regulated by signalling through Delta-like1

The above data are supportive of an interaction between Aire and Notch signalling, but the cells in this system are TCR activated and therefore a multitude of complex processes will be occurring simultaneously. In view of this, it was important to investigate the effect on Aire expression when a direct Notch signal is delivered in the absence of a TCR signal.

A mouse fibroblast cell line (L cell), which has been transfected with class II MHC ($I\text{-}A^b$) (designated parental L cells) and the Notch ligand Delta-like1 (Dl1), a kind gift from Prof M Dallman, was utilised for this purpose (155). Characterisation of the Dl1 L cells was recently reported by Wong et al, and they have been shown to express higher levels of Dl1 mRNA than parental L cells, to actively signal through the Notch receptor in a reporter assay for Notch ligand activity and to up-regulate expression of the target gene *hes1* in T cells co-cultured with Dl1 L cells compared to parental L cells (155).

C57Bl6/J mice were used for these experiments to match the class II on the L cells. CD4+ T cells were purified from pooled spleens by positive selection (Section 2.14) and co-cultured with Mitomycin C treated L cells (section 2.15.2) for 24 hours. Aire protein expression was determined by immunofluorescence and RNA was obtained for real time RT-PCR to assess *Aire* and *hes1* mRNA expression. To verify that T cell activation was not occurring, cell surface activation markers were analysed by flow cytometry, cell proliferation was assessed by the incorporation of tritiated thymidine and cell division was determined by CFSE staining (Section 2.17). The

gamma-secretase inhibitor MW167 was also added to four out of six experiments to inhibit the Notch signal delivered by the Dl1 L cells. Cell purity was assessed by flow cytometry and was 89-97% in the experiments in which MW167 was added. The cell purities for the remaining experiments were 63% and 83%, data from the experiment with a cell purity of 63% are not included, as this level of contamination was considered to be unacceptably high.

6.6.1 Signalling through Delta-like1 up-regulates hes1 expression

To ensure that Notch signalling is activated by co-culture with Dl1 L cells, hes1 mRNA and protein expression were determined. As can be seen in Figure 6.12, in this preliminary experiment, both mRNA and protein expression are up-regulated after 24 hours of co-culture, in comparison to co-culture with the parental cells.

Having shown that Notch signalling is up-regulated in CD4+ T cells co-cultured with Dl1 L cells, it was important to inhibit this Notch signal using the gamma-secretase inhibitor MW167. Due to the fact that the Notch signal delivered by the Dl1 L cells was likely to be greater than that seen upon T cell activation, MW167 was used at 20,50 and 100μM (Fig 6.13), and 100μM was required to decrease hes1 mRNA expression in T cells co-cultured with either the parental L cells or Dl1 L cells back to baseline levels (Fig 6.13), thus MW167 was used at 100μM in all subsequent experiments.

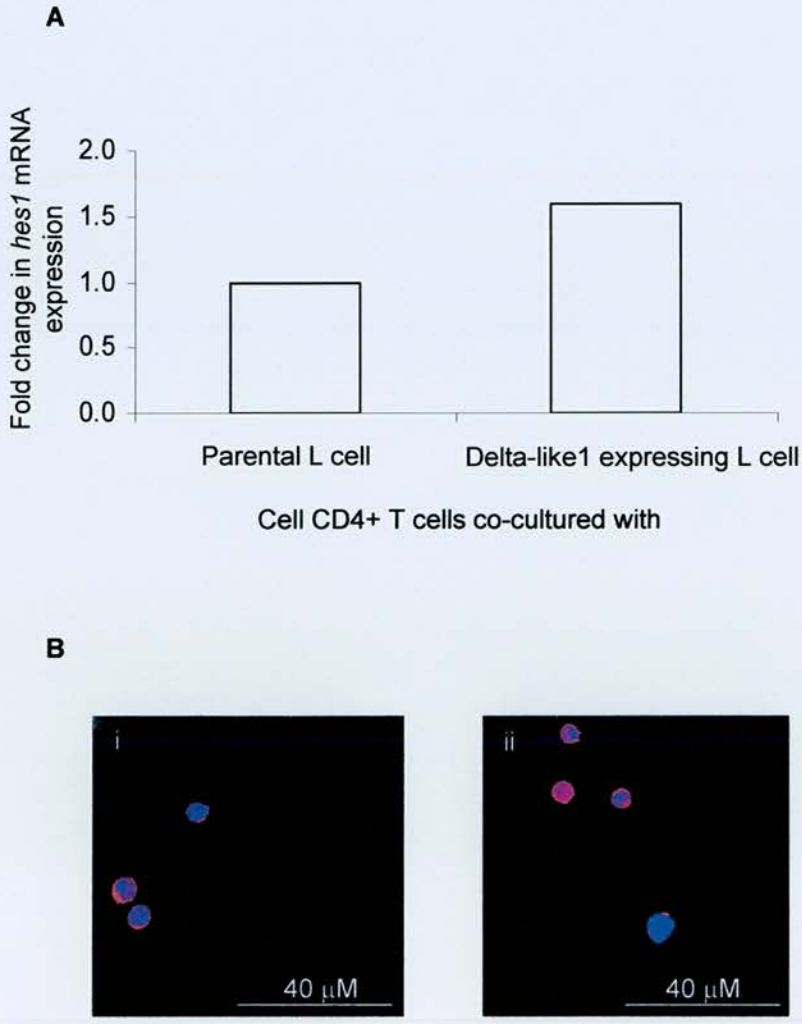

Fig 6.12 Notch signalling is up-regulated in CD4+ T cells co-cultured with Delta-like1 expressing L cells. A *hes1* mRNA expression as measured by Real Time RT-PCR in CD4+ T cells co-cultured with either parental or Delta-like1 expressing L cells; **B** Hes1 protein expression by immunofluorescence in CD4+ T cells co-cultured with either (i) parental or (ii) Delta-like1 expressing L cells; Hes1 (red), Nucleus (Blue).

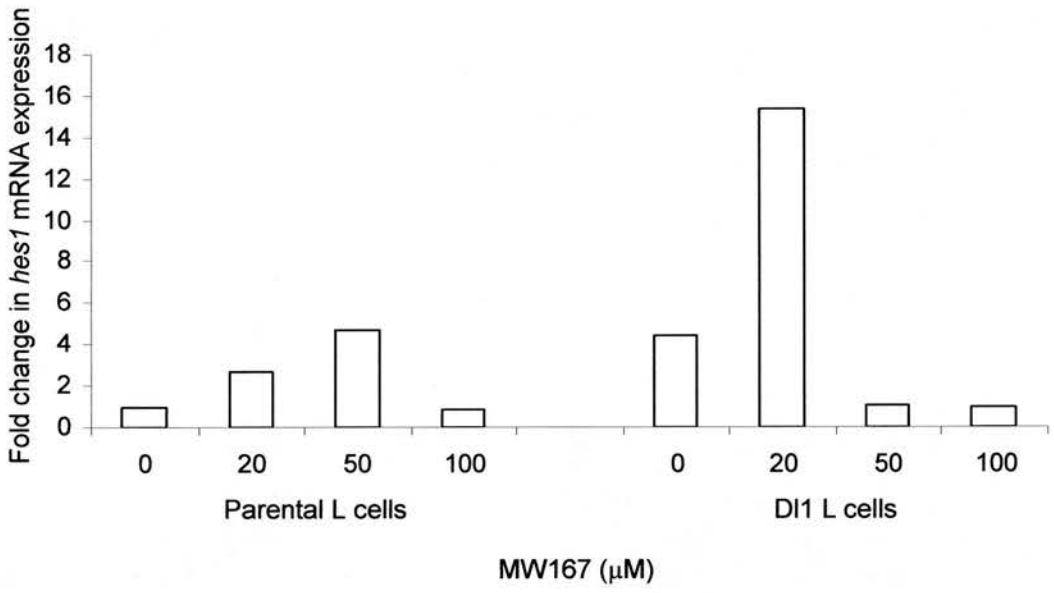

Fig 6.13 *Hes1* mRNA expression is decreased by MW167 at 100μM. *Hes1* mRNA expression was determined by Real Time RT-PCR. All values are relative to CD4+ T cells co-cultured with parental L cells in the absence of MW167.

6.6.2 CD4+ T cells are not activated by co-culture with Delta-like1 expressing L cells

Prior to co-culture with parental or Dl1 L cells, CD4+ T cells were CFSE stained (Section 2.17). After 24 hours of culture, cells were stained with anti-CD4 PE antibody (Section 2.18) and CFSE labelling of the CD4+ cells was analysed by flow cytometry. The cells did not divide in this 24 hour period (n=3) (Fig 6.14).

Cell proliferation by the incorporation of tritiated thymidine was also assessed. No difference in proliferation was observed by culture with Dl1 L cells compared to parental L cells in the presence or absence of MW167 at 100 μM (n=3) (Fig 6.15).

Surface expression of the T cell activation markers, CD25 and CD69, was determined by flow cytometry (section 2.18). No difference in expression of these 2 markers was seen on CD4+ T cells co-cultured with parental or Dl1 L cells, and no difference was observed by the addition of MW167 at 100 μM (Fig 6.16 and 6.17).

As for activated CD4+ T cells, it was important to determine that the γ-secretase inhibitor was not causing increased apoptosis. Cells were stained with 7AAD and for Annexin V and no differences in the amount of apoptosis were observed (Fig 6.18).

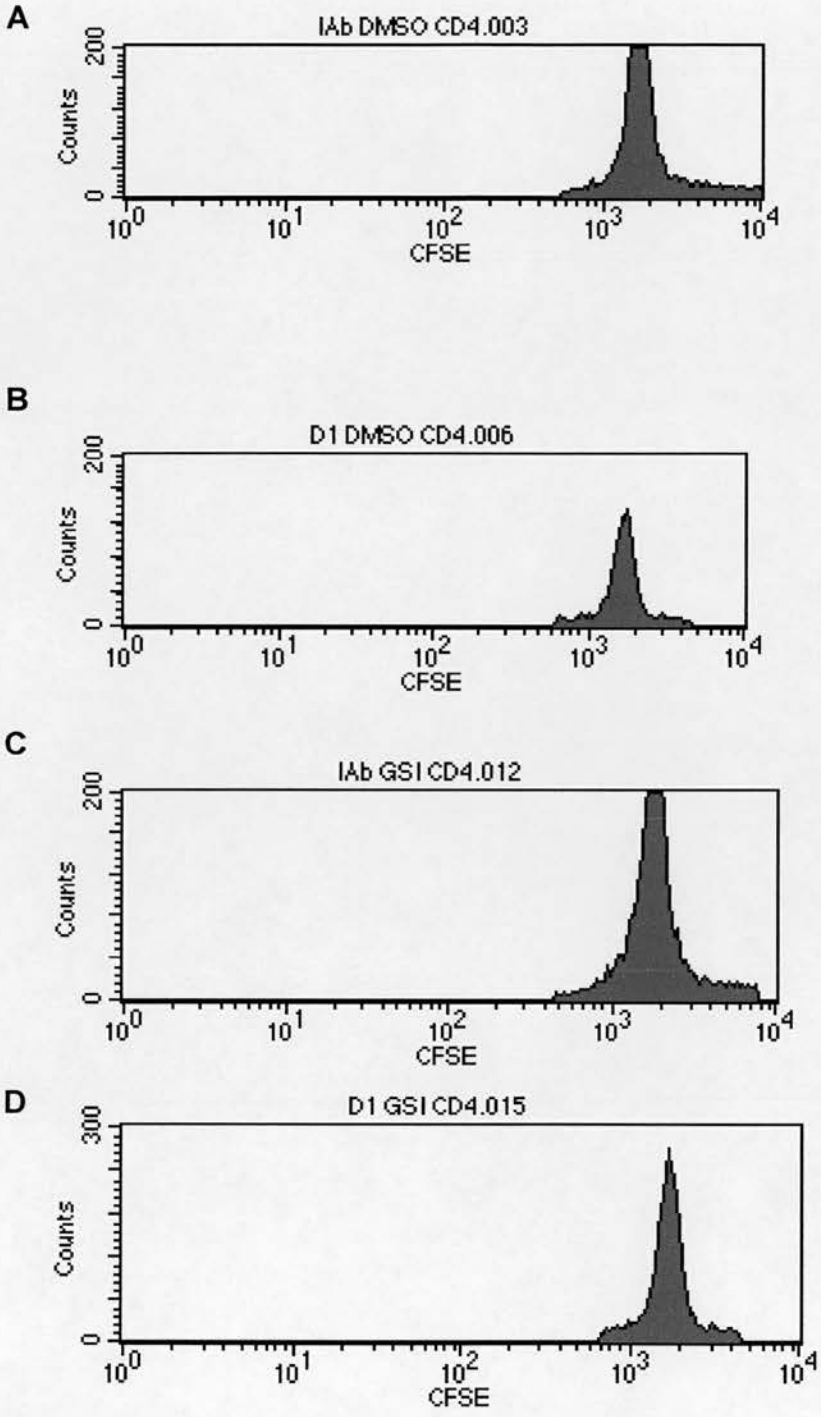

Fig 6.14 CD4+ T cells co-cultured with L cells do not divide. CFSE staining of CD4+ T cells co-cultured with **A** Parental L cells; **B** Parental L cells and 100μM MW167; **C** Delta-like 1 expressing L cells; **D** Delta-like1 expressing L cells and 100μM MW167. Data are representative of 3 experiments.

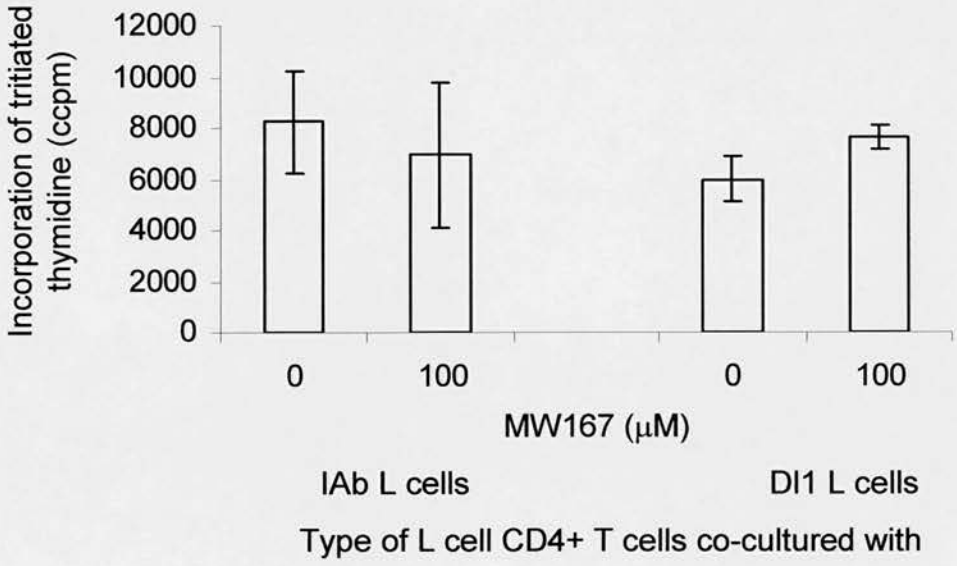

Fig 6.15 CD4+ T cells co-cultured with L cells do not proliferate.
Incorporation of tritiated thymidine by CD4+ T cells co-cultured with Parental L cells +/- 100μM MW167 or Delta-like1 expressing L cells +/- 100μM MW167. Data represents the mean +/- SEM; n= 3.

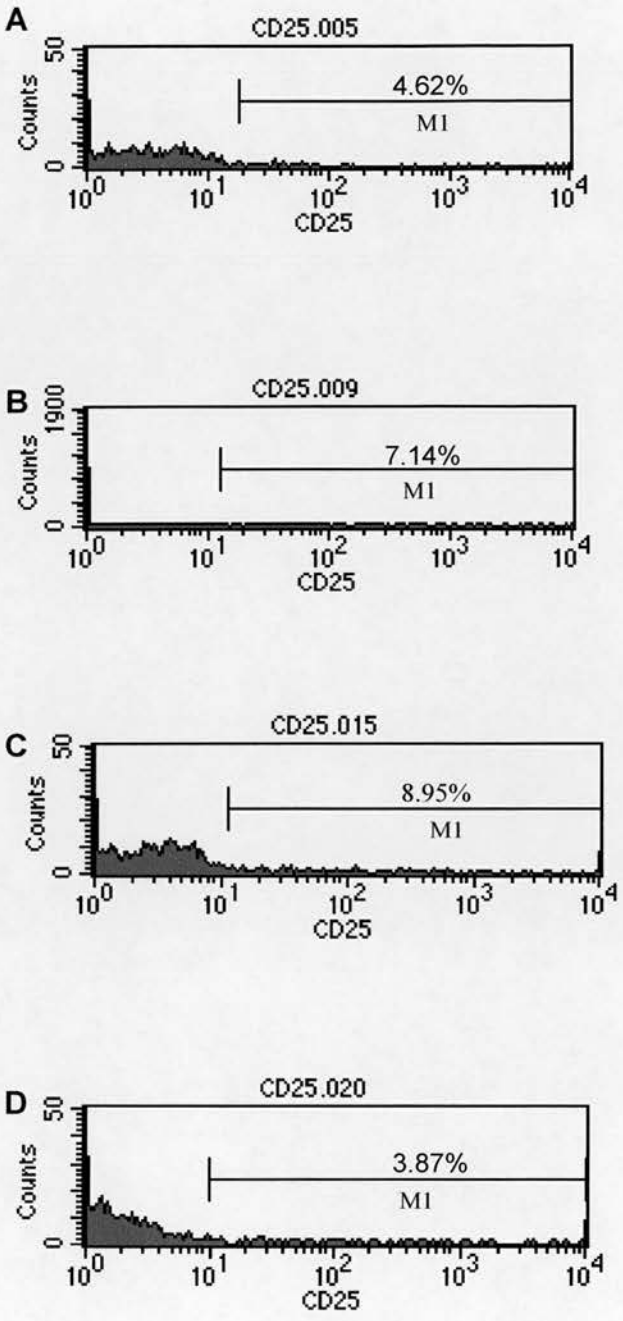

Fig 6.16 CD25 on CD4+ T cells is not up-regulated by co-culture with L cells. FACS analysis of CD4+ T cells, gated on a lymphocyte gate, stained with anti-CD25 antibody, co-cultured with **A** Parental L cells; **B** Parental L cells and 100μM MW167; **C** Delta-like1 expressing L cells; **D** Delta-like1 expressing L cells and 100μM MW167. Data are representative of 3 experiments.

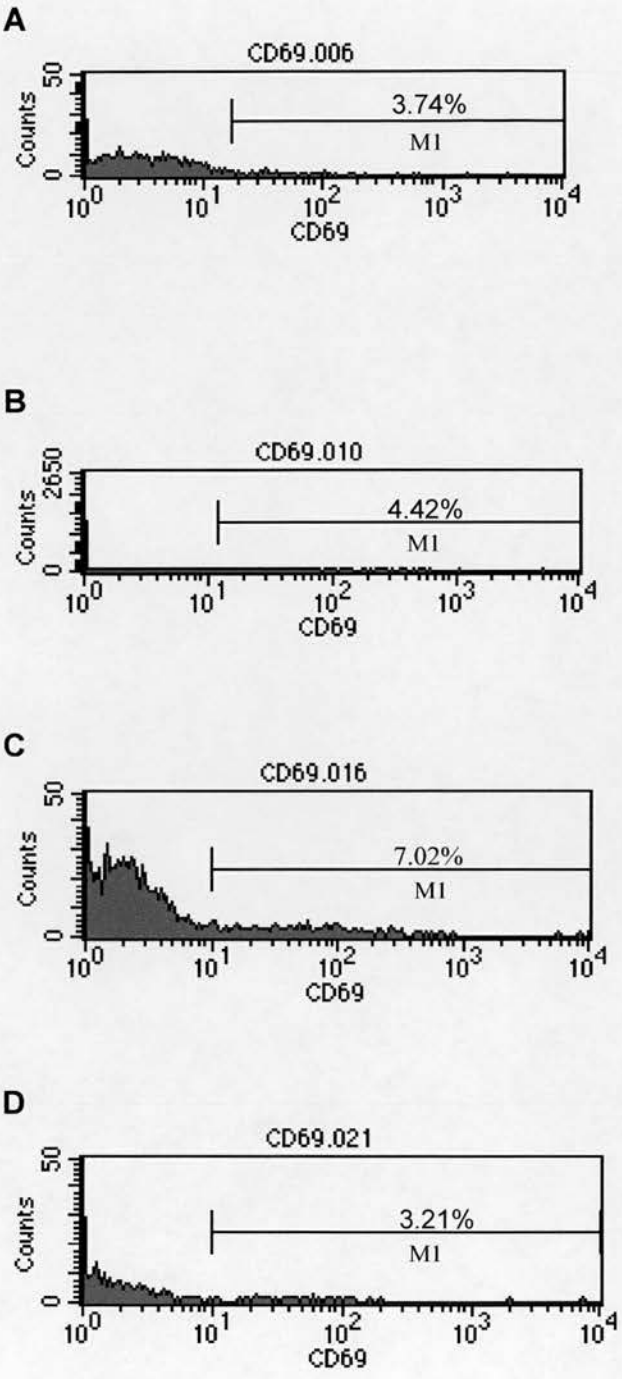

Fig 6.17 CD69 on CD4+ T cells is not up-regulated by co-culture with L cells. FACS analysis of CD4+ T cells, gated on a lymphocyte gate, stained with anti-CD69 antibody, co-cultured with **A** Parental L cells; **B** Parental L cells and 100μM MW167; **C** Delta-like1 expressing L cells; **D** Delta-like1 expressing L cells and 100μM MW167. Data are representative of 3 experiments.

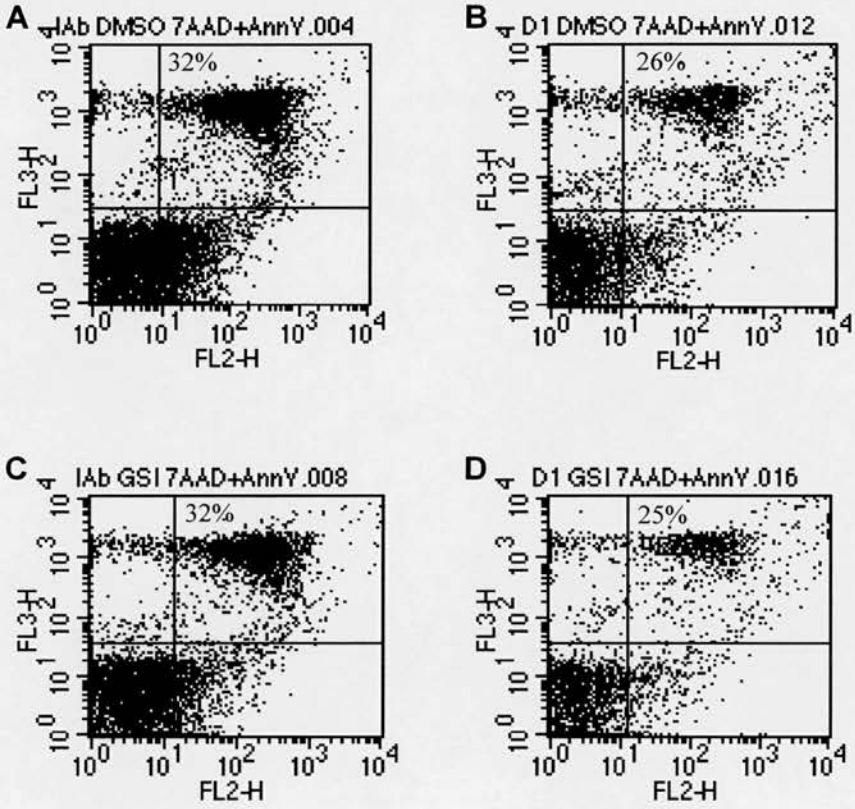

Fig 6.18 Co-culture of CD4+ T cells with Delta-like 1 expressing L cells has no effect on the degree of apoptosis observed. AnnexinV/7AAD staining of CD4+ T cells to determine the degree of apoptosis. **A** Co-culture with parental L cells + DMSO; **B** Co-culture with Delta-like 1 expressing L cells + DMSO; **C** Co-culture with parental L cells + 100μM MW167; **D** Co-culture with Delta-like 1 expressing L cells + 100μM MW167. Representative data from 2 experiments.

6.6.3 Aire expression is up-regulated by signalling through Delta-like1

In all 4 experiments in which immunofluorescence was undertaken, Aire protein expression was increased in CD4+ T cells co-cultured with Dl1 L cells compared to co-culture with parental L cells (Fig 6.19).

6.6.4 Inhibition of Notch signalling inhibits Aire up-regulation by Delta-like1

The up-regulation of Aire protein expression observed following co-culture with Dl1 L cells is not seen when these cells are cultured in the presence of 100μM MW167 (n=3) (Fig 6.20).

A

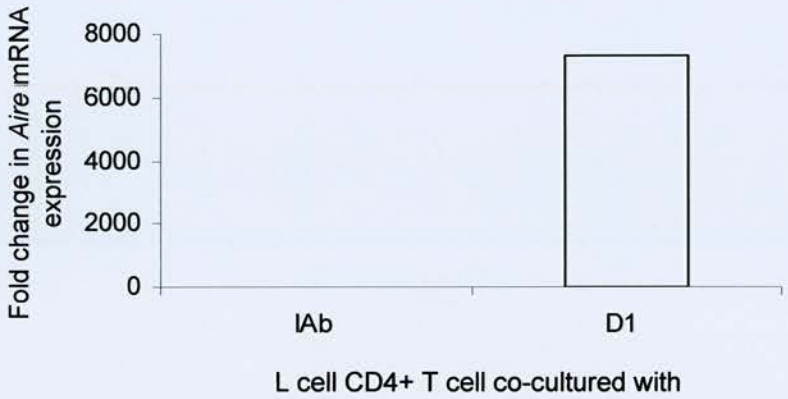

B

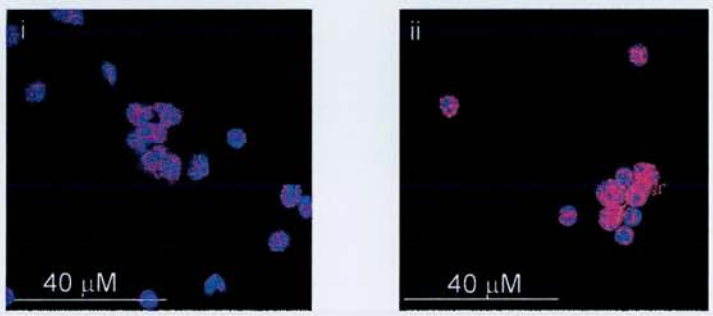

Fig 6.19 Aire expression is up-regulated in CD4+ T cells co-cultured with Delta 1 expressing L cells. A *Aire* mRNA expression as measured by Real Time RT-PCR in CD4+ T cells co-cultured with either parental or Delta-like 1 expressing L cells; **B** Aire protein expression by immunofluorescence in CD4+ T cells co-cultured with either (i) Parental or (ii) Delta-like 1 expressing L cells; Aire (red), Nucleus (Blue); n=4.

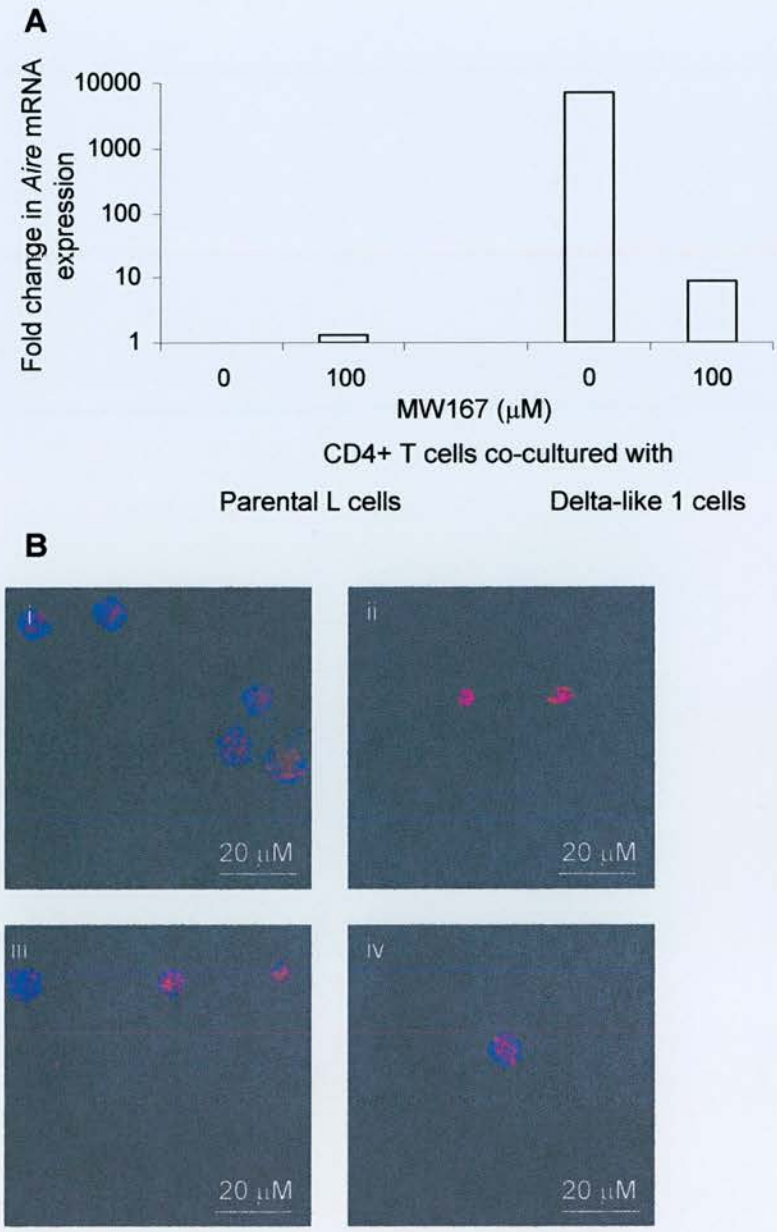

Fig 6.20 Aire expression is not up-regulated in the presence of MW167. CD4+ T cells co-cultured with either Parental or Delta-like1 L cells in the presence or absence of MW167. **A** Real time RT-PCR; **B** Immunofluoresence for Aire (red), the nucleus is stained with ToPro3 (blue); i) CD4+ T cells co-cultured with parental L cells – MW167; ii) CD4+ T cells co-cultured with Delta-like1 L cells – MW167; iii) CD4+ T cells co-cultured with parental L cells + MW167; iv) CD4+ T cells co-cultured with Delta-like1 L cells + MW167. Data are representative of 3 individual experiments.

6.7 Discussion

Following the observation that Aire is up-regulated under the same conditions as Hes1, one of the target genes of Notch signalling, the possibility of an interaction between Aire and Notch was investigated. Further evidence for Notch signalling occurring under these conditions is provided in 2 recent publications (146,145). In work by Palaga et al, Notch 1 protein expression was increased upon activation. Furthermore, Hes1 was also up-regulated upon activation as was the active intra-cellular portion of Notch 1, demonstrating that signalling through Notch is occurring to give cleavage and release of the intra-cellular portion which is then signalling to Hes1 (146). This was also demonstrated by Adler et al, who show that mRNA expression of all Notch receptors is increased after antigen specific stimulation and at the protein level, the active intra-cellular portion of Notch1 was detected within 12 hours of activation (145).

For the data presented in this chapter, the increase in Notch signalling seen on T cell activation was inhibited by the γ-secretase inhibitor, MW167, this prevented the up-regulation in Aire protein seen in the presence of co-stimulation. However, the up-regulation of Aire protein seen when activation occurs solely through the TCR is not inhibited by MW167.

Although it is arguably more relevant to have protein data, as presented here, as it is this that will effect a biological response, the relative mRNA expression would also be interesting. However, deriving any meaningful results from the real time RT-PCR data obtained was problematic. This was mainly because Aire is expressed at very low levels, and as such was at the limit of detection by real-time RT-PCR. As the

cycle threshold was occurring within the plateau phase of the reaction rather than the logarithmic phase any differences in expression are much more difficult to detect. An added problem was determining the optimal kinetics for the reaction, as this appeared to be slightly different in each experiment. Thus, to accurately determine the true change in mRNA expression in each experiment would have involved a large number of time points and would have been impossible in terms of the size of the experiment and the cost of reagents.

Given its effects on cell proliferation and survival, it was important to ensure that any differences seen were due to Notch signalling itself and not due to any effects its absence may have on the cell. This was demonstrated in the system used here, i.e. inhibition of Notch signalling, by the absence of any differences in cell proliferation, up-regulation of activation markers and measurement of apoptosis. However, in work using an alternative γ-secretase inhibitor, compound E, Adler et al, find that inhibiting Notch signalling decreases T cell proliferation, IL-2 production and CD25 expression (145). A decrease in proliferation of T cells is also described by Palaga et al, when the γ-secretase inhibitor, IL-CHO is used to inhibit Notch signalling, in addition, they find a decrease in IFN-γ production and NF-κB activity when Notch signalling is inhibited (146). In a preliminary experiment using one of these alternative γ-secretase inhibitors, Compound E, no difference in proliferation was observed, but a diminution in the up-regulation of CD25 upon activation was observed in the absence of notch signalling. The same pattern of Aire expression was observed, i.e. in the presence of co-stimulation Aire up-regulation was prevented by inhibiting Notch signalling, this did not occur in the absence of co-stimulation. Aire protein expression was also increased by delivering a direct Notch signal in the

absence of TCR signalling providing further evidence that it is the Notch signal, and not the TCR signalling that is leading to up-regulation of Aire. Again this up-regulation could be prevented by the γ-secretase inhibitor MW167.

An important question to address is the specificity of the gamma secretase inhibitor, at the time this work was commenced MW167 was one of only two gamma secretase inhibitors available. MW167 was chosen as there was data in the literature showing a 90% reduction in signalling through Notch (156). However, the gamma secretase complex also cleaves amyloid precursor protein (APP) (133). APP is expressed at low levels in lymphocytes (157,158) and its surface expression is increased upon activation (158). APP has been shown to affect lymphocytes as APP peptides are able to stimulate lymphocyte proliferation in humans (159). Thus, there is a possibility that the results shown in this chapter are due to APP being affected by MW167 rather than Notch signalling. A preliminary experiment with a γ-secretase inhibitor XI that inhibits cleavage of APP but not Notch, completely inhibited proliferation of CD4+ T cells to either anti-CD3 antibody alone or anti-CD3/28 antibodies. However, as described above, no difference was observed in proliferation when MW167 was used. These data suggests that MW167 was not affecting APP in the system used here, and also raises the question, whether the difference in proliferation observed by Adler et al (145) and Palaga et al (146) is due to effects on APP cleavage as well as Notch.

CHAPTER 7

7 Discussion

The hypothesis of this work was that lack of functional Aire affects peripheral T cell function. This was addressed in the following ways.

In chapter 3, the UK population of APS1 patients was characterised with regard to phenotype and genotype. The predominant genotype consisted of the presence a mutation in exon 8 of the *AIRE* gene (964del13), which has previously been suggested to be the common UK mutation (1). These patients have a wide variety of autoimmune diseases, with no apparent genotype-phenotype correlation. This disease heterogeneity led to problems investigating peripheral T cell responses in APS1 patients and therefore no significant differences were seen. One way to have more confidence in the limited data set presented here, would be to increase the number of controls studied, as this would ensure that the 'normal range' against which the patients are compared is as accurate as possible. The use of the Aire deficient mouse may help to clarify this issue, as these mice are all on the same genetic background, which would eliminate any bias in phenotype due to the genetic variability seen in humans.

In keeping with other reports (51,8,6,7), the data in chapter 4 show the presence of Aire mRNA and protein in the murine thymus, predominantly within the medulla. In the lymph node and spleen, Aire expression was seen in B and T cell areas, in contrast to the 'T cell area only' staining reported previously (6). This Aire staining was confirmed to be expression in both T and B cells by staining of purified lymphocyte populations (Chapter 5). This may suggest a role for Aire in the peripheral immune response in addition to its recently characterised role in the development of central tolerance.

Expression of Aire in other tissues was more restricted than in the previously reported study (6). It is difficult to resolve these differences, as all the antibodies currently in use, are polyclonal sera raised in house by the individual groups, and at present there are no commercially available antibodies. A GFP construct under the control of the Aire promoter could be developed to clarify this issue.

To further investigate the possibility of a role for Aire in peripheral T cells, CD4+ T cells were activated through the TCR in the presence and absence of co-stimulation and an increase in Aire mRNA and protein expression was observed (Chapter 5). This observation was then investigated further with regard to an interaction with the Notch signalling pathway, as components of this pathway had been observed to be up-regulated under the same conditions (146,145).

When Notch signalling was inhibited by the γ-secretase inhibitor, MW167, the up-regulation of Aire observed in the presence of co-stimulation was inhibited. In CD4+ T cells that received only a TCR signal, Aire expression was increased irrespective of the presence of a Notch signal (Chapter 6). In addition, evidence for an increase in Aire expression caused by a direct Notch signal is presented, this increase is also abrogated by the use of MW167 (Chapter 6).

As co-stimulation appears to be required to inhibit Aire expression in the absence of Notch signalling, the role of co-stimulation in the regulation of Aire expression is of interest. One possibility would be to explore this further using alternative methods of co-stimulation e.g. CD40-CD40L, ICOS-B7, however as it is CD28 that is a major source of co-stimulation this approach may not succeed. A more successful approach may be to substitute IL2 for the CD28 signal, however, this assumes that the effects

mediated by CD28 are through it up-regulating other transcription factors and not through IL2 production.

There have been many difficulties in investigating the role of Aire in peripheral T cell function. As this is a rapidly evolving field with limited reagents the first challenge was to characterise the distribution of Aire in the system used here. This lack of commercially available reagents has also meant that the work has been descriptive, as the resources required to address these issues in a mechanistic way are not freely available.

It is disappointing that no differences were observed in the distribution of peripheral cell subsets and the responses of T cells to a polyclonal stimulus and this work clearly needs to be expanded both in terms of numbers and the methods used to confirm that this lack of a difference is not an artefact of the methods used. An alternative approach would be to characterise antigen specific responses, e.g. to tetanus toxoid, as this may reveal more subtle differences in the T cell proliferative response than can be seen with the use of a polyclonal stimulus such as anti-CD3/28 antibodies. Use of an animal model rather than patients with APS1 to investigate the role of Aire in the periphery would enable the investigation of antigen specific responses in more detail, as although looking at a recall response to common immunogens eg tetanus toxoid would be preferable to a polyclonal response, the numbers of cells involved would, relatively speaking be small. However, if this were investigated in a TCR transgenic mouse crossed with the Aire knock-out mouse, the chances of seeing any differences present would be greatly enhanced.

The development of an all-encompassing hypothesis based on the results presented here has been challenging. The systems investigated are complex, with numerous interactions, at a variety of different levels, such that completely dissecting out the pathways will be a difficult process.

The results in chapter 6, suggest that Aire up-regulation is mediated by Notch signalling. Thus, when a T cell is activated, surface expression of Notch1 is increased (146) leading to increased Notch signalling, which is able to mediate Aire up-regulation. However, the lack of inhibition of Aire expression seen when Notch signalling is inhibited in an anti-CD3 activated T cell is not in keeping with this (Chapter 6). One possible explanation of this observation, is that Notch is required to prevent CD28 mediated down-regulation of Aire. Signalling through CD28 leads to the activation of cJun (160) which is able to bind to the Aire promoter, but functional assays of AP-1 binding to Aire, which appears to be solely mediated through Jun and not Fos, reveal that AP-1 binding activates a luciferase reporter construct and that this activation is decreased when the AP-1 binding site in the Aire promoter is mutated (63). If Notch is required to prevent CD28 down-regulation of Aire, then one possible mechanism would be that binding of the Aire promoter by Jun has an inhibitory effect on Aire transcription, which is not suggested by the available data on Aire and AP-1 binding, but AP-1 has been shown to have inhibitory effects on mdr-1 gene expression (161).

However, Notch signalling also affects AP-1, as binding of NICD to CBF1 represses AP-1 transactivation (162) and inhibiting Notch signalling leads to a defect in NF-κB

activation (146). Therefore, there are many different pathways through which Notch signalling may affect the T cell, all of which will undoubtedly interact.

This putative interaction between Aire and Notch signalling clearly needs further investigation, this may either be mediated through one of the components of the Notch signalling pathway directly, or alternatively through alterations in cytokine secretion in the presence of Notch signalling. To take this aspect of the thesis further forward, the experiments described here, should first be repeated using the alternative methods of inhibiting the Notch signal that are now available. The data presented here would suggest that Aire is up-regulated by Notch signalling. Notch signalling is up-regulated in an activated T cell, therefore, is it Notch signalling rather than T cell activation that is leading to Aire up-regulation in activated T cells. The investigation of Aire expression in a Notch knock-out mouse would help to delineate this, however, due to redundancy in the Notch signalling system, this is likely to prove difficult. If it is the effects of Notch signalling on cytokine secretion that bring about the effect on Aire expression, a different approach will need to be taken. Inhibition of Notch signalling decreases IFN-γ production (146), and data presented as a poster in 2002 by Moratto et al, shows that there is an AIRE binding site in the promoter region of IFN-γ, therefore the inhibition of Aire seen on Notch signalling may reflect a decrease in IFN-γ. This could be investigated further by blocking IFN-γ activity with a specific antibody and assessing the impact on Aire expression in activated cells.

What might be the function of this regulation of Aire expression in CD4+ T cells? In the Aire deficient mouse, a 3-5 fold increase in proliferation was observed upon *in-vitro* re-challenge with HEL (74). This, coupled with the observation in chapter 5

that Aire expression is increased upon activation, led to the thought that Aire may be required to terminate the proliferative response. This hypothesis needs further investigation and the approaches described above, namely the use of antigen specific responses, and in particular TCR transgenic mice crossed with the Aire knock-out mouse, should go some way to determining this.

Final thoughts

This work has started to address the issue of whether Aire has a role in the peripheral T cell. In view of the widespread autoimmune disease seen in the absence of Aire, the role of Aire in peripheral tolerance would be of interest, as although Aire has been shown to affect central tolerance, not all autoreactive T cells will be deleted within the thymus, thus mechanisms are required in the periphery to control these cells. One avenue to explore in this respect would be the expression of Aire in regulatory T cells, both resting and upon activation, or perhaps it would be more interesting to investigate the effect upon Aire expression in the cells suppressed by the regulatory population. In addition to CD4+ T cells subsets, work described here reveals the presence of Aire in CD8+ T cells and in B cells, and the investigation of the role of Aire in these cells will be of interest.

The hope when starting this work was that, as the absence of Aire mediates the development of a monogenic form of autoimmune disease, the study of this gene would provide insights into the mechanisms of autoimmunity not just in this small population of patients, but also in the more common complex autoimmune diseases. Work published during the course of this work has demonstrated an important role

for Aire in central tolerance (13,75), which despite the lack of a correlation between heterozygosity for AIRE mutations and complex autoimmune diseases, may still prove to be of relevance in non-APS1 patients. However, it is unlikely that Aire only acts to regulate the ectopic expression of tissue specific antigens, making the data presented here regarding a possible role for Aire in the periphery all the more intriguing.

Reference List

1. Pearce, S. H. et al 1998 A common and recurrent 13-bp deletion in the autoimmune regulator gene in British kindreds with autoimmune polyendocrinopathy type 1. Am.J.Hum.Genet. 63;1675-1684.

2. 1997 An autoimmune disease, APECED, caused by mutations in a novel gene featuring two PHD-type zinc-finger domains. The Finnish-German APECED Consortium. Autoimmune Polyendocrinopathy-Candidiasis-Ectodermal Dystrophy. Nat.Genet. 17;399-403.

3. Nagamine, K. et al 1997 Positional cloning of the APECED gene. Nat.Genet. 17;393-398.

4. Ahonen, P. et al 1990 Clinical variation of autoimmune polyendocrinopathy-candidiasis- ectodermal dystrophy (APECED) in a series of 68 patients. N.Engl.J.Med. 322;1829-1836.

5. Mittaz, L. et al 1999 Isolation and characterization of the mouse Aire gene. Biochem.Biophys.Res.Commun. 255;483-490.

6. Halonen, M. et al 2001 Subcellular location and expression pattern of autoimmune regulator (Aire), the mouse orthologue for human gene defective in autoimmune polyendocrinopathy candidiasis ectodermal dystrophy (APECED). J.Histochem.Cytochem. 49;197-208.

7. Heino, M. et al 2000 RNA and protein expression of the murine autoimmune regulator gene (Aire) in normal, RelB-deficient and in NOD mouse. Eur.J.Immunol. 30;1884-1893.

8. Heino, M. et al 1999 Autoimmune regulator is expressed in the cells regulating immune tolerance in thymus medulla. Biochem.Biophys.Res.Commun. 257;821-825.

9. Laufer, T. M., Glimcher, L. H., and Lo, D. 1999 Using thymus anatomy to dissect T cell repertoire selection. Semin.Immunol. 11;65-70.

10. Klein, L. et al 2000 Shaping of the autoreactive T-cell repertoire by a splice variant of self protein expressed in thymic epithelial cells. Nat.Med. 6;56-61.

11. Derbinski, J. et al 2001 Promiscuous gene expression in medullary thymic epithelial cells mirrors the peripheral self. Nat.Immunol. 2;1032-1039.

12. Kyewski, B. et al 2002 Promiscuous gene expression and central T-cell tolerance: more than meets the eye. Trends Immunol. 23;364-371.

13. Anderson, M. S. et al 2002 Projection of an immunological self shadow within the thymus by the aire protein. Science. 298;1395-1401.

14. Heino, M. et al 1999 Mutation analyses of North American APS-1 patients. Hum.Mutat. 13;69-74.

15. Heino, M. et al 2001 APECED mutations in the autoimmune regulator (AIRE) gene. Hum.Mutat. 18;205-211.

16. Rosatelli, M. C. et al 1998 A common mutation in Sardinian autoimmune polyendocrinopathy- candidiasis-ectodermal dystrophy patients. Hum.Genet. 103;428-434.

17. Scott, H. S. et al 1998 Common mutations in autoimmune polyendocrinopathy-candidiasis- ectodermal dystrophy patients of different origins. Mol.Endocrinol. 12;1112-1119.

18. Wang, C. Y. et al 1998 Characterization of mutations in patients with autoimmune polyglandular syndrome type 1 (APS1). Hum.Genet. 103;681-685.

19. Esselborn VM et al 1956 The syndrome of familial juvenile hypoadreocorticism, hypoparathyroidism and superficial moniliasis. Journal of Clinical Endocrinology Metabolism. 16;1374-1387.

20. Thorpe ES and Handley HE 1929 Chronic tetany and chronic mycelial stomatitis in a child aged 4 and half years. Am J Dis Child. 38;328-338.

21. Leonard MF 1946 Chronic idiopathic hypoparathyroidism with superimposed Addison's disease in a child. Journal of Clinical Endocrinology Metabolism. 6;493-495.

22. Aaltonen, J. et al 1994 An autosomal locus causing autoimmune disease: autoimmune polyglandular disease type I assigned to chromosome 21. Nat.Genet. 8;83-87.

23. Blechschmidt, K. et al 1999 The mouse Aire gene: comparative genomic sequencing, gene organization, and expression. Genome Res. 9;158-166.

24. Wang, C. Y. et al 1999 Cloning of Aire, the mouse homologue of the autoimmune regulator (AIRE) gene responsible for autoimmune polyglandular syndrome type 1 (APS1). Genomics. 55;322-326.

25. Gibson, T. J. et al 1998 The APECED polyglandular autoimmune syndrome protein, AIRE-1, contains the SAND domain and is probably a transcription factor. Trends Biochem.Sci. 23;242-244.

26. Bottomley, M. J. et al 2001 The SAND domain structure defines a novel DNA-binding fold in transcriptional regulation. Nat.Struct.Biol. 8;626-633.

27. Kumar, P. G. et al 2001 The autoimmune regulator (AIRE) is a DNA-binding protein. Journal of Biological Chemistry. 276;41357-41364.

28. Pitkanen, J. and Peterson, P. 2003 Autoimmune regulator: from loss of function to autoimmunity. Genes Immun. 4;12-21.

29. Ahonen, P. et al 1988 The expression of autoimmune polyglandular disease type I appears associated with several HLA-A antigens but not with HLA-DR. Journal of Clinical Endocrinology Metabolism. 66;1152-1157.

30. Gylling, M. et al 2000 {beta}-Cell Autoantibodies, Human Leukocyte Antigen II Alleles, and Type 1 Diabetes in Autoimmune Polyendocrinopathy-Candidiasis-Ectodermal Dystrophy. Journal of Clinical Endocrinology Metabolism. 85;4434-.

31. Betterle, C. et al 2002 Autoimmune adrenal insufficiency and autoimmune polyendocrine syndromes: autoantibodies, autoantigens, and their applicability in diagnosis and disease prediction. Endocr.Rev. 23;327-364.

32. Betterle, C., Greggio, N. A., and Volpato, M. 1998 Clinical review 93: Autoimmune polyglandular syndrome type 1. Journal of Clinical Endocrinology Metabolism. 83;1049-1055.

33. Zlotogora, J. and Shapiro, M. S. 1992 Polyglandular autoimmune syndrome type I among Iranian Jews. J Med.Genet. 29;824-826.

34. Neufeld M, Maclaren NK, and Blizzard RM 1981 Two types of autoimmune Addison's disease associated with different polyglandular autoimmune (PGA) syndromes. Medicine. 60;355-362.

35. Li, Y. et al 1996 Autoantibodies to the extracellular domain of the calcium sensing receptor in patients with acquired hypoparathyroidism. J.Clin.Invest. 97;910-914.

36. Winqvist, O. et al 1993 Two different cytochrome P450 enzymes are the adrenal antigens in autoimmune polyendocrine syndrome type I and Addison's disease. J.Clin.Invest. 92;2377-2385.

37. Winqvist, O. et al 1995 Identification of the main gonadal autoantigens in patients with adrenal insufficiency and associated ovarian failure. J.Clin.Endocrinol.Metab. 80;1717-1723.

38. Song, Y. H. et al 1994 Autoantibody epitope mapping of the 21-hydroxylase antigen in autoimmune Addison's disease. J.Clin.Endocrinol.Metab. 78;1108-1112.

39. Uibo, R. et al 1994 Characterization of adrenal autoantigens recognized by sera from patients with autoimmune polyglandular syndrome (APS) type I. J.Autoimmun. 7;399-411.

40. Craig JM, Schiff LH, and Boone JE 1955 Chronic moniliasis associated with Addison's disease. Am J Dis Child. 89;669-683.

41. Ekwall, O. et al 1998 Identification of tryptophan hydroxylase as an intestinal autoantigen. Lancet. 352;279-283.

42. Friedman, T. C. et al 1991 Frequent occurrence of asplenism and cholelithiasis in patients with autoimmune polyglandular disease type 1. Am J Med. 91;625-630.

43. Tuomi, T. et al 1996 Antibodies to glutamic acid decarboxylase and insulin-dependent diabetes in patients with autoimmune polyendocrine syndrome type I. J.Clin.Endocrinol.Metab. 81;1488-1494.

44. Myhre, A. G. et al 2001 Autoimmune polyendocrine syndrome type 1 (APS I) in Norway. Clin.Endocrinol.(Oxf). 54;211-217.

45. Pearce, S. H. and Cheetham, T. D. 2001 Autoimmune polyendocrinopathy syndrome type 1: treat with kid gloves. Clin Endocrinol (Oxf). 54;433-435.

46. Klemetti, P. et al 2000 Autoimmunity to glutamic acid decarboxylase in patients with autoimmune polyendocrinopathy-candidiasis-ectodermal dystrophy (APECED). Clin.Exp.Immunol. 119;419-425.

47. Vaidya, B. et al 2000 Association analysis of the cytotoxic T lymphocyte antigen-4 (CTLA-4) and autoimmune regulator-1 (AIRE-1) genes in sporadic autoimmune Addison's disease. J.Clin.Endocrinol.Metab. 85;688-691.

48. Nithiyananthan, R. et al 2000 A heterozygous deletion of the autoimmune regulator (AIRE1) gene, autoimmune thyroid disease, and type 1 diabetes: no evidence for association. J.Clin.Endocrinol.Metab. 85;1320-1322.

49. Meyer, G. et al 2001 Screening for an AIRE-1 mutation in patients with Addison's disease, type 1 diabetes, Graves' disease and Hashimoto's thyroiditis as well as in APECED syndrome. Clin.Endocrinol.(Oxf). 54;335-338.

50. Pitkanen, J. et al 2001 Subcellular localization of the autoimmune regulator protein. characterization of nuclear targeting and transcriptional activation domain. Journal of Biological Chemistry. 276;19597-19602.

51. Bjorses, P. et al 1999 Localization of the APECED protein in distinct nuclear structures. Hum.Mol.Genet. 8;259-266.

52. Rinderle, C. et al 1999 AIRE encodes a nuclear protein co-localizing with cytoskeletal filaments: altered sub-cellular distribution of mutants lacking the PHD zinc fingers. Hum.Mol.Genet. 8;277-290.

53. Bjorses, P. et al 2000 Mutations in the AIRE gene: effects on subcellular location and transactivation function of the autoimmune polyendocrinopathy-candidiasis-ectodermal dystrophy protein. Am.J.Hum.Genet. 66;378-392.

54. Pitkanen, J. et al 2000 The autoimmune regulator protein has transcriptional transactivating properties and interacts with the common coactivator CREB-binding protein. Journal of Biological Chemistry. 275;16802-16809.

55. Janknecht, R. and Hunter, T. 1996 Versatile molecular glue. Transcriptional control. Curr.Biol. 6;951-954.

56. Goldman, P. S., Tran, V. K., and Goodman, R. H. 1997 The multifunctional role of the co-activator CBP in transcriptional regulation. Recent Prog.Horm.Res. 52;103-119.

57. Kamei, Y. et al 1996 A CBP integrator complex mediates transcriptional activation and AP-1 inhibition by nuclear receptors. Cell. 85;403-414.

58. Chakravarti, D. et al 1996 Role of CBP/P300 in nuclear receptor signalling. Nature. 383;99-103.

59. Heery, D. M. et al 1997 A signature motif in transcriptional co-activators mediates binding to nuclear receptors. Nature. 387;733-736.

60. Ogryzko, V. V. et al 1996 The transcriptional coactivators p300 and CBP are histone acetyltransferases. Cell. 87;953-959.

61. Bannister, A. J. and Kouzarides, T. 1996 The CBP co-activator is a histone acetyltransferase. Nature. 384;641-643.

62. Doucas, V. et al 1999 Modulation of CREB binding protein function by the promyelocytic (PML) oncoprotein suggests a role for nuclear bodies in hormone signaling. Proc.Natl.Acad.Sci.U.S.A. 96;2627-2632.

63. Murumagi, A., Vahamurto, P., and Peterson, P. 2003 Characterization of regulatory elements and methylation pattern of AIRE (autoimmune regulator) promoter. Journal of Biological Chemistry. M210437200-.

64. Karin, M., Liu, Z., and Zandi, E. 1997 AP-1 function and regulation. Curr.Opin.Cell Biol. 9;240-246.

65. Mantovani, R. 1999 The molecular biology of the CCAAT-binding factor NF-Y. Gene. 239;15-27.

66. Suske, G. 1999 The Sp-family of transcription factors. Gene. 238;291-300.

67. Cao, Y. X., Jean, J. C., and Williams, M. C. 2000 Cytosine methylation of an Sp1 site contributes to organ-specific and cell-specific regulation of expression of the lung epithelial gene t1alpha. Biochem.J. 350 Pt 3;883-890.

68. Uchida, D. et al 2004 AIRE Functions As an E3 Ubiquitin Ligase. The Journal of Experimental Medicine. 199;167-172.

69. Hochstrasser, M. 1998 There's the Rub: a novel ubiquitin-like modification linked to cell cycle regulation. Genes and Development. 12;901-907.

70. Pickart, C. M. 2001 Mechanisms underlying ubiquitination. Annu.Rev.Biochem. 70;503-533.

71. Zuklys, S. et al 2000 Normal thymic architecture and negative selection are associated with Aire expression, the gene defective in the autoimmune-polyendocrinopathy-candidiasis-ectodermal dystrophy (APECED). J.Immunol. 165;1976-1983.

72. Kogawa, K. et al 2002 Expression of AIRE gene in peripheral monocyte/dendritic cell lineage. Immunol.Lett. 80;195-198.

73. Ruan, Q. G. et al 1999 Expression and alternative splicing of the mouse autoimmune regulator gene (Aire). J.Autoimmun. 13;307-313.

74. Ramsey, C. et al 2002 Aire deficient mice develop multiple features of APECED phenotype and show altered immune response. Hum.Mol.Genet. 11;397-409.

75. Liston, A. et al 2003 Aire regulates negative selection of organ-specific T cells. Nat Imm 4;350-354.

76. Jolicoeur, C., Hanahan, D., and Smith, K. M. 1994 T-cell tolerance toward a transgenic beta-cell antigen and transcription of endogenous pancreatic genes in thymus. Proc.Natl.Acad.Sci.U.S.A. 91;6707-6711.

77. Chin, R. K. et al 2003 Lymphotoxin pathway directs thymic Aire expression. Nat.Immunol. 4;1121-1127.

78. Park, Y., Moon, Y., and Chung, H. Y. 2003 AIRE-1 (autoimmune regulator type 1) as a regulator of the thymic induction of negative selection. Ann.N.Y.Acad.Sci. 1005;431-435.

79. Sospedra M et al 1998 Transcription of a broad range of self-antigens in human thymus suggests a role for central mechanisms in tolerance toward peripheral antigens. J.Immunol. 161;5918-5929.

80. Vafiadis, P. et al 1997 Insulin expression in human thymus is modulated by INS VNTR alleles at the IDDM2 locus. Nat.Genet. 15;289-292.

81. Pugliese, A. et al 1997 The insulin gene is transcribed in the human thymus and transcription levels correlated with allelic variation at the INS VNTR-IDDM2 susceptibility locus for type 1 diabetes. Nat.Genet. 15;293-297.

82. Mosmann, T. R. et al 1986 Two types of murine helper T cell clone. I. Definition according to profiles of lymphokine activities and secreted proteins. J.Immunol. 136;2348-2357.

83. Lighvani, A. A. et al 2001 T-bet is rapidly induced by interferon-gamma in lymphoid and myeloid cells. Proc.Natl.Acad.Sci.U.S.A. 98;15137-15142.

84. Afkarian, M. et al 2002 T-bet is a STAT1-induced regulator of IL-12R expression in naive CD4+ T cells. Nat.Immunol. 3;549-557.

85. Swain, S. L. et al 1990 IL-4 directs the development of Th2-like helper effectors. J.Immunol. 145;3796-3806.

86. Kaplan, M. H. et al 1996 Stat6 is required for mediating responses to IL-4 and for development of Th2 cells. Immunity. 4;313-319.

87. Zheng, W. and Flavell, R. A. 1997 The transcription factor GATA-3 is necessary and sufficient for Th2 cytokine gene expression in CD4 T cells. Cell. 89;587-596.

88. Hoyne, G. F. et al 2000 Serrate1-induced notch signalling regulates the decision between immunity and tolerance made by peripheral CD4(+) T cells. Int.Immunol. 12;177-185.

89. Yvon, E. S. et al 2003 Over expression of the Notch ligand, Jagged-1 induces alloantigen-specific human regulatory T cells. Blood 102;3815-3821.

90. Anastasi, E. et al 2003 Expression of activated Notch3 in transgenic mice enhances generation of T regulatory cells and protects against experimental autoimmune diabetes. J.Immunol. 171;4504-4511.

91. Maekawa, Y. et al 2003 Delta1-Notch3 interactions bias the functional differentiation of activated CD4+ T cells. Immunity. 19;549-559.

92. Bennett, S. T. et al 1995 Susceptibility to human type 1 diabetes at IDDM2 is determined by tandem repeat variation at the insulin gene minisatellite locus. Nat.Genet. 9;284-292.

93. Bennett, S. T. and Todd, J. A. 1996 Human type 1 diabetes and the insulin gene: principles of mapping polygenes. Annu.Rev.Genet. 30;343-370.

94. Ward, L. et al 1999 Severe autoimmune polyendocrinopathy-candidiasis-ectodermal dystrophy in an adolescent girl with a novel AIRE mutation: response to immunosuppressive therapy. J.Clin.Endocrinol.Metab. 84;844-852.

95. Todd, J. A. and Wicker, L. S. 2001 Genetic protection from the inflammatory disease type 1 diabetes in humans and animal models. Immunity. 15;387-395.

96. Tait, B. D. et al 2003 HLA genes associated with autoimmunity and progression to disease in type 1 diabetes. Tissue Antigens. 61;146-153.

97. Todd, J. A., Bell, J. I., and McDevitt, H. O. 1987 HLA-DQ beta gene contributes to susceptibility and resistance to insulin-dependent diabetes mellitus. Nature. 329;599-604.

98. Badenhoop, K. et al 1995 Susceptibility and resistance alleles of human leukocyte antigen (HLA) DQA1 and HLA DQB1 are shared in endocrine autoimmune disease. J.Clin.Endocrinol.Metab. 80;2112-2117.

99. Pugliese, A. et al 1995 HLA-DQB1*0602 is associated with dominant protection from diabetes even among islet cell antibody-positive first-degree relatives of patients with IDDM. Diabetes. 44;608-613.

100. Gylling, M. et al 2000 ss-cell autoantibodies, human leukocyte antigen II alleles, and type 1 diabetes in autoimmune polyendocrinopathy-candidiasis-ectodermal dystrophy. J.Clin.Endocrinol.Metab. 85;4434-4440.

101. Arulanantham, K., Dwyer, J. M., and Genel, M. 1979 Evidence for defective immunoregulation in the syndrome of familial candidiasis endocrinopathy. N.Engl.J.Med. 300;164-168.

102. Kirkpatrick, C. H. 1989 Chronic mucocutaneous candidiasis. Eur.J.Clin.Microbiol.Infect.Dis. 8;448-456.

103. Sediva, A., Cihakova, D., and Lebl, J. 2002 Immunological findings in patients with autoimmune polyendocrinopathy-candidiasis-ectodermal dystrophy (APECED) and their family members: are heterozygotes subclinically affected? J.Pediatr.Endocrinol.Metab. 15;1491-1496.

104. Kobrynski, L. J. et al 1996 Production of T-helper cell subsets and cytokines by lymphocytes from patients with chronic mucocutaneous candidiasis. Clin.Diagn.Lab Immunol. 3;740-745.

105. Lilic, D. and Gravenor, I. 2001 Immunology of chronic mucocutaneous candidiasis. J.Clin.Pathol. 54;81-83.

106. Moraes-Vasconcelos, D. et al 2001 Characterization of the cellular immune function of patients with chronic mucocutaneous candidiasis. Clin.Exp.Immunol. 123;247-253.

107. Ashwell, J. D., Lu, F. W., and Vacchio, M. S. 2000 Glucocorticoids in T cell development and function*. Annu.Rev.Immunol. 18;309-345.

108. Hayes, C. E. et al 2003 The immunological functions of the vitamin D endocrine system. Cell Mol.Biol.(Noisy.-le-grand). 49;277-300.

109. Maret, A. et al 2003 Estradiol enhances primary antigen-specific CD4 T cell responses and Th1 development in vivo. Essential role of estrogen receptor alpha expression in hematopoietic cells. Eur.J.Immunol. 33;512-521.

110. Murch, S. H. et al 1999 Autoimmune enteropathy with distinct mucosal features in T-cell activation deficiency: the contribution of T cells to the mucosal lesion. J.Pediatr.Gastroenterol.Nutr. 28;393-399.

111. Moore, L. et al 1995 Autoimmune enteropathy with anti-goblet cell antibodies. Hum.Pathol. 26;1162-1168.

112. Burkly, L. C. et al 1993 Clonal deletion of V beta 5+ T cells by transgenic I-E restricted to thymic medullary epithelium. J.Immunol. 151;3954-3960.

113. Schonrich, G. et al 1992 Anergy induced by thymic medullary epithelium. Eur.J.Immunol. 22;1687-1691.

114. Modigliani, Y. et al 1995 Lymphocytes selected in allogeneic thymic epithelium mediate dominant tolerance toward tissue grafts of the thymic epithelium haplotype. Proc.Natl.Acad.Sci.U.S.A. 92;7555-7559.

115. Kumar, P. G., Laloraya, M., and She, J. X. 2002 Population genetics and functions of the autoimmune regulator (AIRE). Endocrinol.Metab Clin.North Am. 31;321-38, vi.

116. Cremer, T. and Cremer, C. 2001 Chromosome territories, nuclear architecture and gene regulation in mammalian cells. Nat.Rev.Genet. 2;292-301.

117. Matera, A. G. 1999 Nuclear bodies: multifaceted subdomains of the interchromatin space. Trends Cell Biol. 9;302-309.

118. Fox, A. H. et al 2002 Paraspeckles: a novel nuclear domain. Curr.Biol. 12;13-25.

119. Thiede, B. et al 2001 Predominant identification of RNA-binding proteins in Fas-induced apoptosis by proteome analysis. J.Biol.Chem. 276;26044-26050.

120. Hallier, M., Tavitian, A., and Moreau-Gachelin, F. 1996 The transcription factor Spi-1/PU.1 binds RNA and interferes with the RNA-binding protein p54nrb. J.Biol.Chem. 271;11177-11181.

121. Basu, A. et al 1997 The intracisternal A-particle proximal enhancer-binding protein activates transcription and is identical to the RNA- and DNA-binding protein p54nrb/NonO. Mol.Cell Biol. 17;677-686.

122. Zhang, Z. and Carmichael, G. G. 2001 The fate of dsRNA in the nucleus: a p54(nrb)-containing complex mediates the nuclear retention of promiscuously A-to-I edited RNAs. Cell. 106;465-475.

123. Mathur, M., Tucker, P. W., and Samuels, H. H. 2001 PSF is a novel corepressor that mediates its effect through Sin3A and the DNA binding domain of nuclear hormone receptors. Mol.Cell Biol. 21;2298-2311.

124. Iwasaki, T., Chin, W. W., and Ko, L. 2001 Identification and characterization of RRM-containing coactivator activator (CoAA) as TRBP-interacting protein, and its splice variant as a coactivator modulator (CoAM). J.Biol.Chem. 276;33375-33383.

125. Macian, F. et al 2002 Transcriptional mechanisms underlying lymphocyte tolerance. Cell. 109;719-731.

126. Lieberman, S. M. et al 2003 Identification of the beta cell antigen targeted by a prevalent population of pathogenic CD8+ T cells in autoimmune diabetes. Proc.Natl.Acad.Sci.U.S.A. 100;8384-8388.

127. Perniola, R. et al 2000 Organ-specific and non-organ-specific autoantibodies in children and young adults with autoimmune polyendocrinopathy-candidiasis-ectodermal dystrophy (APECED). Eur.J.Endocrinol. 143;497-503.

128. Portin, P. 2002 General outlines of the molecular genetics of the Notch signalling pathway in Drosophila melanogaster: a review. Hereditas. 136;89-96.

129. Baron, M. 2003 An overview of the Notch signalling pathway. Semin.Cell Dev.Biol. 14;113-119.

130. Logeat, F. et al 1998 The Notch1 receptor is cleaved constitutively by a furin-like convertase. Proc.Natl.Acad.Sci.U.S.A. 95;8108-8112.

131. Brou, C. et al 2000 A novel proteolytic cleavage involved in Notch signaling: the role of the disintegrin-metalloprotease TACE. Mol.Cell. 5;207-216.

132. Schroeter, E. H., Kisslinger, J. A., and Kopan, R. 1998 Notch-1 signalling requires ligand-induced proteolytic release of intracellular domain. Nature. 393;382-386.

133. Fortini, M. E. 2002 Gamma-secretase-mediated proteolysis in cell-surface-receptor signalling. Nat.Rev.Mol.Cell Biol. 3;673-684.

134. Yu, G. et al 2000 Nicastrin modulates presenilin-mediated notch/glp-1 signal transduction and betaAPP processing. Nature. 407;48-54.

135. Francis, R. et al 2002 aph-1 and pen-2 are required for Notch pathway signaling, gamma-secretase cleavage of betaAPP, and presenilin protein accumulation. Dev.Cell. 3;85-97.

136. Li, Y. M. et al 2000 Presenilin 1 is linked with gamma-secretase activity in the detergent solubilized state. Proc.Natl.Acad.Sci.U.S.A. 97;6138-6143.

137. Kao, H. Y. et al 1998 A histone deacetylase corepressor complex regulates the Notch signal transduction pathway. Genes Dev. 12;2269-2277.

138. Wu, L. et al 2000 MAML1, a human homologue of Drosophila mastermind, is a transcriptional co-activator for NOTCH receptors. Nat.Genet. 26;484-489.

139. Osborne, B. and Miele, L. 1999 Notch and the immune system. Immunity. 11;653-663.

140. Oswald, F. et al 1998 NF-kappaB2 is a putative target gene of activated Notch-1 via RBP-Jkappa. Mol.Cell Biol. 18;2077-2088.

141. Radtke, F. et al 1999 Deficient T cell fate specification in mice with an induced inactivation of Notch1. Immunity. 10;547-558.

142. Pui, J. C. et al 1999 Notch1 expression in early lymphopoiesis influences B versus T lineage determination. Immunity. 11;299-308.

143. Maillard, I., Adler, S. H., and Pear, W. S. 2003 Notch and the immune system. Immunity. 19;781-791.

144. Fowlkes, B. J. and Robey, E. A. 2002 A reassessment of the effect of activated Notch1 on CD4 and CD8 T cell development. J.Immunol. 169;1817-1821.

145. Adler, S. H. et al 2003 Notch signaling augments T cell responsiveness by enhancing CD25 expression. J.Immunol. 171;2896-2903.

146. Palaga, T. et al 2003 TCR-mediated Notch signaling regulates proliferation and IFN-gamma production in peripheral T cells. J.Immunol. 171;3019-3024.

147. De Strooper, B. et al 1999 A presenilin-1-dependent gamma-secretase-like protease mediates release of Notch intracellular domain. Nature. 398;518-522.

148. Mizutani, T. et al 2001 Conservation of the biochemical mechanisms of signal transduction among mammalian Notch family members. Proc.Natl.Acad.Sci.U.S.A. 98;9026-9031.

149. Berezovska, O. et al 2000 Rapid Notch1 nuclear translocation after ligand binding depends on presenilin-associated gamma-secretase activity. Ann.N.Y.Acad.Sci. 920;223-226.

150. Berezovska, O. et al 2000 Aspartate mutations in presenilin and gamma-secretase inhibitors both impair notch1 proteolysis and nuclear translocation with relative preservation of notch1 signaling. J.Neurochem. 75;583-593.

151. Xia, W. et al 2000 FAD mutations in presenilin-1 or amyloid precursor protein decrease the efficacy of a gamma-secretase inhibitor: evidence for direct involvement of PS1 in the gamma-secretase cleavage complex. Neurobiol.Dis. 7;673-681.

152. Campbell, W. A. et al 2003 Presenilin endoproteolysis mediated by an aspartyl protease activity pharmacologically distinct from gamma-secretase. J.Neurochem. 85;1563-1574.

153. Levitan, D. et al 2001 PS1 N- and C-terminal fragments form a complex that functions in APP processing and Notch signaling. Proceedings of the National Academy of Sciences. 98;12186-12190.

154. Sade, H., Krishna, S., and Sarin, A. 2004 The Anti-apoptotic Effect of Notch-1 Requires p56lck-dependent, Akt/PKB-mediated Signaling in T Cells. J.Biol.Chem. 279;2937-2944.

155. Wong, K. K. et al 2003 Notch ligation by Delta1 inhibits peripheral immune responses to transplantation antigens by a CD8+ cell-dependent mechanism. J.Clin.Invest. 112;1741-1750.

156. Taniguchi, Y. et al 2002 Notch receptor cleavage depends on but is not directly executed by presenilins. Proc.Natl.Acad.Sci.U.S.A. 99;4014-4019.

157. Suh, Y. H. et al 1997 Expression of Alzheimer's amyloid precursor protein in human lymphocyte. Archives of Gerontology and Geriatrics. 24;1-7.

158. Bullido, M. J. et al 1996 Alzheimer's amyloid precursor protein is expressed on the surface of hematopoietic cells upon activation. Biochim.Biophys.Acta. 1313;54-62.

159. Trieb, K. et al 1996 APP peptides stimulate lymphocyte proliferation in normals, but not in patients with Alzheimer's disease. Neurobiol.Aging. 17;541-547.

160. Su, B. et al 1994 JNK is involved in signal integration during costimulation of T lymphocytes. Cell. 77;727-736.

161. Miao, Z. H. and Ding, J. 2003 Transcription factor c-Jun activation represses mdr-1 gene expression. Cancer Res. 63;4527-4532.

162. Chu, J. and Bresnick, E. H. 2003 Evidence that CBF1 binding is required for notch-1-mediated repression of activator protein-1. J.Biol.Chem.

163. Macian, F. et al 2004 T-cell anergy. Curr.Opin.Immunol. 16;209-216.

164. Negre, N., Ghysen, A., and Martinez, A. M. 2003 Mitotic G2-arrest is required for neural cell fate determination in Drosophila. Mech.Dev. 120;253-265.

Papers arising from this thesis

Adamson KA, Pearce SHS, Lamb JR, Seckl JR and Howie SEM. A comparative study of expression of the autoimmune regulator gene (*Aire*) at the mRNA and protein level in embryonic and adult murine tissues. Journal of Pathology 2004;202:180-187.

Rajendram R, Deane JA, Barnes M, Swift PGF, **Adamson K**, Pearce S and Woodruff G. Rapid onset childhood cataracts leading to the diagnosis of autoimmune polyendocrinopathy candidiasis ectodermal dystrophy. American Journal of Ophthalmology 2004; Vol 136 (5) 951-952.

Adamson KA, Cheetham TD, Kendall-Taylor P, Pearce SHS. Role of insulin gene polymorphisms in the IDDM susceptibility of APS1 subjects.

J Endo Vol 163 Supp

Presented as a poster at 190th meeting of the Society for Endocrinology

Adamson KA, Cheetham TD, Kendall-Taylor P and Pearce SHS. Spectrum of mutations in the AIRE-1 gene in UK APS1 (APECED) kindreds.

J Med Genet 2000 Vol 37, Supp 1

Presented as a poster at BSHG 2000

Adamson KA, Marley J, Howie SEM, Pearce SHS, Lamb JR, Seckl JR and Turner AN. Abnormalities in T cell receptor induced stimulation in patients with APS1.

Presented as a poster at the 1st Functional genomics and Disease conference 2003.

Adamson KA, Benson RA, Pearce SHS, Lamb JR, Seckl JR and Howie SEM. The autoimmune regulator gene (Aire) is up-regulated upon activation of peripheral T cells.

Immunology 2003 Vol 10, Supp 1

Presented as a poster at the Annual Congress of the British Society for Immunology 2003.

Benson RA, **Adamson KA**, Lamb JR and Howie SEM. Notch1 co-localises with CD4 upon T-cell activation.

Immunology 2003 Vol 10, Supp 1

Presented as a poster at the Annual Congress of the British Society for Immunology 2003.

Journal of Pathology
J Pathol 2004; **202**: 180–187.
Published online in Wiley InterScience (www.interscience.wiley.com). **DOI:** 10.1002/path.1493

Original Paper

A comparative study of mRNA and protein expression of the autoimmune regulator gene (*Aire*) in embryonic and adult murine tissues

KA Adamson,[1,2]* SHS Pearce,[3] JR Lamb,[1,4] JR Seckl[2] and SFM Howie[1,5]

[1]*Immunobiology Group, MRC Centre for Inflammation Research, University of Edinburgh, Medical School, Teviot Place, Edinburgh, EH8 9AG, UK*
[2]*Molecular Medicine Centre, Western General Hospital, Crewe Road, Edinburgh, EH4 2XU, UK*
[3]*Institute of Human Genetics, International Centre for Life, Central Parkway, Newcastle upon Tyne, NE1 3BZ, UK*
[4]*Respiratory Medicine Unit, University of Edinburgh, Medical School, Teviot Place, Edinburgh, EH8 9AG, UK*
[5]*Department of Pathology, University of Edinburgh, Medical School, Teviot Place, Edinburgh, EH8 9AG, UK*

**Correspondence to:*
Dr KA Adamson, Immunobiology Group, MRC Centre for Inflammation Research, University of Edinburgh, Medical School, Teviot Place, Edinburgh, EH8 9AG, UK.
E-mail: K.A.Adamson@ed.ac.uk

Received: 23 September 2002
Revised: 11 June 2003
Accepted: 2 October 2003

Abstract

Autoimmune polyendocrine syndrome type 1 (APS1) is a rare autosomal recessive human disorder caused by mutations in the autoimmune regulator gene (*AIRE*) and characterized by multiple autoimmune diseases. As reports of the tissue expression pattern of the murine *Aire* gene are discordant, a comprehensive survey of Aire expression was undertaken in adult and embryonic tissues at the mRNA and protein levels using real-time RT-PCR, *in situ* hybridization, and immunohistochemistry. In the adult, the highest *Aire* mRNA expression was in the thymus. All the other tissues investigated expressed *Aire* mRNA at low levels, but it was barely detectable in the adrenal gland. Aire protein expression was observed in the thymus, spleen, and lymph nodes. A common pattern was observed in other tissues, with staining in epithelial cells. An exception to this was the gut, where staining was seen in the mucin spaces. In embryonic tissue, *Aire* mRNA and protein expression was detected from E14.5 in the thymus. In the fetal liver, unlike the adult, staining was observed at E14.5 and decreased towards term. Thus, Aire is expressed in immunologically relevant tissues and in a restricted number of extra-immunological tissues in the adult. Furthermore, the presence of Aire protein is reported in extra-thymic tissues of the embryo. Copyright © 2004 John Wiley & Sons, Ltd.

Keywords: **autoimmune polyendocrine syndrome type 1; APS1; APECED; Aire**

Introduction

Autoimmune polyendocrine syndrome type 1 (APS1), also known as autoimmune polyendocrinopathy candidiasis and ectodermal dystrophy (APECED), is a rare autosomal recessive disorder characterized by multiple autoimmune diseases [1]. As one of two monogenic forms of human autoimmunity [2], APS1 represents an important paradigm in the study of autoimmune diseases. The autoimmune regulator gene (*AIRE*), mutations in which cause APS1 [3], encodes a number of highly conserved motifs (four LXXLL motifs, two PHD fingers, and a SAND domain), suggesting that it functions as a transcription factor [4–7]. Recently, AIRE was shown to form homodimers and homotetramers that can bind DNA [8]. Murine *Aire* cDNA shares a high degree of homology with human *AIRE* [9–11] and the homozygous Aire knock-out mice manifest similar autoimmune features to those in patients with APS1 [12,13].

The pattern of human *AIRE* mRNA expression was first described in 1997 by two independent groups [4,5]. Northern analyses showed expression in the thymus, lymph node, and fetal liver. AIRE expression was also reported in the spleen and tissues affected in APS1, such as the adrenal cortex and pancreas by one group [4], but not by another [5]. These differences have been attributed to false-positive hybridization due, perhaps, to non-specific binding by a GC-rich probe [7]. Human AIRE protein expression, as determined by immunohistochemical staining, is also seen in thymic medulla, lymph node, spleen, and fetal liver [14,15], but expression was not observed in tissues other than these [15].

Reports of the tissue distribution of murine *Aire* mRNA are also discordant. Although *Aire* mRNA could not be detected by northern blot analysis [9,10,16], RT-PCR revealed the presence of *Aire* transcripts in the heart, lung, testis [9,15,16], thymus [16–18], and lymph node [17,18]. However, there are conflicting reports of *Aire* mRNA expression in the spleen [9,16,18], kidney, brain [9,17], and liver [16,17]. Furthermore, a single report found *Aire* mRNA in the ovary, adrenal gland, and thyroid [16].

Similarly, Aire protein has been found in adult thymic medullary epithelial cells [12,17,18] and in the thyroid, gut, pancreas, and brain [12,18]. However, Aire protein expression in the spleen, lymph node,

Copyright © 2004 John Wiley & Sons, Ltd.

adrenal gland, lung, ovary, liver, kidney, and testis is discordant between studies [12,17,18].

In the murine embryo, Aire expression can be seen using RT-PCR, *in situ* hybridization, and immunohistochemistry from embryonic day 14.5 in thymic medullary epithelial cells [9,10,18].

Thus, not only is there a discrepancy between the reported expression of Aire at the protein and mRNA levels, but there is also variability in expression as determined by the same technique between studies. Since the distribution of Aire is crucial to the understanding of its role in organ-specific pathogenesis, we carried out a comprehensive survey of Aire expression in adult tissues at the mRNA and protein levels using *in situ* hybridization and the more sensitive technique of real-time RT-PCR and immunohistochemistry to clarify this issue. We determined protein expression in the whole embryo, as, to date, only Aire expression in the embryonic thymus has been described and we present novel data on the expression of Aire in peripheral immunological tissues.

Materials and methods

Mice

CD1 and C57BL/6J mice (B&K, Hull, UK) were housed in the University of Edinburgh Animal Facilities in accordance with local guidelines. Embryonic tissue was taken at embryonic (E) days 14.5, 16.5, and 18.5 from time-mated pregnancies, where embryonic day 0 (E0) was determined by detection of the vaginal plug.

RNA extraction

RNA was obtained from whole tissue by homogenization, followed by extraction using Trizol (Life Sciences, Paisley, UK), according to the manufacturer's instructions. All samples for use in real-time RT-PCR were DNAse-treated (Promega, Southampton, UK).

Real-time RT-PCR

A Taqman-based system and an ABI Prism 7700 sequence detector were used for real-time RT-PCR. All reagents were obtained from Applied Biosystems (Warrington, UK). Reverse transcription was performed using the Multiscribe RT™ kit and random hexamer primers, according to the manufacturer's instructions.

Primers were designed using Primer Express for murine Aire [F — 5′CCT GGA TTT CTG GAG GAT TCT CT 3′ (nucleotides 282–304); R — 5′CCG TCC AGG ATG CTA TGC A3′ (nucleotides 339–356); probe — 5′6FamCGG CTG TAC CGC TCC AGA TTG TAG TCC T Tamra3′ (nucleotides 308–335)] (sequence accession number NM_009646.1) and PCR was performed using Taqman Universal PCR Master Mix™ plus 18S as an internal calibrator for each sample. All samples were run in triplicate. cDNA from whole thymus from an adult CD1 mouse was used as a positive control for all runs; all mRNA levels were determined in relation to this.

In situ hybridization (ISH)

Aire was amplified from mouse thymus by RT-PCR (primers: F — AAG AAG CCA GAT GGC AAC TT; R — CGA GGA TGA GTG TGC CGT GT) (nucleotide numbers 550–569 and 948–967; accession number NM_009646.1) and the 418 bp product was cloned into PGEMTeasy vector. The insert was confirmed by sequencing and the orientation by restriction digest. Sense (control) and anti-sense ^{35}S-labelled RNA probes were generated from this plasmid using an appropriate RNA polymerase. Tissue was obtained from 6- to 8-week-old CD1 mice, and C57BL/6J embryos. Frozen sections (10 μm) were cut and mounted onto poly-l-lysine-coated slides. Sections were fixed in 4% paraformaldehyde, washed in PBS, and acetylated (0.25% acetic anhydride in 0.1 M triethanolamine, pH 8.0). After pre-hybridization in an SSC humidified chamber, the sections were hybridized at 50 °C overnight with ^{35}S-labelled probe (1×10^7 cps/slide) in an SSC humidified chamber. Slides were washed and then RNAse-treated for 1 h at 37 °C, followed by further washes and dehydration in alcohol. Slides were dipped in Kodak NTB2 emulsion (Kodak, Hemel Hempstead, UK) and developed 2 weeks later. Tissue was counterstained with haematoxylin and eosin and then coverslipped.

Antibody

A rabbit polyclonal anti-human Aire antibody (designated 2328.1) was raised by giving six injections of a peptide consisting of Aire amino acids 147–165 conjugated to BSA. The immunoglobulin (Ig) was then protein A-purified from serum according to the manufacturer's instructions (HiTrap protein A affinity column, Amersham Pharmacia Biotech, Bucks, UK).

Immunohistochemistry (IHC)

All IHC was performed on a Biogenex Optimax plus automated staining system (Biogenex, Berkshire, UK). Tissue was taken from C57BL/6J and CD1 mice into 4% buffered formalin and then processed into paraffin wax blocks. Three-micrometre sections were cut and mounted on Vectabond-treated slides (Vector Laboratories, Peterborough, UK). Slides were dewaxed in xylene, followed by antigen retrieval using Vector antigen retrieval solution (Vector Laboratories). Slides were blocked with 2% hydrogen peroxide, followed by normal goat serum. The Aire antibody was pre-absorbed with 20% mouse serum and 20% goat serum overnight at 4 °C. Slides were incubated with the primary antibody (0.675 ng of Ig per slide) for 2 h at room temperature, washed, incubated with

Copyright © 2004 John Wiley & Sons, Ltd.

a goat biotinylated anti-rabbit secondary antibody (DAKO, Ely, Cambridgeshire, UK), washed and then Vector RTU ABC (Vector Laboratories) was applied and positive signal was detected by the addition of diaminobenzidine (DAB) (DAKO). The slides were counterstained with haematoxylin and coverslipped. Avidin/biotin blocking (Avidin/Biotin blocking kit, Vector Laboratories) was used on all tissues.

Western blotting

Protein was extracted from adult thymus, liver, and adrenal glands by homogenization in lysis buffer [50 mM Hepes (pH 7.5), 1% Triton X-100, 50 mM NaCl, 50 mM NaF, 10 mM sodium pyrophosphate, 1% aprotinin, 1 mM PMSF, 0.5 M sodium orthovanadate; all from Sigma Aldrich, UK]. Fifteen micrograms of protein was resolved on a 10% SDS-PAGE gel and analysed using the specific Aire antibody.

Cell purification

T and B cells were magnetically sorted from adult C57BL/6J murine spleens. T cells were isolated using a Pan T cell isolation kit, and B cells positively selected using CD19 microbeads on an AutoMACS machine (Miltenyi Biotech, Germany), according to the manufacturer's instructions. Cell purity was assessed using anti-CD3 antibody for T cells and anti-CD19 antibody for B cells; both antibodies were labelled with PE (Pharmingen, UK) and analysed on a FACSCalibur flow cytometer (Becton Dickinson, UK).

Immunofluorescence

Cells were smeared onto superfrost slides, air-dried, fixed in 90% dry acetone–10% methanol, blocked in Dako diluent, incubated with Aire antibody, washed, incubated with a goat anti-rabbit unconjugated antibody, washed, and incubated with an Alexa Fluor 568 goat anti-rabbit antibody (Molecular Probes, Leiden, The Netherlands). All incubations were at room temperature for 30 min. Slides were then incubated with ToPro3 (Molecular Probes) to allow visualization of the nucleus, prior to coverslipping. Images were captured using a Leica TCS NT confocal system (Leica Microsystems, GmbH Mannheim, Germany).

Results

Characterization of antibody

Western blotting of murine thymic protein with the rabbit polyclonal anti-human Aire antiserum revealed a band of the expected molecular weight of Aire (58 kD). The amino acid sequence of the peptide used for immunization is homologous between mouse and human at 11 of 19 amino acids. Specificity in mouse was confirmed by immunohistochemistry, in control sections by pre-absorption with peptide in excess, and incubation of additional control sections with protein A-purified Ig from pre-immune serum (Figure 1). Staining was within the nucleus in a punctate pattern, consistent with the subcellular expression previously reported [14].

Expression of *Aire* in tissues of adult mice as determined by real-time RT-PCR, ISH, and IHC

Aire mRNA expression was determined by real-time RT-PCR and is presented relative to expression in adult CD1 mouse thymus. The same cDNA sample was used on each real-time PCR plate to standardize between runs. The highest expression was seen in C57BL/6J thymus and was over four times higher than that seen in CD1 thymus. All the other tissues investigated expressed *Aire* mRNA at varying levels which were less than in the positive control. Low levels of mRNA relative to thymus were seen in the spleen, testis, kidney, liver, brain, lung, ovary, heart, and gut, with barely detectable expression in adrenal gland (Figure 2).

The level of expression of *Aire* mRNA was confirmed by *in situ* hybridization, where detectable *Aire* mRNA expression was limited to the thymic medulla.

Immunohistochemistry was performed on tissues from C57BL/6J mice. Aire expression within the thymus (Figure 3A) was most marked within the thymic medullary epithelial cells, with occasional medullary and cortical non-epithelial cells also staining. In lymph nodes (Figure 3B), the light zone of the germinal centre of the lymphoid follicles showed positive staining, whilst in the dark zone there was some staining but the majority of cells were negative. Positive staining was seen in the T-cell areas of the lymph node. This was

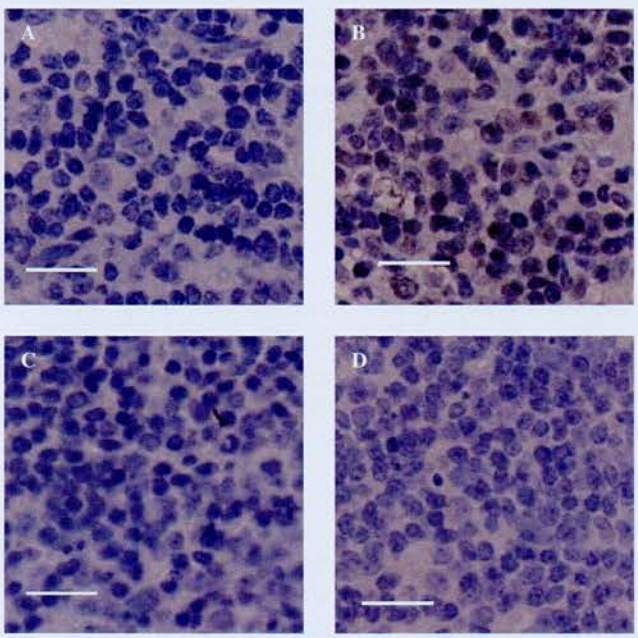

Figure 1. Immunohistochemistry of murine thymus (×200; scale bar represents 20 μm). (A) Negative control; (B) incubated with Aire antiserum; (C) incubated with pre-immune serum; (D) incubated with Aire antiserum pre-absorbed with peptide

Copyright © 2004 John Wiley & Sons, Ltd.

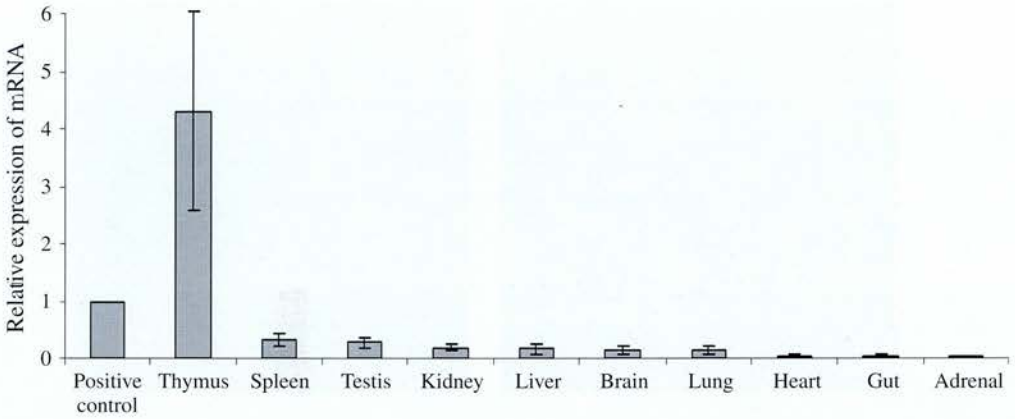

Figure 2. Real-time PCR. mRNA from whole tissues was reverse-transcribed and used as the template for PCR with specific primers and probes to Aire. All samples were normalized to a positive control, which is given a value of 1

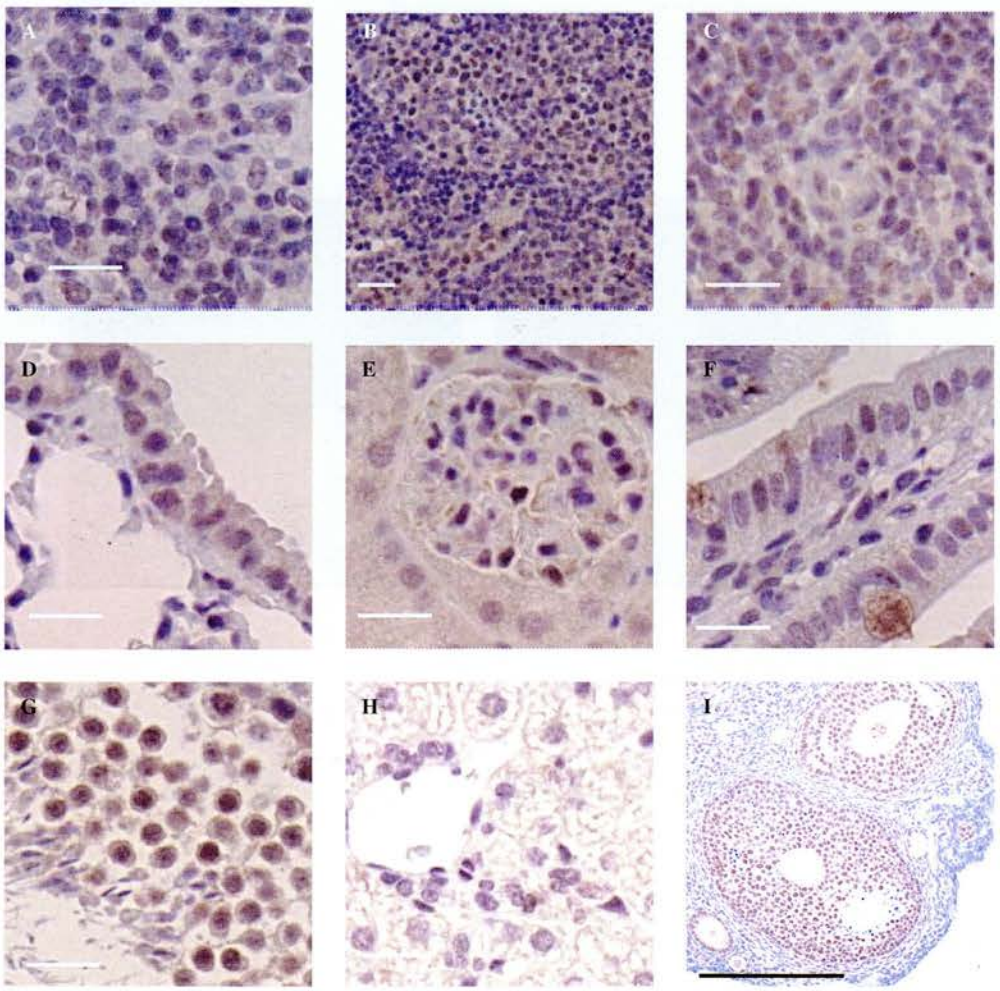

Figure 3. Immunohistochemistry of murine adult tissues. (A) Thymus; (B) lymph node; (C) spleen; (D) lung; (E) kidney; (F) gut; (G) testis; (H) liver; (I) ovary. (A, C–I) ×200; (B) ×100; scale bar represents 20 μm

also the case in the spleen, where the positive staining was seen in the nuclei of cells in T-cell areas of the white pulp. There was no staining in the red pulp (Figure 3C). No staining was seen with either peptide pre-absorbed antiserum or pre-immune antisera. The presence of Aire protein in the T and B cells of the spleen was confirmed by staining purified cells. Positive staining for Aire was seen in both T and B cells, although the staining in B cells was less marked than in T cells (Figure 4).

In many other tissues including the lung, kidney, and Fallopian tube, there was expression within epithelial cells. This is illustrated in the large airways of the lung (Figure 3D), where the only positive staining is in the epithelial cells. No staining was detected within the small airways or alveoli.

Copyright © 2004 John Wiley & Sons, Ltd.

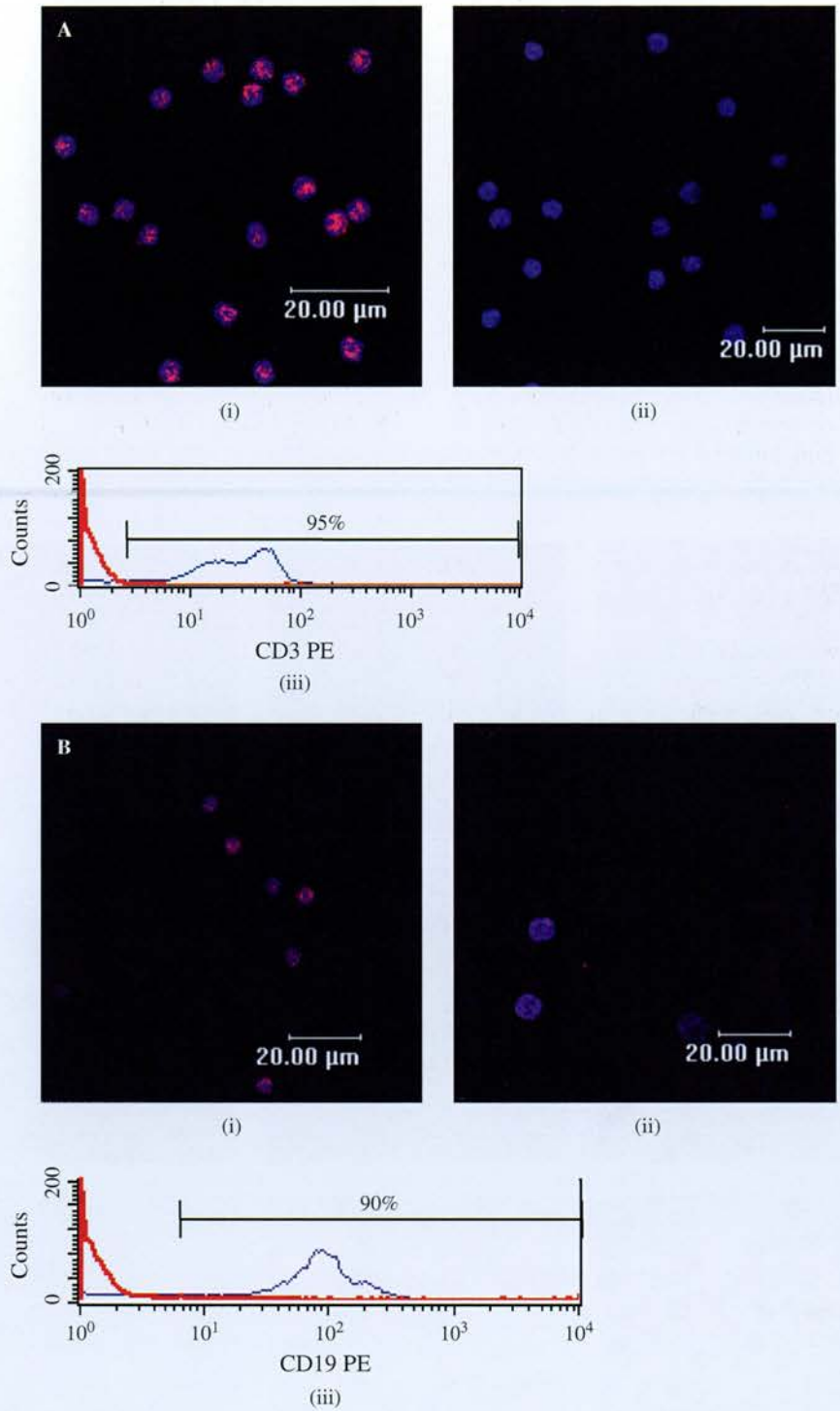

Figure 4. Aire protein expression in T and B cells. (A) T cells. (i) Positive staining for Aire in CD3-positive T cells; (ii) negative control; (iii) flow cytometry to demonstrate the purity of the T cells using an anti-CD3 antibody (isotype control shown in red). (B) B cells. (i) Positive staining for Aire in CD19-positive B cells; (ii) negative control; (iii) flow cytometry to demonstrate the purity of the B cells using an anti-CD19 antibody(isotype control shown in red)

Staining was observed in epithelial cells of the kidney (Figure 3E), within the tubules and the glomerulus. Similarly, the columnar epithelium of the Fallopian tubes also stained positively.

No specific staining was seen in the epithelial cells of the small intestinal villi or in the neuroendocrine cells of the gut, but strong staining was seen in the mucin spaces of the goblet cells (Figure 3F). The significance of this is unclear, but loss of goblet cells is a feature of autoimmune disease of the gut [19,20].

Within the testis (Figure 3G), Aire staining was seen in the developing spermatocytes, but not in the mature haploid cells, whilst in the ovary, staining was seen in the follicular cells. In the brain, staining was present in the neurones of the hippocampus and cortex. All of this staining was absent in sections incubated with pre-immune serum and was abolished by pre-absorption

Copyright © 2004 John Wiley & Sons, Ltd.

with a blocking peptide. No staining was seen in the heart, liver (Figure 3H), or any zone of the adrenal gland.

This pattern mimics that seen by real-time RT-PCR, as tissues where a greater population of cells stain have higher expression, eg thymus, spleen, and kidney. The only discrepancies between the real-time RT-PCR data and IHC are for the liver and heart. IHC was also performed on tissues from the outbred strain CD1: the pattern of staining seen is consistent with that in the inbred strain C57BL/6J (data not shown).

In view of the difference in tissue distribution in this study compared with that of Halonen *et al* [17], western blotting of the liver and adrenal gland was undertaken. This confirms the absence of Aire protein in these tissues.

Expression of Aire in murine embryonic tissues as determined by ISH and IHC

Aire expression was detected by ISH from E14.5 in the thymus as previously reported [9,18]. No other specific expression was seen by ISH. Additionally, Aire expression in the embryo in relation to the adult was studied using real-time RT-PCR. In the spleen, expression in the embryo at E16.5 was 20-fold less than in the adult (Figure 5D). A lower level of expression in the embryo than in the adult was also seen in the thymus (data not shown). IHC was undertaken from E14.5; expression within the thymus was seen from E14.5 to term (Figure 5A). Unlike the adult, expression was seen at E14.5 in the liver and decreased towards term, presumably reflecting that this is the main site of haematopoiesis in the embryo.

Staining was also observed in the epithelial cells of the developing lung (Figure 5B), in the large airways, and in the epithelial cells of the developing renal tubules, as demonstrated in the adult. Unlike the adult, positive staining was detected in the epithelial cells of the gut. This staining decreased towards term and was accompanied by the presence of staining in the mucin spaces of goblet cells, in the same pattern as the adult (Figure 5C).

Discussion

Our results reveal the presence of Aire protein in immunologically relevant tissues and a restricted number of peripheral tissues. In the thymus, mRNA and protein were detected primarily within the medulla, as previously published for both human and murine tissue [14,15,17,18]. Thymic medullary epithelial cells have a role in tolerance induction through clonal deletion [21], the induction of anergy [22], and by supporting the development of regulatory T cells [23]. As patients with APS1 have a breakdown in tolerance leading to autoimmune disease, the expression of Aire in this particular tissue is not surprising. Defects in the appropriate negative selection of autoreactive T cells within the thymus are an important mechanism in the aetiology of autoimmune disease. Therefore, the increased expression of Aire seen in models of negative selection and the absence of Aire in the RelB-deficient

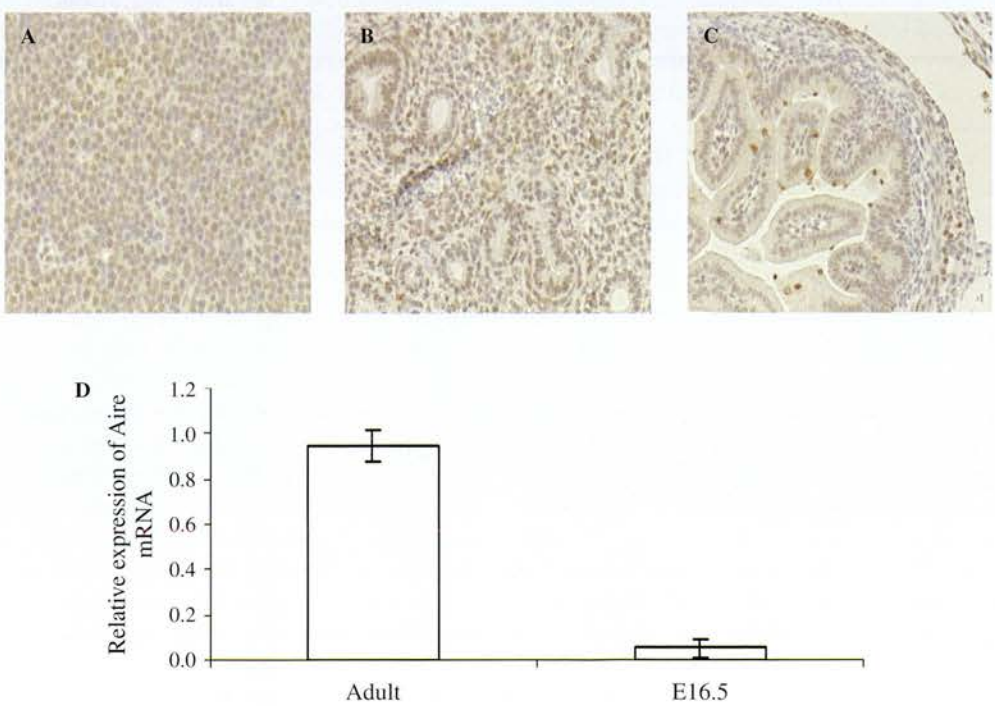

Figure 5. Immunohistochemistry (IHC) and real-time RT-PCR of murine embryonic tissues. (A) Thymus 18.5; (B) lung E14.5; (C) gut E18.5 (×100). (D) mRNA from whole adult and embryonic (E16.5) spleen was reverse-transcribed and used as the template for PCR with specific primers and probes to Aire. All samples were normalized to the adult tissue, which is given a value of 1

Copyright © 2004 John Wiley & Sons, Ltd.

mouse, in which there is a defect in negative selection, are important clues to Aire's function, although interpretation of the data in the RelB-deficient mouse is complicated by the fact that it has defective thymic development [18,24]. These data, in addition to the recently described Aire knock-out mice, in which there is a defect in ectopic expression of peripheral antigens in the thymus [13] and failure of deletion of organ-specific T cells within the thymus [25], show the importance of Aire in the induction of central (thymic) tolerance.

In the lymph node, Aire expression has previously been reported in human and mouse. However, in this study, the pattern of expression in the lymph node and spleen is different from that reported by Halonen *et al* [17], who found no staining in B-cell areas, whilst we found staining in both B- and T-cell areas. Halonen *et al* [17] failed to detect Aire in the white pulp of the spleen. In contrast, we showed specific staining in the T-cell areas of the white pulp (Figure 3C). This staining in the T- and B-cell areas was confirmed by the presence of staining in T and B cells isolated from the spleen (Figure 4).

In addition to the immune system, immunostaining was seen in epithelial cells of the lung, kidney, neurones within the cortex and hippocampus, in the ovary and testis, and in the goblet cells of the gut. Expression of the Aire protein in the lung, kidney, and brain is more restricted in this study than in the earlier ones [17,26].

These discrepancies may be explained by the use of different antibodies in the two studies. The antibodies may recognize different epitopes: the peptide used by Halonen *et al* is slightly different from that used here, as it overlaps the sequence that we used by five amino acids. Strain differences between the inbred C57BL/6J mice used in this study and the outbred NMRI mice used by Halonen *et al* [17] may also account for the variation in the pattern of staining. However, the pattern of protein expression in the outbred strain CD1 was similar to that in C57BL/6J mice. A study on BALB/C mice [18] revealed protein expression in the thymic medulla as demonstrated here, but not in other tissues examined including the testis, adrenal gland, lymph node, spleen, and liver. Therefore, in the adult, we would agree that Aire is seen within immunologically relevant tissues and in some non-immunological tissues. However, protein expression as detected by our antibody appears not to be as widespread as that reported by Halonen *et al* [17].

The staining detected within T cells is of great interest and clearly needs to be investigated further. These data clearly show that Aire is expressed in splenic T cells, as was suggested by the positive staining seen by Halonen *et al* in the T-cell areas of the spleen. Aire has been reported to be present in some bone marrow lymphoblast stem cells [17]. However, its expression is less marked in thymocytes, but is then detectable in the majority of splenic T cells: this observation is in agreement with that of Ramsey *et al* [27]. As described above, it is established that Aire has a role in central tolerance, by controlling the expression of some tissue-specific antigens [13] and through Aire-mediated central tolerance to high-affinity T cells [25]. However, the presence of Aire in peripheral T cells may suggest a role in mediating peripheral tolerance. Ramsey *et al* found that Aire knock-out mice have a greater proliferative response to *in vitro* re-challenge with HEL than wild-type mice [12]. It is therefore possible that Aire has a role in controlling the proliferative response in the periphery.

In the embryo, in common with another report, we detected *Aire* mRNA in the thymus by *in situ* hybridization from E14.5 [9] and using the more sensitive technique of real-time RT-PCR, we detected *Aire* mRNA at low level in the spleen. Protein expression was also seen from E14.5 and persisted through to E18.5. Expression was also seen within the embryonic liver from E14.5 and towards term, the expression of Aire was less marked, consistent with a decline in the liver's role in haematopoiesis. Expression of protein and mRNA has also been reported in the human fetal liver [15].

In the embryo, as in the adult, Aire expression was present in the epithelial cells of the lung and developing renal tubules. Additionally, Aire expression was seen in the epithelial cells of the gut at E14.5, as reported by Halonen *et al* [17] in the adult. In the embryo, Aire was absent by E18.5 and we observed the same pattern of expression as in the adult, namely expression in the mucin spaces of the goblet cells only.

Positive staining for mRNA by *in situ* hybridization was seen only in the thymus and not in the other tissues studied. This may reflect either absent or very low levels of expression in these tissues, below the limit of detection of this technique. These findings complement those of others, as this is a common theme in previously published work in the mouse and human [9,15,16]. In BALB/C mice, *Aire* mRNA could be detected outside the immune system, but nested PCR was required due to low levels of signal [18]. The presence of low-level expression is strongly suggested by real-time PCR. The lack of staining seen in the adrenal gland suggests either that the barely detectable signal from real-time PCR may be from a migrating cell type, as described by Heino *et al* [18], due to the higher sensitivity of this technique, or that *Aire* mRNA may be short-lived in comparison to protein.

In conclusion, we have demonstrated that Aire is expressed at the protein and mRNA levels in immunologically relevant tissues and in a restricted number of extra-immunological tissues in the adult. For the first time, we have shown that Aire protein can be detected in extra-thymic tissues of the embryo. Of particular interest is the expression seen, firstly, within the immune privileged sites of the testis and brain, especially in view of the high proportion of male patients who develop testicular failure [1]; secondly, in the goblet cells of the gut, which are lost in autoimmune disease at this site; and thirdly, in splenic

Copyright © 2004 John Wiley & Sons, Ltd.

T and B cells. The role of Aire in these tissues remains to be elucidated, but these data raise questions regarding its role in the regulation of tolerance in the periphery, in addition to its role in the maintenance of central tolerance [13,25,28].

Acknowledgements

The advice of June Noble, Anne Grant, Linda Wilson, and Lynn Forsyth with *in situ* hybridization, immunohistochemistry, confocal microscopy, and real-time RT-PCR primer design, respectively, is gratefully appreciated. This work was funded by the Medical Research Council (UK) and The Wellcome Trust.

References

1. Ahonen P, Myllarniemi S, Sipila, Perheentupa J. Clinical variation of autoimmune polyendocrinopathy–candidiasis–ectodermal dystrophy (APECED). *N Engl J Med* 1990; **322**: 1829–1836.
2. Bleesing JJ, Cooper E. Autoimmune lymphoproliferative syndrome (ALPS). *Curr Pharm Des* 2003; **9**: 265–278.
3. Pearce SHS, Cheetham T, Imrie H, *et al*. A common and recurrent 13-bp deletion in the autoimmune regulator gene in British kindreds with autoimmune polyendocrinopathy type 1. *Am J Hum Genet* 1998; **63**: 1675–1684.
4. Finnish–German APECED Consortium. An autoimmune disease, APECED, caused by mutations in a novel gene featuring two PHD-type zinc-finger domains. The Finnish–German APECED Consortium. Autoimmune polyendocrinopathy–candidiasis–ectodermal dystrophy. *Nature Genet* 1997; **17**: 399–403.
5. Nagamine K, Peterson P, Scott HS, *et al*. Positional cloning of the APECED gene. *Nature Genet* 1997; **17**: 393–398.
6. Aasland R, Gibson TJ, Stewart AF. The PHD finger implications for chromatin-mediated transcriptional regulation. *Trends Biochem Sci* 1995; **20**: 56–59.
7. Gibson TJ, Ramu C, Gemund C, Aasland R. The APECED polyglandular autoimmune syndrome protein, AIRE-1, contains the SAND domain and is probably a transcription factor. *Trends Biochem Sci* 1998; **23**: 242–244.
8. Kumar GP, Laloraya M, Wang CY, *et al*. The autoimmune regulator (AIRE) is a DNA-binding protein. *J Biol Chem* 2001; **276**: 41 357–41 364.
9. Blechschmidt K, Schweiger M, Wertz K, *et al*. The mouse *Aire* gene: comparative genomic sequencing, gene organisation, and expression. *Gen Res* 1999; **9**: 158–166.
10. Mittaz L, Rossier C, Heino M, *et al*. Isolation and characterisation of the mouse *Aire* gene. *Biochem Biophys Res Commun* 1999; **255**: 483–490.
11. Wang C, Shi J, Davoodi-Semiromi A, She J. Cloning of *Aire*, the mouse homologue of the autoimmune regulator (*AIRE*) gene responsible for autoimmune polyglandular syndrome type 1 (APS1). *Genomics* 1999; **55**: 322–326.
12. Ramsey C, Winqvist O, Puhakka L, *et al*. Aire deficient mice develop multiple features of APECED phenotype and show altered immune response. *Hum Mol Genet* 2002; **11**: 397–409.
13. Anderson MS, Venanzi ES, Klein L, *et al*. Projection of an immunological self shadow within the thymus by the aire protein. *Science* 2002; **298**: 1395–1401.
14. Bjorses P, Pelto-Huikko M, Kaukonen J, Aaltonen J, Peltonen L, Ulmanen I. Localization of the APECED protein in distinct nuclear structures. *Hum Mol Genet* 1999; **8**: 259–266.
15. Heino M, Peterson P, Kudoh J, *et al*. Autoimmune regulator is expressed in the cells regulating immune tolerance in thymus medulla. *Biochem Biophys Res Commun* 1999; **257**: 821–825.
16. Ruan Q, Wang C, Shi J, She J. Expression and alternative splicing of the mouse autoimmune regulator gene (*Aire*). *J Autoimmun* 1999; **13**: 307–313.
17. Halonen M, Pelto-Huikko M, Eskelin P, Peltonen L, Ulmanen I, Kolmer M. Subcellular location and expression pattern of autoimmune regulator (Aire), the mouse orthologue for human gene defective in autoimmune polyendocrinopathy candidiasis ectodermal dystrophy (APECED). *J Histochem Cytochem* 2001; **49**: 197–208.
18. Heino M, Peterson P, Sillanpaa N, *et al*. RNA and protein expression of the murine autoimmune regulator gene (Aire) in normal, RelB-deficient and in NOD mouse. *Eur J Immunol* 2000; **30**: 1884–1893.
19. Murch SH, Fertleman CR, Rodrigues C, *et al*. Autoimmune enteropathy with distinct mucosal features in T-cell activation deficiency: the contribution of T cells to the mucosal lesion. *J Pediatr Gastroenterol Nutr* 1999; **28**: 393–399.
20. Moore L, Xu X, Davidson G, Moore D, Carli M, Ferrante A. Autoimmune enteropathy with anti-goblet cell antibodies. *Hum Pathol* 1995; **26**: 1162–1168.
21. Burkly LC, Degermann S, Longley J, *et al*. Clonal deletion of V beta 5^+ T cells by transgenic I-E restricted to thymic medullary epithelium. *J Immunol* 1993; **151**: 3954–3960.
22. Schonrich G, Momberg F, Hammerling GJ, Arnold B. Anergy induced by thymic medullary epithelium. *Eur J Immunol* 1992; **22**: 1687–1691.
23. Modigliani Y, Thomas-Vaslin V, Bandeira A, *et al*. Lymphocytes selected in allogenic thymic epithelium mediate dominant tolerance toward tissue grafts of the thymic epithelium haplotype. *Proc Natl Acad Sci U S A* 1995; **92**: 7555–7559.
24. Zuklys S, Balciunaite G, Agarwal A, Fasler-Kan E, Palmer E, Hollander G. Normal thymic architecture and negative selection are associated with Aire expression, the gene defective in the autoimmune-polyendocrinopathy–candidiasis–ectodermal dystrophy (APECED). *J Immunol* 2000; **165**: 1976–1983.
25. Liston A, Lesage S, Wilson J, Peltonen L, Goodnow CC. Aire regulates negative selection of organ-specific T cells. *Nature Immunol* 2003; **4**: 350–354.
26. Kumar PG, Laloraya M, She JX. Population genetics and functions of the autoimmune regulator (AIRE). *Endocrinol Metab Clin North Am* 2002; **31**: 321–338.
27. Ramsey C, Kaukonen J, Palotie A, Peltonen L. Developmentally regulated expression of AIRE during human leukocyte differentiation. 49th Annual Meeting of the American Society of Human Genetics, 1999.
28. Peterson P, Nagamine K, Scott H, *et al*. APECED: a monogenic autoimmune disease providing new clues to self-tolerance. *Immunol Today* 1998; **19**: 384–386.

Copyright © 2004 John Wiley & Sons, Ltd.

Rapid Onset Childhood Cataracts Leading to the Diagnosis of Autoimmune Polyendocrinopathy-candidiasis-ectodermal Dystrophy

Ranjan Rajendram, MRCOphth,
James A. Deane, FRCOphth,
Martin Barnes, MRCOphth,
Peter G.F. Swift, FRCPCH,
Karen Adamson, MRCP, Simon Pearce, MRCP,
and Geoffrey Woodruff, FRCOphth

PURPOSE: To report a case of bilateral cataracts in a child that led to diagnosis of autoimmune polyendocrinopathy-candidiasis-ectodermal dystrophy.

DESIGN: Observational case report.

METHODS: A 12-year-old boy was being investigated for weakness, lethargy, short stature, and blurred vision. He developed bilateral, dense cataracts over a 2-week period. He was found to be hypocalcemic and diagnosed with hypoparathyroidism and autoimmune polyendocrinopathy-candidiasis-ectodermal dystrophy.

RESULTS: Because of hypoparathyroidism, adrenocortical failure, and insulin-dependent diabetes, it was 9 months before the patient's metabolic imbalance was brought under sufficient control to allow cataract surgery.

CONCLUSION: Autoimmune polyendocrinopathy-candidiasis-ectodermal dystrophy should be considered with diagnoses of hypocalcemic cataract. (Am J Ophthalmol 2003;136:951–952. © 2003 by Elsevier Inc. All rights reserved.)

AUTOIMMUNE POLYENDOCRINOPATHY-CANDIDIASIS-ectodermal dystrophy (APECED), also known as autoimmune polyendocrinopathy syndrome type 1, is a rare autosomal recessive disease characterized by a variable combination of (A) failure of the parathyroid glands, adrenal cortex, gonads, pancreatic beta cells, gastric parietal cells, thyroid gland, and hepatitis; (B) chronic mucocutaneous candidiasis; (C) dystrophy of dental enamel and nails; alopecia; vitiligo; and keratopathy.[1]

A 12-year-old boy was seen in the ophthalmology department of the Leicester Royal Infirmary with a 6-week history of intermittent double vision. He was found to have an intermittent right esotropia. A general deterioration in his health was noted, with symptoms of weakness and lethargy and problems with speech and writing. His height was below the third percentile. He was admitted to the pediatric department for further investigation. He later complained of blurred vision; on review, he had developed bilateral cortical lens opacities, that had not been present 2 weeks earlier (Figure 1). His visual acuity had deteriorated from 20/40 (OD) and 20/20 (OS) to 20/200 in each eye.

Serum calcium was 0.68 mmol/l (normal, 2.10–2.60), with a phosphate level of 3.22 mmol/l (normal, 1.20–2.30). The parathyroid hormone level was below detectable limits at <0.1 pmol/l. Control of the mineral and electrolyte balance proved to be difficult to achieve and was complicated by the development of adrenocortical failure. A clinical diagnosis of APECED was made.

Nine months after the appearance of the cataracts, when the patient's general medical condition was sufficiently stable, bilateral phacoemulsification with intraocular lens placement was carried out without complication. Preoperative visual acuity had deteriorated to 3/180 in each eye; postoperative visual acuity was 20/20 part in each eye. The patient also developed a large-angle (48 prism diopter, near and distance) right convergent squint, which was corrected following the cataract surgery. Systemic features of APECED seen in this case included intestinal malabsorption without enterocyte antibodies, alopecia, skin and nail changes, insulin-dependent diabetes mellitus, and delayed puberty.

Autoimmune polyendocrinopathy-candidiasis-ectodermal dystrophy is caused by mutations in the autoimmune regulator gene (AIRE).[2] Analysis of this gene demonstrated that the patient was a compound heterozygote for the most common UK mutation, 964del13, which is thought to give rise to a truncated nonfunctional protein, and a second, as yet unidentified mutation.

Other ocular associations with this disease include bilateral chronic keratitis, which may be a presenting feature. The outcome following keratoplasty in these patients is poor, with rejection occurring in all four transplants of one series.[3,4] Iridocyclitis, retinal detachment, and optic nerve atrophy may occur in rare cases.[4,5]

Rapidly progressive cataracts were the key feature leading to the diagnosis of hypoparathyroidism and APECED in this child. It is not known whether the emergence of the convergent squint was related to the disease. Ophthalmologists and pediatricians should consider APECED when making a diagnosis of cataract in a patient with hypocalcaemia. Because some manifestations may not appear until the fifth decade, all patients need lifelong follow-up to detect new components of the disease.[1]

Accepted for publication April 30, 2003.

From the Departments of Ophthalmology (R.R., J.A.D., M.B., G.H.W.) and Paediatrics (P.G.F.S.), The Leicester Royal Infirmary, University Hospitals of Leicester NHS Trust, Leicester, England; Immunobiology Group, MRC Centre for Inflammation Research and Department of Molecular Endocrinology, University of Edinburgh, Edinburgh, Scotland (K.A.); and Institute of Human Genetics, University of Newcastle Upon Tyne, Newcastle Upon Tyne, England (S.P.).

Inquiries to Ranjan Rajendram, MRCOphth, Department of Ophthalmology, Doheny Eye Institute, 1450 San Pablo Street, DVRC 211, Los Angeles, CA 90033; fax: (323) 442-6688; e-mail: RRajendram@DohenyEyeInstitute.org

FIGURE 1. One of the bilateral, dense anterior and posterior cortical lens opacities, that appeared and progressed rapidly over a 2-week period.

REFERENCES

1. Ahonen P, Myllarniemi S, Sipila I, Perheentupa J. Clinical variation of autoimmune polyendocrinopathy-candidiasis-ectodermal dystrophy (APECED) in a series of 68 patients. N Engl J Med 1990;322:1829–1836.
2. Pearce SH, Cheetham T, Imrie H, et al. A common and recurrent 13-bp deletion in the autoimmune regulator gene in British kindreds with autoimmune polyendocrinopathy type 1. Am J Hum Genet 1998;63:1675–1684.
3. Tarkkanen A, Merenmies L. Corneal pathology and outcome of keratoplasty in autoimmune polyendocrinopathy-candidiasis-ectodermal dystrophy (APECED). Acta Ophthalmol Scand 2001;79:204–207.
4. Merenmies L, Tarkkanen A. Chronic bilateral keratitis in autoimmune polyendocrinopathy-candidiadis-ectodermal dystrophy (APECED). A long-term follow-up and visual prognosis. Acta Ophthalmol Scand 2000;78:532–535.
5. Perheentupa J. APS-I/APECED: the clinical disease and therapy. Endocrinol Metab Clin N Am 2002;31:295–320.

Exudative Retinal Detachment Due to Small Noncalcified Retinal Astrocytic Hamartoma

Tamara R. Vrabec, MD, and James J. Augsburger, MD

Accepted for publication May 9, 2003.

From the Wills Eye Hospital (T.R.V.), Thomas Jefferson University, Philadelphia, Pennsylvania, and Department of Ophthalmology (J.J.A.), College of Medicine, University of Cincinnati, Cincinnati, Ohio.

Inquiries to Tamara R. Vrabec, MD, 3244 Midvale Ave, Philadelphia, PA 19129; fax: (215) 849-9989; e-mail: TRVRDMD@aol.com

PURPOSE: To report a case of exudative retinal detachment due to small noncalcified retinal astrocytic hamartoma and review pertinent literature.

DESIGN: Case report and review of literature.

METHODS: Clinical examination, fluorescein angiography, optical coherence tomography, and laser treatment were performed.

RESULTS: Exudative macular detachment caused by a small noncalcified retinal astrocytic hamartoma confirmed by optical coherence tomography regressed completely after laser therapy. Visual acuity improved only slightly because lamellar macular thinning developed after subretinal fluid and macular exudates resolved.

CONCLUSIONS: Small noncalcified, parafoveal retinal astrocytic hamartomas may cause macular retinal detachment. Optical coherence tomography may aid in the diagnosis of the tumor. Argon laser photocoagulation may induce tumor regression and resolution of exudative detachment. Final visual acuity may be limited in some cases. (Am J Ophthalmol 2003;136:952–954. **© 2003 by Elsevier Inc. All rights reserved.)**

FOUR TYPES OF RETINAL ASTROCYTIC HAMARTOMAS are described. Large atypical retinal astrocytic hamartomas are usually not associated with tuberous sclerosis or neurofibromatosis especially when single and peripapillary.[1] Most develop before age 20; few adult cases are reported. Complications include exudative retinal detachment, vitreous hemorrhage, infarction, neovascular glaucoma, and blindness.[1,2] Three typical forms, small